



Figlus, Marek (2008) *Synthesis of new recoverable catalysts and their application in asymmetric reduction of ketimines with trichlorosilane*. PhD thesis.

<http://theses.gla.ac.uk/1640/>

Copyright and moral rights for this thesis are retained by the author

A copy can be downloaded for personal non-commercial research or study, without prior permission or charge

This thesis cannot be reproduced or quoted extensively from without first obtaining permission in writing from the Author

The content must not be changed in any way or sold commercially in any format or medium without the formal permission of the Author

When referring to this work, full bibliographic details including the author, title, awarding institution and date of the thesis must be given

**A thesis submitted in part fulfillment of the requirements of the degree of Doctor of
Philosophy**



**UNIVERSITY
of
GLASGOW**

**SYNTHESIS OF NEW RECOVERABLE CATALYSTS AND
THEIR APPLICATION IN ASYMMETRIC REDUCTION OF
KETIMINES WITH TRICHLROSILANE**

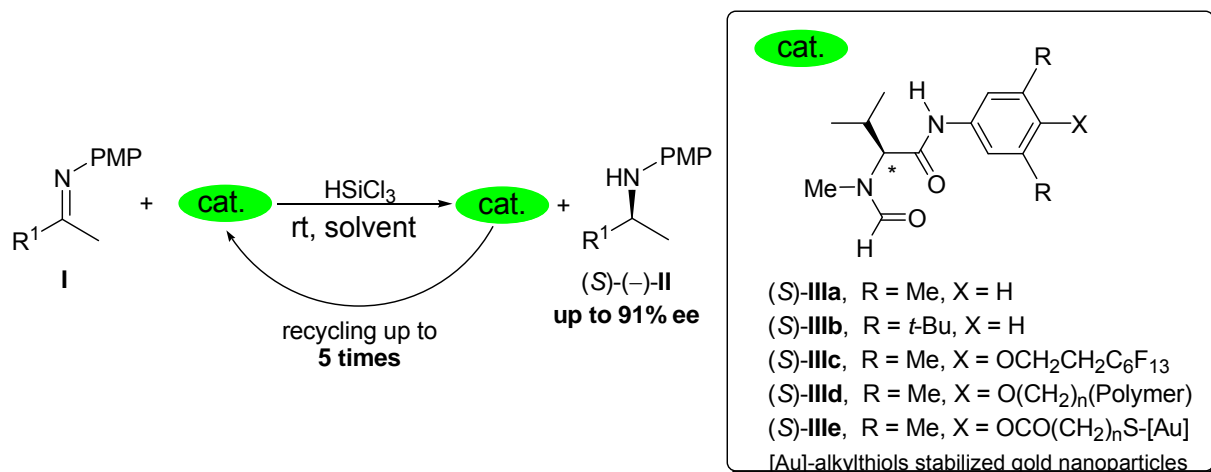
Marek Figlus

Department of Chemistry

University of Glasgow

i. Abstract

Obtaining chiral amines from ketones via imine intermediates represents an attractive strategy that opens a straightforward route to valuable building blocks for the pharmaceutical and other fine chemicals industries. Metal-free organocatalysis can be viewed as an attractive and broadly applicable methodology in which the metal is not vital for the key bond-forming event. Previously developed in our laboratory, *N*-methylvaline-derived formamides **IIIa,b** proved to be efficient catalysts for asymmetric reduction of prochiral ketimines with trichlorosilane, (up to 98%, 95% ee).^{136,137} Tagging the catalyst to a fluorosilyl tail **IIIc**, soluble and insoluble polymers **IIId**, or gold nanoparticles **IIIe** simplified the isolation procedure, while preserving high activities and stereoselectivities (up to 98%, 91% ee). The recovered catalysts could be reused at least 5 times without the loss of activity or stereoselectivity. This technology appears to be particularly suited to the small-scale parallel chemistry.



ii. Acknowledgements

I would like to thank the University of Glasgow for a Graduate Fellowship and AstraZeneca for additional financial support. My supervisors Prof. Pavel Kočovský, Dr Andrei Malkov (University of Glasgow), and Prof. Iwao Ojima (State University of New York at Stony Brook) for general support and help, and Prof. Francis Johnson for funding my stay at New York State University at Stony Brook.

Also thanks to Dr Graeme Cook and Dr Richard Hartley for useful advice regarding fluororous chemistry, polymers, gold nanoparticles, and dendrimers, to Sigita (Dr S. Stončius) for introducing me to asymmetric reduction of imines, and to Stuart (Dr. S. Caldwell) for a nice collaboration

Great thanks to the Polish gang of the Chemistry Department: Kasia, Teresa, Aska, Maciek, Dawid, and Mikhail (actually a Russian) for fun and nice atmosphere.

Finally great thanks to all people who have helped me to push my project forward.

iii. Abbreviations

Å	Ångström
Aq	Aqueous
BINOL	1,1'-Binaphthol
Bn	Benzyl
Boc	<i>tert</i> -Butoxycarbonyl
Bp	Boiling Point
<i>tert</i> -Bu	Tertiary butyl
Bz	Benzoyl
°C	Degrees centigrade
cat	Catalytic
CI	Chemical ionization
cm	Centimetre
conc	Concentrated
Cy	Cyclohexyl
d	Doublet (NMR spectroscopy)
D-A	Diels-Alder
DMAP	4-Dimethylaminopyridine
DMF	Dimethylformamide
DMSO	Dimethylsulfoxide
ee	Enantiomeric excess
EI	Electron Impact
Equiv	Equivalents
FAB	Fast Atom Bombard
GC	Gas Chromatography
h	Hours
HPLC	High Performance Liquid Chromatography
Hz	Hertz
IR	Infrared
JJ	JandaJel
M	Molarity
m	Multiplet (NMR spectroscopy)
min(s)	Minutes
MS	Mass Spectroscopy
Naph	Naphtyl
NMO	<i>N</i> -methylmorpholine- <i>N</i> -oxide
NMR	Nuclear Magnetic Resonance
PMP	<i>para</i> -Methoxyphenyl
PS	Polystyrene
q	Quartet (NMR spectroscopy)
rt	Room Temperature
satd	Saturated
t	Triplet (NMR spectroscopy)
TLC	Thin Layer Chromatography
UV	Ultraviolet
WR	Wang resin

CONTENTS

i. Abstract	2
ii. Acknowledgements	3
iii. Abbreviations	4

LITERATURE PART

	Introduction	8
1	Immobilization of chiral homogeneous catalysts	8
1.1	Immobilization of catalysts for metal catalysed reactions	8
1.1.1	Covalent immobilization on polymers	8
1.1.2	Covalent immobilization on an inorganic support	16
1.1.2.1	Covalent immobilization on metal oxides	16
1.1.2.2	Immobilization on metal nanoparticles	23
1.2	Immobilization of organocatalysts	28
1.3	Immobilization of homogeneous catalysts – conclusions	38
2	Application of ionic liquids in asymmetric catalysis	39
2.1	Application of ionic liquids in asymmetric catalysis – conclusions	47
3	Application of chiral fluorine catalysts in asymmetric synthesis	48
3.1	Application of chiral fluorine catalysts in asymmetric synthesis – conclusions	51
4	Asymmetric catalytic reduction of imines	53
4.1	Introduction	53
4.2	Catalytic reduction of imines using hydride reagents	53
4.3	Catalytic asymmetric hydrogenation of imines	55
4.4	Catalytic asymmetric hydrosilylation of imines	64
4.4.1	Catalytic asymmetric hydrosilylation of imines with trichlorosilane	68
4.5	Catalytic asymmetric transfer hydrogenation of imines	74

RESEARCH

5	Synthesis and application of new recoverable catalysts – Introduction	78
5.1	Catalysts synthesis	79
5.1.1	Synthesis of substituted anilines	79
5.1.2	Synthesis of fluorine catalysts	80
5.1.3	Application of fluorine catalysts in asymmetric reduction of imines	81
5.1.4	Conclusions	84
5.2	Immobilization of organocatalysts on insoluble polymers	84
5.2.1	Synthesis of the amino-acid moieties suitable for immobilization	85

5.2.2	Immobilization of amino-acid moieties	87
5.2.3	Asymmetric reduction of imines catalysed by solid-supported catalysts	91
5.2.4	Conclusions	96
5.3	Asymmetric reduction of imines catalysed by ionic catalyst	96
5.4	Immobilization of the catalyst on gold nanoparticles	99
5.4.1	Synthesis of organic intermediates	100
5.4.2	Immobilization of the catalyst on the surface of gold nanoparticles	102
5.4.3	Gold nanoparticles supported catalysts-application	105
5.4.4	Conclusions	107
5.5	Immobilization of the catalyst on a soluble polymer	108
5.5.1	Catalyst synthesis	108
5.5.2	Soluble polymer supported catalyst – application	110
5.5.3	Conclusions	111
5.6	Immobilization of the catalyst on inorganic support	112
5.7	Silica gel supported catalyst – application	115
5.8	General Conclusions	116
	EXPERIMENTAL	118
	REFERENCES	172
	APPENDICES	182

LITERATURE PART

Introduction

In view of an increasing demand for affordable enantiomerically pure compounds, preparation of organic molecules in an enantioselective way, under catalytic reaction conditions, is becoming a key technology.¹ The field of asymmetric catalysis has been dominated for a long time by homogeneous catalysis as a result of high activities and selectivities obtained. However significant development of solid phase chemistry has resulted in the progress of heterogeneous catalysis.² The advantages of heterogeneous catalysis are as follows: easy separation, efficient recycling, minimization of the metal leaching (in the case of metal catalysed reactions), improved handling, and process control. In an ideal case the activity of a heterogeneous catalyst should be comparable to a homogeneous counterpart in combination with an easy and quantitative separation. Heterogeneous asymmetric catalysis can be divided into three major categories: application of immobilized homogeneous catalysts, catalysis on surfaces that are chiral themselves or modified with chiral modifiers, and diastereoselective reactions of chiral substrates promoted by an achiral catalyst. This review presents only the examples of application of heterogeneous catalysts derived from the homogeneous counterparts.

1 Immobilization of chiral homogeneous catalysts

Immobilization of a homogeneous catalyst can occur by covalent, or noncovalent attachment of the chiral ligand, the metal, or pre-assembled complex to the support.³ The choice of a suitable support is not trivial, as numerous problems can occur that influence the performance of the final catalyst. First, the optimal geometry of the catalyst can be disturbed by the support. Second, undesired interactions between the catalyst and the support can occur. Unsatisfactory stability of the linkage between the catalyst, and the support and accessibility of the active site of the catalyst should also be considered. Among the supports employed for immobilization of homogeneous catalysts, the most popular are organic polymers (soluble and insoluble), metal oxides, metal nano-particles, nanotubes, and dendrimers. This review covers chiral homogeneous catalyst covalently bonded to polymers, metal-nanoparticles, and metal oxides.

1.1 Immobilization of catalysts for metal catalysed reactions

1.1.1 Covalent immobilization on polymers

A successful application of polystyrene-based resins (PS) in peptide synthesis, developed by Merrifield in the 1960s, has evolved in the application of the polymers as

supports for homogeneous catalysts. Ready availability, mechanical robustness, chemical inertness, and facile functionalization makes polystyrene a very popular polymeric material used in heterogeneous catalysis.⁴ The polymer is usually prepared by copolymerization with active monomers such as chloromethylstyrene or bromomethylstyrene, which ensure an equal distribution of active sites within the polymer matrix.⁴ Various percentages of various cross-linking agents can be used to ensure different solvation properties, among which divinylbenzyl (DVB) is the most commonly used. Polystyrene-based resins containing 2% of the cross-linking agent are called microporous, and require solvent swelling for reagents to access internal functional group.⁵ This can be a problem when a highly polar solvent is to be used. The application of long and flexible cross-linkers can improve swelling properties as in the case of JandaJel (Figure 1 A).⁶ Also grafting of PS with poly(ethylene glycol) (PEG) dramatically increase resin compatibility with polar solvents. TentaGel and ArgoGel are two commercially available examples (Figure 1).⁷ Another way to overcome the problem of polar solvents is the use of macroporous resin, which contain 10-15% of cross linkers.⁸ These polymers do not undergo significant swelling and due to the permanent pore structure reagents simply fill the pores throughout the polymer beads, regardless of the reaction medium. However, macroporous resins can suffer from poor loading capacity and brittleness.

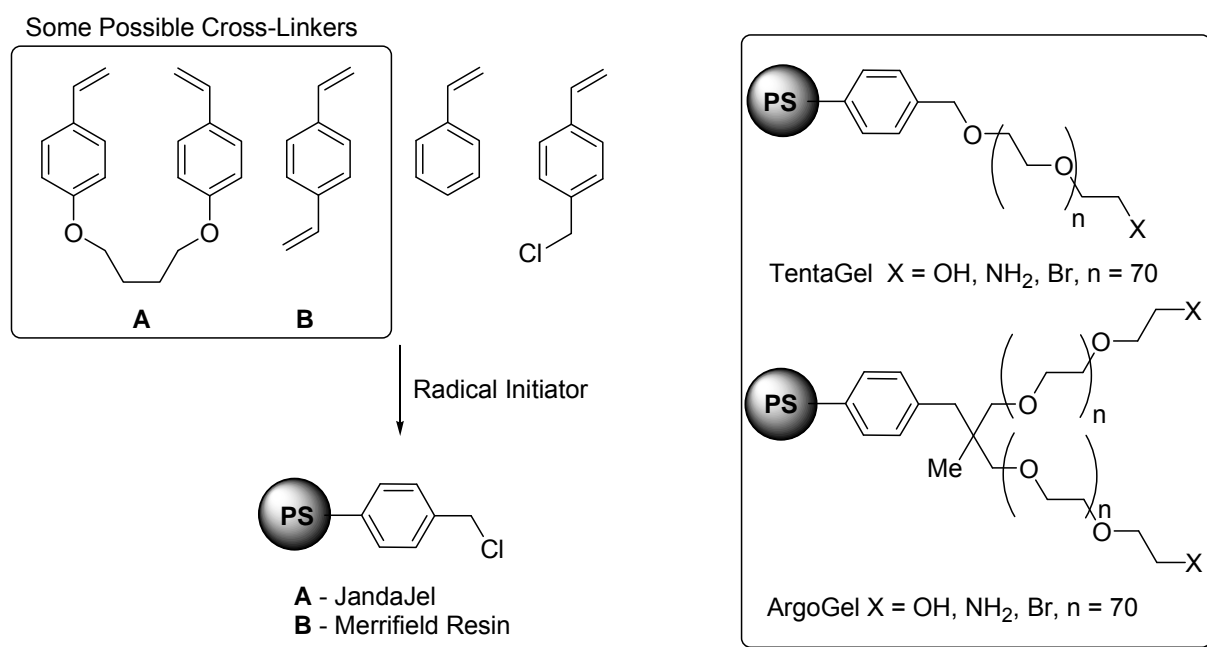


Figure 1. Examples of resins used for catalyst immobilization

Despite the well known advantages of the use of insoluble support, there are some disadvantages related to heterogeneous nature of the reaction conditions including: nonlinear kinetic behavior, an unequal distribution and access of the supported reagents (catalysts) to

the reaction partners from a solution, solvation problems, synthetic problems to transfer a homogeneous reaction to the solid phase.⁸ Therefore, alternative methodologies were developed in order to restore homogeneous reaction conditions. Replacement of an insoluble resin with a soluble polymer results in the reinstalling of classical organic chemistry reaction conditions, while the supported catalyst can still be easily separated (by precipitation, centrifugation, dialysis, or gel chromatography) due to its macromolecular properties.⁸ The most representative example of this class of polymers is poly(ethylene glycol) (PEG) also successfully used as support for chiral catalysts.⁸

Due to the successful application in many asymmetric transformations, BINAP has often been used for investigation of new immobilization techniques.

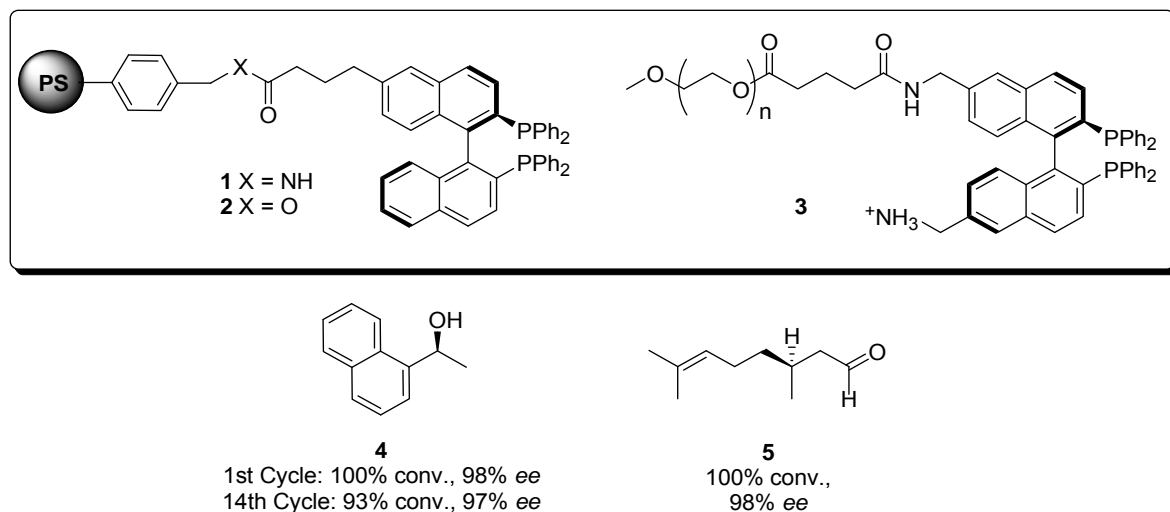


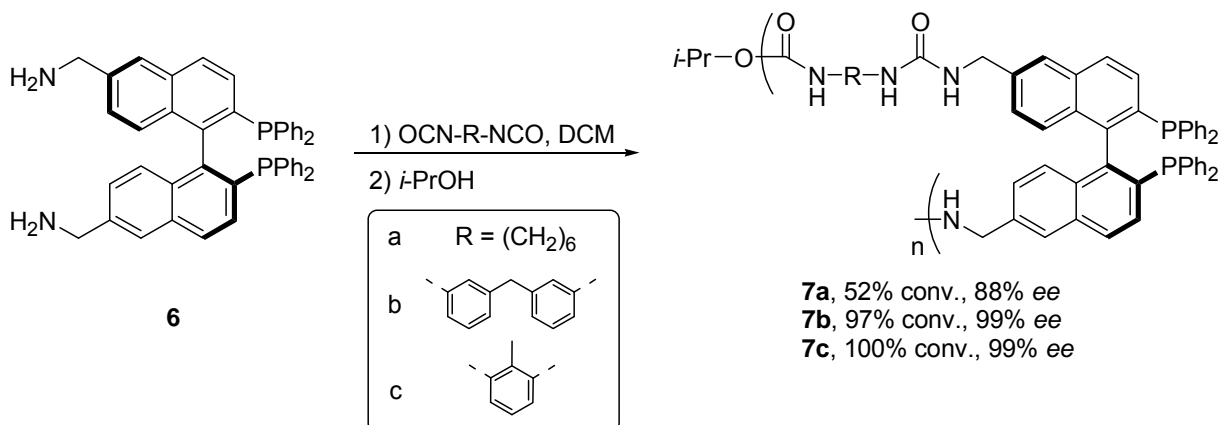
Figure. 2 Examples of polymer supported BINAP

Bayston reported on the use of PS-supported BINAP **1** (Figure 2) in the ruthenium-catalysed hydrogenation of β-ketoesters.⁹ In a model reaction, hydrogenation of methylpropionyl acetate, resulted in the formation of the corresponding β-hydroxy ester with excellent yield (99%) and enantioselectivity (97% ee). The application of BINAP anchored to a soluble polymer (**3**) (Figure 2), gave nearly identical results (99%, 99% ee) and in addition, the recycled catalysts retained high activity over four cycles.¹⁰ The application of the polymer-supported BINAP **1** in the ruthenium catalysed hydrogenation of ketones was also investigated by Noyori.¹¹ For example, reduction of acetophenone afforded alcohol **4** (Figure 2) in excellent enantioselectivities in total of 14 experiments.

Polymer-supported BINAP **2** (Figure 2) is commercially available, and has been successfully applied to many reactions such as the palladium-catalysed Mukaiyama-aldol reaction and the asymmetric Mannich reaction.¹² In the industrially important isomerization of (E)-diethylgeranylamine to citronellal **5** (Figure 2), catalyst **2** afforded the product with

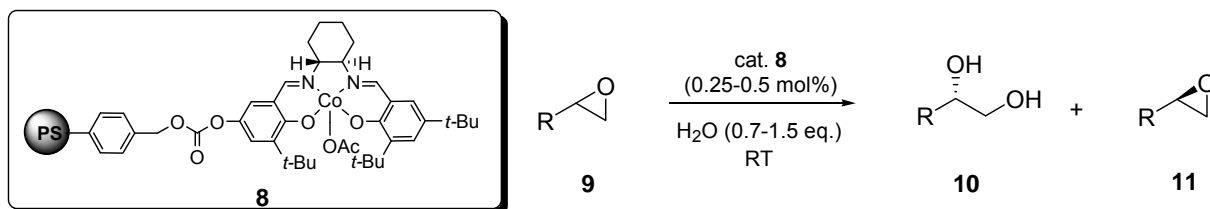
excellent yield and selectivity (100% conversion, 98% ee) was recovered by simple filtration and could be reused up to 37 times.¹³

Lemaire prepared solid-supported BINAP by co-polymerization of 6,6'-diaminomethyl-binap **6** (Scheme 1) with various diisocyanates¹⁴ and found an increase in enantioselectivities in ruthenium-catalysed asymmetric hydrogenation of methyl acetoacetate as the rigidity of the linker moiety increased. Polymer **7** was recycled three times without loss of activity.



Scheme 1. Immobilization of 6,6'-diaminomethyl-binap by copolymerization with diisocyanates

Immobilization of another privileged ligand was reported by Jacobsen: his chiral [Co(salen)] complex was attached to polystyrene through a carbonate linker.¹⁵



Scheme 2. Kinetic resolution with immobilized [Co(salen)] complex **8**

The heterogeneous catalyst **8** was tested in kinetic hydrolytic resolution of epoxides (Scheme 2) and the results are shown in Table 1. The recycled catalyst was re-used up to five cycles without the loss of activity.¹⁵

Table 1. Kinetic resolution of epoxides **9** with **8**

R	Yield of 10 (conversion) [%]	<i>ee</i> (S)- 10 [%]	<i>ee</i> (R)- 11 [%]
-CH ₂ Cl	41 (51-52)	92-95 ^a	>99 ^a
-CH ₂ Br	94 ^b	96 ^a	-
-(CH ₂) ₂ OH	36 (40)	94 ^a	59 ^a

a-Results over 5 cycles, b-Dynamic kinetic resolution of epibromohydrin

In addition, catalyst **8** was successfully applied to epoxide opening by phenols with up to 99% ee.¹⁶

The influence of the support in epoxidation of olefins catalysed by [Mn(salen)] complexes was investigated by Janda.¹⁷ In the reaction of styrene with *m*-CPBA in the presence of NMO, moderate, but comparable to homogeneous salen complex **12** (Figure 3), enantioselectivities were obtained with catalysts anchored to soluble resins, PEG **13** and NCPS **14** (non-cross-linked polystyrene, Figure 3). The application of insoluble JandJel polymer with flexible cross-linkers afforded analogous results, whereas some loss of enantioselectivity was observed with Merrifield resin.

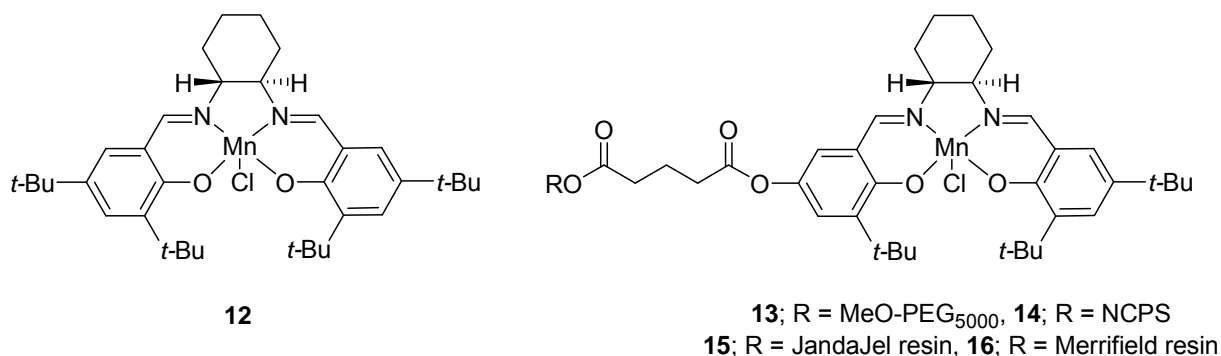


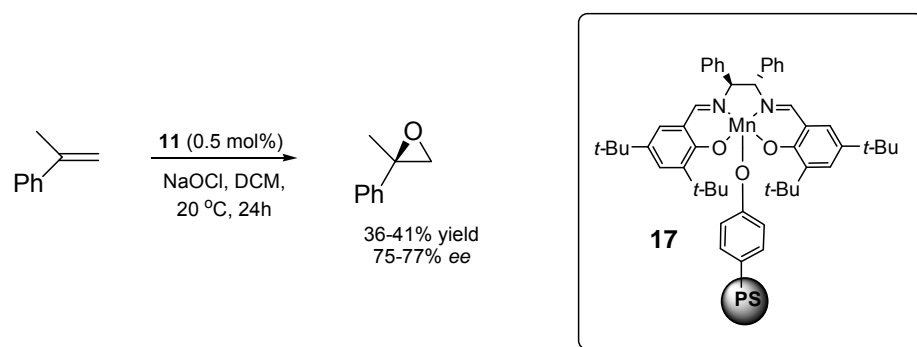
Figure 3. Examples of immobilized [(Mn)salen] complexes

Higher enantioselectivities were observed when *cis*- β -methylstyrene was used as a substrate with almost similar effect of the support. Due to catalysts degradation in all cases supported catalysts could be reused only once without the loss of activity.¹⁷

Table 2. Asymmetric epoxydation of olefins in the presence of **12-16**.

Catalyst	styrene		<i>cis</i> - β -methylstyrene	
	ee (%)	yield (%)	ee (%)	yield (%)
12	57	84	88	82
13	52	82	88	79
14	51	76	90	79
15	51	81	88	77
16	35	61	86	75

Recycling of immobilized [Mn(salen)] complexes has often proved to be a problem owing to the complex instability under the reaction conditions.

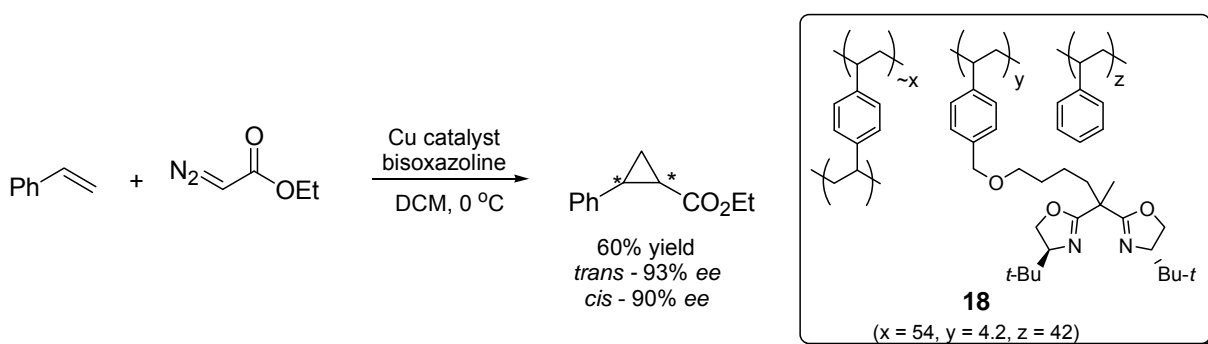


Scheme 3. Epoxidation of an unfunctionalized olefin in the presence of **17**

However, Li¹⁸ was able to immobilize [Mn-(salen)] complex by binding it axially to the phenoxy ligand on highly cross linked PS. The resulting catalyst **17** could then be reused up to three times without loss of activity in epoxidation of olefins (Scheme 3).

Chiral bisoxazolines have been successfully used in many metal-catalysed reactions¹⁹; however, due to a high catalyst loading (up 10 mol%) an efficient recycling method was desired.

Salvadori^{20a} reported on the use of highly cross-linked (ca. 54%) heterogeneous ligand **18** in the copper-catalysed cyclopropanation of styrene (Scheme 4). The catalyst exhibits activity comparable to its homogeneous counterpart even though the C_2 -symmetry was lost upon the attachment to a support.



Scheme 4. Copper catalyzed cyclopropanation of styrene in the presence of **18**

Immobilization of bis(oxazolines) on a soluble polymer was reported by Glos and Reiser.^{20b} Catalyst **19** (Figure 4) was tested in copper-catalysed cyclopropanation of 1,1-diphenylethylene, and found to afford the product in 78% yield and with 90% enantioselectivity. Analogous transformation in the presence of the catalyst anchored to an insoluble polymer afforded the cyclopropane product in 49% yield and 56% ee. In addition, catalyst **19** was reused in 9 cycles, exhibiting identical activity.

Another example of PEG-supported bis(oxazoline) was reported by Cozzi.²¹ Catalyst **20** (Figure 4) exhibited high level of activity and enantioselectivity in asymmetric cyclopropanation and ene reaction, whereas significantly worse results were obtained for the Diels-Alder (D-A) reaction (*endo*, ≤45% ee) compared to the homogenous counterpart.

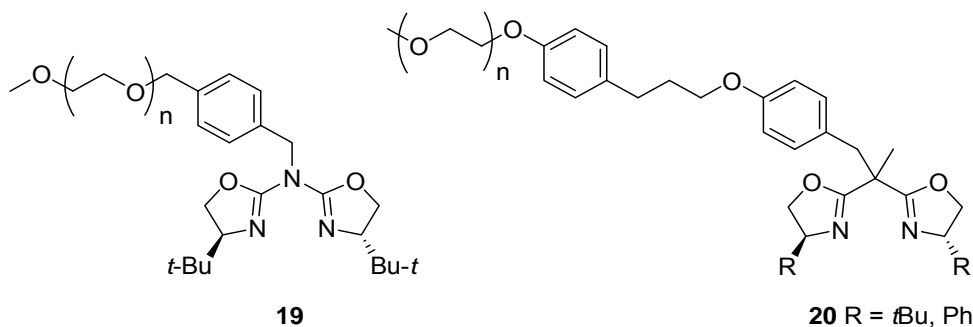


Figure 4. Examples of PEG supported bis(oxazolines)

To eliminate the possible factors responsible for low asymmetric inductions in D-A reaction, control experiments were performed. However, the possibility of the oxygen atoms of the polymer chain to coordinating copper, the loss of C_2 -symmetry, and the presence of inorganic impurities were all excluded. The real reason(s) remained unknown.

Itsuno²² reported on the synthesis of solid-supported chiral oxazaborolidinones as catalysts for D-A reaction. Two synthetic options were investigated, namely grafting of L-valine to polystyrene (**21**) and a co-polymerization of the amino acid moiety **22** with styrene and various cross-linkers (Figure 5). In the addition of methacrolein to cyclopentadiene, the catalysts derived from monomer **22** and cross linker **23** afforded the *exo* product (96:4) in 95% ee, whereas its polystyrene-supported analogue exhibited much lower enantioselectivity (99:1, 60% ee).

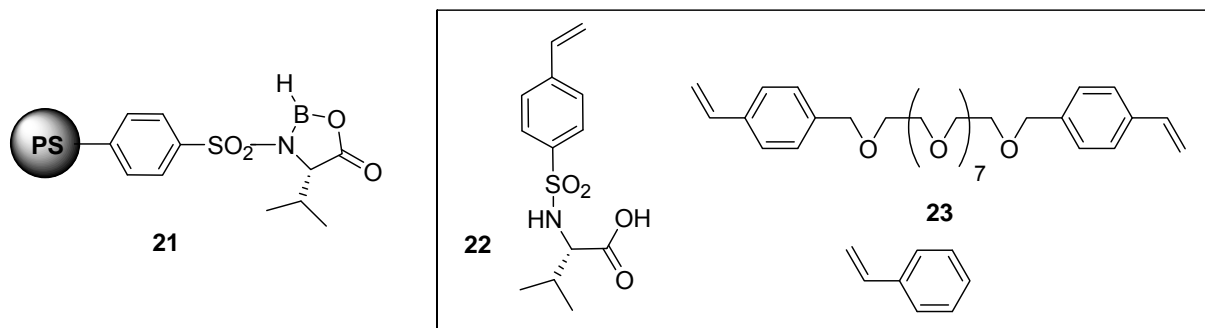


Figure 5. Catalysts for asymmetric D-A reaction developed by Itsuno

It is believed that the presence of more flexible cross linking agent **23** is crucial for higher enantioselectivities obtained. The champion catalyst could be recycled multiple times and used in a flow reactor, although the use of such a highly swelling resins is not recommended for continuous flow processes²².

Polystyrene-supported metal complexes of TADDOLates were also intensively tested as potential catalysts for the D-A reaction,²³ however, in all cases the enantioselectivities were poor and did not exceed ~ 50% ee.

Chiral amino alcohols immobilized on polymers were reported as useful catalysts for the asymmetric addition of diethylzinc to aldehydes. Itsuno and Frechet supported the amino-isoborneol moiety on DVB cross-linked PS (cat. **24**, Figure 6) and in the model reaction, addition of diethyl zinc to benzaldehyde produced the corresponding alcohol in 91% yield and 92% ee.²⁴ The immobilization of (-)-ephedrine reported by Soai²⁵ afforded the highly stereoselective catalyst **25** (89% ee, Figure 6) however, attempted application of **25** beyond benzaldehyde failed. The same group presented an interesting example of the spacer effect.²⁶ The use of one-carbon linker between the polymer and the amino-alcohol moiety, as in the case of **26a**, afforded the product of diethylzinc addition to benzaldehyde in 24% ee, whereas

extension of the linker to six carbon atoms (cat. **26b**, Figure 6) improved the results to 61% ee.

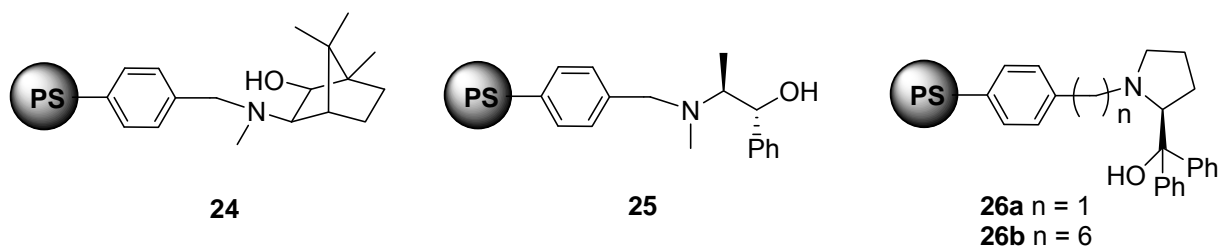


Figure 6. Examples of polymer supported chiral amino alcohols

The addition of diethylzinc to aldehydes catalysed by polymer supported cyclo-BINOL **27** (Figure 7) was reported by Lipshutz.²⁷ Excellent enantioselectivities (84-96%), higher than for homogeneous BINOL, were observed in the case of benzaldehyde and a broad range of its substituted derivatives. The catalyst was reused up to 4 cycles without loss of activity.

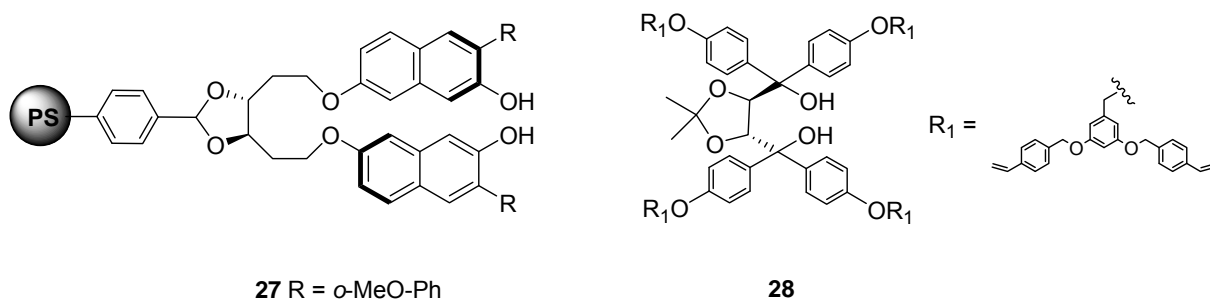


Figure 7. Polymer supported BINOL and TADDOL

Polymer-bound *di*isopropoxy-Ti-TADDOLate catalyst prepared by co-polymerization of monomer **28** (Figure 7) with styrene was reported by Seebach.²⁸ It was found that high enantiomeric excess was induced in the addition of diethylzinc to benzaldehyde (96% ee) and the catalyst retained full activity over 20 cycles.

The first example of osmium-catalysed asymmetric dihydroxylation using a polymer-bound alkaloid was reported by Sharpless.²⁹ In the presence of insoluble polyacrylonitrile-supported dihydroquinidine (DHQD) **29** (Figure 8) and NMO as a stoichiometric oxidant, *trans*-stilbene was transformed into the corresponding diol in 87% chemical and 82% ee. Using analogous reaction conditions and DHQD anchored to soluble PEG (cat. **30**, Figure 8), Janda³⁰ reported an improvement of the results. The enantiomerically enriched product was obtained in 88% ee, which corresponds to the results obtained with the homogeneous catalyst.³⁰ Moreover, catalyst **30** retained full activity over five cycles. Further modification of the reaction conditions and the catalyst structure allowed the product formation in 99% ee³¹. In the improved procedure, the soluble catalyst **31** (Figure 8) was used in the presence of K₃Fe(CN)₆ as a stoichiometric oxidant. Catalyst **31** was recycled six times without any loss of activity.

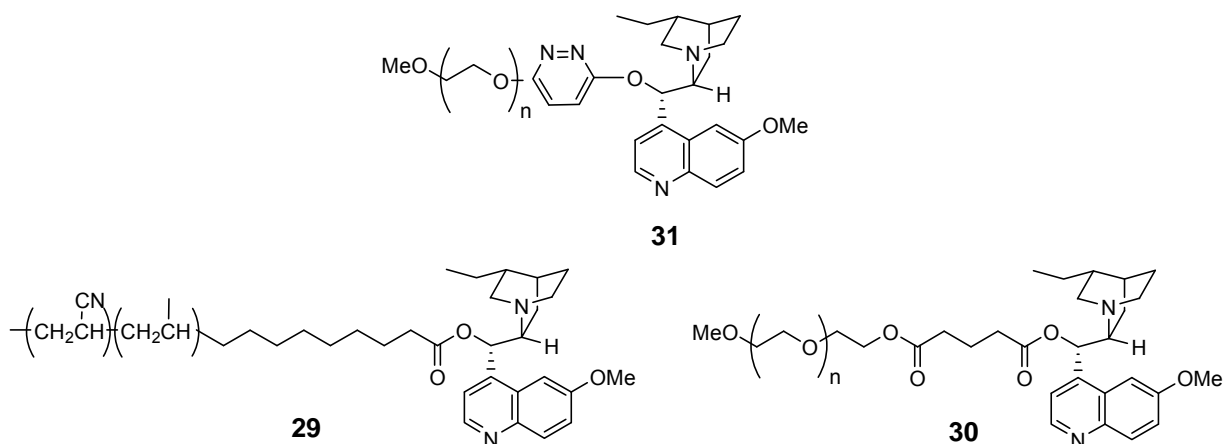
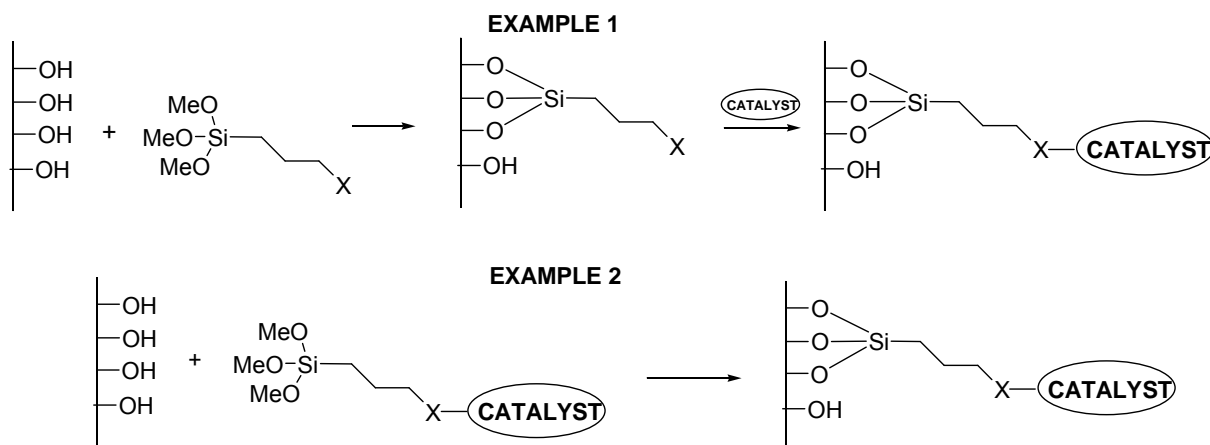


Figure 8. Polymer supported ligands for asymmetric dihydroxylation

1.1.2 Covalent immobilization on an inorganic support

1.1.2.1 Covalent immobilization on metal oxides

The application of inorganic materials as support for heterogeneous catalysts offers a number of benefits: their rigid structure does not allow the aggregation of active catalysts, they do not swell, and they are insoluble in organic solvent.³² The lack of swelling properties and the insolubility in organic solvents make them an interesting material for the use in a continuous process. In addition, inorganic materials possess high thermal and mechanical stability.



Scheme 5. Immobilization of catalysts on silicon based supports

The most popular inorganic supports used in heterogeneous catalysis are silicon-based materials. Prominent examples are as follows:³ synthetic amorphous silica, silica gel, nonporous silica (e.g., cabosil), and mesoporous materials, characterized by high surface area and easily accessible pores, such as MCM-41, MCM-48, Grace 332, USY, SBA15. There are two commonly used ways of functionalization of these supports. First, the linker can be attached to the surface through a silanol moiety, followed by the attachment of catalyst³

(example 1, Scheme 5), second, a pre-synthesized catalyst-linker building block is directly attached to the support³ (example 2).

Tu³³ reported the successful immobilization of TsDPEN **32** (Figure 9) on different inorganic supports namely, amorphous silica gel (cat. **33**), mesoporous silicas of MCM-41 (cat. **34**) and SBA-15 (cat. **35**). Heterogeneous catalysts were tested in the ruthenium-catalysed transfer hydrogenation of acetophenone, as a model reaction, which afforded the corresponding alcohols in excellent enantioselectivities (96-97%) and conversions >99% regardless of the support. The silica gel supported catalyst **33** could be used in 1000:1 s/c ration and was reused 10 times without the loss of activity.

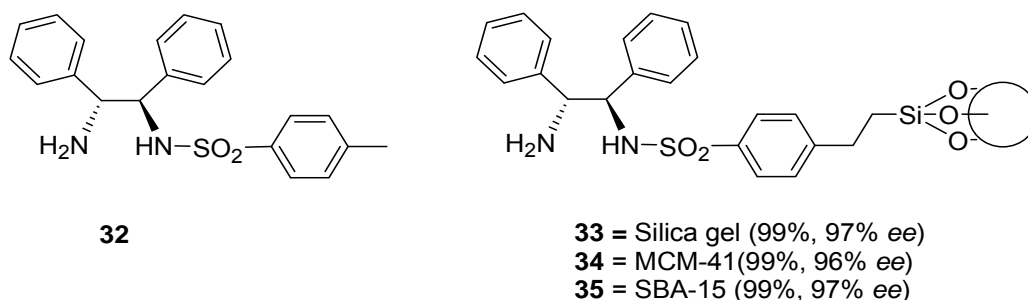
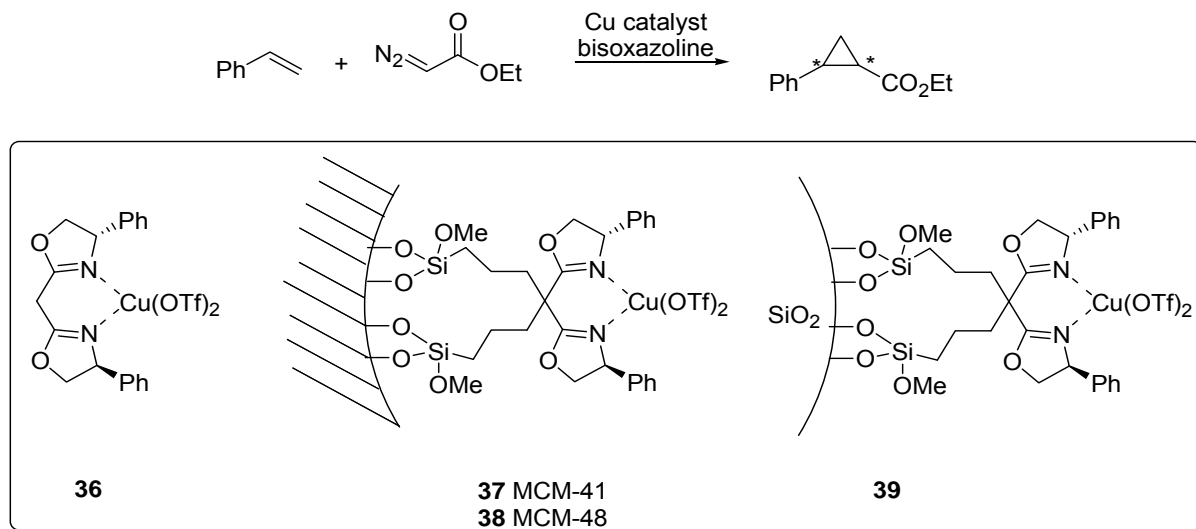


Figure 9. Immobilization of TsDPEN on inorganic support

Copper bis(oxazoline) complexes immobilized on MCM-41 and MCM-48 as catalysts for cyclopropanation of olefins were reported by Shannon (Scheme 6).³⁴



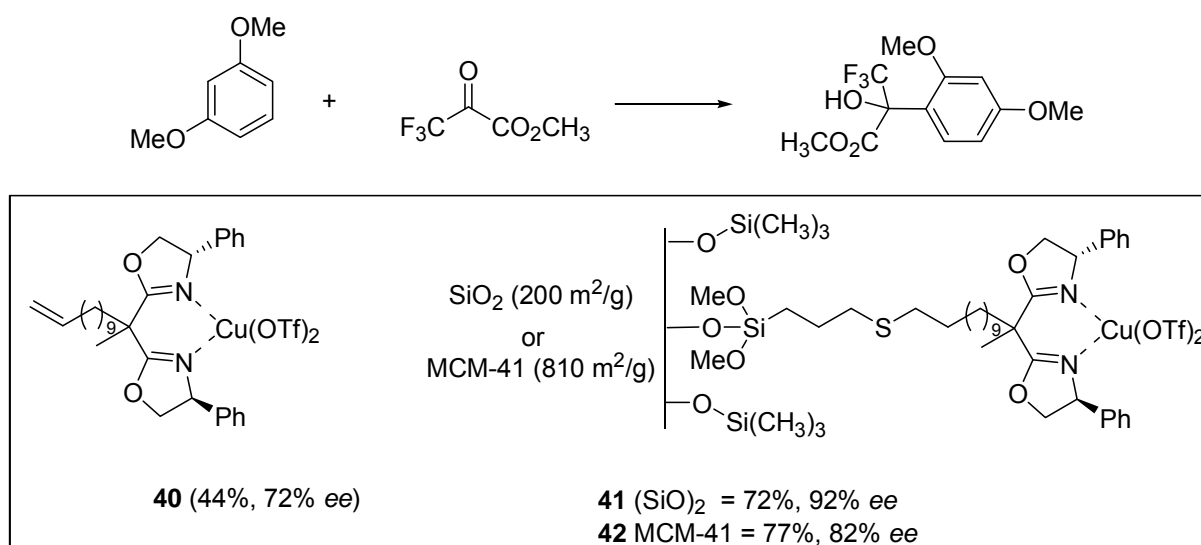
Scheme 6. Copper catalyzed cyclopropanation of styrene in the presence of **36-39**

In the reaction of styrene with diazoacetate, moderate yields and enantioselectivities were obtained (Table 3). However, these results were comparable to the application of homogeneous catalyst **36**. The use of regenerated **37** and **38** resulted in the formation of the product of comparable enantiopurity.³⁴ The immobilization of the copper bis(oxazoline) complex on the surface of silica gel reported by Mayoral³⁵ afforded the less selective catalyst **39**.

Table 3. Copper catalysed asymmetric cyclopropanation of styrene in the presence of **36-39**

Catalyst	Run	Yield [%]	<i>trans/cis</i>	ee (<i>cis</i>) [%]	ee (<i>trans</i>) [%]
36	-	46	2.05	49	58
37	1	39	1.89	48	54
	2	24	1.80	48	52
38	1	47	1.95	46	51
	2	47	1.78	42	45
39	1	24	1.63	32	33

Another example of immobilization of copper bis(oxazoline) complexes was presented by Corma.³⁶ The catalyst was anchored to the surface of amorphous silica and MCM-41, following standard procedure; however, in addition, the remaining hydroxyl functionalities were deactivated using hexamethyldisilazane. Heterogeneous catalysts **41** and **42** were then tested in the enantioselective Friedel-Crafts hydroxyalkylation of 1,3-dimethoxybenzene with 3,3,3-trifluoropyruvate (Scheme 7).³⁶



Scheme 7. Friedel-Crafts hydroxylation catalyzed by **40-42**

In all cases the product was formed with high selectivity however surprisingly, the heterogeneous catalysts were more active and enantioselective than the homogeneous precursor **40**. However, this issue was not explained by the authors. The difference between the performance of the catalyst immobilized on silica and MCM-41 was explained by the incompletely deactivated hydroxyl groups on the surface of MCM-41.

The copper bis(oxazoline) complexes anchored to a mesoporous silica (Figure 10) were also applied in D-A reaction.^{37, 38}

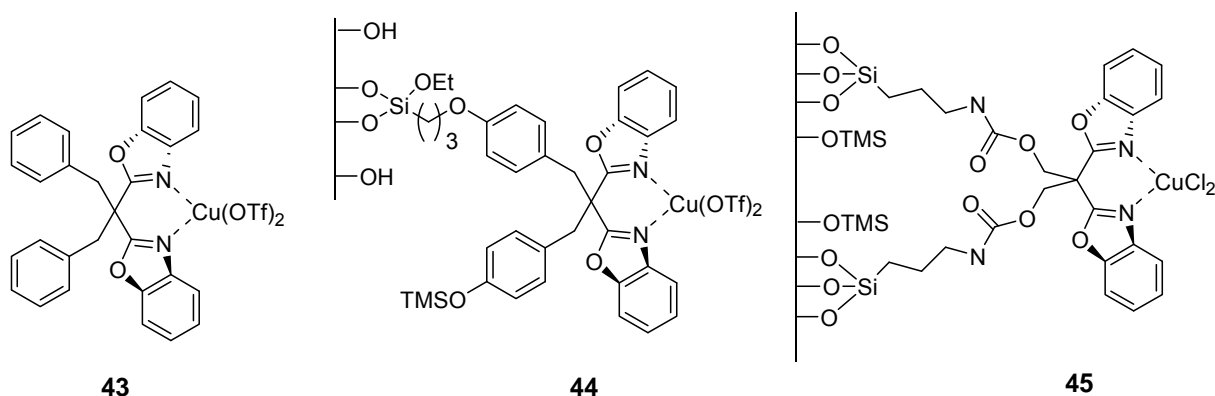
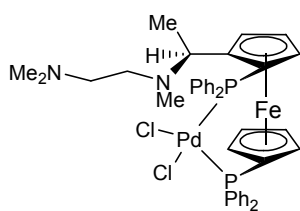


Figure 10. The copper bis(oxazoline) complexes anchored to a mesoporous silica

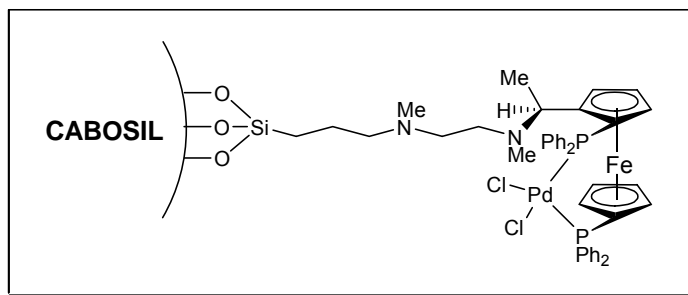
Kim³⁷ reported the addition of 3-(2-propenoyl)-2-oxazolidinone to cyclopentadiene in the presence of catalyst **44** (Figure 10). The product was formed in excellent yield (99%), high selectivity (*endo/exo* 17:1) and enantioselectivity (78% ee). In comparison with the results obtained with the parent homogeneous catalyst **43**, the enantioselectivity decreased by about 10% but the selectivity increased (9:1). The attempt to improve the performance of heterogeneous catalysts by deactivation of free hydroxyl groups of the support surface with hexamethyldisiloxane failed. In the experiment with a subsequent reuse of the catalyst, a gradual decrease in enantioselectivity was observed after each run.³⁷

The immobilization of an analogous catalyst on the surface of silica was reported simultaneously by Lemaire.³⁸ However, in the previously described reaction, the new catalyst **45** (Figure 10) exhibited higher enantioselectivity (up to 92%), and could be reused at least 4 times. The improved reusability stems from the application of a new catalyst precursor, $\text{Cu}(\text{ClO}_4)_2$ – (Lemaire’s work) versus $\text{Cu}(\text{OTf})_2$ – (Kim’s work). However the improvement of enantioselectivity is not clearly understood. In sharp contrast to Kim’s work, Lemaire reported the influence of free hydroxyl groups of the support surface on the enantioselectivities. It was crucial to deactivate hydroxyl functionalities from the support with *N*-trimethylsilylimidazole prior to the catalyst use, otherwise enantioselectivity decreased to 65%.

The immobilization of the catalyst on mesoporous materials can occur on the surface or inside the pore of the support. Selective immobilization of the catalyst inside the pore can improve catalyst’s selectivity either by restriction of its conformation³⁹ or by the restriction of substrate access.⁴⁰ Johnson⁴¹ reported on a comparison of results from the asymmetric allylic amination catalysed by Pd-dppf complex immobilized on the non-porous silica (cabosil) (cat. **47**, Figure 11) and inside the pore of MCM-41 (cat. **48**, Figure 12).



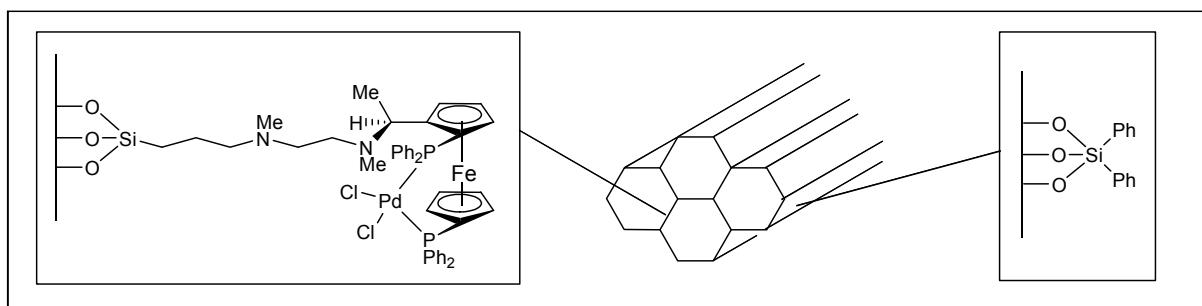
46



47

Figure 11. Pd-dppf complex immobilized on the non-porous silica (cabosil)

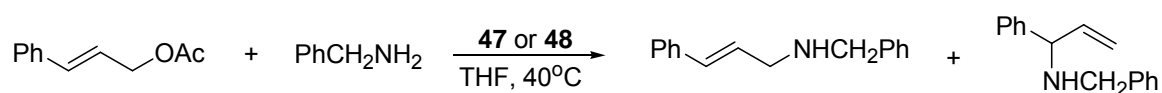
The anchoring of catalyst to the surface of cabosil was performed using a standard protocol but great care was taken to attach Pd-complex only to the inner walls of MCM-41; to this end, the outer walls were functionalized with bulky silylating agent prior to the attachment of the catalyst.



48

Figure 12. Pd-dppf complex immobilized inside the pore of MCM-41

In a model reaction, substitution cinnamyl acetate with benzylamine (Scheme 8), the catalyst immobilized on silica afforded mainly, the less favorable, straight chain product, with just a tiny amount of the enantimerically enriched branched amine. These results were comparable to the application of the homogeneous catalyst **46**. However, when the catalyst **48** was used in this reaction, the branched product was formed in an enantiomerically pure form in 50% yield, which indicated that the control exercised by MCM-41 on the activity of the ferrocenyl catalyst is considerable.



Scheme 8. Substitution of cinnamyl acetate with benzylamine in the presence of **47** or **48**

Similar phenomenon was observed by Thomas in the ruthenium catalysed asymmetric hydrogenation of phenylcinnamic acid.⁴⁰

Catalytic activity of chiral salen complex immobilized on MCM-41 was investigated by Kim.⁴² In the presence of complex **49** (Figure 12), the product of styrene epoxidation was

obtained in 65% ee. This result is comparable to the application of the polymer-supported catalysts **13-15** (Table 2). Further modification of the structure afforded more selective catalyst **50** and improved the enantioselectivity of epoxidation to 89%.

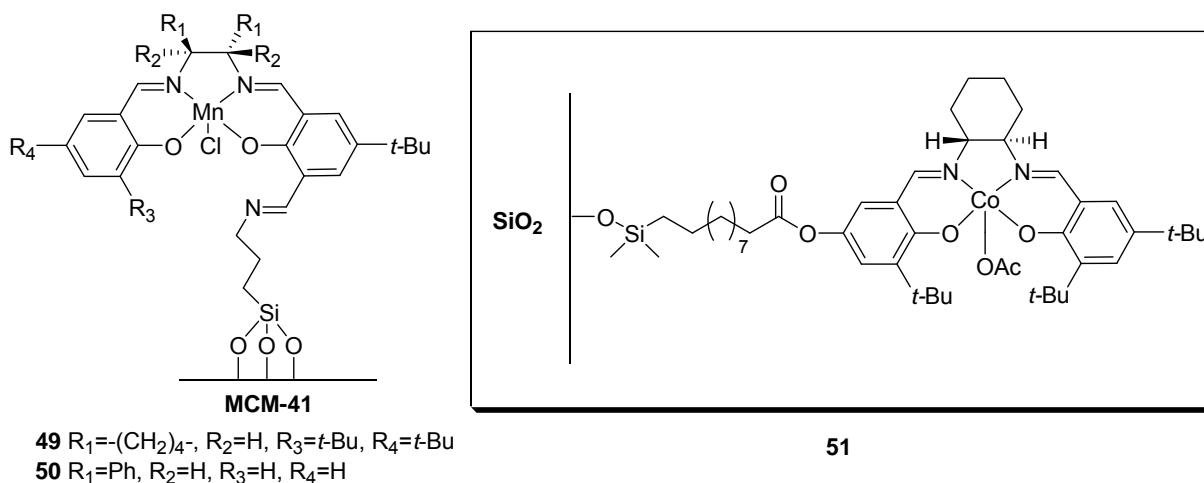


Figure 13. MCM-41 and silica gel-supported Co-salen complex

Silica gel-supported Co-salen complex was reported by Jacobsen.¹⁵ The catalyst was tested in the kinetic resolution of epoxides, giving the results comparable to polymer supported salen complex **8** (Table 1, Scheme 2). In addition, **51** was applied as a stationary phase in a continuous flow reactor¹⁵.

The use of silica gel supported *bis*-cinchona alkaloid as the catalyst of Sharpless asymmetric dihydroxylation was reported by Song.⁴³ When *trans*-stilbene was used as substrate in the presence of **52** (Figure 14), osmium tetroxide, and K₃Fe(CN)₆ as the stoichiometric oxidant, the corresponding enantiopure diol (>99% ee) was obtained in 88% yield. This result is analogous to the application of soluble polymer supported catalyst **31**. Moreover, the silica gel supported alkaloid **52** exhibited much greater binding ability for OsO₄ than its homogeneous analogue. For the best results, the reaction usually requires excess of the expensive alkaloid ligands to osmium. However, in the heterogeneous system, excellent ee was obtained with only an equimolar amount of ligand to osmium. The osmium complex with **52** was reused once in dihydroxylation of *trans*-stilbene giving the result comparable to the first run.

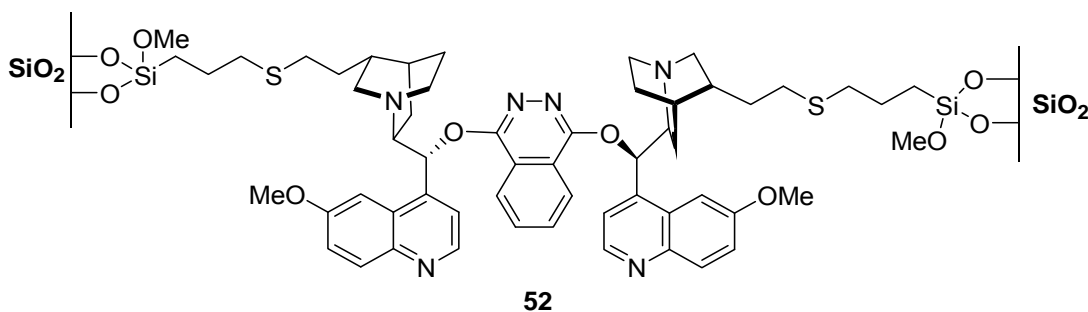


Figure 14. An example of silica gel supported catalyst for Sharpless asymmetric dihydroxylation

Lin⁴⁴ investigated the properties of the BINAP-derived heterogeneous catalyst **53** (Figure 15). The authors used SBA-15 as an inorganic support because of a very large pore size. As a result, the diffusion of substrate and products would be more facile. In the presence of 1 mol% of **53**, β -alkyl β -ketoesters were hydrogenated in complete conversion and e.e. values in a range of 96-98%. These values are comparable to those of parent homogeneous and polymer supported Ru(BINAP) catalysts (catalyst **1** and **3**). The hydrogenation of β -aryl β -ketoesters was carried out in the presence of 2 mol% of **53** and e.e. values in a range of 82-95% were obtained. These values are higher (by ca. 6%) than those afforded by the parent homogeneous Ru(BINAP)(DMF)₂Cl₂ catalyst, which agrees with the earlier observation of the positive influence of substituents in 4,4'-positions.⁴⁵ Comparison of the catalytic performance of **53** and that of the parent homogeneous Ru[4,4'-(1-cyclopentanol)₂BINAP](DMF)₂Cl₂ indicates some loss of enantiopurity in the reaction (by ca. 7%). Catalyst **53** could be recycled three times with full conversion and comparable ee values.

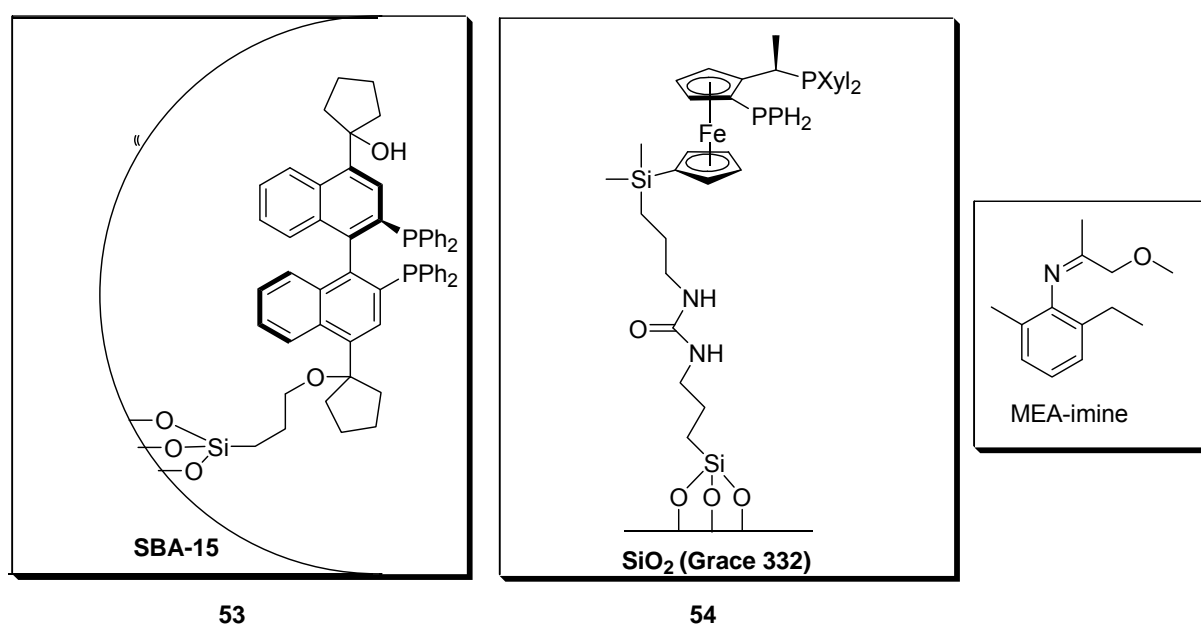


Figure 15. Examples of the catalysts immobilized on SBA-15 and silica Grace 332

An example of the catalyst supported on silica Grace 332 (cat. **54**, Figure 15) was reported by Blaser.⁴⁶

Table 4. Comparison of homogeneous and heterogeneous Ir-xyliphos systems

Catalyst	s/c	TOF [h ⁻¹]	<i>Ee</i> [%]
Ir-xyliphos	120000	55385	80
Ir-xyliphos-SiO ₂	120000	12000	78

Ir-xyliphos complex was immobilized, and tested as a heterogeneous catalyst in hydrogenation of sterically hindered MEA-imine (the importance of this process is described in chapter 4.3). Although a very good, and comparable to homogeneous system (Table 4)

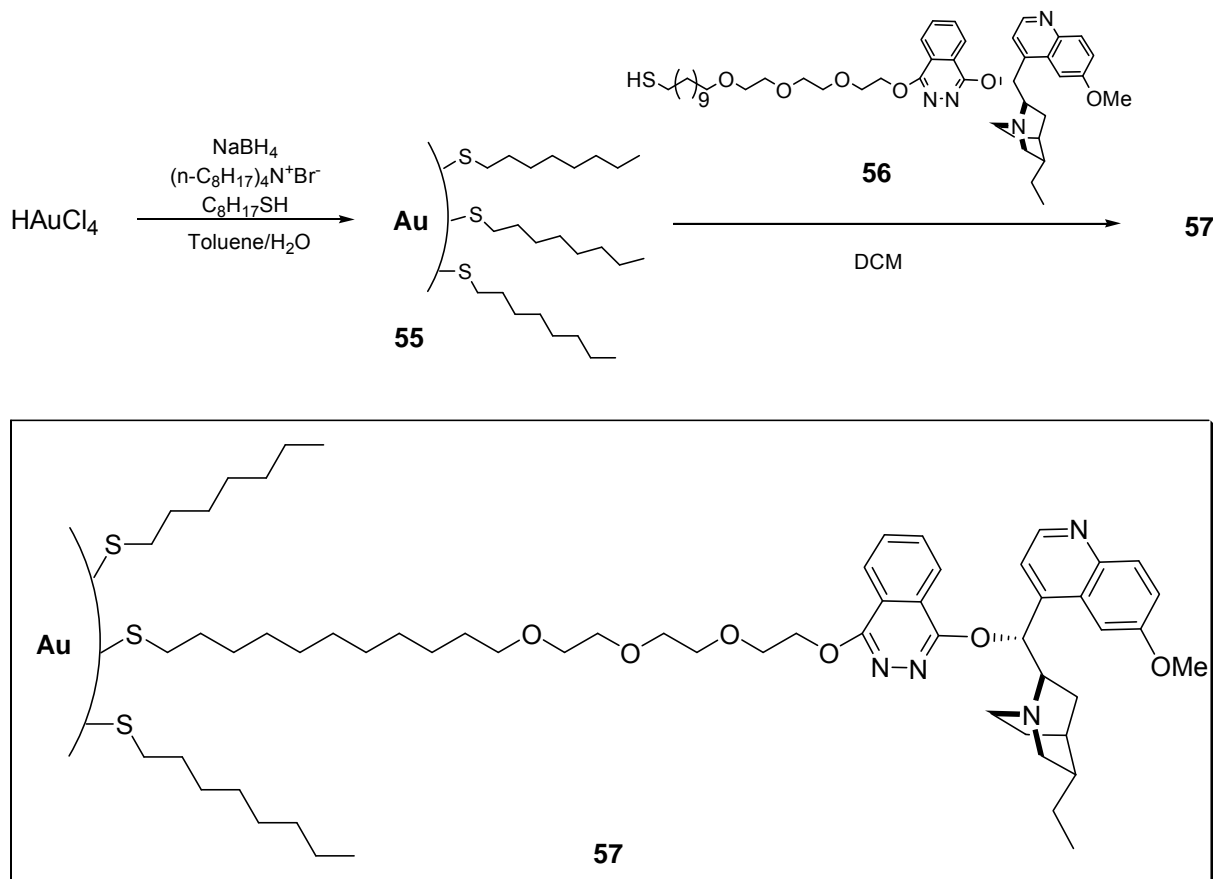
enantioselectivities were obtained, the TOF number for the heterogeneous catalyst was significantly lower. Moreover, because of fast deactivation of the heterogeneous catalyst, full conversion was never achievable, and re-use seems not to be possible.

1.1.2.2 Immobilization on metal nanoparticles

As it has already been shown, the attempt at immobilization of homogeneous catalyst on insoluble support can result in the loss of the catalytic activity due to the limited catalyst mobility. For example, the catalyst immobilized on the Merrifield resin is surrounded by the mass of the polymer and the catalytic site remains deep inside the polymer backbone. This can limit the access to the reaction partners, which would result in a substantial decrease in activity. It has also been shown that the use of soluble polymers can overcome those difficulties and restore the homogeneous reaction conditions. The reinstatement of homogeneous reaction conditions, combined with the benefits of heterogeneous catalysis, can also be achieved by the use of metal nanoparticles as a support for homogeneous catalysts. In this case, functionalized metal nanoparticles with appropriate surface coating can act as nearly homogeneous catalysts at the stage of reaction in one solvent while at the work-up stage they are aggregated in another solvent so that the catalyst can be separated from the product by simple filtration. If the catalyst is stable enough under the reaction conditions, it can be recovered and used again. Functionalized gold nanoparticles are structurally more ordered than polymers, hence the environment in which the catalyst is presented, is better defined and can be rationally modified. Moreover, owing to their small size, nanoparticles tend to have a very high surface area. Spherical nanoparticles of 10 nm diameter, for example, have a calculated surface area of $600 \text{ m}^2/\text{cm}^3$, which is comparable to that of many porous materials used for immobilization. Nanoparticles can thus be viewed as novel supports for the preparation of heterogenized asymmetric catalysts.

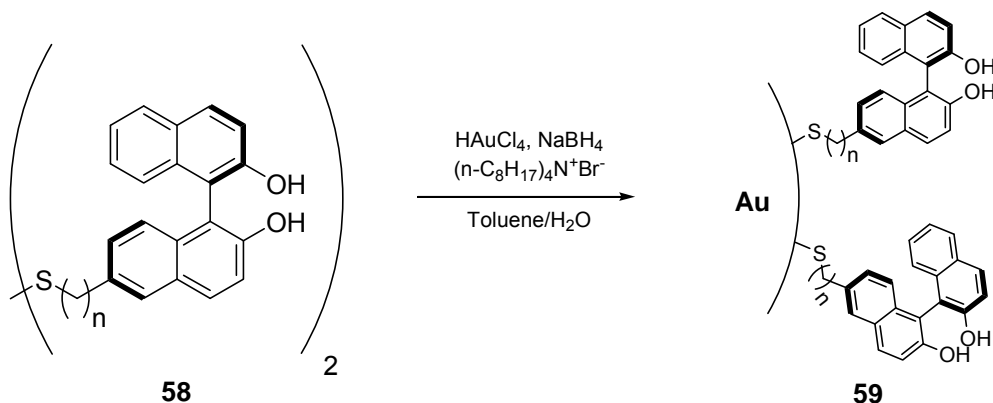
Markish⁴⁷ reported on the use of gold nanoparticles as a support for dihydroquinidine ligands. The key transformations of the reaction sequence is presented in Scheme 9. First, gold colloids modified with a monolayer of octanethiolate (**55**) were prepared from HAuCl_4 by organic-phase reduction with sodium borohydride in the presence of octanethiol. Treatment of gold colloids **55** with sulfur-containing ligand precursor **56** resulted in partial ligand exchange and the formation of **57**. Gold nanoparticles functionalized with dihydroquinidine ligands were then tested in the osmium-catalysed asymmetric dihydroxylation of olefins. When *trans*-styrene was used a substrate, the corresponding diol was obtained in 90% enantioselectivity, a result comparable to the application of soluble

polymer supported catalyst **30** (88% ee) Catalyst **57** was re-used twice in dihydroxylation of β -methylstyrene but after each run some loss of enantiopurity was observed, namely: 90% ee, 86% and 79% after the third run.



Scheme 9. Immobilization of dihydroquinidine on the surface of gold nanoparticles

Sasai⁴⁸ reported on the use of gold nanoparticles for immobilization of BINOL. In the synthetic approach presented in Scheme 10, monolayer-protected Au clusters bearing BINOL moieties (**59a-c**) were prepared by treatment of HAuCl_4 with sodium borohydride in the presence of disulfides **58a-c**. This approach allowed a coating of gold nanoparticles with alkyl chains and the introduction of the ligand in a one pot reaction.



Scheme 10. Immobilization of BINOL on gold nanoparticles

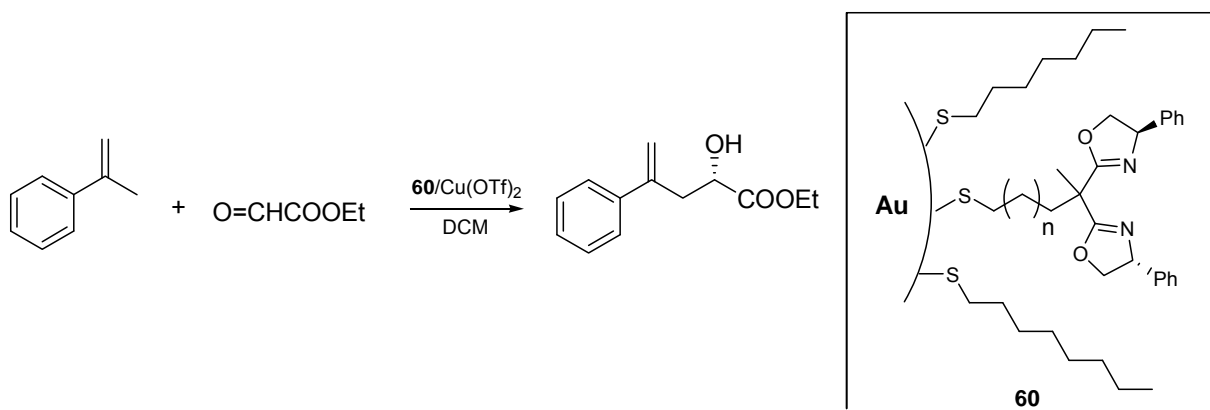
The catalytic activity of these new ligands was investigated in the addition of diethyl zinc to benzaldehyde in the presence of titanium *iso*-propoxide. The results are summarized in Table 5.

Table 5. Asymmetric addition of diethyl zinc to benzaldehyde in the presence of **59a-c**.

MPC	n	yield [%]	ee [%]
59a (10 mol%)	4	92	80
59b (10 mol%)	5	98	86
59c (10 mol%)	6	95	72
59b (5 mol%)	5	95	84

At 10 mol% loading, all Au-MPC-supported catalysts showed excellent reactivity, producing the corresponding alcohols in high yield and good enantioselectivity. The authors noticed the influence of the spacer length on the enantioselectivities obtained and 5 carbons linker appeared to be optimal. The catalyst amount could be decreased to 5 mol% without the loss of activity. Notably, the activity of heterogeneous Au-MPC catalysts was comparable to those of homogeneous parent Ti-BINOLate complexes. No attempts of subsequent re-use of the new catalysts was reported.

Preparation of reusable nano-sized chiral bisoxazolines catalysts was reported by Kanemasa.⁴⁹ New catalysts were tested in the copper-catalysed ene reaction between 2-phenyl-propene and ethyl glyoxalate (Scheme 11). The reaction was carried out in dichloromethane as it is a solvent in which nanoparticles-supported catalysts **60** are highly soluble. After completion of the reaction, the addition of hexane resulted in aggregation of the supported catalyst, which was separated from the product by centrifugation.



Scheme 11. Copper-catalysed ene reaction in the presence of gold nanoparticles supported bis(oxazolines) **60**

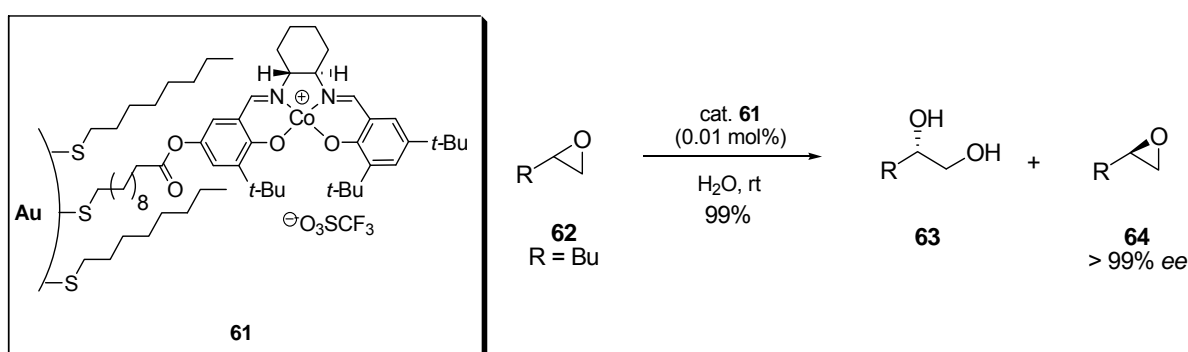
The recovered catalyst was used in the next transformations without purification and the results are summarized in Table 6.

Table 6. Copper catalysed ene reaction in the presence of **60**.

Catalyst	60a (n = 2)	60b (n = 4)	60c (n = 6)	60d (n = 8)
run	yield (ee)	yield (ee)	yield (ee)	yield (ee)
1	99 (86)	95 (85)	97 (85)	93 (85)
2	99 (84)	98 (86)	90 (86)	80 (85)
3	94 (85)	73 (85)	55 (84)	39 (86)
4	92 (86)	-	-	-

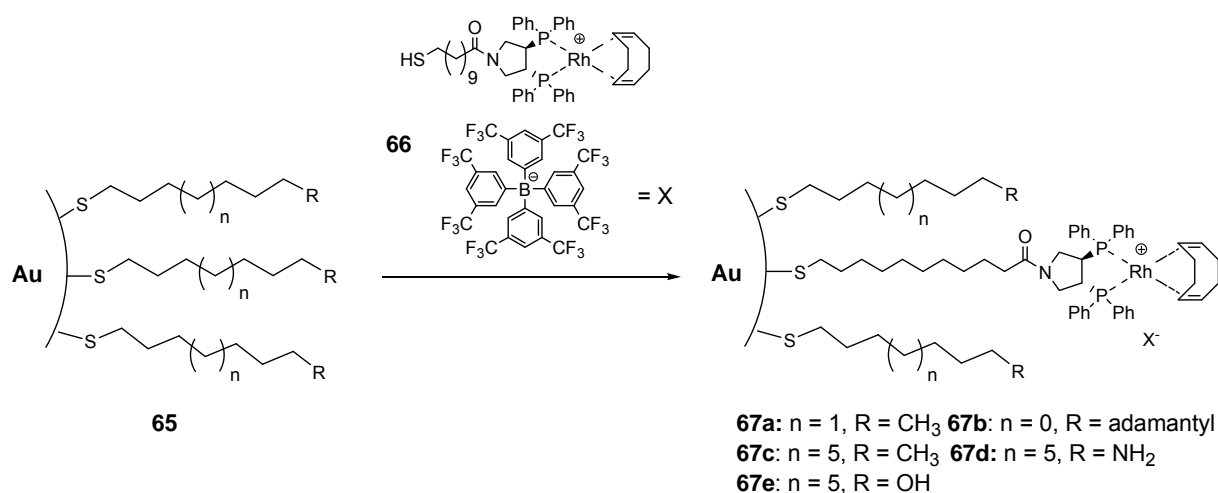
The best results were obtained with the copper(II) complex derived from **60a**. Although it is not indicated in Table 6, with **60a**, the reactions were completed two times faster than in the case of **60b-d**. According to the authors, the copper complex of **60a** showed the highest dispersion, and hence minimized aggregation in dichloromethane solution, as the complex parts are buried in an array of neighboring hexanethiol ligands. However, highly dispersed in dichloromethane, the copper complex of **60a** shows the effective aggregation in hexane forming large-sized particles which could be separable. This indicated that the size of the spacer is essential to attain the optimised homogeneous reusable catalyst.

Chiral Salen-Co complex immobilized on gold colloids was reported by Jacobsen.⁵²

**Scheme 12.** Kinetic resolution with immobilized [Co(salen)] complex **61**

In the kinetic resolution of hexane-1-oxide (Scheme 12), complete resolution was achieved within 5 h at 0.01 mol% catalyst loading. The catalyst was simply recovered after each transformation by centrifugation and was found to retain full activity over six cycles.

Rhodium-PHYRPHOS complex immobilized on gold colloids has been reported by Pfaltz.⁵³ A series of *n*-alkanethiolate-protected gold colloids **65** was treated with complex **66** to obtain Rh-PHYRPHOS-functionalized nanoparticles **67** (Scheme 13). The catalytic activity was tested using asymmetric hydrogenation of methyl α -acetamidocinnamate as a model reaction, and the results are summarized in Table 7.



Scheme 13. Immobilization of Rh-PHYRPHOS on gold nanoparticles

High enantioselectivities, comparable to homogeneous catalysts, were obtained with apolar colloids **67a-c**. Polar colloids **67d-e** with amino and hydroxy group terminal group proved to be less reactive and enantioselective.

Table 7. Hydrogenation of methyl α -acetamidocinnamate with functionalized gold colloids

colloid	spacer/[Rh]	conversion [%]	ee [%]
67a	1:3	>99 [>99]	93 [93]
67b	1:6	>99	93
67c	1:8	>99	93
67d	1:5	94	86
67e	1:6	32	82

The values in brackets correspond to the homogeneous reaction using $[\text{Rh}(\text{COD})(n\text{-octanoyl-PYRPHOS})]\text{BAR}_\text{F}$

Although the authors could not explain the observed negative effect of the amino and hydroxy groups, the results show that the spacer can strongly influence the performance of the catalyst. Furthermore, recycling the functionalized gold colloids **67a** was investigated. The enantioselectivities remained constant during three recycling steps, while conversion decreased from 99 to 74% in the fourth cycle.

Magnetically recoverable chiral catalyst were reported by Li,⁵⁰ who immobilized $[\text{Ru}(\text{binap})(\text{dpen})]$ complex on super-paramagnetic magnetite nanoparticles (cat. **68**, Figure 16). Magnetite nanoparticles are intrinsically not magnetic but can be readily magnetized by an external magnet. In the presence of **68**, excellent conversions ($>99\%$) and high asymmetric inductions were obtained in the hydrogenation of aromatic ketones

and these results correspond to those obtained with the corresponding homogeneous BINAP complex. Catalyst **68** can be separated by simple magnetic decantation, and was recycled up to 14 times without the loss of activity in the hydrogenation of 1-acetophenone (100%, 97-99% ee).

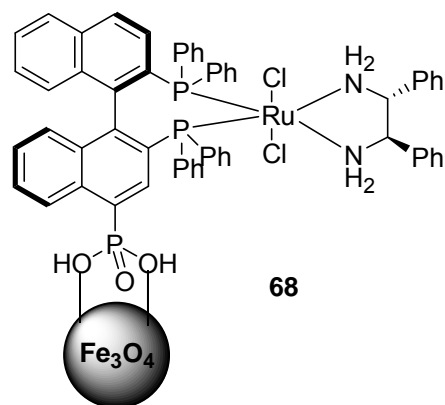


Figure 16. An example of magnetically recoverable BINAP complex

The application of BINAP-palladium nanoparticles in the asymmetric hydrosilylation of styrene was reported by Fujihara.⁵¹ The catalyst was prepared by the reduction of K_2PdCl_4 with sodium borohydride in the presence of BINAP. In contrast to the previously described examples, where nanoparticles were stabilized with thiols, this approach is an adaptation of the previously described idea, where gold nanoparticles were functionalized with triphenyl phosphine. Thus, the BINAP moieties plays the role of Pd-nanoparticles stabilizers and catalyst in the same time. This nanoparticles-based catalyst gave up to 95% ee in hydrosilylation of styrene, as determined after oxidation to the corresponding alcohol. Strikingly, the homogeneous palladium-BINAP complex does not promote the reaction.

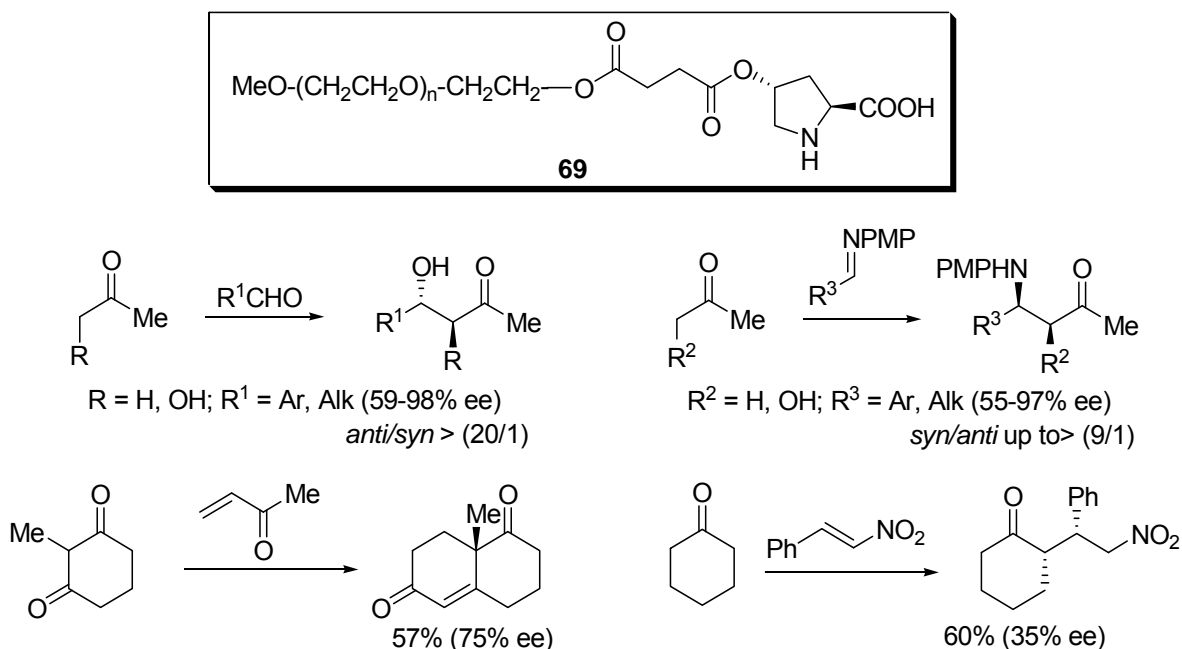
1.2 Immobilization of organocatalysts

It was recently proposed to define an organic catalyst as: “an organic compound of relatively low molecular weight and simple structure capable of promoting a given transformation in substoichiometric quantity”.^{54a} The term organic emphasizes the advantages of performing a catalytic reaction under metal-free conditions including: working in wet solvents and an under aerobic atmosphere, dealing with stable and robust catalysts, avoiding from the outset the problem of the metal leaching into the organic product. Organic catalysts can be seen as minimalistic version of enzymes from which they are conceptually derived,^{54c} the organic catalysts are generally more stable, less expensive, and enjoy a wider application under a variety of conditions unsustainable for enzymes. In addition, organic catalysts are also more readily amenable than their metal-based counterparts and biocatalysts to anchoring on a

support with the aim of facilitating catalyst recovery and recycling. In many cases the main goal of immobilization is the simplification of the work-up by the easy separation of the organo-catalyst from the product. The continuing discovery of more sophisticated structures, recovery and recycling will become a priority.

Proline is one of the first amino acids recognized as an organocatalyst and since that time proline has been employed in a number of enantioselective syntheses including aldol, iminoaldol reactions, and Michael addition.

A soluble polymer-supported version of this versatile catalyst was reported by Cozzi.⁵⁵ (2*S*,4*R*)-4-hydroxy proline was anchored on PEG₅₀₀₀ via a succinate spacer, affording catalyst **69** (Scheme 14). In the presence of 0.25-0.35 mol% of this catalyst, acetone reacted with enolizable and nonenolizable aldehydes (Scheme 14) in DMF or DMSO at room temperature (40-60 h) to afford β -hydroxy ketones with high enantioselectivity ($\leq 98\%$) and chemical (80%) yields.^{55a} These results are comparable to the use of proline as the catalyst. In the condensation of hydroxy-acetone with cyclohexanecarboxaldehyde catalysed by **69**, the corresponding *anti*- α,β -dihydroxyketone was obtained in 48% yield and 96% ee (*anti/syn* >20:1).^{55a} Replacement of the aldehyde component with imines opened the way for the synthesis of β -amino- and *syn*- β -amino- α -hydroxy-ketones (Scheme 14),^{55b} which were obtained in up to 97% ee and good chemical yields (up to 80%).

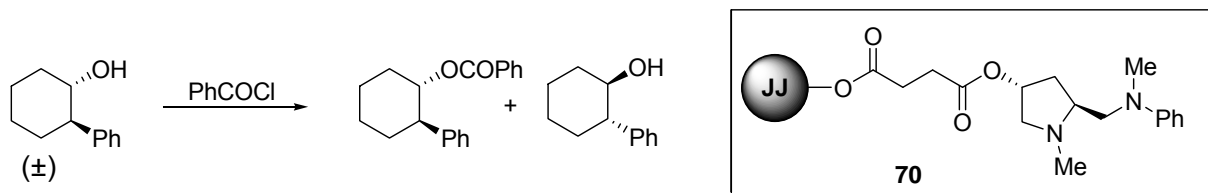


Scheme 14. Examples of reactions catalysed by PEG supported proline **69**

The use **69** in the Robinson annulation^{55b} of 2-methyl-1,3-cyclohexanedione and 3-buten-2-one in DMSO at room temperature (Scheme 14) afforded the product in 55% yield and 75% enantioselectivity, in agreement with the application of proline. Analogous transformation promoted by the proline supported on insoluble polystyrene resulted in significant loss both

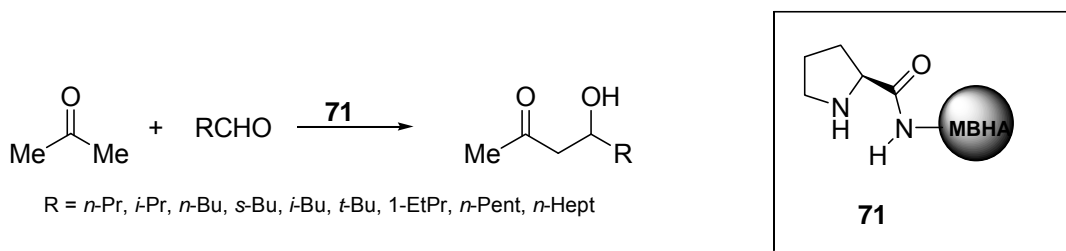
chemical yield (29%) and enantioselectivity (39% ee).⁵⁶ In all reactions discussed here, catalyst **69** can be reused up to three times without a significant loss of activity. Finally the catalyst **69** was employed in the Michel-type synthesis of γ -nitroketones.⁵⁷ For example, in the addition of cyclohexanone to nitrostyrene, the product was obtained in 60% yield and 35% ee displaying enantioselectivity inferior than that observed with the non-supported catalyst.⁵⁸

Kinetic resolution of cyclic secondary alcohols catalysed by 4-hydroxy-*N*-methylproline derivative supported on JandaJel (JJ) (cat. **70**) was reported by Janda.⁵⁹ In the presence of 0.15 mol equiv of the catalyst **70**, racemic *trans*-2-phenylcyclohexanol was reacted with benzoyl chloride, affording the enantiomerically enriched benzoate in 44% yield and 96% ee. Unreacted alcohol was recovered in 45% yield and 85% ee. The catalysts **70** could be reused in up to five reactions cycles with unchanged yield and ee.



Scheme 15. Kinetic resolution of cyclic secondary alcohols in the presence of the catalyst **70**

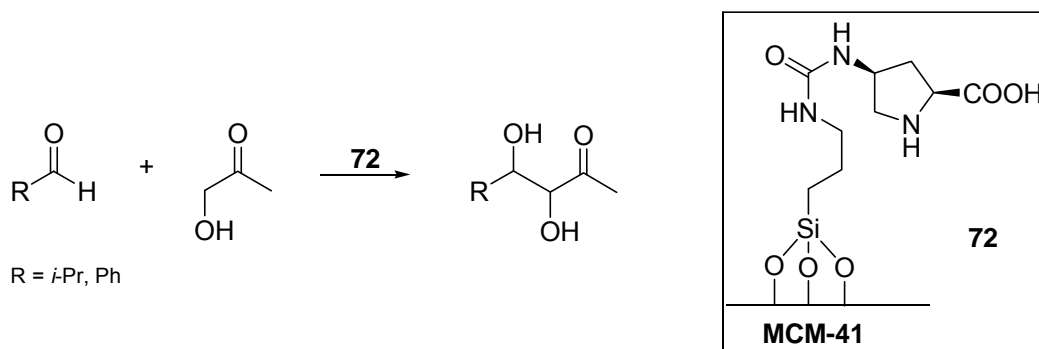
The use of proline amide **71**, obtained by a condensation of proline with benzhydrylamino polystyrene (MBHA) was reported by Bartok and co-workers.⁶⁰ In the presence of 20 mol% of catalyst **71**, acetone reacted with linear and branched aldehydes to afford the aldol product in moderate yields (40-75%). Products derived from aliphatic aldehydes showed enantiomeric excess averaging around 50% ee, whereas significant improvement was observed with hindered substrates such as pivalaldehyde (86% ee). Slightly lower yield and ee values were obtained when recycled catalyst was used in the transformation.



Scheme 16. Aldol reaction in the presence of MBHA supported proline **71**

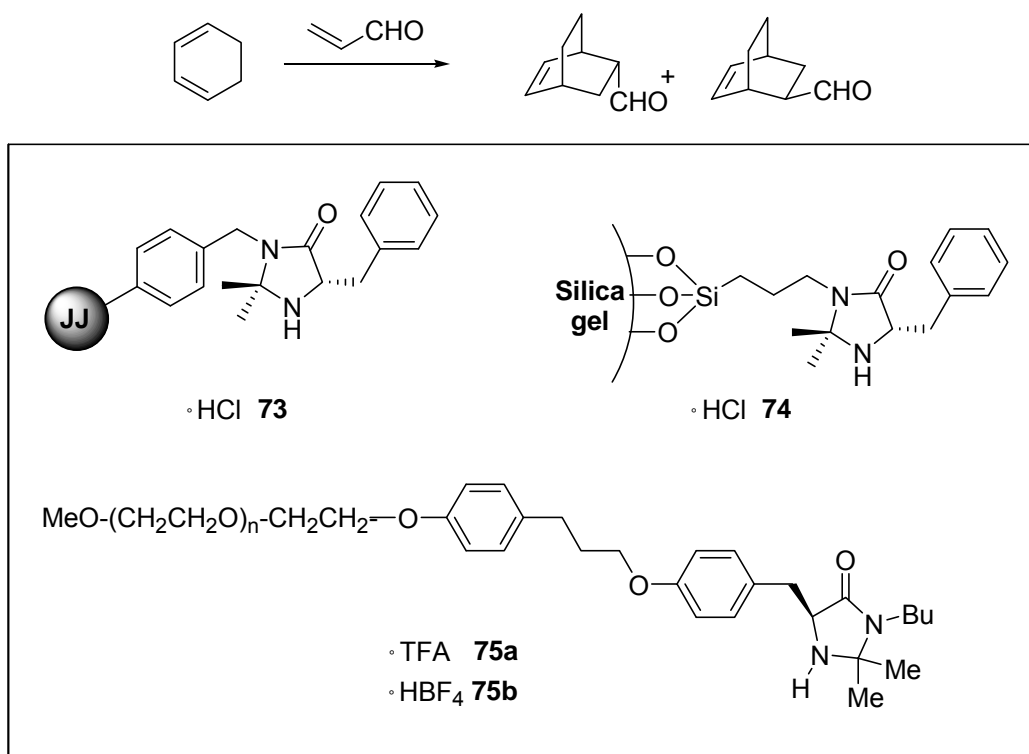
The modified proline immobilized on mesoporous siliceous material (Scheme 17) was reported by Fernandez-Mayoralas.⁶¹ The use 52 mol% of catalyst **72** in the reaction between hydroxy-acetone and isobutyraldehyde at room temperature in DMSO, led to the exclusive formation of *anti* diols of >99% ee in 55% yield. In comparison to proline itself, catalyst **72** exhibited identical enantioselectivity though some loss of chemical yield (*ca.*~20%) was

observed. When benzaldehyde was used as a substrate, the product was obtained in 55% yield, 70% ee and in 1:1.4 dr ratio, which corresponds to some loss of activity and selectivity compared to proline (80%, 2.5:1 dr ratio, 80% ee). The recovered catalyst was re-used twice with unchanged stereoselectivity, though with slow decrease of yields.



Scheme 17. Aldol condensation in the presence of MCM-41 supported proline

Imidazolidin-4-ones were originally proposed as organo-catalysts by MacMillan.⁶² The importance of these catalysts led to their immobilization on soluble^{55b} and insoluble⁶³ supports (Scheme 18).



Scheme 18. Diels Alder reaction in the presence of supported Imidazolidin-4-ones **73**, **74**, **75a,b**

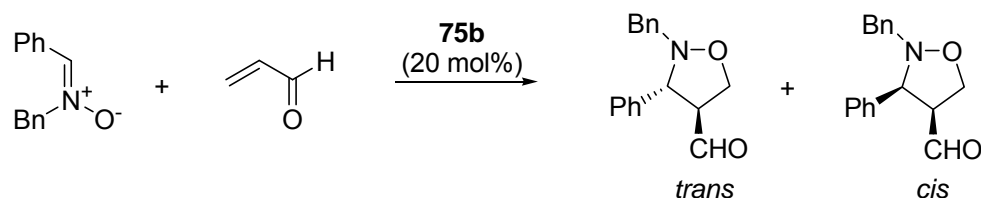
The activity was tested using the enantioselective Diels-Alder reaction and the results are summarized in Table 8.

Table 8. Asymmetric D-A cycloaddition catalysed by **73-75a**

Catalyst [mol%]	Time [h]	Yield [%]	Endo (ee%)	Exo (ee%)
73 (20)	25	30	13 (98)	1
74 (20)	24	83	14 (90)	1
75a (10)	40	67	94 (92)	6 (86)

JandaJel-supported catalyst **73** afforded the product with the highest enantioselectivity though in a very low yield. Interestingly, the heterogeneous catalyst induced higher ee than the non-supported MacMillan's catalyst.⁶² An improvement of activity was achieved by immobilization on silica gel but at the expense of enantioselectivity. The authors believed that the increase in the polarity of the support on passing from *JandaJel* to silica increase the efficiency of the catalyst in the reaction, which involves a highly polar transition state. Finally, the use of soluble polymer supported catalyst **75a** combines good enantioselectivity with a reasonable yield. Both *JandaJel* and PEG supported catalysts could be reused at least once, but a small loss of activity and stereoselectivity was observed.

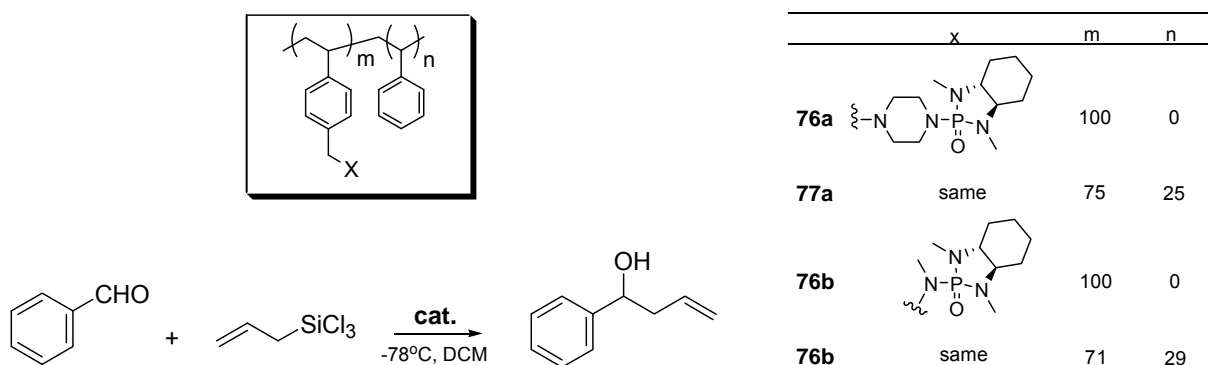
Following the development of organocatalysts for 1,3-dipolar cycloaddition reported by MacMillan⁶⁴, Cozzi⁶⁵ prepared a soluble polymer-supported version of this catalyst (**75b**, Scheme 18) and investigated its properties in the addition of nitrones to α,β -unsaturated aldehydes. By reacting *N*-benzyl-*C*-phenyl nitron with acrolein in the presence of 20 mol% of **75b** (Scheme 19) the product was obtained in 71% yield as an 85:15 *trans/cis* mixture of isomers with major having 87% ee. Extension of the reaction to crotonaldehyde and other nitrones led to similar results. Comparison with MacMillan catalyst indicates that the difference between the PEG-supported and non-supported catalyst resides in chemical rather than stereochemical efficiency (3-9% lower ee, 9-27% lower yields). Catalyst **75b** could be recycled twice, affording the product with unchanged ee but significant decrease in chemical yields was observed after each run.

**Scheme 19.** Asymmetric addition of *N*-benzyl-*C*-phenylnitron to acrolein catalyzed by **75b**

The use of immobilized polyamino acids as organocatalysts in asymmetric synthesis is described in the literature^{54a,b} but these examples are not covered by this review.

The first and only example of chiral phosphoramides immobilized on polymer was reported by in 2005.⁶⁶ Two synthetic approaches were explored in order to synthesize this

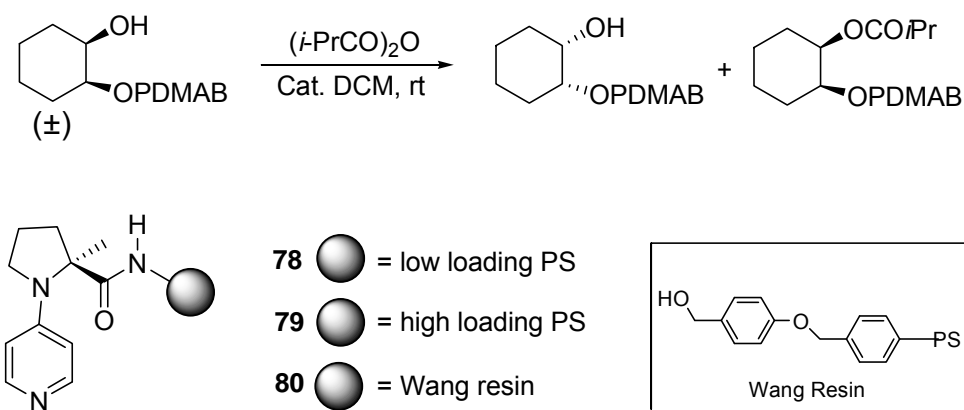
catatalyst. In the first approach, polymerization of styrene monomers containing phosphoramidate afforded catalyst **76**, whereas copolymerization of the same monomers with unfunctionalized styrene furnished catalyst **77**.



Scheme 20. Asymmetric allylation of aldehydes allyltrichlorosilane catalyzed by **76**, **77**

The addition of allyltrichlorosilane to benzaldehyde in the presence of 10 mol % of **76a,b** (Scheme 20) afforded the product with high chemical and moderate enantioselectivities (82-84%, 62-63% ee). Catalyst **77a,b** exhibited lower activity and stereoselectivity (43-62%, 49-51% ee). Interestingly enough, all heterogeneous catalysts were more efficient than the corresponding non-supported derivatives featuring benzyl group rather than polymer residue. Better results obtained with catalysts **76** were explained on the basis of an earlier observation that bisphosphoramides are more efficient than mono-phosphoramidate.^{67a} Apparently, the polymer backbone can force two catalyst sites into a close proximity so that they behave as *bis*-phosphoramidate. Both recycling and extension of the application were not mentioned by the authors.

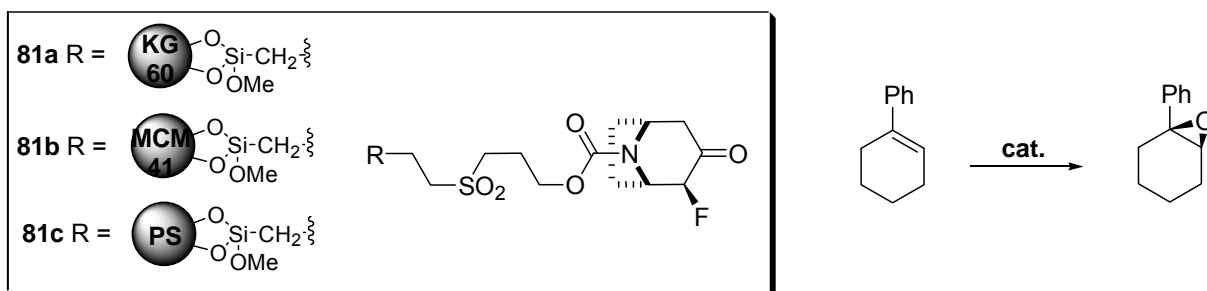
The use of chiral DMAP analogues anchored to a polymeric matrix was described by Priem and Campbell.^{67b} Heterogeneous organo-catalysts were prepared by condensation of *N*-4-pyridinyl- α -methylproline with low and high loading polystyrene and with Wang resin.



Scheme 21. The kinetic resolution of *cis*-1,2-cyclohexanediol mono-4-dimethylaminobenzoate

In a kinetic resolution of *cis*-1,2-cyclohexanediol mono-4-dimethylaminobenzoate, carried out in the presence of 5 mol% of supported catalyst **80** and deficiency of isobutyric anhydride (0.7 equivalent), the unreacted (-)-alcohol was recovered in about 75% ee after 50% conversion (Scheme 21). When the reaction was stopped at 67% conversion, the enantiopurity of the unreacted alcohol increased to 93%. All catalysts exhibited similar level of chemical and stereochemical activity regardless of the resin used. Recovered catalyst **80** was used in the next transformation to afford the product of slightly higher enantiopurity, and the same conversion although the activity of the recycled catalyst decreased and the reaction time to reach the same level of conversion increased.

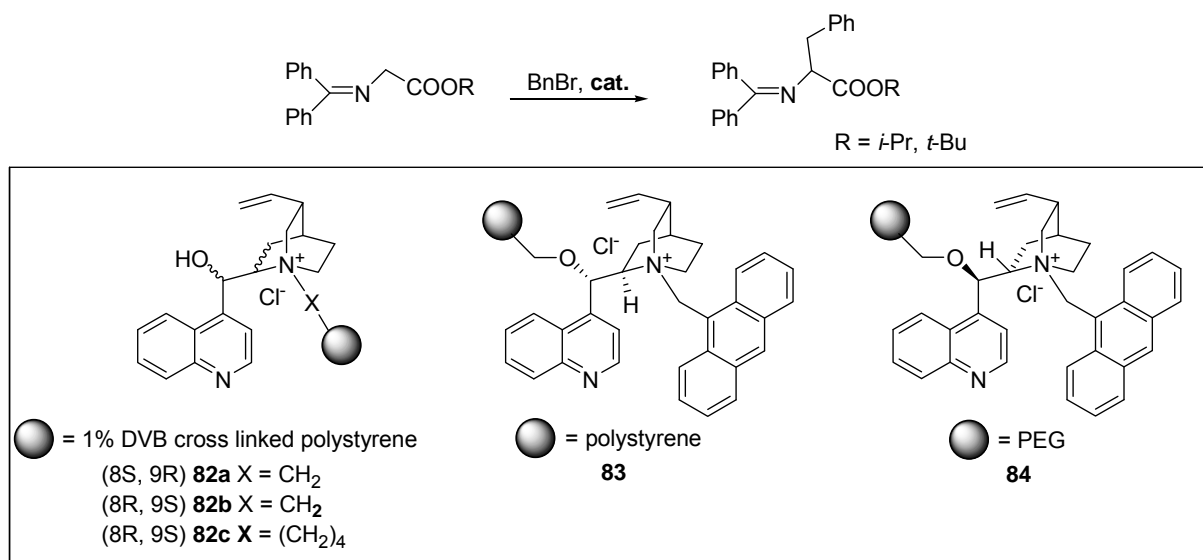
Dioxiranes derived from chiral ketones are known as organocatalysts and have been extensively studied in epoxidation of olefins. The heterogeneous version of these catalysts was reported first by Sartori, Armando and co-workers.⁶⁸ In the initial study, racemic tropinone was anchored to amorphous silica KG-60, mesoporous silica MCM-41, and 2% cross-linked polystyrene (Scheme 22).



Scheme 22. Asymmetric epoxidation of 1-phenylcyclohexene in the presence of **81a-c**

In the epoxidation of 1-phenylcyclohexene, in the presence of 40 mol% of supported catalysts and using oxone as the oxidant (Scheme 22), catalysts immobilized on siliceous material performed much better than the polystyrene-based analogues. When the enantiomerically enriched tropinone (78% ee) anchored to siliceous material was tested in the epoxidation of a series of trisubstituted alkenes, the corresponding epoxides were obtained in very good chemical yields (>91%) and acceptable enantioselectivities (58-80% ee; corrected for the ee of tropinone). These results corresponds to those obtained with the homogeneous catalyst. Recovered catalysts could be reused three times, furnishing the products of unchanged ee.⁶⁸

An important group of heterogeneous organocatalysts derives from the immobilization of alkaloids. A large number of these catalysts and their application in the asymmetric synthesis has been described.^{54a} However, because of the limited space, only selected examples are presented in this review.



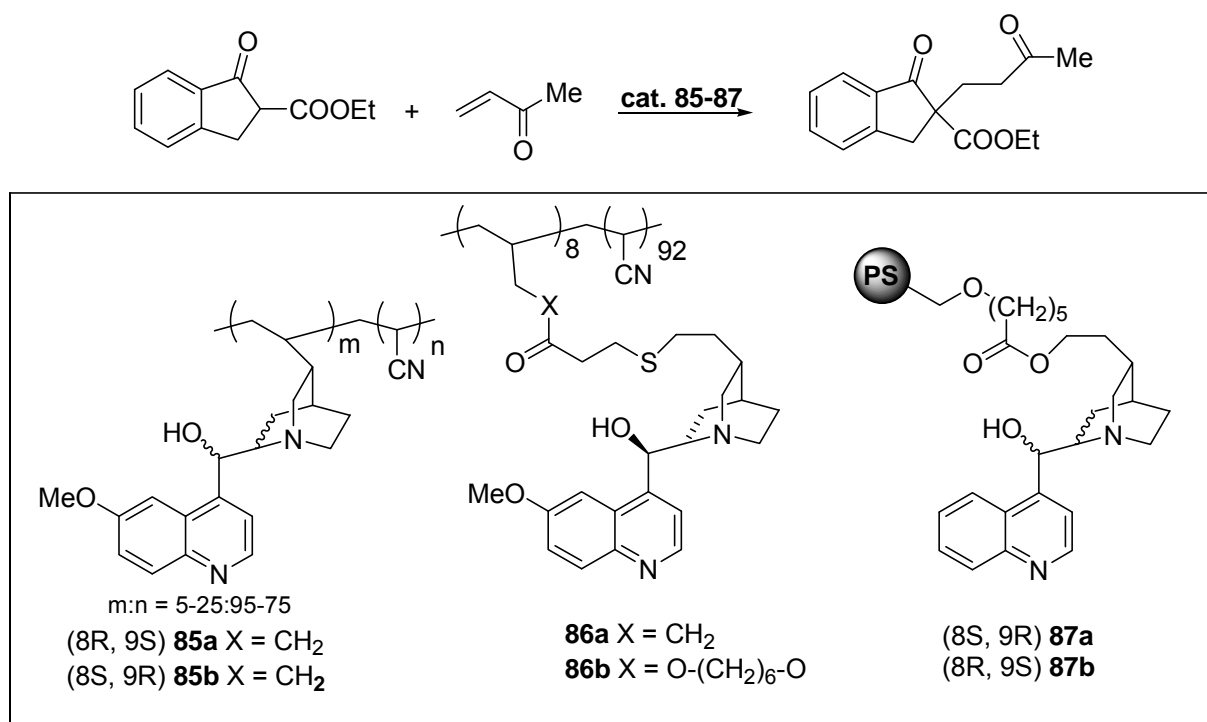
Scheme 23. Asymmetric alkylation of amino acid imines catalyzed by **82-84**.

Development of the O'Donnell-Corey-Lygo protocol for asymmetric alkylation of amino acid imines under PTC conditions, catalysed by quaternized cinchona alkaloids,⁶⁹ led to the preparation of an immobilized version of these catalyst. Najera^{70a} anchored cinchonine and cinchonidine to 1% DVB cross-linked chloromethylated polystyrene to afford adducts **82a,b** (Scheme 23). When the benzylation of the benzophenone imine of glycine *i*-propylester was carried out in a mixture of aqueous 25% NaOH and toluene in the presence of catalyst **82a** at 0 °C, the corresponding (*S*)-product was obtained in 90% yield and 90% ee. Rather surprisingly, the use of the catalyst **82b** afforded the (*R*)-product in only 40% ee. The use of different substrates and different reactions conditions depressed the ee to 40-60%.^{70a} The recovered catalyst can be reused at least once without the loss of activity.

An improvement in enantiopurity in the formation of the (*R*)-product derived from benzophenone imine glycine *tert*-butyl ester (81% ee) was observed after incorporation of a spacer between the catalyst and polystyrene (cat **82c**, Scheme 23), but this had a dramatic effect on the stereochemical outcome of the reaction. In this case, both the catalyst derived from cinchonine and cinchonidine induced the formation of the (*R*)-product.^{70b} Further improvement in enantioselectivities was attained by the use of the second generation catalyst with 9-antracenylmethyl residue at the quinuclidine nitrogen.^{70c} In the presence of 10 mol% of **83** at -50 °C in toluene (Scheme 23) the (*S*) product deriving from benzophenone imine glycine *tert*-butyl ester was formed in 94% ee, a value similar to that obtained with unsupported catalyst. Unfortunately, the pseudoenantiomer of **83** was less effective, affording the (*R*)-product in only 23% ee. An attempt to improve the result by anchoring the quaternary salt to a soluble polymer has been made⁷¹ but in the best case (cat. **84**, DCM,

-70 °C, solid CsOH, 60 h) the (*S*)-product was formed in 64% ee. It was found in a controlled experiment, that the presence of polyethylene glycol has a negative influence on the outcome of the reaction as the polymer solubilizes inorganic species in the organic phase, which leads to poorly stereocontrolled reaction pathway.

Non-ionic organocatalysts deriving from anchoring of cinchona alkaloids were reported by Kobayashi and Iwai.⁷² Quinine and quinidine were supported through the double bond by a copolymerization with acrylnitrile. The resulting polymers were soluble in polar aprotic solvents, such as DMF and DMSO, but insoluble in less polar solvents, which created a possibility for their simple recovery. When the Michael addition was promoted by catalyst **85a** (Scheme 24) in toluene at rt, the product was formed in 92% yield and 42% ee. The use of **85b** under the same reaction conditions was slightly less efficient as it induced 30% ee.



Scheme 24. Asymmetric Michael Addition catalyzed by **85-87**.

The separation of supported catalysts from the product was simplified to a filtration but a subsequent reuse of regenerated catalysts in a cycle of transformation was not described by the authors. An improvement of enantioselectivity was observed after the introduction of a spacer group between the polymer backbone and the alkaloid moiety:⁷³ When 0.05 mol equiv of catalyst **86a** or **86b** (Scheme 24) was used in toluene at -48 °C, enantioselectivity increased to 65% ee. Further improvement was observed after the replacement of the support. When alkaloids were anchored to 1% DVB cross-linked polystyrene, the enantioselectivity increased to 87% as in the case of **87a**. However, rather surprisingly, the quinidine-based catalyst **87b**

became much less selective (39% ee). These results demonstrate that even small changes in the polymer-supported catalyst ensemble may produce dramatic changes in the stereochemical outcome of the reaction.

Beside the Michael addition, the catalyst **85a** was tested in the addition of dodecanethiol to 3-methyl-3-buten-2-one (76%, 57% ee),⁷² the addition of benzylmercaptan to β -nitrostyrene (54%, 18% ee),⁷⁴ and the addition of hydrogen cyanide to 3-phenoxybenzaldehyde (98%, 46% ee).⁷⁵

The use of oxygen atom at C-9 of cinchonine and quinine as the attachment point to a polymer led to catalyst **88a,b** (Figure 17).⁷⁶ Application of **88a** in a low-temperature addition of methanol to methylphenyl ketene afforded the corresponding (*S*)-ester in 34% ee. For comparison, the quinine-derived analogue induced formation of the (*R*)-product in 12% ee. The attachment of quinine to 2% DVB polystyrene via oxygen atom at C-9 led to catalysts **88c,d** (Figure 17).⁷⁷ However, in the previously described Michael addition, the product was almost racemic (11% ee).

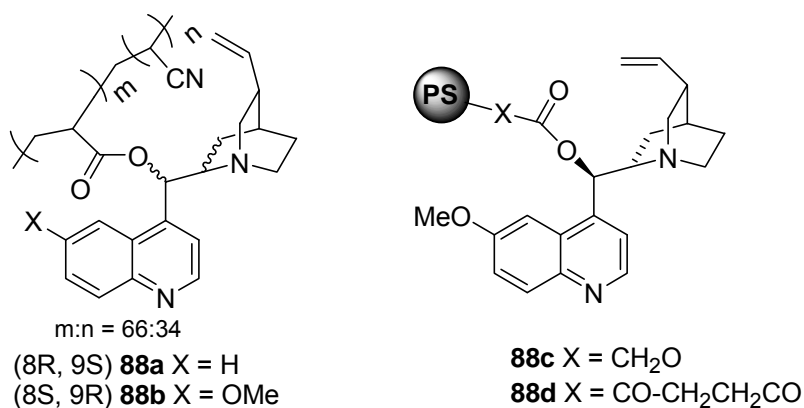
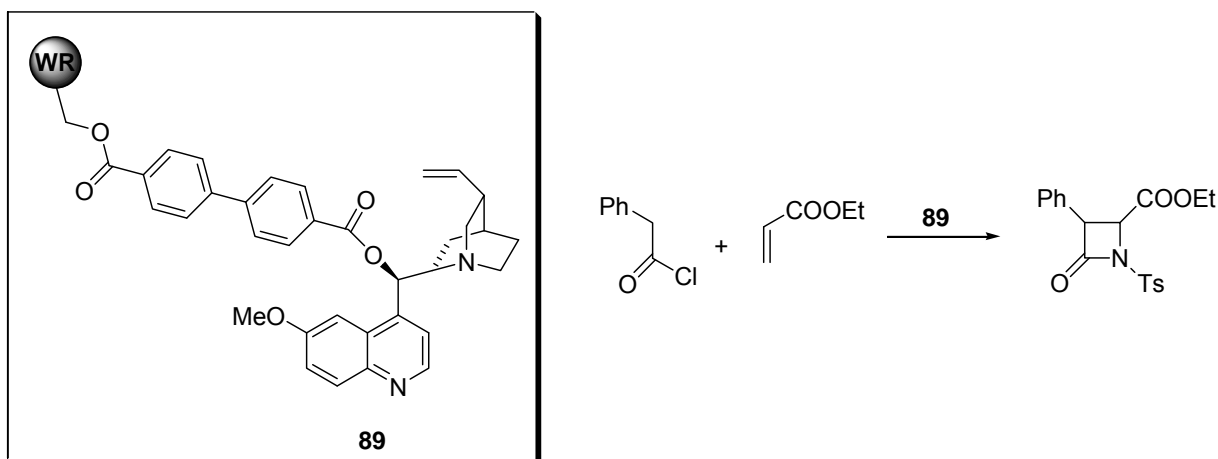


Figure 17. Polymer supported cinchonine and quinine obtained by the use of oxygen atom at C9 as an attachment point

Lectka⁷⁸ reported on the application of quinine supported on 1% DVB cross-linked, highly loaded Wang resin (**WR**), as catalyst for the [2+2] Staudinger reaction between ketenes and imines. In the synthesis of 1-*p*-tolylsulfonyl-3-phenyl-4-carbethoxy β -lactam by the cycloaddition of phenyl ketene to the *N*-tosylimine of ethyl glyoxalate catalysed by **89** (Scheme 25), the product was obtained in 62% yield as a 93:7 mixtures of *cis* and *trans* azetidinones with the major isomer having 90% ee. Several runs were necessary before the catalyst aged enough to afford consistent results. The aged catalyst was used in 6 cycles, affording the product with unchanged ee.



Scheme 25. Cycloaddition of phenyl ketene to N-tosylimine of ethyl glyoxalate in the presence of **89**

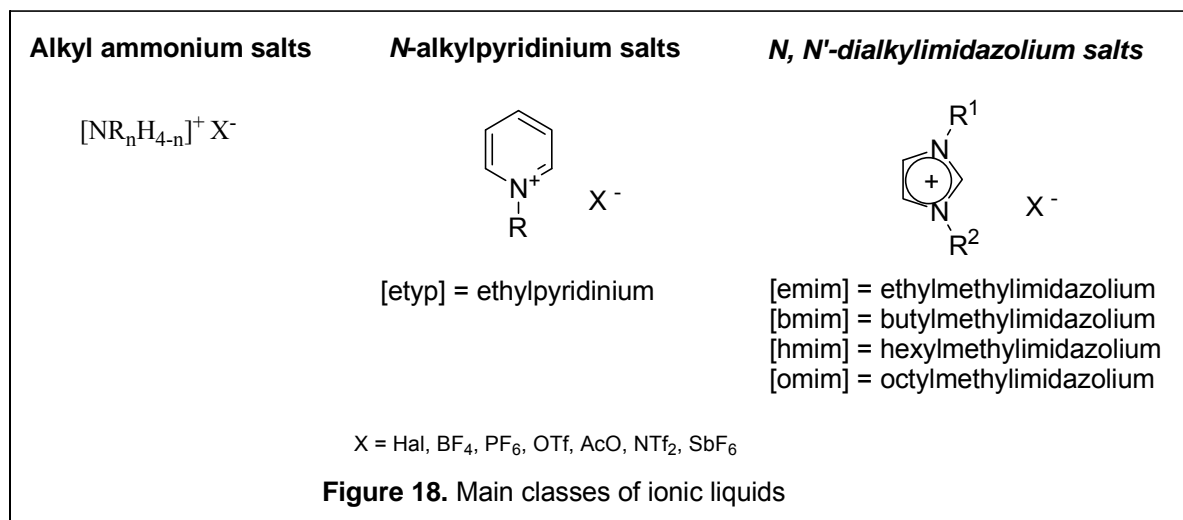
1.3 Immobilization of homogeneous catalysts – conclusions

A number of reasons justify the immobilization of the homogeneous catalysts. Among the most important are: (1) simpler separation of the catalyst from the reaction mixture; (2) easier isolation of the reaction products; and (3) catalyst recovery and recycling. Immobilization is convenient if the catalyst is expensive or has been obtained after a complex synthesis or is employed in a relatively large amount. However, the candidate for immobilization should be capable to promote more than one reaction or tolerate a variety of substrates in a given transformation. Another very important feature is the catalyst stability since this can decisively affect recycling, which represents the major goal of catalyst immobilization. The attachment point on the catalyst for the connection to the support ranks second followed by what kind of linker, if any, must be inserted between the catalyst and the support. Finally, the choice of the support for immobilization is most important, because the properties of the support can influence the catalyst behavior at every level.

For a long time, immobilization of homogeneous chiral catalysts had been accompanied by loss in activity and selectivity. Today, however by choosing a suitable support a heterogeneous catalyst can be prepared that gives similar or even enhanced selectivity and activities. Although the knowledge about immobilized catalysts has increased significantly during the last three decades, our understanding of the factors underlying the efficiency and selectivity of supported catalysts is incomplete.

2 Application of Ionic Liquids in Asymmetric Catalysis

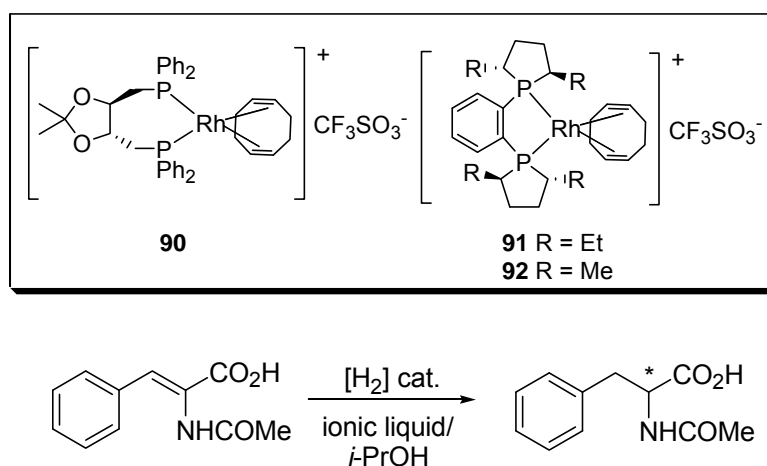
Ionic liquids (ILs), which combine good solubility properties, negligible vapor pressure, and excellent thermal stabilities, can serve as valuable substitutes for many volatile solvents. The common classes of ILs derive from: alkylammonium salts, alkyl pyridinium salts and *N,N'*-dialkyl imidazolium salts (Figure 18).



Many reaction were carried out with success in this reaction medium⁷⁹ and in some cases, an improvement of process performance was observed. In asymmetric catalysis, the use of ionic liquids can simplify the catalyst recovery, and allow its undemanding recycling. Two main strategies have evolved. First, a chiral catalyst having polar or ionic character can be immobilized in an ionic liquid, which is used to allow the recovery of chiral catalyst. Second, chiral discrimination is promoted by chiral ionic liquid itself, which acts as a promoter. Separation of the organic product from the catalyst is usually simplified to a phase separation (biphasic systems) or the extraction with nonpolar solvents (monophasic system).

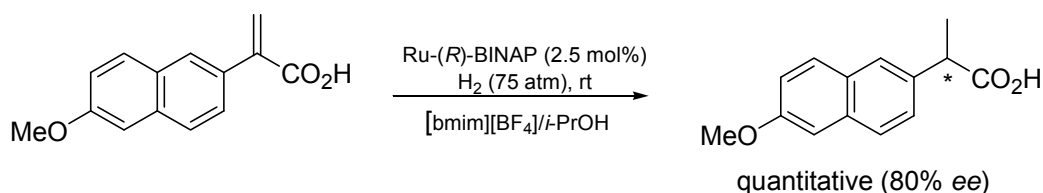
The first example of application of ILs in asymmetric synthesis was reported by Chauvin.⁸⁰ α -acetamidocinnamic acid was hydrogenated in the presence of [Rh(cod)]{(-)-diop}][PF₆] (**90**) using [bmim][SbF₆]/*i*-PrOH biphasic system (Scheme 25). After completion of the reaction, the product of 64% ee was easily and quantitatively separated from the catalyst immobilized in ionic liquid by means of phase separation. Further improvement was reported by Dupont.⁸¹ Carrying out the reaction in [bmim][BF₄]/*i*-PrOH biphasic system in the presence of [(-)-1,2-bis((2*R*,5*R*)-2,5-diethylphospholano)benzene(cyclooctadiene)rhodium(I)-trifluoro-methyl sulfonate (**91**) as a catalyst, α -acetamidocinnamic acid was hydrogenated in 73% conv., and 93% ee (Scheme 26). After extraction of the organic product, the catalyst immobilized in IL was reused 4 times, affording the product with similar ee however the loss of conversion after fourth cycle was observed (35%). The loss of conversion

was explained by partial leaching of the catalyst to the extraction solvent after each cycle, which decreased the amount of catalyst presence in [bmim][BF₄]. Hydrogenation of α -acetamidocinnamic acid catalysed by [Rh-MeDuPHOS] (**92**) immobilized in [bmim][PF₆] afforded the corresponding product in 96% ee (Scheme 26).⁸² Although the reaction was carried out in the biphasic system of [bmim][PF₆]/*i*-PrOH, the result is very close to that obtained in pure *iso*-propanol (99% ee). In comparison to organic solvents, ionic liquids provide superior stability to the air sensitive Rh-complex. The recycling of the catalyst was possible and good enantioselectivities were obtained after five cycles, but with continuous loss of catalytic activity.



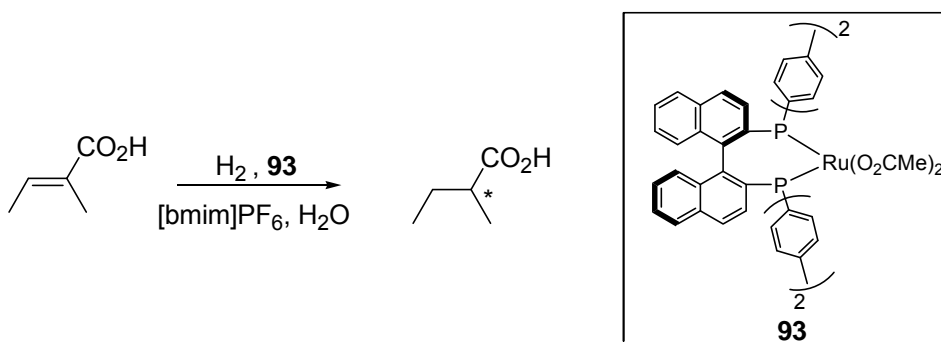
Scheme 26. Asymmetric hydrogenation of α -acetamidocinnamic acid in the presence of **90**, **91** or **92**

Dupont⁸³ investigated hydrogenation of 2-arylacrylic acids catalysed by [BINAP-Ru(OAc)₂] complex in [bmim][BF₄]/alcohol medium (Scheme 27). High conversions (>95%) and enantioselectivities (86% ee) were observed both in homogeneous MeOH/[bmim][BF₄] and biphasic *i*-PrOH/[bmim][BF₄]. The isolation of the organic product was simplified to the separation of the *iso*-propanol phase and the catalyst immobilized in ILs could be reused several times without significant loss of activity or enantioselectivity. This system was applied to the synthesis of (*S*)-naproxen.



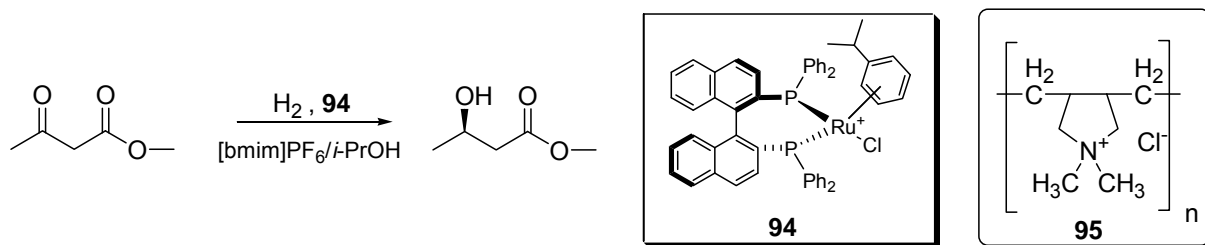
Scheme 27. Asymmetric synthesis of (*S*)-naproxen in ionic liquids

Asymmetric hydrogenation of tiglic acid catalysed by the $[\text{Ru}(\text{O}_2\text{CMe})_2((R)\text{-tolBINAP})]$ complex (**93**) in $[\text{bmim}][\text{PF}_6]/\text{H}_2\text{O}$ system was reported by Jessop.⁸⁴ Excellent conversion (99%) and good enantioselectivity (85% ee) were attained. The reaction was shown to be hydrogen pressure dependent. At low temperature, the presence of water did not influence the enantioselectivity but at high temperature, the enantioselectivity was enhanced. After completion of the reaction the product was extracted from the reaction mixture using scCO_2 , so that the use of organic solvents was avoided. The recovered catalyst was reused five times retaining the activity and even enhancing enantioselectivity (up to 91% ee).



Scheme 28. Asymmetric hydrogenation of Tiglic Acid in the presence of **93**

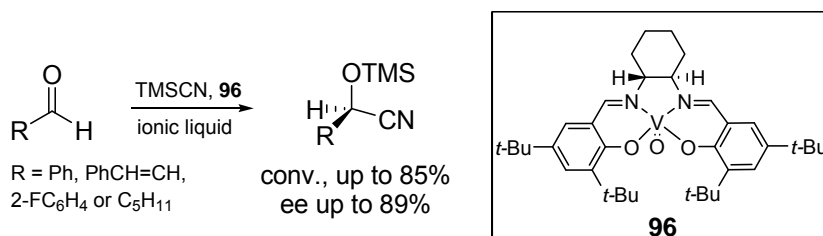
Asymmetric hydrogenation of methylacetoacetate catalysed by $[\text{Ru}(\text{BINAP})]$ complex (**94**) in ionic liquids was reported by Vankelecom.^{85a} In a biphasic $[\text{bmim}][\text{PF}_6]/i\text{-PrOH}$ system, good selectivity^{85b} (83%) and excellent enantiomeric excess (97% ee) were observed. (Comparable to those from homogeneous system (93%, 99% ee)). The addition of the third component, poly(diallyldimethylammonium chloride) (**95**) to the system resulted in a complete avoidance of the catalyst leaching into the alcohol phase while preserving identical selectivity and enantioselectivity. Immobilized catalyst was reused without the loss of activity or selectivity.



Scheme 29. Asymmetric hydrogenation methylacetoacetate in the presence of **94** or **95**

Immobilization of chiral vanadyl-(salen) complex (**96**, Scheme 30) in ionic liquids was reported by Baleizao.⁸⁶ In the addition of TMSCN to aldehydes, good conversions (up to 85%) and very good enantioselectivities ($\leq 89\%$ ee) were observed in $[\text{emim}][\text{PF}_6]$ and $[\text{bmim}][\text{PF}_6]$, which corresponds to the use of CH_2Cl_2 . However, significant loss of activity

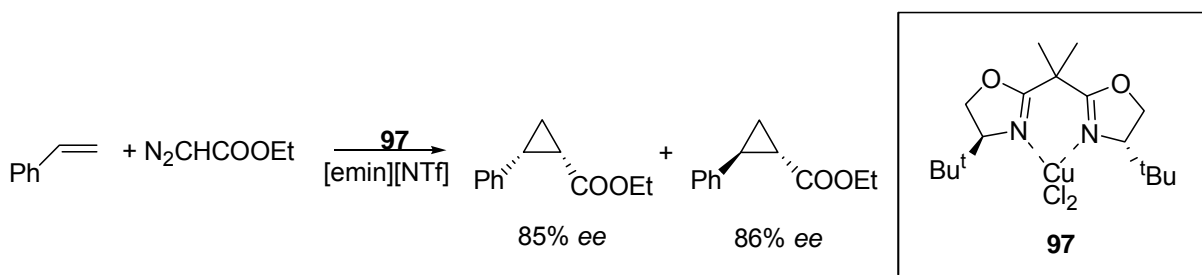
and stereocontrol were recorded for [bmim]Cl and [bmim]BF₄, showing a dramatic effect of the counter ion. The product of reaction carried out in [emim][PF₆] was separated by extraction with hexane and the recovered catalyst was reused up to 4 times without the loss of activity and stereoselectivity.



Scheme 30. The addition of TMSCN to aldehydes in the presence of **96**

Chiral salen complexes immobilized in ionic liquids were also successfully applied in the asymmetric ring-opening of epoxides,⁸⁷ hydrolytic kinetic resolution of racemic epoxides,⁸⁸ and asymmetric epoxidation of alkenes.⁸⁹

The immobilization of (bis)-oxazoline **97** copper catalysts in ionic liquids was reported by Mayoral (Scheme 31).⁹⁰ The usefulness of three ionic liquids, namely [emin][NTf], [emin][BF₄], and [Oct₃NMe][NTf], was investigated. In the asymmetric cyclopropanation of styrene with ethyldiazoacetate, the best results were obtained with low cost CuCl₂ in [emin][NTf], and matched those attained with the expensive Cu(OTf)₂ in CH₂Cl₂ (*cis/trans*: 71:29, 91% ee *trans*, 88% ee *cis*). The crucial role of the anion of ionic liquid and its influence on catalytic performance, is believed to originate from the fast anion exchange between the two salts, i.e., the catalyst precursor and ionic liquid, which explains the problems related to the use of ionic liquids other than those derived from triflates.

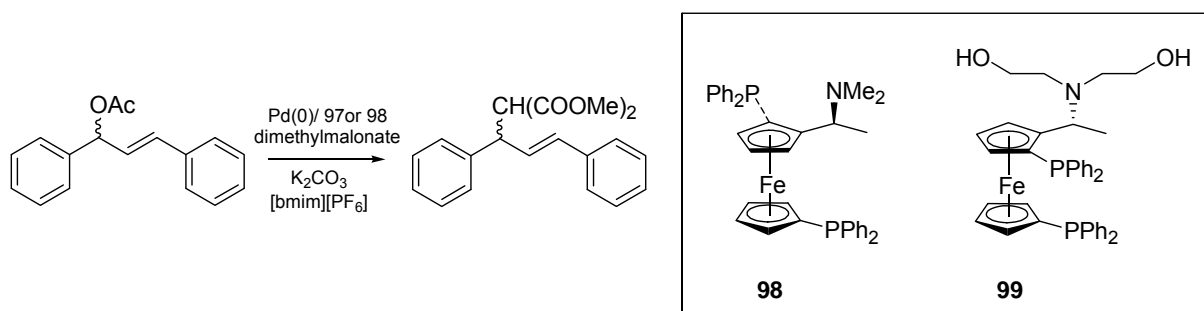


Scheme 31. Asymmetric cyclopropanation of styrene with ethyl diazoacetate promoted by **97**

However, the reaction performed in [Oct₃NMe][NTf] afforded the product in only 22% ee, showing the influence of the positive counter ion as well. The authors believe that in this case the difference in polarity between [emin][NTf] and [Oct₃NMe][NTf] plays a crucial role in the dramatic decrease of enantioselectivity. The isolation of the product was simplified to

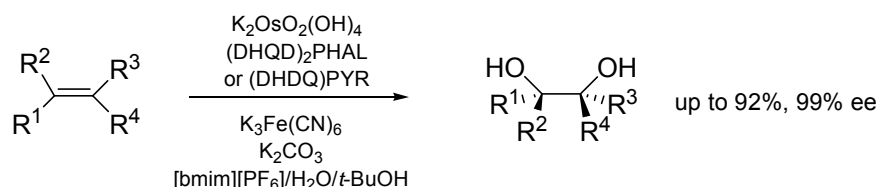
extraction with hexane; the recovered catalyst could be reused twice retaining high activity and selectivity.

The use of ionic liquids in palladium catalysed asymmetric allylic substitutions was reported by Toma.⁹¹ Two palladium complexes derived from (*S,R*)-BPPFA **98** and (*R,S*)-BPPFDEA **99** were immobilized in [bmim][PF]₆ and tested in the reaction between dimethylmalonate and racemic (*E*)-1,3-diphenyl-3-acetoxyprop-1-ene; the substitution product was obtained in 68 and 74% ee, respectively. In both cases, the reaction carried out in ionic liquids afforded product of a higher enantiopurity than those carried out in THF (40% ee). After completion of the reaction, the organic product was extracted into toluene and the recovered catalyst could be reused without the loss of stereoselectivity, though the product was formed with lower chemical yield (ca. 30%). The attempt to the use the latter catalytic systems in a biphasic, [bmim][PF]₆/toluene mixture, afforded the analogous results.



Scheme 32. Asymmetric allylic substitution in the presence of **98**, **99**

Recycling of osmium-based catalyst for asymmetric dihydroxylation of alkenes was reported by two groups independently. In the work by Alfonso,⁹² the reaction was carried out using K₂OsO₂(OH)₄/K₃Fe(CN)₆ in two systems: biphasic [bmim][PF]₆/water or monophasic [bmim][PF]₆/water/*t*-butanol.

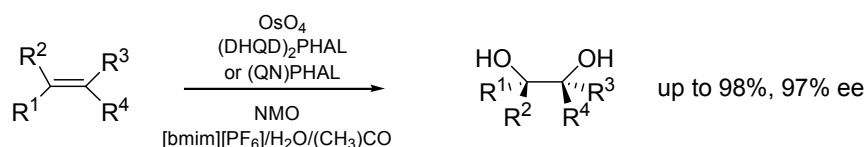


Scheme 33. Asymmetric dihydroxylation of olefins in the presence of [bmim][PF]₆

Depending on the system used and the nature of the substrate, the complex derived from (1,4-bis (9-*O*-dihydroquinidiny) phthalazine) [(DHQD)PHAL] and (1,4-bis (9-*O*-dihydroquinidiny) biphenyl-pyrimidine) [(DHQD)PYR] afforded products of slightly different enantiopurities with the highest value of 99% ee. However, for each substrate there is always one system affording product of comparable or higher yield and ee values than the

original water/t-butanol system. The immobilization of the latter catalysts in ionic liquids allowed the recycling up to 11 times without the loss of activity or stereoselectivity. The author reported that leaching of the toxic osmium into the organic phase was reduced to less than three percent.

Song⁹³ investigated dihydroxylation of *trans*-stilbene and methyl *trans*-cinnamate in the presence of (1,4-bis (9-*O*-quininyl) phthalazine) (QN)PHAL and (DHQ)PHAL as ligands. When the reaction was performed in a mixture of acetone, water, and [bmim][PF₆] in the presence of *N*-methylmorpholine-*N*-oxide (NMO) as a co-oxidant, the obtained results were comparable to those recorded without ionic liquids (up to 98%, 97% ee). However, the use (QN)PHAL in ionic liquid afforded a recoverable system, which can be reused at least 5 times retaining high activity and excellent stereoselectivity; by contrast, significant leaching of the osmium complex into the organic phase was observed with (DHQ)PHAL which makes this system less useful.



Scheme 34. Asymmetric dihydroxylation of stilbene and methyl *trans*-cinnamate in the presence of [bmim][PF₆]

The first example of direct asymmetric aldol reaction carried out in ionic liquids was reported by Loh.⁹⁴ In the presence of 30 mol% of L-proline, a condensation of acetone and benzaldehyde was performed in various ionic liquids and the results are summarized in Table 9.

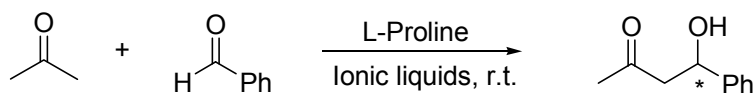


Table 9. L-Proline catalysed asymmetric direct aldol reaction of acetone and benzaldehyde in various ionic liquids

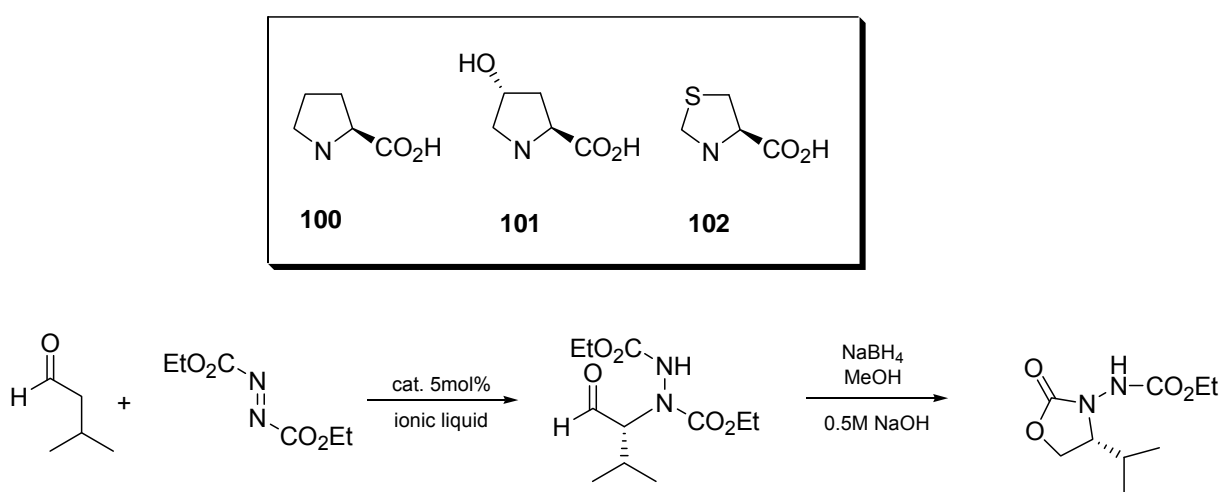
entry	ionic liquid	time (h)	ST:EP:AP	isolated yield (%)	ee (%)
1	hmim BF ₄	45	6:34:60	50	58
2	omim Cl	20	0:55:45	30	78
3	omim BF ₄	20	11:16:73	59	71
4	bmim PF ₆	20	40:0:60	48	71

ST-starting material, EP-elimination product, AP-aldol product

It can be seen that in all cases the aldol product (AP) was formed in comparable or better enantiopurities (58-78% ee) than in the original protocol (60% ee in DMSO). It was found that the reaction performed in [omim]Cl was faster than those carried out in other ionic liquids, but formation of the dehydration product (DP) affected the yield of the desired product. The dehydration product was not observed when bmim PF₆ was used as a solvent.

Separation of the product from the catalyst was simplified to a washing with diethyl ether, and the recovered catalyst could be reused 3 times without the loss of activity or selectivity as demonstrated for [bmim]PF₆. The methodology was further extended to substrates other than benzaldehyde with best results obtained for cyclohexanecarboxaldehyde (65%, 89% ee).

The proline-catalysed addition of aldehydes to diethyl azodicarboxylate (DEAD) in ionic liquids was reported by Toma (Scheme 35).⁹⁵ Using 5 mol% of proline, 3-methylbutanal, DEAD, and various ionic liquids, the addition product was obtained and transform directly into the more stable *N*-(ethoxycarbonylamino)-oxazolidinone derivative by reduction with NaBH₄ and subsequent treatment with aqueous NaOH.



Scheme 35. Proline catalysed asymmetric addition of 3-methylbutanal to DEAD in various ionic liquids

The best results were obtained in the case of [bmim]BF₄ (85%, 84% ee) and the product could be separated by extraction with ether; the recovered catalyst retained full activity over the next 3 cycles. Further improvement of enantioselectivity was observed when the reaction was carried out in [bmim]BF₄ in the presence of catalysts **101** (94% ee) and **102** (92% ee) though significant loss of chemical yields was observed.

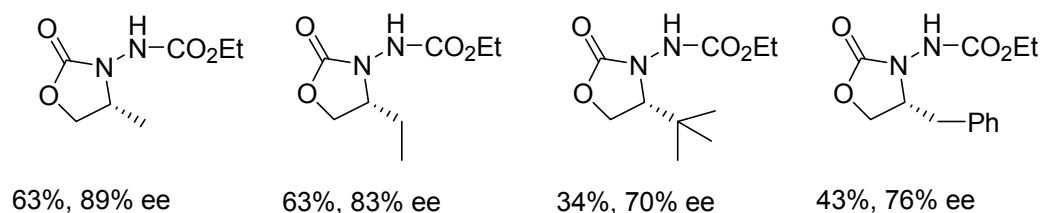
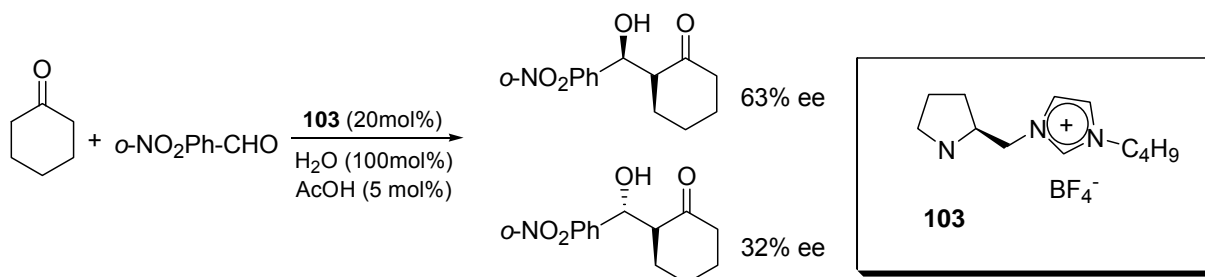


Figure 19. Proline-catalysed asymmetric addition of aldehydes to DEAD in [bmim]BF₄

The scope of application of the proline-catalysed reaction in [bmim]BF₄ was extended to other aldehydes and the results are summarized in Figure 19.⁹⁵ The attempts to extend the application to ketones failed due to the low chemical yields obtained.

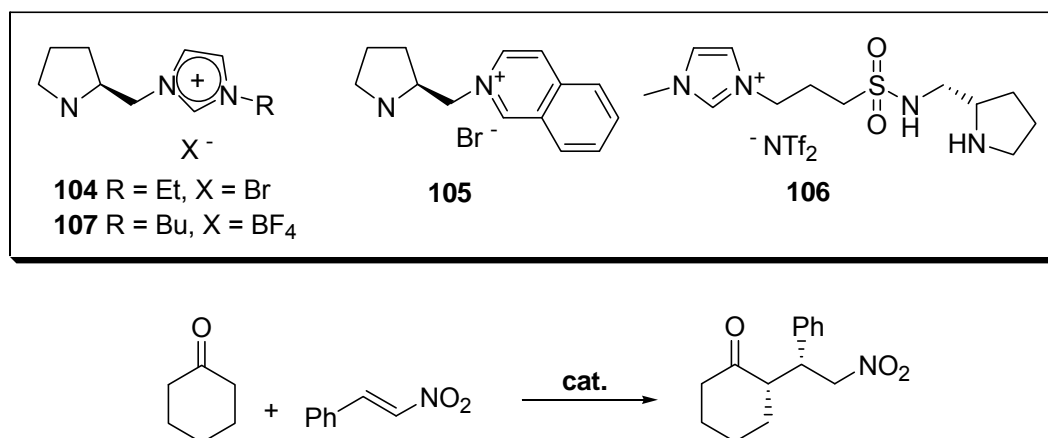
Ion supported chiral pyrrolidines as catalyst for direct aldol reaction were reported by Luo.⁹⁶ Under the best reaction conditions (H₂O/CH₃CO₂H) in the presence of 20 mol% of the catalyst **103**, the aldol products were formed with moderate to excellent yields (35-93%) but with rather low enantioselectivity ($\leq 25\%$ ee).



Scheme 36. Direct aldol condensation catalysed by **103**

An improvement was attained with cyclic ketones, for example in the reaction of cyclohexanone and *o*-nitro-benzaldehyde the product was obtained as a 1:1 mixture of *syn* and *anti* adducts in excellent chemical yield (99%). The reaction product could be separated by simple extraction, and the recycled catalyst could be reused 5 times without the loss of stereoselectivity.

Functionalized chiral ionic liquids as recyclable organocatalysts for asymmetric Michael addition to nitrostyrenes were reported independently by several groups. Xu⁹⁷ reported on the application of catalysts **104** and **105**, Headley⁹⁸ employed catalyst **106**, and Luo^{99a} used catalyst **107** (Scheme 37).



Scheme 37. Asymmetric Michael addition of cyclohexanone to nitrostyrene catalysed by **104-107**

Comparison of the new catalysts in a model reaction, addition of cyclohexanone to *trans*- β -nitrostyrene is presented in Table 10. When the reaction was carried out in the presence of 20 mol% of the catalyst **104** in [bmim]PF₆, the addition product was formed in good selectivity, excellent enantiomeric excess and high chemical yield after 24 h (entry 1). These results could not be reached in any other solvents (entries 2-4); hence, the use of ionic liquids benefits both from an easy catalysts recycling and the enhancement of the catalyst selectivity. Separation of the catalyst from the product was possible by simple extraction with diethyl ether; the recovered catalyst could be reused 3 times affording product with unchanged yield and enantiopurity. Similar results were obtained when catalyst **105** was used in the model reaction. A dramatic loss of catalytic activity was observed for catalyst **106**, though the product was formed in good enantioselectivity and the catalyst could be reused 4 times (entry 6). Finally, catalyst **107** combines an excellent activity, stereoselectivity and reusability with low catalyst loading which makes it a champion in this group. In all cases, lower *ees* products were observed when acyclic ketones were used as substrates.

Table 10. Enantioselective Michael addition of cyclohexanone to *trans*- β -nitrostyrene catalysed **104-107**.

entry	catalyst (mol%)	conditions	time[h]	yield [%]	syn/anti	ee [%]	recycling ^a
1	104 (20)	[bmim]PF ₆ , rt	24	98	92:8	97	4
2	104 (20)	DMSO, rt	96	53	91:9	79	-
3	104 (20)	DMF, rt	96	49	90:10	81	-
4	104 (20)	<i>i</i> -PrOH, rt	96	45	93:7	98	-
5	105 (20)	[bmim]PF ₆ , rt	20	95	93:7	99	5
6	106 (20)	Et ₂ O, 4°C	6 days	38	95:5	88	4
7	107 (15)	TFA - 15 mol%	8	100	99:1	99	4

^a number of runs without the loss of chemical and enantioselectivities.

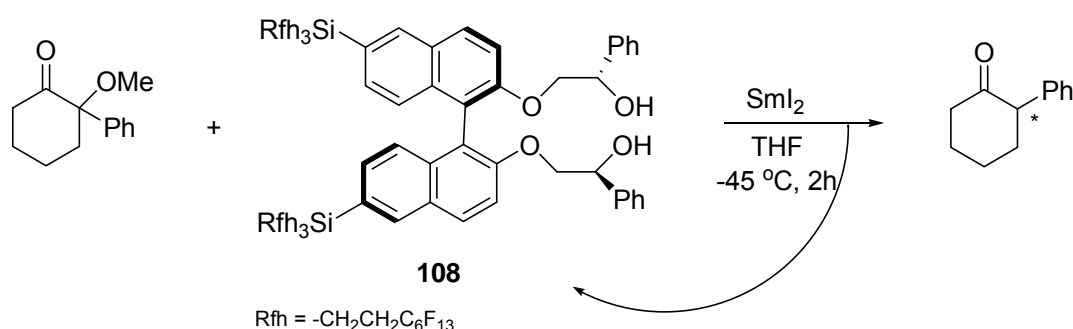
2.1 Application of Ionic Liquids in Asymmetric Catalysis – conclusions

It is now established that a number of classical asymmetric reactions can be realized in ILs with comparable or better efficiency in terms of yields and stereoselectivities. One of the most important aspect of this chemistry is the possibility to immobilize chiral catalytic systems thus allowing to recycle both the solvent and the catalyst for further use. The ionic liquid has to be fine-tuned to the substrate and the catalyst. However, due to the large choice of ionic liquids, it is likely to find one with satisfactory properties. Only a few chiral ionic liquids have been described and their real potential in asymmetric synthesis has yet to be proven; therefore, chiral ionic liquids will be a subject of further development.

3 Application of chiral fluorous catalysts in asymmetric synthesis

Compounds that have long perfluorinated carbon chains are called “fluorous” and can be easily separable from organic compounds by a simple partitioning procedure with fluorous solvents, such as perfluorinated hexane (FC-72), and a standard organic solvent. In an ideal case, after the partitioning work up, almost pure products are obtained from the organic phase, and the fluorous products or reagents are recovered from the fluorous phase. The organic product and the fluorous product can also be separated by a simple filtration through fluorous reverse phase (FRP) silica gel.^{99b} These techniques allow a recovery of fluorous chiral ligands that often are laborious and expensive, thus making them attractive compounds for catalytic systems.

In 2000 Nakamura reported on the synthesis of chiral fluorous BINOL **108** and its application in asymmetric protonation of samarium enolates.¹⁰⁰ Starting from 2-methoxy-2-phenylcyclohexanone and samarium iodide, the corresponding enolate was generated and then protonated enantioselectively (85% ee) by (*R,S*)-FDHPEB (Scheme 38).



Scheme 38. Asymmetric protonation of samarium enolates in the presence of **108**

The reaction was performed in THF and after completion washed with FC-72 to recover the fluorous reagent quantitatively. The separation procedure was much simpler and more effective when the reaction mixture was filtered through the fluorous reverse silica gel (FRP silica gel). The product and the fluorous reagent were separated simply by eluting first with a fluorophobic solvent (acetonitrile) to obtain the organic product and then by fluorophilic solvent (FC-72) to recover FDHPEB. Recovered FDHPEB was used for the next reaction without further purification (see Table 11)¹⁰⁰.

Table 11. Asymmetric protonation of samarium enolate with (*R,S*)-FDHPEB

run	yield [%]	ee [%]	108 recovery [%]
1	82	81	98
2	81	85	97
3	78	86	98
4	74	89	99
5	73	87	99

Another example of application of fluorous BINOLs was reported by the same group in 2002.¹⁰¹ In the presence of **109** and titanium isopropoxide, a family of aromatic aldehydes was alkylated by diethyl zinc with high enantiomeric excess. The ligand was separated from the organic product with excellent recovery by filtration through FRP silica gel. The results are summarized in Table 12.

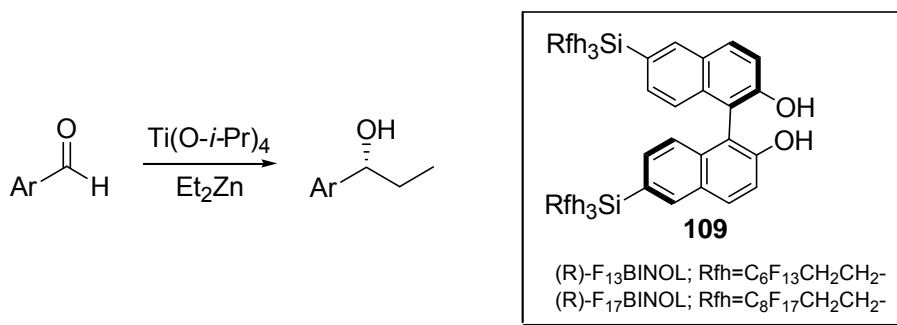


Table 12. Alkylation of aromatic aldehydes with Et₂Zn in the presence of fluorous BINOL

solvent	FBINOL	Ar	yield [%]	ee [%]	109 Recovery [%]
BTF/hexane(1:1)	F ₁₃ BINOL	Ph	92	84	99
BTF/hexane(1:1)	F ₁₇ BINOL	Ph	86	83	100
BTF/hexane(1:1)	F ₁₃ BINOL	4-MeO-C ₆ H ₄ -	97	80	96
BTF/hexane(1:1)	F ₁₃ BINOL	1-Naphthyl	98	91	98
BTF/hexane(1:1)	F ₁₃ BINOL	4-Cl-C ₆ H ₄	93	82	100

The same reaction was also performed in the FC-72/organic solvent biphasic system. In the mixture of toluene, hexane, and perfluorinated hexane the reaction proceeded easily, affording the product in the organic fraction in 81% yield and with 83% ee. The FC-72 fraction consisted of the fluorous ligand but about 10% of the ligand was also detected in the organic fraction. The problem was resolved by increasing the number of fluorine atoms from 13 to 17, which allowed an almost quantitative recovery (99%) of the ligand from the fluorous fraction.

Finally, the utility of the system was confirmed by experiment with consecutive reactions using (R)-F₁₃BINOL recovered from the fluorous silica gel. After the fourth runs the results were the same as after first one (see Table 13).

Table 13. Catalytic asymmetric addition of Et₂Zn to benzaldehyde reusing the same (R)-F₁₃BINOL

run	FBINOL	yield [%]	ee [%]	cat. recovery
1	F ₁₃ BINOL	92	84	99
2	F ₁₃ BINOL	93	85	97
3	F ₁₃ BINOL	96	84	99
4	F ₁₃ BINOL	89	83	99

Another family of ligands successfully applied in the fluororous realm are bis(oxazolines). In 2004 Simonelli¹⁰² reported on the synthesis of new perfluoroalkyl-substituted bisoxazolines **110-113** as chiral ligands for asymmetric Cu^{II}-catalysed reactions (Figure 20).

The utility of these new ligands was demonstrated in two enantioselective C-C bond-forming processes: the ene reaction and Mukaiyama aldol addition. The reactions were performed in dichloromethane and after completion the ligands were recovered by filtration through FRP silica gel. In the case of more highly fluorinated ligand **113** the use of a mixture of THF and FC-72 as the reaction solvent allowed the recovery of the ligand by simple separation of the solvents. Results from the ene reaction are summarized in Table 14.

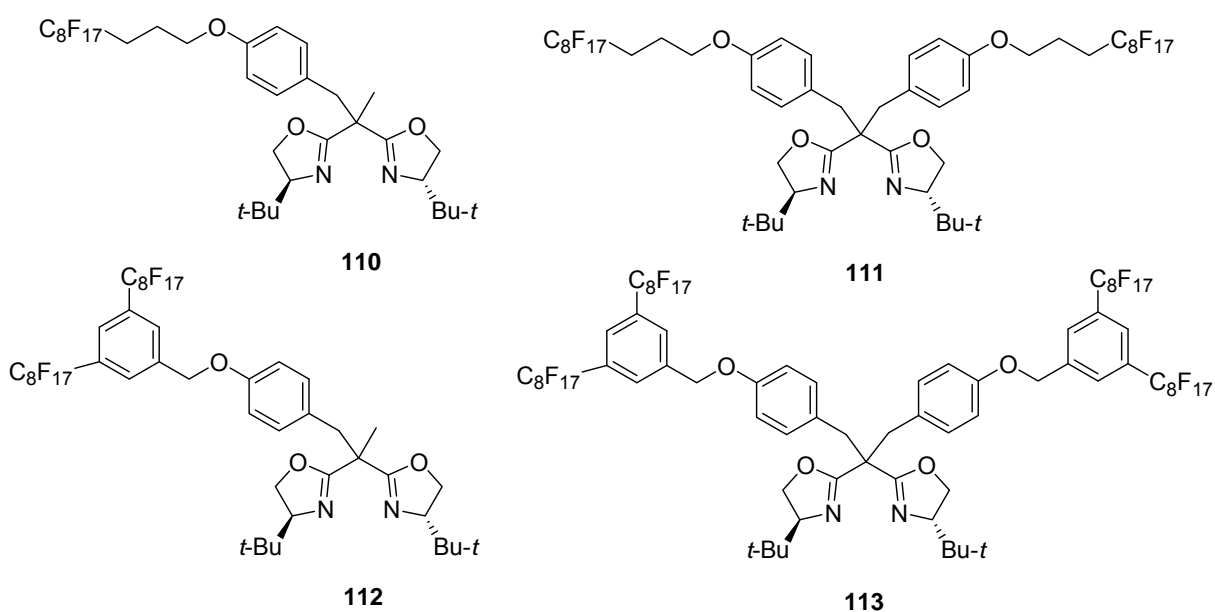


Figure 20. Structures of fluororous (bis)oxazolines

Recycled ligand **110** was used for the next reaction without purification, affording product **115** with similar results to the experiment carried out with a fresh sample of **110**. Ligands **112** and **113** were also applied to asymmetric cyclopropanation of styrene with enantioselectivities of 44-76%.¹⁰²

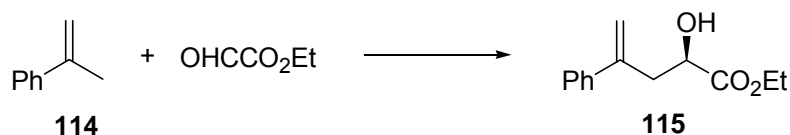


Table 14. An application of fluororous Bisoxazolines in Cu^{II}-catalysed ene reaction

catalyst	yield [%]	ee [%]	cat. recovery [%]
110 /Cu(OTf) ₂	65	74	78
111 /Cu(OTf) ₂	73	7	80
112 /Cu(OTf) ₂	99	67	77
113 /Cu(OTf) ₂	64	26	89

A few other examples of application of fluororous chiral ligand in asymmetric synthesis are shown below (Figures 21).¹⁰³

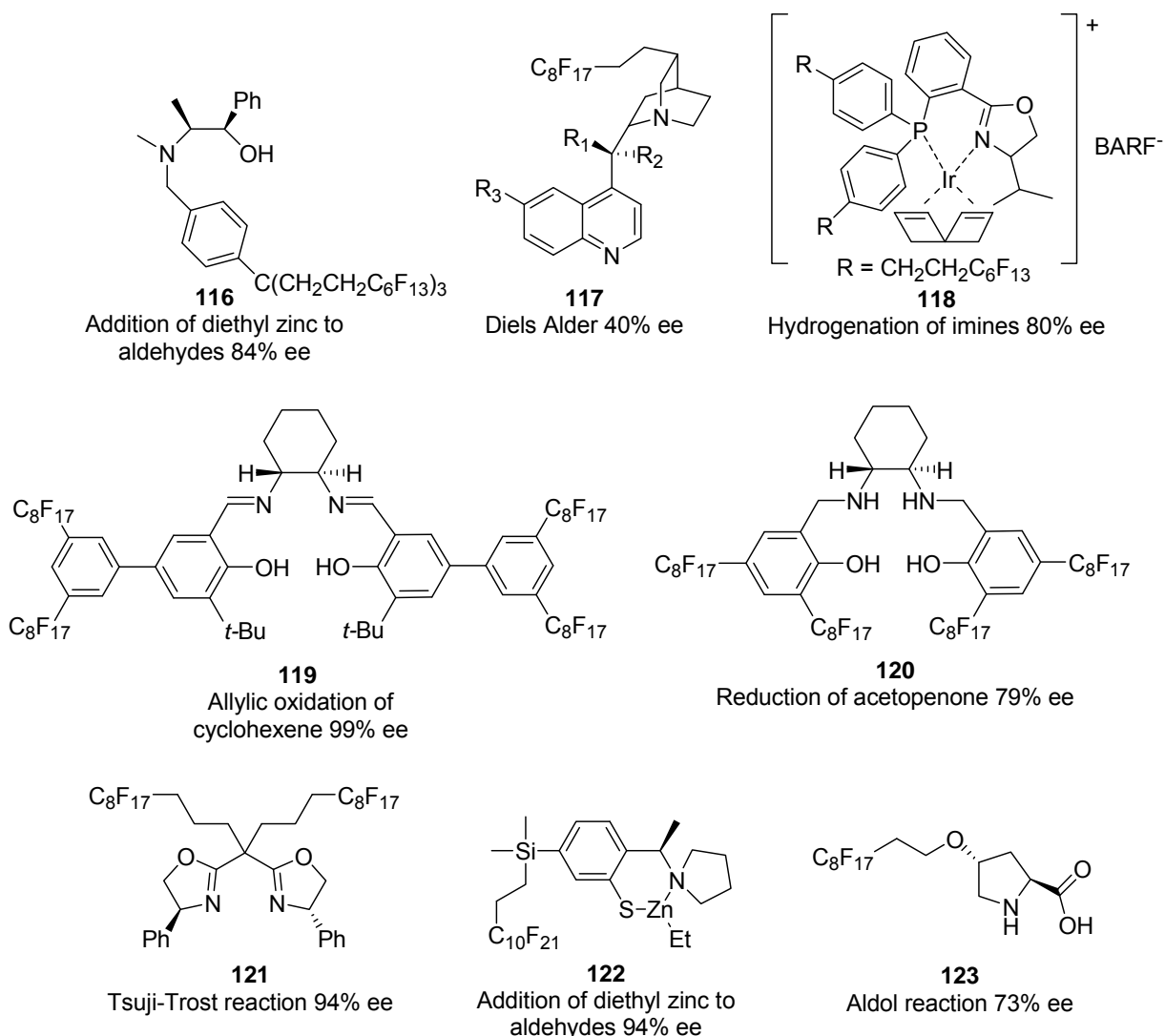


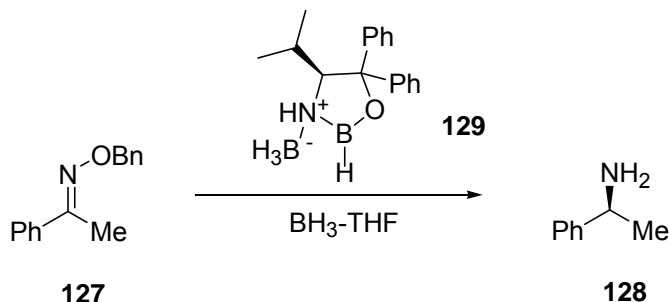
Figure 21. Fluororous ligands and catalysts in asymmetric catalysis

3.1 Application of chiral fluororous catalysts in asymmetric synthesis – conclusions

In conclusion, the primary objective of application of fluororous ligands is the creation of a catalytic system where fluororous ligand could be easily separated from the organic product(s) and recycled after each transformation. The numerous results published since 1994 show that asymmetric catalysis with fluorine containing ligands is now well established. However, the scope and limitations of this approach are far from being assessed. First, it is difficult to apply a fluororous biphasic technique, due to their low fluorine content which makes them also soluble in organic solvent. There must be 60% of fluorine content to ensure a biphasic catalysis and easy separation. Moreover, it is better to have several polyfluoralkyl chains spread around the carbon skeleton rather than only one even if the overall fluorine

content is the same. In the case of light fluororous ligands, the separation of the products from the catalytic system is possible by chromatography techniques, thanks to the difference of polarity induced by the fluorinated part of the ligand. The electron-withdrawing properties of fluorine often deactivate the catalyst, but the use of a carefully chosen spacer allows this problem to be avoided. In most cases, fluororous catalytic systems are recyclable at most one or two times with the same activity and selectivity. After a few runs, the ligand is decomposed, poisoned or there is metal leaching

(52% ee) was obtained when 10 mol% of the amino alcohol was used. Cho¹⁰⁶ reported on the application of **129** for the reduction of the imine derived from propiophenone and aniline; however, in the presence of 10 mol % of the catalyst, the product was formed in only 66% ee.



Scheme 40. Catalytic asymmetric hydroboration in the presence of **129**

Few other examples of catalytic asymmetric hydroborations of imines are shown in Table 15. Bolm¹⁰⁷ used the chiral β -hydroxy sulfoximine **131** and in the presence of 10 mol% of the catalyst, the product was formed in 70% ee (entry 2).

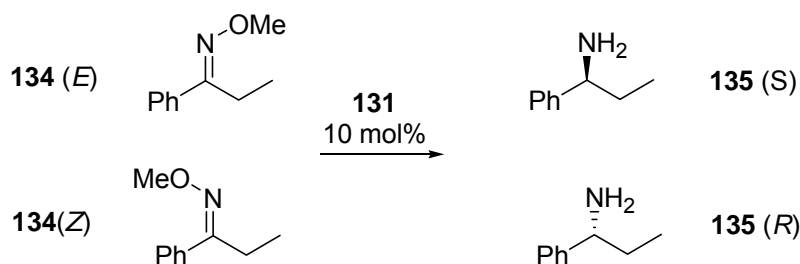
Table 15. Catalytic enantioselective reduction of imines with chirally modified boranes

entry	substrate	chiral source	borane	Yield (%)	Ee (%)
1			BH ₃ *THF	92	70
2			BH ₃ *SMe ₂	64	70
3			BH ₃ *SMe ₂	59	63
4			BH ₃ *THF	90	99

The same group revealed that the absolute configuration of the resulting amine depends of the substrate geometry.¹⁰⁷ In the reduction of oxime-ether **134** catalysed by **131**

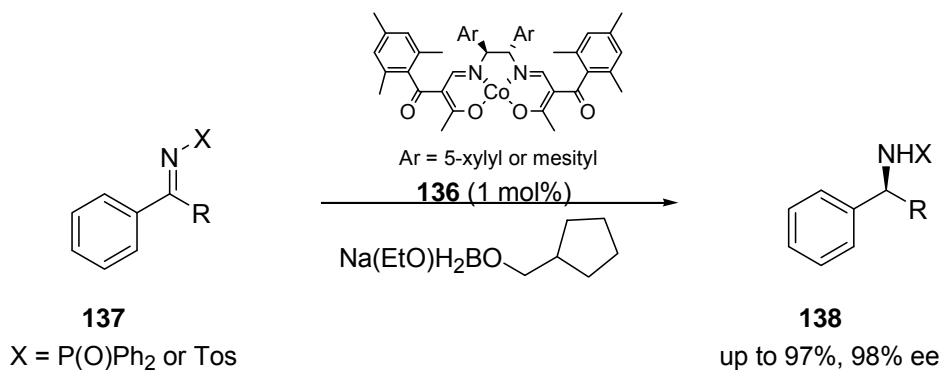
the (*E*)-isomer afforded the (*S*)-product, whereas the (*Z*)-imine produced the (*R*)-amine (Scheme 41).

Buono¹⁰⁸ performed the reduction of imines in the presence of 10 mol% of oxazaphospholidine **132** as the catalyst but the enantiopurity of the product was moderate (entry 3). Fujisawa¹⁰⁹ reported on the reduction of bisimine in the presence of **133** (entry 4). When 50 mol% of amino-alcohol **133** was used in the reduction, the product was formed with high yield (90%) and excellent selectivity (chiral/meso 95:5, 99% ee) but the distereoselectivity decreased in the presence of 10 mol% of **133** (71%, 73% ee).



Scheme 41. Asymmetric reduction of oxime ethers

A highly enantioselective borohydride reduction of imines using chiral cobalt(II) complex **136** was developed by Mukaiyama.¹¹⁰ Various *N*-tosyl or *N*-diphenylphosphinyl imines were reduced by pre-modified sodium borohydride with high chemical yield and enantioselectivity (Scheme 42).

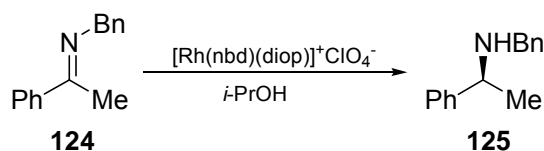


Scheme 42. Mukaiyama's catalytic enantioselective borohydride reductions

4.3 Catalytic asymmetric hydrogenation of imines

The catalytic asymmetric hydrogenation of imines, which utilizes inexpensive molecular hydrogen and metal complexes (Rh, Ru, Ir, Ti), has drawn much attention, since it provides one of the most efficient routes to the synthesis of chiral amines. However, in spite of great efforts in the recent decades and some excellent results, the process still remains a challenge in modern synthesis, which sharply contrasts with the relatively easy hydrogenation of olefins or ketones.

Reductive amination via catalytic asymmetric hydrogenation was first demonstrated in 1974 by Scorano,¹¹¹ who reported on reduction of imine **124** in the presence of a catalytic amount of the rhodium complex with (-)-DIOP. However, the resulting amine was obtained with in only 22% ee.



Scheme 43. Scorano's asymmetric reduction of imine **124**

An improvement of enantioselectivities was reported by Marko,¹¹² who tested a variety of diphosphine ligands in the reduction of imine **124** (Table 16). Almost racemic product was obtained when the reaction was carried out in the presence of (+)-DIOP in a mixture (1:1) of methanol and benzene at room temperature (entry 1). Significant improvement of the enantiopurity of the product was observed with diphosphine **139** under analogous reaction conditions (entry 2). Finally application of **140** in methanol in the presence of triethyl amine as an additive at 0 °C afforded the most efficient system as the product was formed in 83% ee (entry 4).

Table 16. Marko and Bakos asymmetric hydrogenation of imine **124**.

entry	Ligand/[Rh(nbd)Cl] ₂	solvent	additive	temp./°C	yield [%]	ee [%]
1	(+)-DIOP	MeOH/C ₆ H ₆ (1:1)	-	25	97	3
2	 139	MeOH/C ₆ H ₆ (1:1)	-	25	100	66
3	 140	MeOH	Et ₃ N	25	96	73
4	140	MeOH	Et ₃ N	0	100	83

James¹¹³ observed an improvement of enantioselectivities in the rhodium catalysed asymmetric hydrogenation of imines in the presence of KI (compare entries 2-4, Table 17). In the presence 1 mol% of an *in situ* generated catalyst based on ruthenium, and KI as an additive at -25 °C, imine **141b** was reduced quantitatively with 91% enantioselectivity.

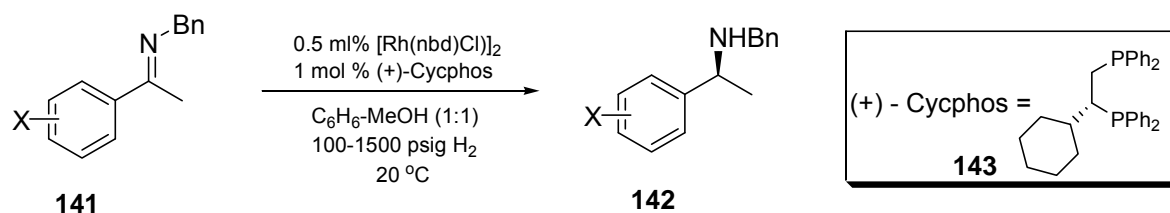
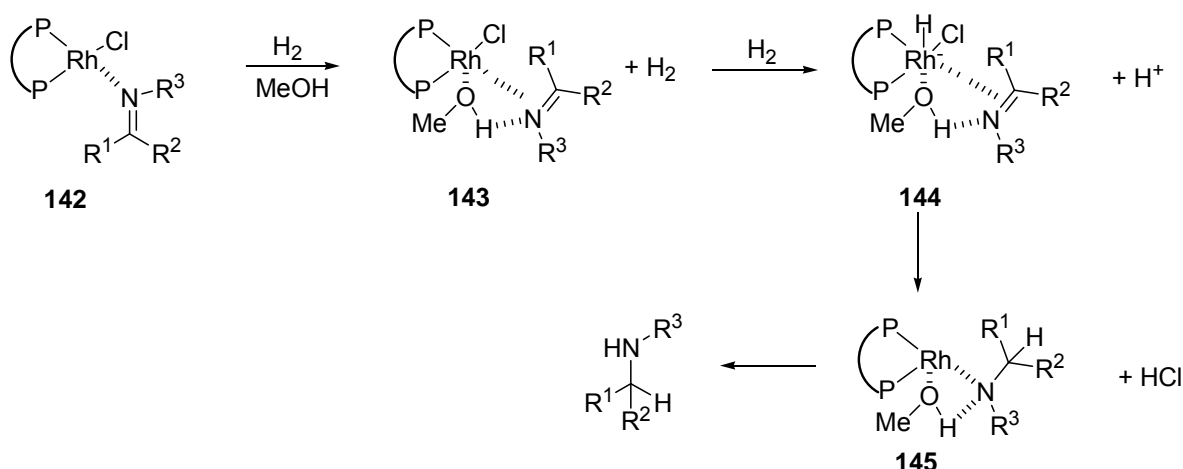


Table 17. Rh-catalysed asymmetric hydrogenation of imines in the presence of (+)-Cycphos

entry	Substrate	conditions	yield [%]	ee [%]
1	141a , X = <i>o</i> -OMe	KI	quant	71
2	141b , X = <i>p</i> -OMe	-	90	71
3	141b , X = <i>p</i> -OMe	KI	quant	84
4	141b , X = <i>p</i> -OMe	KI, Tol-MeOH(1:2), -25°C	quant	91
5	141b , X = <i>p</i> -OMe	Pre-formed[Rh(nbd)(cycphos)][PF] ₆	quant	0
6	141c , X = <i>o</i> -OH	-	0	

The same group also presented some mechanistic consideration.¹¹⁴ They suggested that chelate formation is not essential to obtain high yields and enantioselectivities.

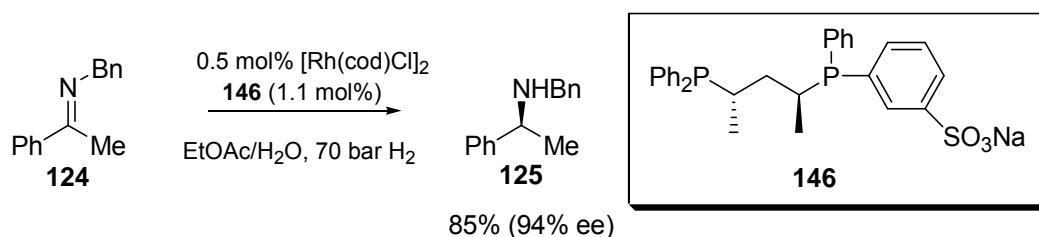


Scheme 44. Proposed mechanism for Rh-diphosphine complex-catalyzed enantioselective hydrogenation. Hydrogenation of imine **141a** resulted in the formation of the corresponding amine in 71% ee (entry 1) but no reaction was observed with **141c** (entry 6). When the reaction of **141b** was performed in the presence of preformed catalyst the yield was quantitative but no chiral induction was observed (entry 5).

According to the reaction mechanism of Rh-mediated hydrogenation by Longely and Wilkinson, oxidative addition of hydrogen to rhodium(I) is the first step of the reaction.¹¹⁵ On the other hand, James suggested that the reaction commences with coordination of the imine nitrogen to the rhodium center,¹¹⁶ followed by formation of the penta-coordinated Rh(I) intermediate, such as **143** (Scheme 44). The next step is a heterolytic cleavage of the

hydrogen molecule and formation of hydride **144**. Finally, hydride shift from rhodium to the imine carbon, and the cleavage of the Rh-N bond by the liberated proton produced the amine and regenerate the catalyst. The role of KI is not completely understood but it is believed that the iodide prevents the binding of two imines to the metal center.

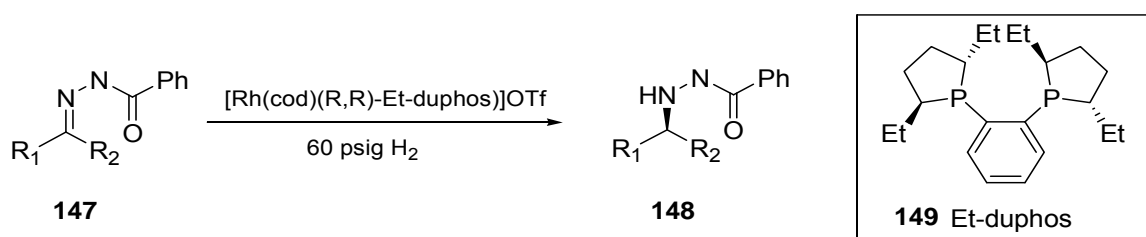
A two phase system for asymmetric hydrogenation of imines was studied by Sinou.¹¹⁷ Using partially sulfonated chiral diphosphine **146** (sulfonation degree = 1) in a water/ethyl acetate solvent system, amine **124** was obtained with excellent ee (94%) despite the fact that ligand **146** consisted of equimolar amounts of two epimers.



Scheme 45. Catalytic hydrogenation of imines in two phase system

In a further study it was revealed that enantioselectivity strongly depends on the degree of sulfonation of the diphosphine ligands, reaching the highest value (96% ee) at the sulfonation degree equal to 1.65.¹¹⁷

A cationic Rh(I)-DuPHOS complex was successfully applied in the enantioselective hydrogenation of various *N*-acylhydrazone derivatives by Burk.¹¹⁸ Benzoylhydrazones derived from acetophenone or pyruvate were hydrogenated enantioselectively up to 95% ee. Lower selectivities and reaction rates were observed for imines derived from aliphatic ketones (43-73% ee).



Scheme 46. Burk's asymmetric hydrogenation of hydrazones

Iridium catalysts for asymmetric reduction of imines were developed independently by Osborn^{119a,b} and Spindler^{119c} (Figure 22).

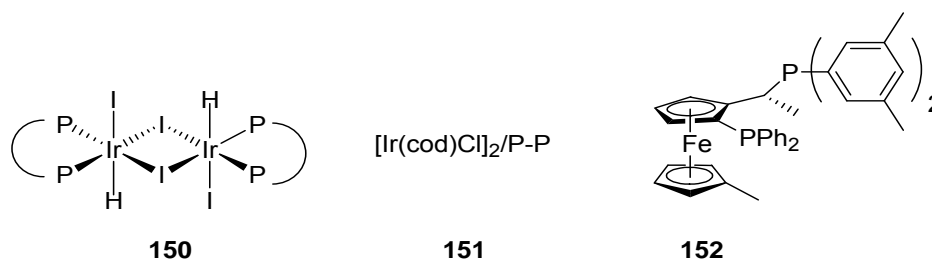
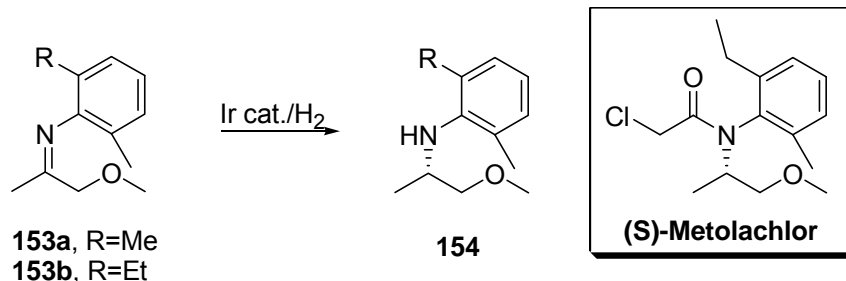


Figure 22. Examples of ligands and catalysts used in Ir-catalyzed hydrogenation of imines

The Osborn group used the catalyst **150**, prepared from [Ir(I)(P-P)(cod)]BF₄ and LiI (Table 18, entry 1), whereas the Spindler group used an *in situ* prepared catalyst (entry 2). In the asymmetric hydrogenation of imine **153a** (Scheme 47), reasonable activities and moderate enantioselectivities (~60-70% ee) were obtained (entries 1,2).



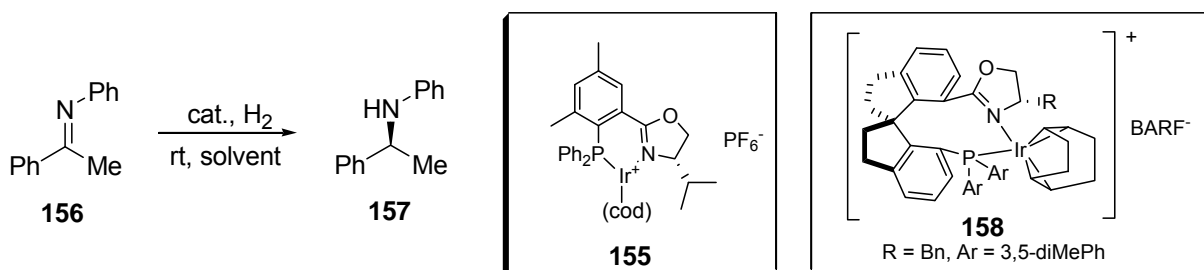
Scheme 47. Ir-catalyzed asymmetric hydrogenation of imines **154a,b**

In a further study, Spindler¹²⁰ used 1 ppm of a new type of ferrocenylphosphine-bound iridium catalyst Ir(I)/**152**/I⁻ to facilitate the hydrogenation of imine **153b**. The product of the transformation was formed in 80% ee (entry 3) and this methodology was applied to an industrial process of preparation of (S)-Metolachlor, a potent herbicide.

Table 18. Osborn and Spindler iridium catalysed asymmetric reduction of imine

Entry	Substrate	Catalyst	Substrate/Ir	ee
1	153a	150 ((+)-DIOP)	2000	63
2	153a	151 /(+)-DIOP/I ⁻	100	70
3	153b	Ir(I)/ 152 /I ⁻	1000000	80

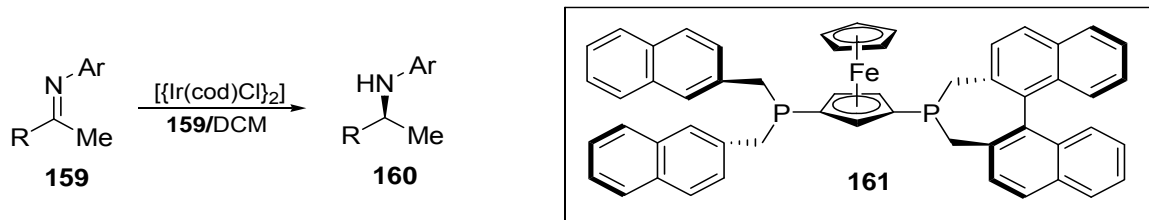
Iridium-phosphine-oxazolidine complexes were reported by Pfaltz¹²¹ as useful catalysts for asymmetric hydrogenation of imines. In the presence of 0.1 mol% of catalyst **155**, at 100 bar of H₂ in dichloromethane, *N*-phenyl imine **156** was reduced to the corresponding aniline in 99% yield and 89% ee (see Scheme 48).



Scheme 48. Catalytic asymmetric hydrogenation of imine **156** in the presence of **155** or **158**

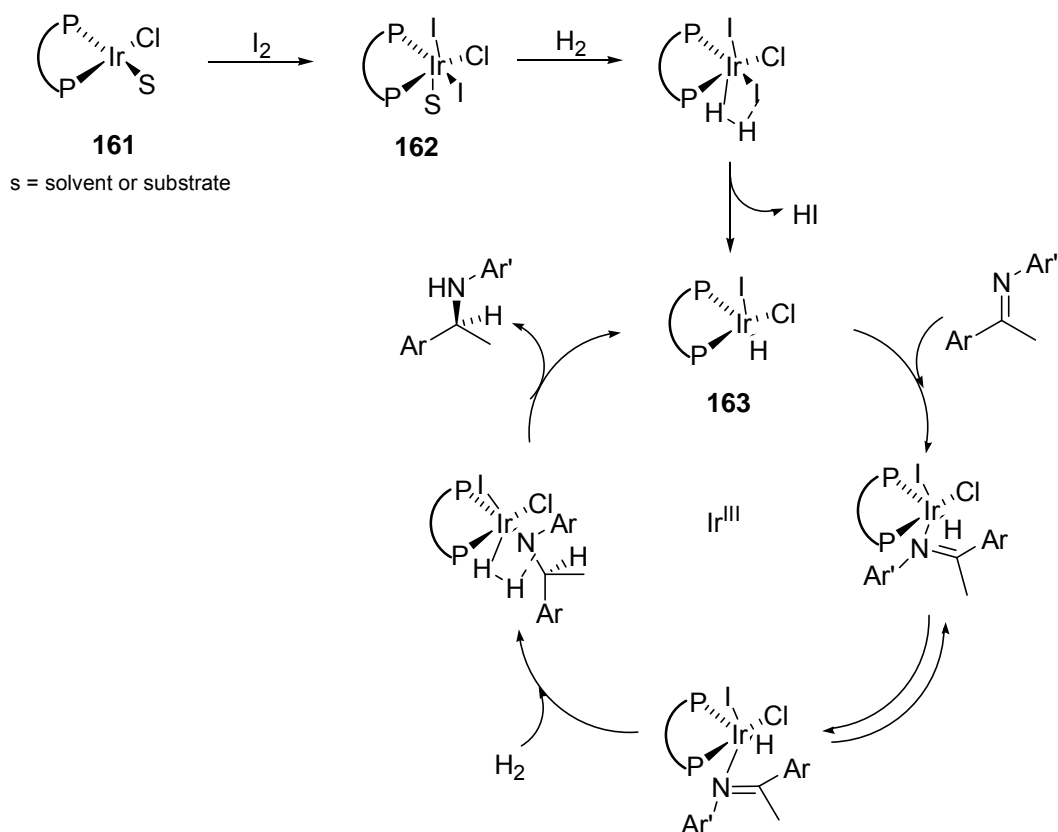
Further improvement of the process was reported by Zhou,¹²² who used the chiral spiro iridium/phosphine-oxazoline cationic complex **158** as the catalyst. The latter catalyst allowed the hydrogenation to be carried out under ambient hydrogen pressure and the product was formed in 93% ee.

Another example of iridium catalysed asymmetric reduction of imines was reported by Zhang.¹²³ Using the binaphane **161**-iridium complex as the catalyst, various aromatic imines were reduced to the corresponding amines (Scheme 49) with excellent enantioselectivities (up to 99%).



Scheme 49. Catalytic asymmetric hydrogenation of **159** in the presence of Ir-**161** as a catalyst

Lower levels of asymmetric induction were observed for the imines derived from aliphatic or acyclic ketones (up to 33% ee). In general, an increase of enantioselectivities (~10%) was observed in the presence of 10 mol% of iodine as an additive. The following mechanistic considerations were then reported¹²³ (Scheme 50).

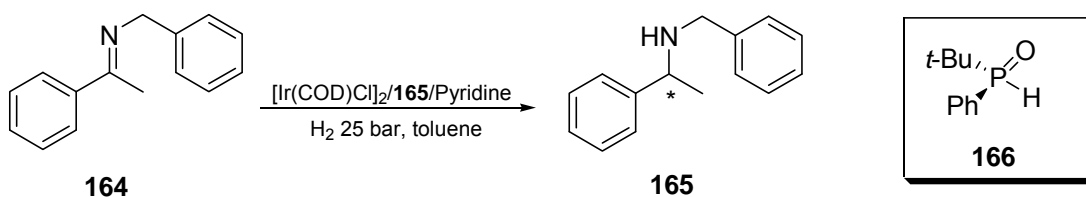


Scheme 50. Proposed mechanism for the Ir-f-binaphane-catalyzed hydrogenation of imines

The oxidative addition of H₂ to Ir^I to give Ir^{III} is a well known fact in hydrogenation of imines. However, Osborn¹²⁴ has demonstrated that Ir complex [$\{\text{Ir}^{\text{III}}(\text{P-P})\text{-HI}_2\}_2$] facilitates the hydrogenation of imines and that Ir^{III} species remains in the same oxidation state over the whole cycle. It was proposed that the heterolytic cleavage of H₂ by the Ir-N species can

generate amine and Ir^{III}-H species. In the industrial process for the synthesis of metolachlor, the addition of I₂ is critical in the hydrogenation of MEA imine and it was suggested that the addition of I₂ leads to the Ir^{III} pathway¹²⁵. Therefore it is believed that the addition of I₂ to the Ir^I precursor **161** generates the Ir^{III} complex **162**. Heterolytic cleavage of H₂ can occur in the presence of an amine to form the Ir^{III}-H species **163**. An imine substrate can coordinate to **163** in an η¹ or η² fashion, followed by migratory insertion of the η²-imine into the Ir^{III}-H bond to form an Ir^{III}-species. The heterolytic cleavage of H₂ by the Ir^{III}-amide intermediate gives an amine and regenerates the Ir^{III}-H species **163**.

Chiral secondary phosphine oxides as ligands in Ir-catalysed hydrogenation of imines were reported by de Vries.¹²⁶ When imine **164** was used as a substrate in the presence of 2.5 mol% of the catalyst precursor and 10 mol% of ligand **166** at room temperature, the reaction went to a completion yielding the product of 76% ee. It was found in a further study¹²⁶ that under the same reaction condition but in the presence of 10 mol% of pyridine, the enantiopurity of the product increased to 80% ee. Further improvement was observed when the reaction was carried out at 0 °C.

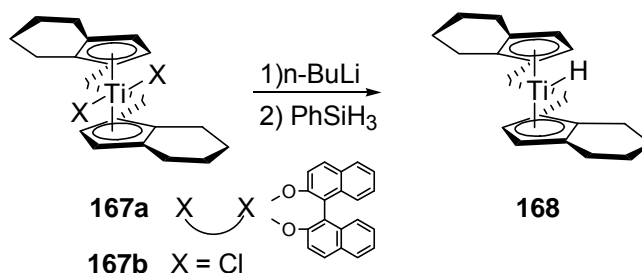


Scheme 51. Ir-catalyzed asymmetric hydrogenation of **164** in the presence of **166**

Although the application of the latter ligand was not as successful as in the previously described examples, the ligand's simplicity is the most important feature. Its preparation involves the reaction of *t*-BuMgBr with PhPCl₂, followed by hydrolysis and resolution by preparative HPLC.

Xylose diphospite and diphosphinite ligands have also been tested in iridium catalysed hydrogenation of imines¹²⁷ but the enantioselectivities did not exceed 57% ee.

The asymmetric hydrogenation of imines with chiral titanocene catalysts was presented by Buchwald.¹²⁸

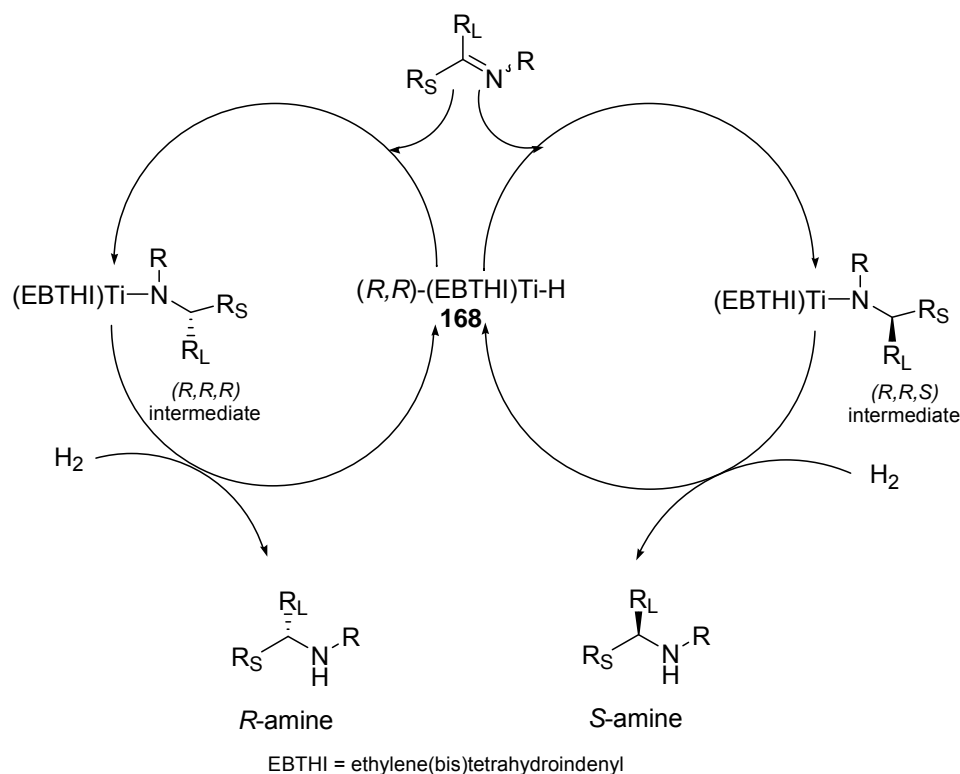


Scheme 52. Formation of the titanium (III) hydride species **168**

The catalyst was prepared by treatment of **167a** or **167b** with 2 equiv of *n*-butyllithium in THF, followed by 3 equiv of phenyl silane. Under these reaction conditions an active hydrogenation catalyst was formed, which is believed to be the titanium(III) hydride species **168** (Scheme 52).

The system was then tested in the hydrogenation of various imines, affording enantiomerically enriched amines with up to 99% ee. Enantioselectivities for acyclic substrates were generally lower ($\leq 81\%$ ee) as the acyclic imines exist as a mixture of slowly interconverting geometric isomers (for explanation see Scheme 53). Moreover, in contrast to cyclic imines, the hydrogenation of acyclic substrates was found to be hydrogen pressure dependant.

The following cycle for the reaction has been proposed (Scheme 53): The first step involves 1,2-insertion of the imine into the titanium hydride to form two diastereoisomeric titanium amide complexes, followed by their hydrogenolysis via a σ -bond metathesis process to form the enantiomeric amines and regenerate the titanium hydride **168**.¹²⁸



Scheme 53. Proposed reaction cycle for asymmetric hydrogenation of imines with chiral titanocene catalyst. Because of the high chemo- and enantio-selectivity observed for the cyclic substrates, it can be concluded that the pathway leading to the minor enantiomer do not contribute significantly to the mechanism.

An interesting example of Pd-catalysed asymmetric hydrogenation of imines was presented by Zhou¹²⁹ Using 2 mol% of palladium trifluoroacetate and *N*-diphenylphosphinyl ketimine **169** the reaction was carried out under 600 psi hydrogen pressure in 2,2,2-trifluoroethanol (TFE) in the presence of various diphosphine ligands. The results are presented in Figure 23.

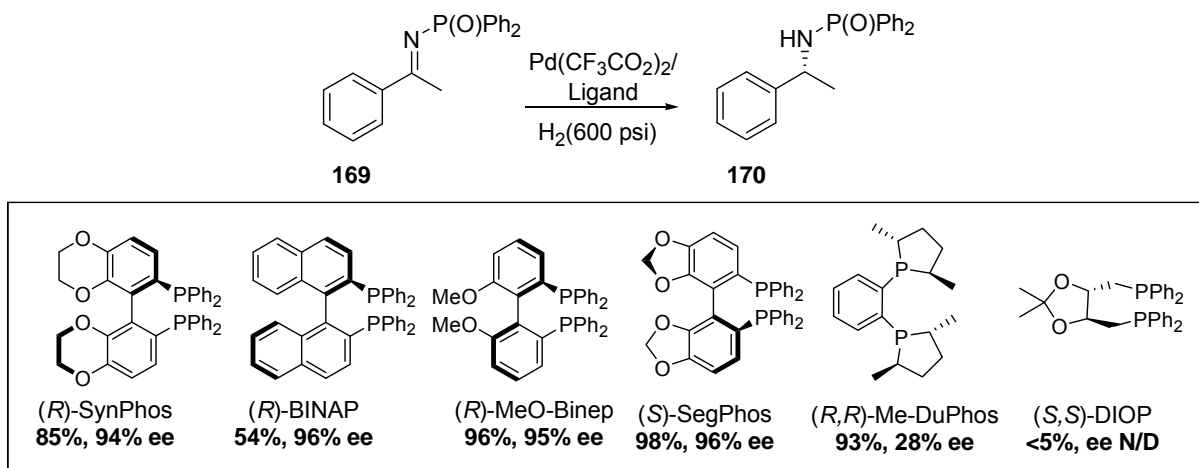
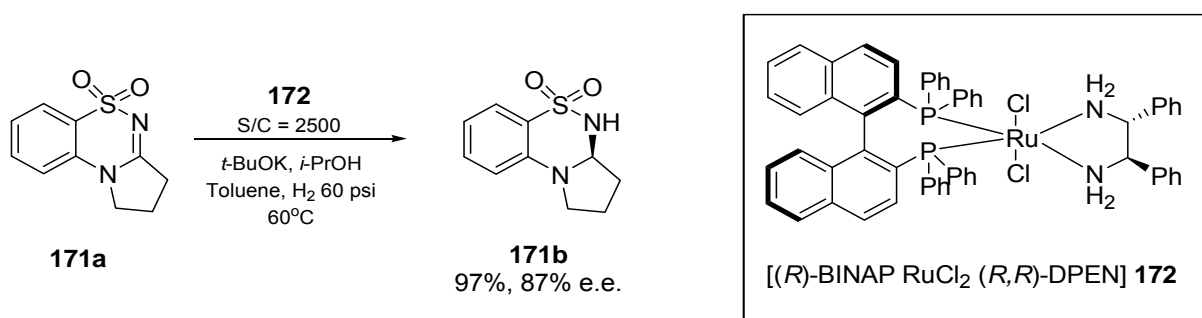


Figure 23. Pd-catalyzed asymmetric hydrogenation of **169** in the presence of various diphosphine ligands

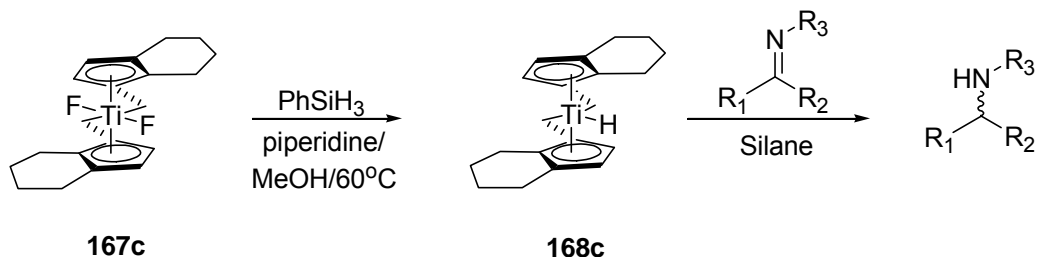
The best results were obtained in the presence of (*S*)-SegPhos (98%, 96% ee) and this ligand was used for further investigation. It was found later that the new catalytic system is tolerant for various substitution patterns for the imines, but only strongly electron-withdrawing groups (tosyl, diphenylphosphinyl) are acceptable as *N*-substituents in order to achieve high chemical yields and enantioselectivities. An attempt to replace trifluoroethanol with any common solvents (MeOH, EtOH, THF, DCM) failed as the yields decreased to the level of 5% and below.

Chiral ruthenium complexes are also recognized as effective catalysts in the asymmetric hydrogenation of imines. Lennon and Ramsden used a catalytic amount of the ruthenium complex **172** for hydrogenation of imine **171a**.^{130a} The corresponding product, which is a selective AMPA receptor modulator, was obtained in high chemical and enantioselectivity.



Scheme 54. Ru-catalyzed asymmetric hydrogenation of **171a**

enantioselectivities ($\leq 99\%$ ee) were observed for cyclic and acyclic *N*-methyl substituted substrates (ex.1, entry 1, Table 19); the worst results were obtained with bulky substituents on the nitrogen atom (entry 3). The authors believe that the titanium hydride **168c** is the active species, in analogy to the previously described hydrogenation process.



Scheme 56. Reduction of imines with silanes in the presence of **167c**

The convenient and inexpensive PMHS (polymethylhydrosiloxane) was much less efficient (entry 2). It was found later that a slow addition of 4 equiv of primary amine to the reaction mixture influenced the activity of the catalytic system. Among various additives investigated (entry 5-8), the best results were obtained with *iso*-buthyl amine (entry 8). The authors suggested the following explanation of the observed results: The rate determining step in the titanium-catalysed hydrogenation of imines has been proposed to be cleavage of the Ti-N bond in the intermediate amido complex through a σ -bond metathesis pathway. It is also believed that the introduction of an aliphatic amine into the reaction mixture might convert the titanium-amido intermediate into the more reactive complex and thereby lead to increase of the reaction rate. ^{132b}

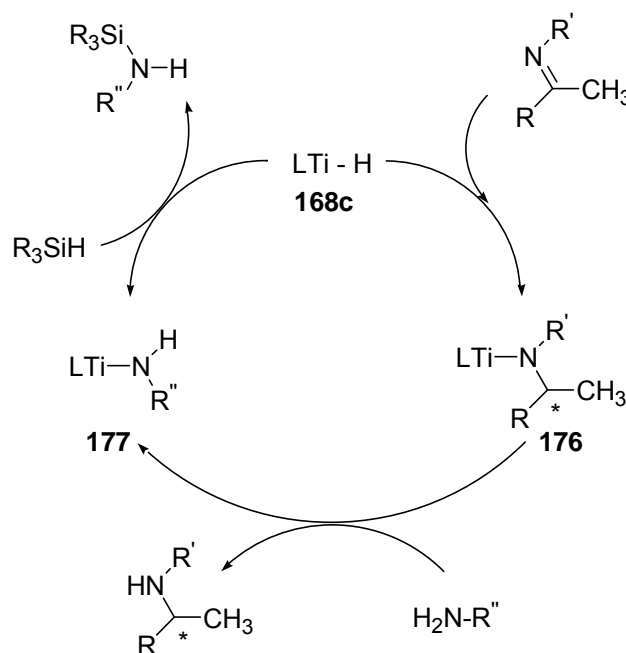
Table 19. Asymmetric hydrosilylation of imines in the presence of chiral titanocene **167c**

Entry	Substrate	Silane	Amine additive	Catalyst/eq.	Yield [%]	Ee [%]
1		PhSiH ₃	-	21/0.01	100	97
2		PMHS	-	21/0.1	50	-
3		PhSiH ₃	-	21/ 0.1	55	47
5		PMHS	-	21/0.05	5	-
6		PMHS	<i>n</i> HexNH ₂	21/0.05	100	85
7		PMHS	<i>t</i> BuNH ₂	21/0.05	39	-
8		PMHS	<i>i</i> BuNH ₂	21/ 0.01	100	92

PMHS – polymethylhydrosiloxane

A possible pathway of the reaction cycle is presented on the Scheme 57. Amines are obtained with the same absolute configuration as in the case of titanium-catalysed

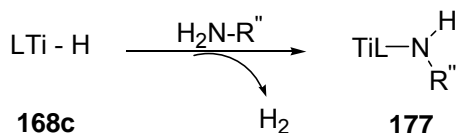
hydrogenation, which suggest that in the chirality-transfer step the imine is inserted into the Ti-H bond of titanocene hydride **167c** in analogy to the hydrogenation process.



Scheme 57. Postulated catalytic cycle

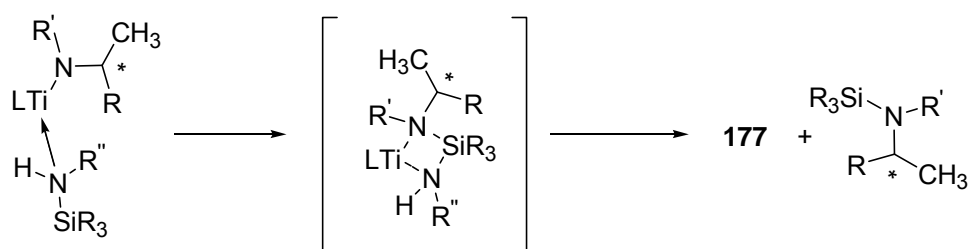
The additive would then react with the titanium – amido complex **176** to release a chiral amine and to regenerate amido complex **177**. Finally, reaction of **177** with silane regenerates **168c**.

The presented catalytic cycle also explains why slow addition of the additive is required. Thus, the promoter can react with titanocene hydride **168c** in a process that competes with imine reduction. When primary amine is present in high concentration, this reaction pathway becomes an important side reaction.



Scheme 58. Postulated catalytic cycle - a meaning of slow addition of primary amine

An alternative explanation of the effect of primary amine as the additive could be as follows: The amido complex **177** is transformed into *N*-silylamine and this species facilitate the cleavage through silylation of the Ti-N bond by coordination to the titanium center followed by σ -bond metathesis. This process is intramolecular, which would make it very facile. The product of amine exchange **177** can then be rapidly converted into **168c** and the silylated primary amine.



Scheme 59. Postulated catalytic cycle - an alternative mechanism of cleavage of Ti-N bond

It is significant that enantioselectivities achieved are not limited by the (*E/Z*) ratio of the starting imine. This methodology was successfully applied to the synthesis of (*S*)-coniine **179** with hydrosilylation of imine **178**^{132b} being the key step (Figure 25).

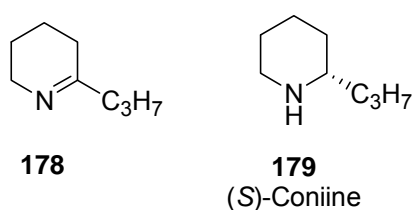


Figure 25. Ti-catalyzed asymmetric hydrosilylation of **178**

Copper-catalysed asymmetric hydrosilylation of imines was reported by Lipshutz in 2004.¹³³ In the presence of a catalytic amount of CuCl, NaOMe and (*R*)-(-)-DTBM-SEGPHOS **182**, various *N*-3,5-dixylylphosphinyl imines were reduced with tetramethyldisiloxane (TMDS) at ambient temperature with high chemical yields and enantioselectivities

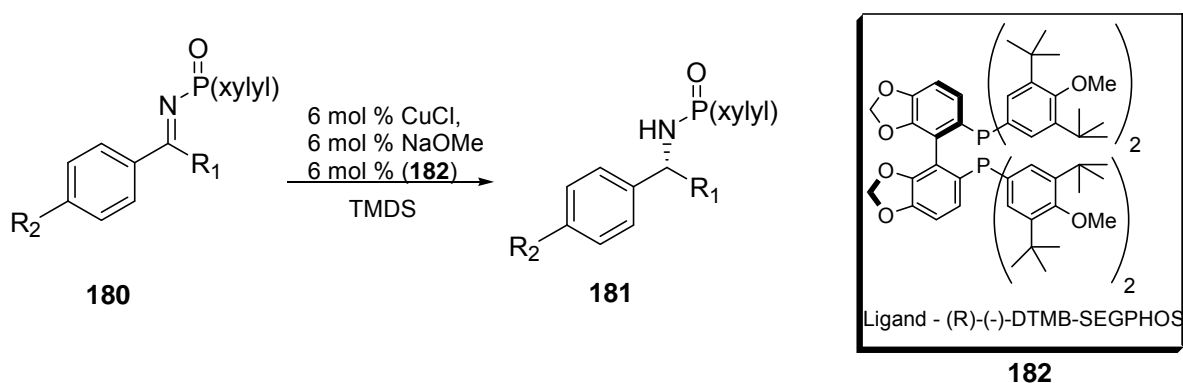


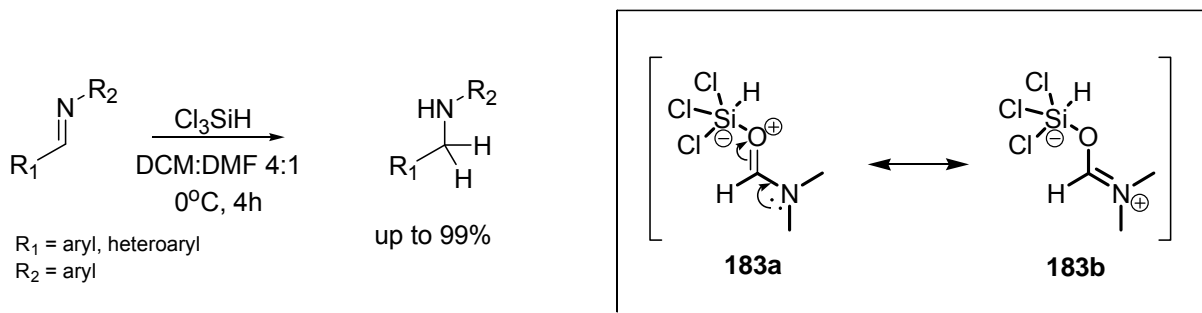
Table 20. Copper catalysed asymmetric hydrosilylation of imines

R ¹	R ²	yield [%]	ee [%]
Me	H	99	96
<i>i</i> Pr	H	93	97
Me	Br	95	96
Me	MeO	98	94
Me	F ₃ C	94	97

Although not indicated in Table 20, excellent enantioselectivities were also observed for cyclic substrates. An attempt to carry out the reaction at -25 °C improved enantioselectivities by about 3% ee. The initial amount of the catalyst can be decreased to as low as 1 mol% with no loss of enantioselectivity, though an increase of the reaction time action is required.

4.4.1 Catalytic asymmetric hydrosilylation of imines with trichlorosilane

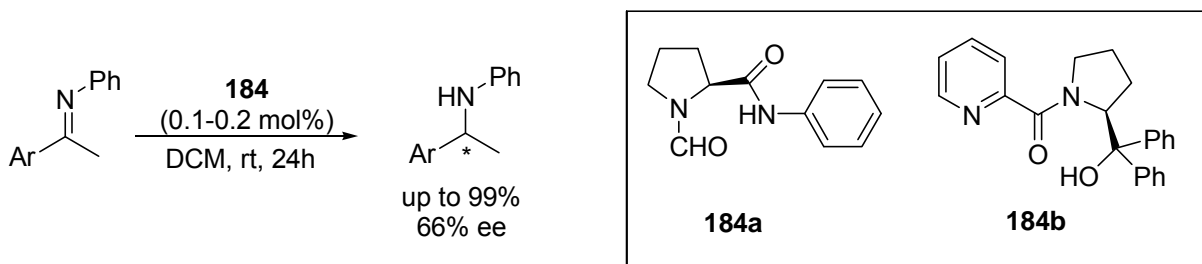
Among the variety of reducing agents developed to date, trichlorosilane, which combines low cost, stability, and easy handling, is one of the most potentially promising. Its activation does not require the presence of transition metals and as a result, its use is free of problems associated with metal catalysed reactions. The reduction of imines with trichlorosilane combines therefore the simplicity of hydrosilylation with the benefits of organocatalysis.



Scheme 60. Reduction of imine with HSiCl₃ in the presence of DMF as an activator

The first example of imine reduction with trichlorosilane was reported by Kobayashi.¹³⁴ In the presence of DMF as an activator, a variety of imines derived from aromatic and hetero-aromatic aldehydes was reduced with chemical yields up to 99%. In this reaction DMF coordinates the silicon reagent to form the hypervalent organosilicate intermediate **183**, which is sufficiently nucleophilic to carbonyl carbon of an aldehyde (Scheme 60).

Based on these findings, Matsumura^{135a} prepared the chiral analogue of DMF based on L-proline (**184a**) and tested it as an activator in the reduction of aromatic ketimines.

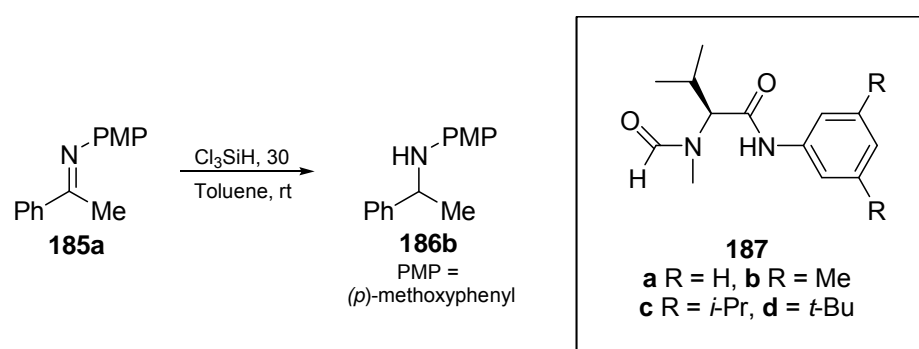


Scheme 61. Asymmetric reduction of aromatic ketimines with HSiCl₃ in the presence **184**

Although the catalytic system exhibited a high selectivity towards the imine bond and high chemical yields were obtained (up to 99%) the enantioselectivities were moderate (up to 66%, Ar = Ph).

Soon after that, the same group^{135b} reported on an improvement of enantioselectivities by using *N*-picolinoylpyrrolidine derivative **184b** (Scheme 61) but 73% ee in the reduction of Schiff base of acetophenone and aniline can still be considered as a moderate yield.

A significant improvement in the process was reported by Malkov and Kočovský.¹³⁶ They investigated the catalytic properties of chiral analogues of DMF deriving from α -amino acids and the best results were obtained with *N*-methyl-L-valine derived formamides **187a-d**.



Scheme 62. Asymmetric reduction of **185a** with HSiCl_3 in the presence **187a-d**

In a model reaction, reduction of Schiff base of acetophenone and *p*-anisidine (Scheme 62), high chemical yields and enantioselectivities were obtained in the presences of 10 mol% of catalyst **187a**¹³⁶ (Table 21, entry 1). Further improvement of enantioselectivity was attained with 3,5-dimethyl substituted derivative **187b**¹³⁶ (entry 2) and especially 3,5-diisopropyl and 3,5-ditertbutyl substituted catalysts¹³⁷ **187c** and **187d** (entries 4 and 6).

Table 21. Asymmetric reduction of imine **185a** with trichlorosilane catalysed by **187a-d**

entry	cat [mol%]	yield [%]	ee [%]
1 ^a	187a (10)	96	85
2	187b (10)	85	91
3 ^a	187b (10)	85	90
4	187c (10)	99	94
5	187c (5)	95	93
6	187d (5)	95	94
7	187d (1)	92	93

a-reaction carried out in chloroform

Although the model reaction was carried out in the presence of 10 mol% of the catalyst, its amount can be decreased to as low as 1 mol% without significant loss of activity or stereoselectivity (entry 7). However, the use of 5 mol% seems to be a compromise between low loading and excellent catalytic performance. The catalyst's performance is comparable in toluene and chloroform (compare entry 2 and 3), which extends the potential application of

the system. Although not indicated in the Table **21**, a decrease of reaction temperature to 0 °C results in a minor improvement in stereoselectivity, but for practical reasons room temperature seems to be the most convenient.

The application of the system can be extended to substrates with different substitution pattern, which afford enantiomerically enriched amines with good to excellent yields and enantioselectivities.¹³⁷ The product of the reduction of imine **185g** can be transformed, into the enantiopure **188**, demonstrating an efficient way of preparation of optically pure aziridines.^{138b}

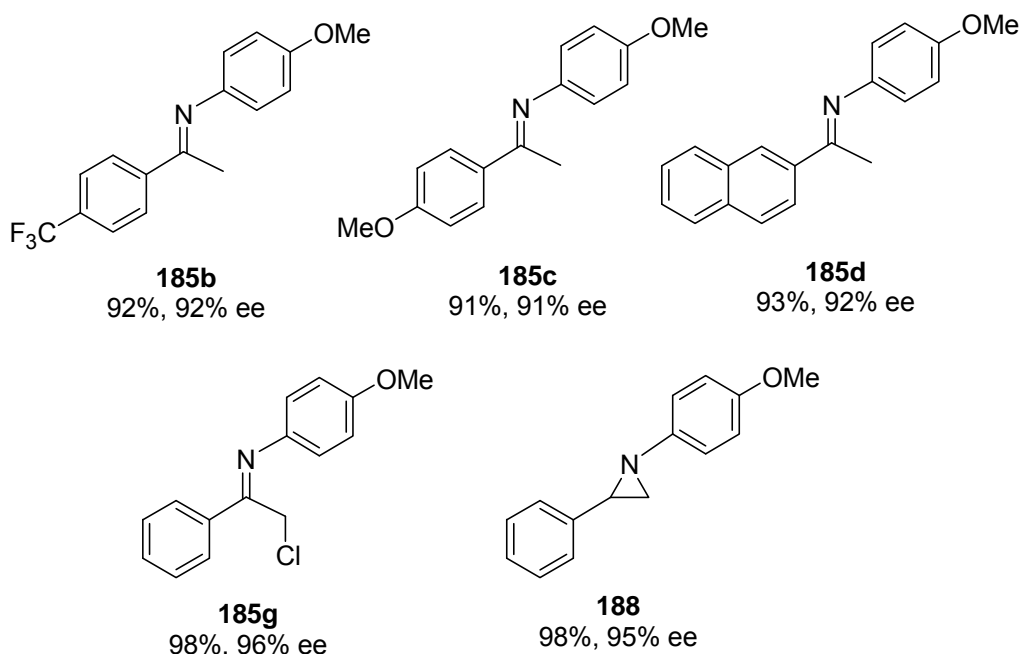


Figure 26. Asymmetric reduction of imines with trichlorosilane catalyzed by **187d** (5 mol%)

Although the exact mechanism of the reaction is not understood, catalysts and substrates screening under various reaction conditions revealed the following facts:^{138a} The catalyst is required to possess two amide groups. Secondary anilides were identified as efficient catalysts, whereas the tertiary anilides proved inert. The reaction does require an *N*-Ar group to be part of the catalyst since *N*-alkyl derivative failed to catalyze the reaction. The presence of electron-withdrawing substituents in 3 and 5 positions of the aryl amide partly decreased enantioselectivity whereas alkyl substituents increase it in the order Me < *i*-Pr ≤ *t*-Bu.

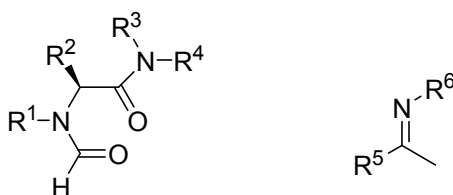


Figure 27. Structural requirements for catalysts and substrates in the reduction of imines with HSiCl₃

The tertiary formamide group is a prerequisite for the catalytic activity. The carbonyl oxygen must be sufficiently Lewis basic and simultaneously the group must be sufficiently small (Me the best). The role of the *N*-Me group in the formamide moiety is important for enantioselectivity, though not crucial for the reaction to occur. It can be hypothesized that the *N*-methyl is responsible for assuming the right conformation of the formamide group that conveys the chiral information from the chiral center. Finally, among various substituents in the side chain of the amino acid investigated (*i*-Pr, *t*-Bu, PhCH₂, *c*-Hex, Me) the best results were obtained with L-valine derivatives. Interestingly, the alanine derivative with the Me substituent induced the formation of the opposite enantiomer with modest enantioselectivity. The side chain is apparently responsible for inducing subtle conformational changes of the catalyst, which play a key role in determining the sense of enantiodifferentiation in the transition state.

The structural requirements for imines are as follows: R⁵ group should preferably be aromatic to attain high conversion and enantioselectivity. Both electron-donating and electron-withdrawing groups are well tolerated. With a non-aromatic group in this position, the reaction does occur but with lower degree of asymmetric induction. The R⁶ must be aromatic to attain high asymmetric induction. The absence of conjugation does not prevent the reaction but results in the formation of a practically racemic product. Steric congestion close to the nitrogen should be avoided as it results in a dramatic decrease in the reaction rate and enantioselectivity. The good enantioselectivity with *p*-methoxy derivative is particularly important, since this electron-rich aryl group can be removed by oxidative methods, which extends this methodology to the synthesis of primary amines.

Another feature of the system is the linear relationship between the enantiomeric purity of the catalyst and the product, suggesting that no more than one molecule of the catalyst is involved in the enantiodifferentiating process.

An important feature of the system is the presence of Brønsted acid necessary for the effective outcome of the reaction. Trichlorosilane is normally contaminated with traces of hydrogen chloride. However when the reaction was carried out in the presence of base as an additive, the formation of product was not observed. Combining this fact with the structural requirements, the following mechanism can be envisaged: as it has already been presented by Kobayashi, the formamide oxygen coordinates trichlorosilane to form a hypervalent organosilicate, which is sufficiently nucleophilic to react with the imine. The importance of acid suggests that protonation of the imine occurs and the resulting protonated imine might coordinate to a carbonyl oxygen of anilide (the approach of protonated imine to the catalyst is

restricted by substituents in the catalyst and the substrate). At this point one side of imine is more accessible for the reducing agent than the other. Stereoselective 1,2-addition of trichlorosilane produces a silylated amine, which undergoes hydrolysis upon aqueous workup.

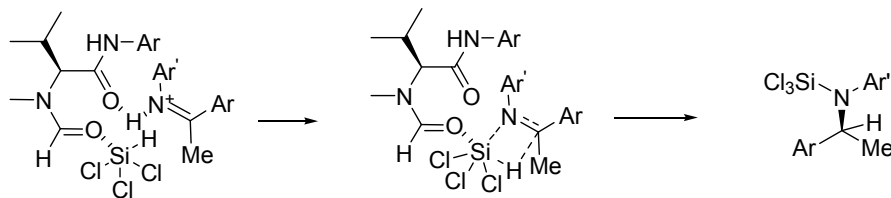


Figure 27a. Postulated outcome of the asymmetric reduction of imines with trichlorosilane catalysed *N*-methyl-L-valine-derived formamides

Several other effective Lewis-basic organocatalysts for the reduction of imines with trichlorosilane were reported by Sun.¹³⁹

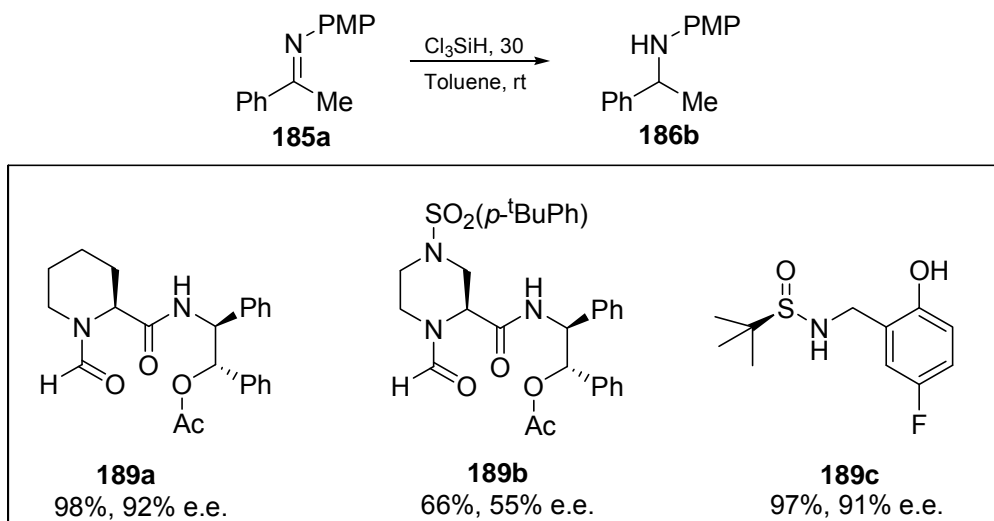
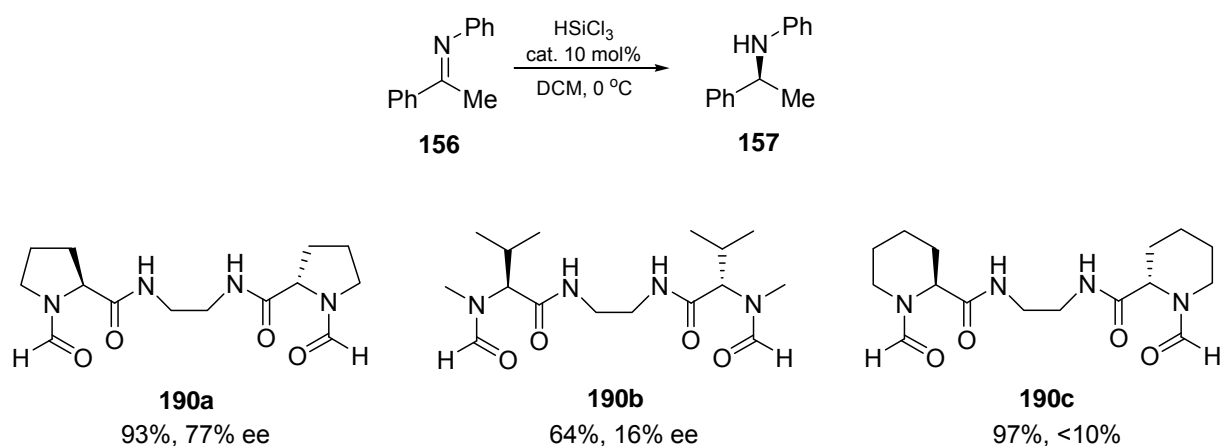


Figure 28. Asymmetric reduction of imine **185** in the presence of **189a-c**

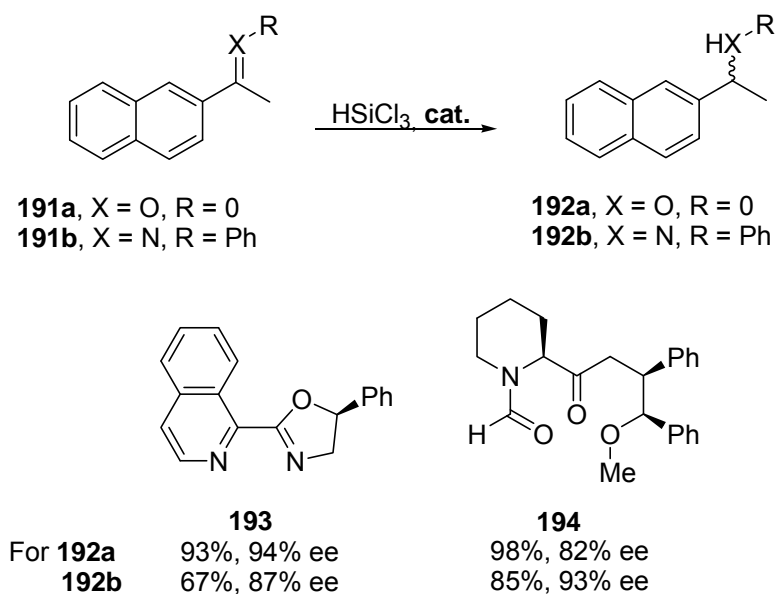
All activators were tested using dichloromethane as a solvent. When 10 mol% of L-pipecolinic acid derivative **189a** was used as an activator at 0 °C imine **185** was reduced with excellent yield and enantioselectivity. Moreover, the scope of application could be extended to substrate with different substituents pattern reaching the level of 96% ee. Catalyst **189b** has also proved to be stereoselective (up to 97% ee at -20 °C) but was generally inefficient for ketimines with substituted *N*-phenyl groups. Finally, the activity and stereoselectivity of the S-chiral sulfonamide **189c** could be compared to that of catalysts **189a**, although higher loading (20 mol%) and lower temperature (-20 °C) were required to reach comparable results. Sulfonamide **189c** is the first efficient organocatalyst relaying solely on a chiral sulfur center for stereochemical induction in this reaction^{139c}.



Scheme 63. Asymmetric reduction of **156** with trichlorosilane catalyzed by **190a-c**

The same group reported a synthesis and investigation of the catalytic activities of C_2 -symmetrical activators.¹⁴⁰ Comparison of the results from the reduction of imine **156** is presented on Scheme 63. Interestingly, while both the L-valine backbone and the L-pipecolic acid backbone have proven to be superior to the L-proline backbone in the diamide catalytic systems, in the C_2 -symmetric tetraamide catalytic system different scenario was observed. Catalysts **190b** and **190c** exhibited much lower enantioselectivity than the L-proline derived catalyst **190a**. It was confirmed later that the synergic effect of two L-proline segments is essential to obtain high stereoselectivities. The application of **190a** could be extended to substrates with different substitution pattern with enantioselectivities up to 86%.

All activators of trichlorosilane described so far could be applied exclusively to the stereoselective reduction of imine bonds. Activators suitable for the reduction of both ketones and imines have been reported by two groups independently.



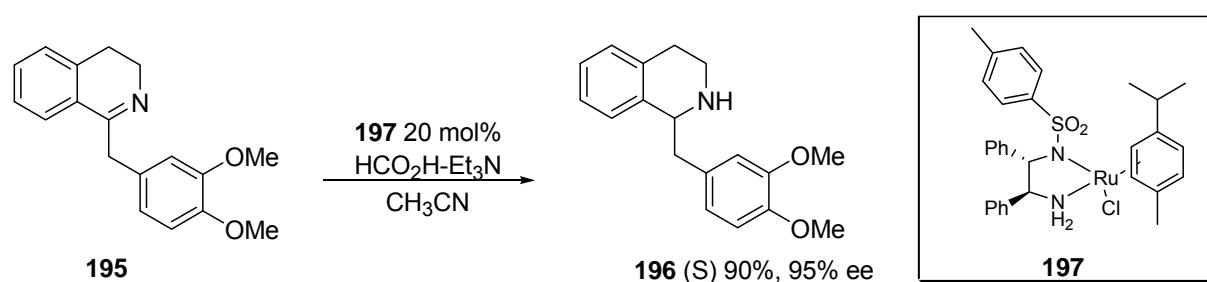
Scheme 64. Asymmetric reduction of imine **191a,b** with trichlorosilane catalyzed by **193** and **194**

Malkov and Kočovský^{141a} successfully applied 1-isoquinolyl catalyst **193**, which provided by far the best enantioselectivities in the organocatalytic hydrosilylation of ketones, (up to 94% ee) and excellent enantioselectivities in the reduction of imines (up to 87% ee). Reduction of the same substrates in the presence of **194**, reported by Sun,^{141b} afforded enantiomerically enriched alcohol in 82% ee and amine in 89% ee.

4.5 Catalytic asymmetric transfer hydrogenation of imines

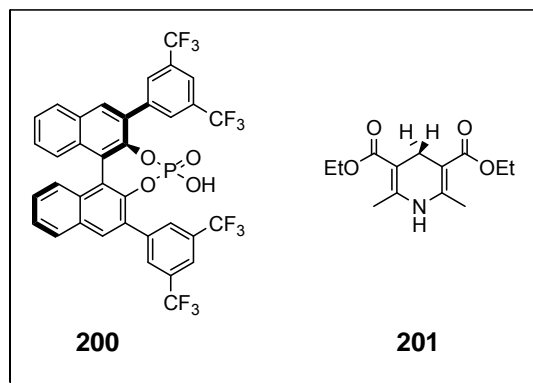
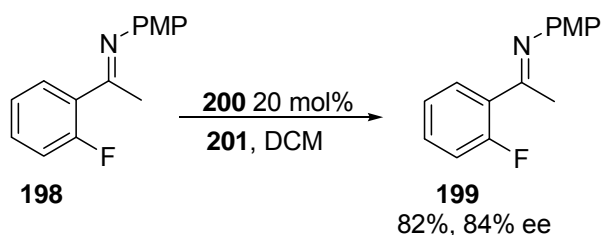
The last general procedure for reduction of imines is called transfer hydrogenation, a reaction using nonhazardous organic molecules, providing a useful complement to catalytic reduction that use molecular hydrogen, particularly for small and medium scale reactions.

An effective protocol for asymmetric reduction of imines *via* transfer hydrogenation was developed by Noyori.¹⁴² In the presence of 0.1-1mol% of the ruthenium complex **197**, a variety of imines were reduced using a 5:2 mixture of formic acid and triethylamine, affording the corresponding amines with moderate to excellent enantioselectivity. Lower enantiomeric excess was observed for geometrically unstable acyclic substrates (77% ee), whereas cyclic imines afforded products with excellent enantioselectivities (Scheme 65).



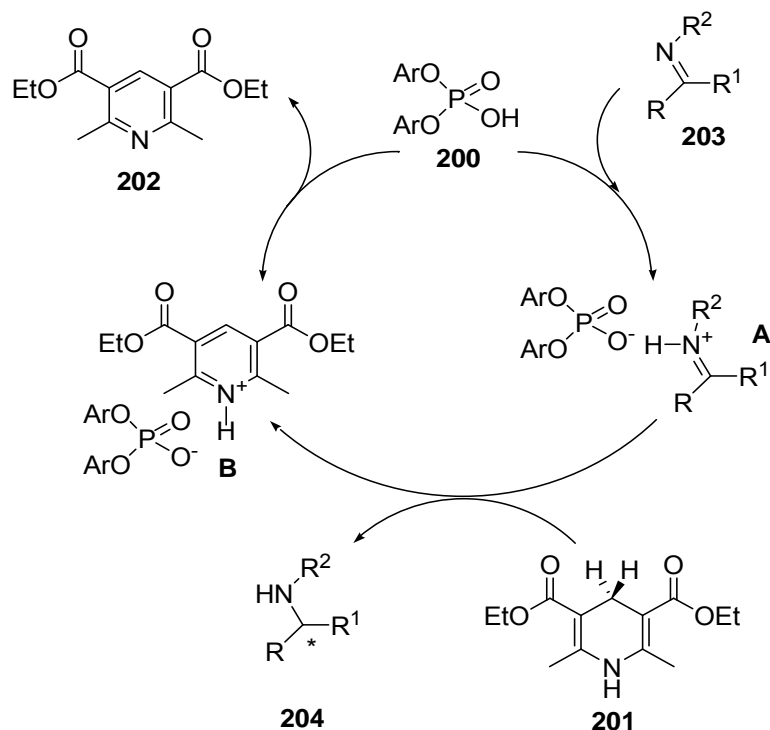
Scheme 65. Asymmetric reduction of imine **195** in the presence of **197**

The rate and enantioselectivity are found to be influenced by η^6 -arene and 1,2-diamine ligands in **197**. The NH_2 and ArSO_2 groups play crucial roles in attaining high reactivity and cannot be modified, while the structure of the aryl substituent of ArSO_2 and the substitution pattern of η^6 -arene ligand may be fine-tuned, depending on the imine substrate. Although the exact mechanism has not been elucidated, the authors believe that in the stereo-determining hydrogen-transfer step, the chiral Ru species, probably a hydride, formally discriminates the enantiofaces at the sp^2 nitrogen atom of the cyclic and acyclic imine, generating a stereogenic sp^3 carbon. The existence of acyclic imines as an interconverting mixture *syn* and *anti* isomers tends to lower the extent of enantioselectivity.



Scheme 66. Asymmetric reduction of imine **198** in the presence of **200**

An organocatalytic version of asymmetric reduction of imines via transfer hydrogenation was presented by two groups independently. Rueping¹⁴³ reported on the use of a catalytic amount of the chiral Brønsted acid **200** in the reduction of imines with Hantzsch dihydropyridine **201** as the hydrogen source. High chemical yields ($\leq 91\%$) and moderate enantioselectivities were obtained, with the best results observed for **198** (Scheme 66). Mechanistically, it is assumed that the activation of ketimine **203** by protonation with Brønsted acid **200** generates the iminium ion **A**. Subsequent hydrogen transfer from dihydropyridine **201** yields the chiral amine **204** and pyridinium salt **B**, which undergoes proton transfer to regenerate Brønsted acid **200** (Scheme 67).



Scheme 67. Postulated catalytic cycle

At the same time a similar study was reported by List.¹⁴⁴ However, the reaction carried out in the presence of Brønsted acid **205** were generally faster (42-71 h versus 72 h), temperatures lower (35 °C versus 60 °C), yields (80-98% versus 46-91%) and ee values

(80-93% versus 68-84%) higher. Most importantly, loading of the catalyst presented by List is much lower than that presented by Rueping (1 mol% versus 20 mol%).

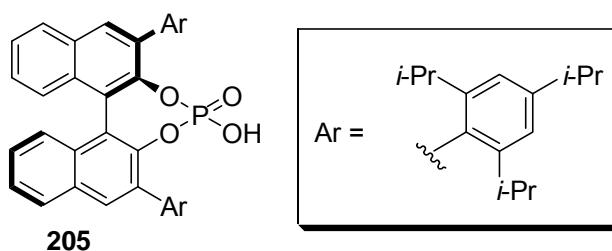


Figure 29. List's catalyst for organocatalytic asymmetric transfer hydrogenation of imines

Brønsted acids of type **205** were also successfully applied in organocatalytic enantioselective reduction of pyridines,^{145a} quinolins,^{145b} benzoxazines, benzothiazines, benzoxazinones,^{145c} asymmetric Strecker reaction^{145d} and asymmetric reductive amination of aldehydes via dynamic kinetic resolution.^{145e}

In conclusion, despite the growing demand for the preparation of chiral secondary amines by pharmaceutical companies, their enantioselective synthesis is still a challenge. Although many methods have been developed to carry out this transformation, none is general. Many effective procedures for aromatic imines failed in the case of aliphatic substrates. The existence of inseparable mixture of (*E/Z*) isomers, especially in the case of acyclic substrates, and the difference in reactivity of imines containing different nitrogen substituents still remain to be a problem only partly solved.

RESEARCH

5 Synthesis of new recoverable catalysts and their application in asymmetric reduction of imines with trichlorosilane - Introduction

Asymmetric reduction of imines represents one of the most efficient method of preparation of chiral amines. Catalytic hydrogenation of imines in the presence of transition metal complexes is a well established method and serves as an example of atom economy process because both atoms of hydrogen molecule are transferred to the product. However, the application of this methodology is associated with some problems: first, a potential metal leaching into the product must be carefully checked at the ppm level for application in drug industry; second, the use of high pressure causes some technological difficulties. Metal recovery constitutes another problem as its cost increases the overall cost of the process. Transition metals are also known as capricious entities since their activity may be suddenly reduced by unforeseen factors, such as impurities in the solvent or substrate imines, which is another limitation for their wider application. Asymmetric hydrosilylation of imines is free of problems related to the use of high pressure but it shares with hydrogenation the problems associated to the use of transitions metals.

Metal-free organocatalysis can be regarded as an attractive alternative to those process in which the metal is not vital for the key bond-forming process. The amino acid-derived formamide catalysts **187** (Figure 30), developed in our laboratory,^{136,137} proved to be very efficient and versatile in asymmetric reduction of imines with trichlorosilane. The catalyst loading could be reduced to 1-5 mol%.^{136,137} However, even this considerably reduced amount appears as a contaminant in the product and has to be separated. It was therefore of a great interest to create the recyclable analogues of the highly efficient catalysts **187**, which could be easily separable from the product after completion of the reaction and suitable for multiple use. In the first part of my research I decide to modify the existing catalysts **187** with a fluororous tag (**206**) and explore the opportunities of fluororous technology.

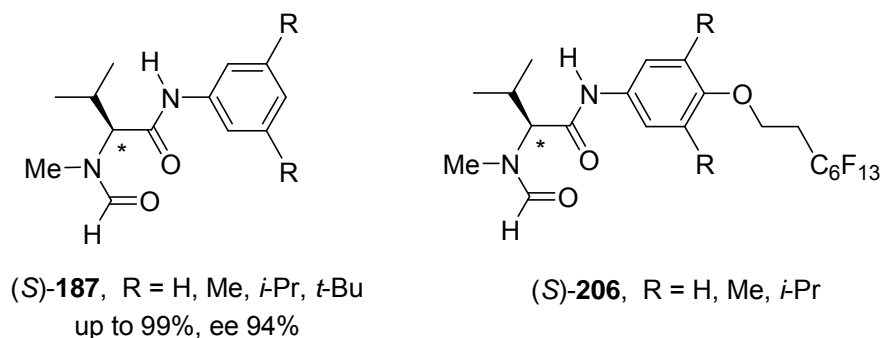


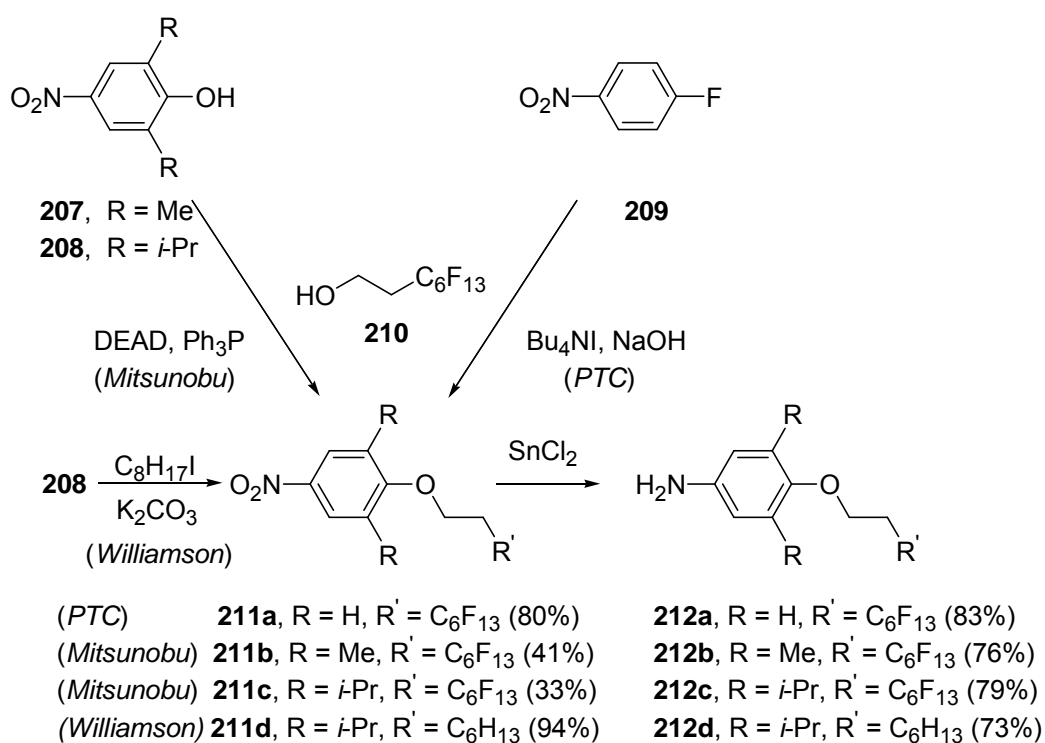
Figure 30. Catalysts for the asymmetric reduction of imines with trichlorosilane **187** and the proposed fluororous modification **206**.

5.1 Synthesis and application of fluoros modification of *N*-methylvaline-derived formamides

A strategy for the synthesis of target catalysts **206** was based on the methodology developed for *N*-methylvaline-derived formamides **187** involving a four-step reaction sequence¹³⁶: *N*-methylation of BOC-protected L-valine, condensation of the product with a substituted aniline, deprotection and formylation of the methylamino group. An important problem was to obtain appropriate anilines bearing suitable fluoros chain that ensure the adaptation of literature methods during synthesis and a good separation of the target molecule during filtration through FRP silica gel. Although the presence of the fluoros chain should not influence chemical properties of target catalysts, their utility in catalytic hydrosilylation of imines remained imponderable.

5.1.1 Synthesis of Substituted Anilines

The key substrate in the synthesis of fluoros anilines was the commercially available alcohol **210** and we envisaged that the attachment of the fluoros tag should be possible via the construction of an ether link, either via alkylation of suitable nitrophenol or via aromatic nucleophilic substitution.



Scheme 68. Synthesis of fluoros anilines

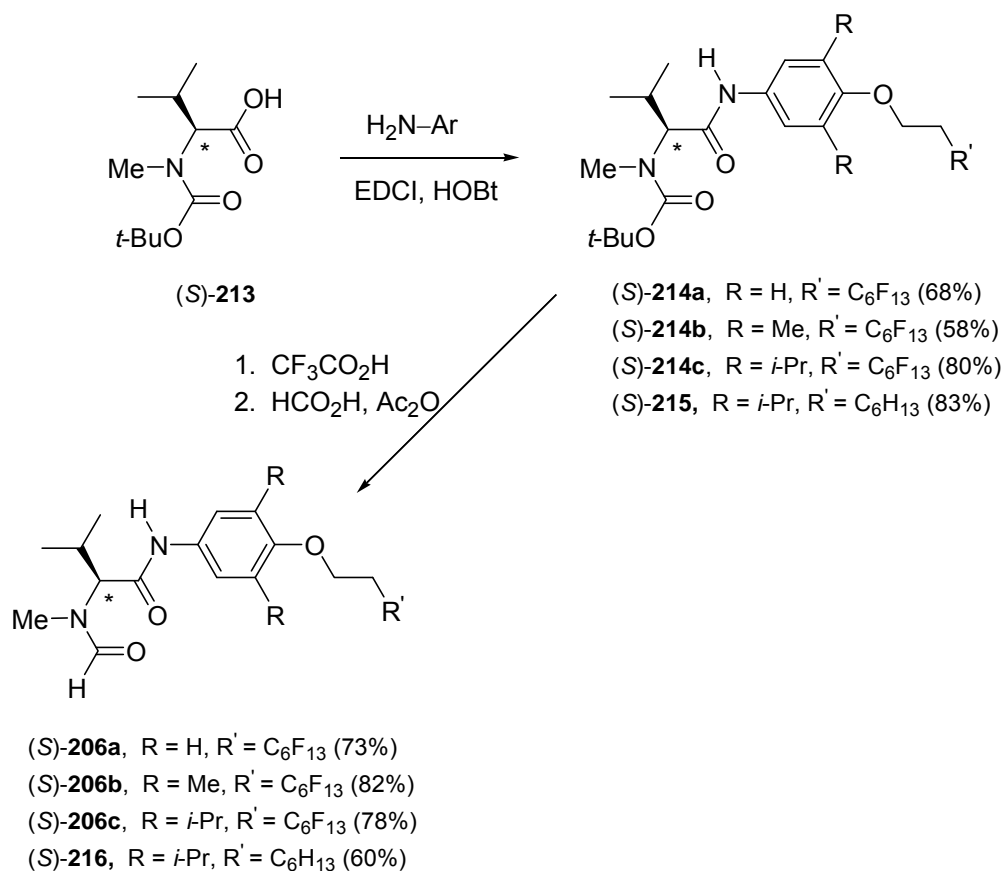
Initial attempts to synthesize ether **211a** via alkylation of *p*-nitrophenol with a triflate derived from the fluoros alcohol **210** or with the corresponding iodide proved fruitless under various conditions (using, e.g., K₂CO₃, KF, or KH as a base). Therefore, aromatic nucleophilic substitution was explored next: the alkoxide, generated from the fluoros alcohol **210** and NaH, was treated with *p*-nitrofluorobenzene (**209**) at 60 °C for 18 h, which resulted in the formation of the desired ether **211a** though in a rather low yield (17%). On the other hand, heating of a mixture of **209**, **210**, and Bu₄NI in a 28% aqueous solution of NaOH at 45 °C for 48 h under the phase-transfer conditions afforded, after optimization, the desired ether **211a** in 80% yield.¹⁴⁶ The more hindered ethers **211b,c** were constructed via the Mitsunobu reaction of phenols **207**, **208**¹⁴⁷ with the fluoros alcohol **210**: standard conditions, using Ph₃P and DEAD (25 °C, 18 h),¹⁴⁸ proved efficient for 2,6-dimethyl-4-nitrophenol (**207**) and the desired ether **211b** was obtained in 41% yield. Rather surprisingly, the Mitsunobu reaction was successful even with the more hindered diisopropyl analogue **211c**, which was converted into ether **211c** in 33% yield. Nitroether **211d** was prepared by heating of nitrophenol **208** with octyl iodide in the presence of K₂CO₃ in acetone at 45 °C. After 19 h, the desired product was obtained in 94% yield.

To reduce the ether **211a** to the corresponding aniline, application of palladium catalysed hydrogenation seemed to be a logical choice. However, the use of palladium supported on activated carbon and sodium phosphate as a reductive agent in THF¹⁴⁹ afforded the required product in only 3% yield. The next attempt to reduce ether **211a** involved the application of tin(II) chloride¹⁵⁰ and the reaction was performed in refluxing absolute ethanol. After 12 h, the desired product **212a** was obtained in 81% yield. Nitro-derivatives **211b,c,d** were reduced in a similar way affording the corresponding anilines **212b,c,d** in 76%, 79%, and 74% yield, respectively.

5.1.2 Synthesis of fluoros catalysts

Having prepared the key fluoros anilines (Ar-NH₂) and BOC protected *N*-methylvaline, synthesized by from BOC-valine and methyl iodide in the presence of sodium hydride,^{138a} a coupling was carried out using standard carbodiimide methodology.¹⁵¹ Thus, amino acid **213** was treated with the fluoros aniline **212a** and EDCI in the presence of HOBt and triethylamine in DCM. After an overnight reaction the corresponding anilide **214a** was obtained in 68% yield (Scheme 69). Using an analogous protocol, anilides **214b,c** were obtained in 58% and 80% yield, respectively. BOC deprotection¹⁵¹ with trifluoroacetic acid in DCM at 0 °C for 1 h, followed by formylation¹⁵¹ using a mixture of formic acid and acetic anhydride (rt, 18 h), afforded the desired catalysts in good yields (73-82%).

Formamide **216** with the *n*-octyl chain instead of fluorous tag was prepared in an analogous way by coupling the aniline **212d** with *N*-methylvaline (83%), followed by BOC-deprotection and formylation of anilide **215** (60%).



Scheme 69. Synthesis of fluorous catalysts

5.1.3 Application of fluorous catalysts in asymmetric reduction of imines with trichlorosilane

The efficiency and possibility of recycling of the new fluorous catalysts was investigated using a modification of the standard procedure developed in this laboratory¹³⁶ using imine **185a** was chosen as a model substrate. Thus, trichlorosilane was added to a stirred solution of the fluorous catalyst and imine **185a** in toluene at 0 °C, and the mixture was allowed to stir at room temperature overnight. After completion of the reaction and a standard workup (washing with NaHCO₃), the crude product was loaded onto a column of fluorous silica gel and the column was washed with fluorophobic solvent (methanol-water, 80:20) to elute the amine and then with a fluorophilic solvent (methanol) to wash out the fluorous catalyst. The results are summarized in Table 22.

All fluorous catalysts exhibited high activities and stereoselectivities. When 10 mol% of the catalyst **206a** was used in the model reaction, the enantiomerically enriched amine (84% ee) was obtained in 80% yield and the catalyst was recovered almost quantitatively (entry 6). These results, comparable to the application of untagged predecessor **187a** (entry 1)

indicates that the presence of the fluororous tag in the catalyst structure does not affect the catalytic performance of the system.

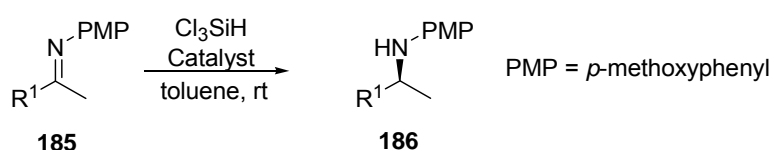
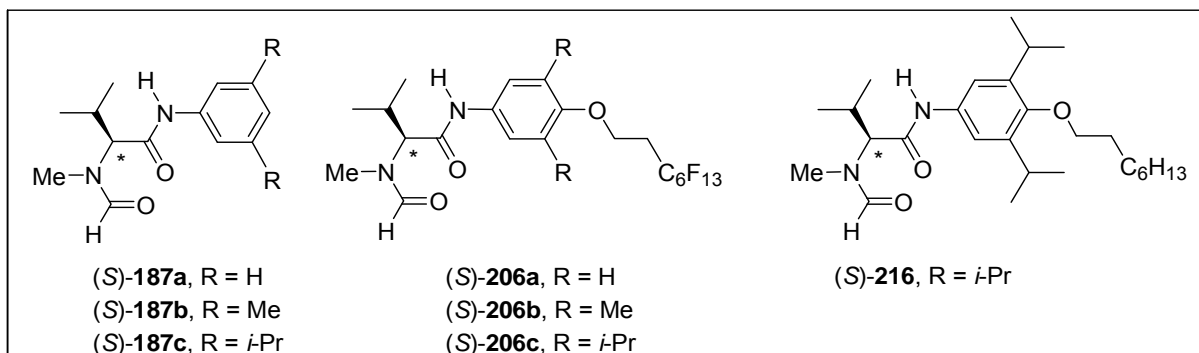


Table 22. Asymmetric reduction of imines with trichlorosilane catalysed by *N*-methylvalin-derived formamides **187, **206**, and **216**.**

entry	catalyst (mol%)	imine	R ¹	yield [%]	ee [%] ^c	catalyst recovery %
1	187a (10)	185a	Ph	96	85 ^a	-
2	187b (10)	185a	Ph	85	91	-
3	187c (10)	185a	Ph	99	94	-
4	187c (5)	185a	Ph	95	93	-
5	216 (10)	185a	Ph	98	90	-
6	206a (10)	185a	Ph	80	84	99
7	206a (5)	185a	Ph	73	82	-
8	206a (3)	185a	Ph	62	74	-
9	206b (10)	185a	Ph	90	91	79
10	206c (10)	185a	Ph	98	89	99
11	206b (10)	185b	4-CF ₃ -C ₄ H ₄	67	88	86
12	206b (5)	185b	4-CF ₃ -C ₄ H ₄	72	92 ^b	71
13	206b (10)	185c	4-MeO-C ₄ H ₄	84	84	71
14	206b (10)	185d	2-Naphth	65	86	86
15	206b (5)	185d	2-Naphth	68	92 ^b	71

^a The reaction was carried out in CHCl₃. ^b The reaction was carried out at 10 °C.

^c Determined by chiral HPLC

The loading of the catalyst could be decreased to 5 mol% with only a marginal effect on both yield and enantioselectivity obtained (73%, 82% ee, entry 7). However, when 3 mol% of the catalyst was used in a model reaction, significant loss of the chemical yield and enantioselectivity were observed (62%, 74% ee, entry 8). In agreement with the earlier observations¹³⁶ (entry 2), further improvement of the catalytic performance was observed with 3,5-dimethyl substituted catalyst **206b** (90%, 91% ee, entry 9). An attempt to improve the results by introducing more bulky *iso*-propyl substituents in the 3,5-position of the aromatic

ring lead to the catalyst **206c**. However, the performance of the new catalyst (98%, 89% ee, entry 10) was slightly worse compared with the untagged predecessor¹³⁷ **187c** (99%, 94% ee, entry 3). To explain the deviation, which has not been observed for catalysts **206a,b**, an analogue of **206c** with an eight-carbon aliphatic chain **206d** instead of the fluororous tag was synthesized and tested in a model reaction. The results were comparable to those obtained with the fluororous catalyst **206c** (compare entries 5 and 10), which indicates that it is the presence of a substituent in the *ortho* position to *iso*-propyls rather than the nature of the fluororous tag that influences the level of the asymmetric induction. Finally, the application of the champion catalyst (**206b**) was extended to the substrates with various substitution patterns, giving the results analogous to those obtained with untagged predecessor **187b** both at 10 and 5 mol% loading (entries 11-15). In addition, the fluororous catalyst could be recovered in reasonable yields (71-86%).

To extend the utility, all new catalysts were tested in experiments with subsequent reuse of the catalyst in a cycle of transformation (reduction of imine **185a**). The reactions and catalyst recovery were carried out as described previously, and the recovered catalyst was used to the next transformation without any purification. 10 mol% of the initial catalyst loading was chosen as we were aware that each run would be followed by some loss of the fluororous catalyst. The results are summarized in Table 23.

Table 23. Asymmetric reduction of imine **185a with trichlorosilane catalysed by recycled *N*-methylvalin-derived formamides **206****

entry	catalyst (run)	yield [%]	ee [%] ^b	catalyst recovery ^a [%]
1	206a (1)	80	84	99
2	206a (2)	82	84	92
3	206a (3)	78	76	83
4	206a (4)	70	74	70
5	206b (1)	90	91	79
6	206b (2)	88	88	72
7	206b (3)	86	88	75
8	206b (4)	86	83	83
9	206c (1)	98	89	99
10	206c (2)	96	87	90
11	206c (3)	90	89	92
12	206c (4)	90	85	92
13	206c (5)	89	87	88

^aObtained by the mass comparison of the catalyst before and after the reaction. ^bDetermined by chiral HPLC

As shown in Table 23, the catalyst **206a** could be reused once affording product with unchanged yield and enantioselectivity (82%, 84% ee). After the second run, due to some loss of the catalyst and its decomposition the enantioselectivity decreased to 76% (entry 3). Enantioselectivity of the process decreased further when the regenerated catalyst was used to

catalyse the reduction in the fourth run (74% ee, entry 4). Similarly to the application of **206a**, a gradual decrease of activity and selectivity after each run was observed when the catalyst **206b** was tested in the experiment (compare entries 5 and 8). In sharp contrast and to our delight, catalyst **206c** retained full activity over five cycles, becoming the best catalyst recycling.

5.1.4 Conclusions

The practicality of the asymmetric reduction of imines with trichlorosilane catalysed by *N*-methylvaline-derived formamides has been considerably enhanced by fluororous tagging of the catalyst. This new methodology allows a very easy isolation of the product and an undemanding recovery of the catalyst that can be used in the next cycle. The fluororous catalysts operate in a homogeneous solution and the difference between their efficiency and that of their untagged predecessors is negligible. Therefore, this technology appears to be particularly suited to the small-scale parallel chemistry.

5.2 Immobilization of *N*-methylvaline-derived formamides on insoluble polymers

As the next step of development of recoverable catalyst for asymmetric reduction of imines with trichlorosilane, we decided to attach our catalyst **187b** to a polymer and explore the benefit of heterogeneous catalysis.

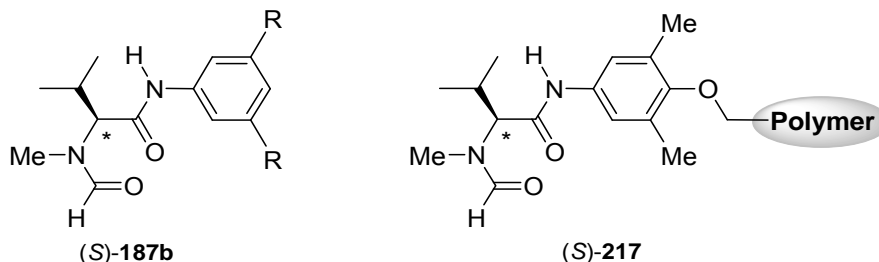


Figure 31. Champion catalyst for asymmetric reduction of imines with trichlorosilane **187b** and its proposed polymer modification **217**

Our strategy for the preparation of heterogeneous catalysts assumed synthesis of amino-acid moieties with various attachment points (**218**, **219**, **220**, Figure 32), followed by the construction of the ether link between the catalyst and polymer in the last step, so that most of the reaction sequences could be carried out in solution.

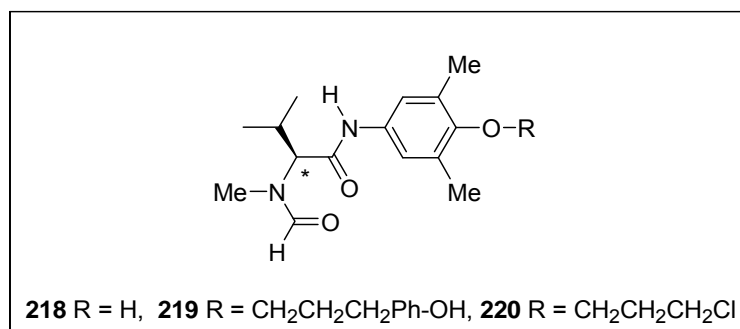
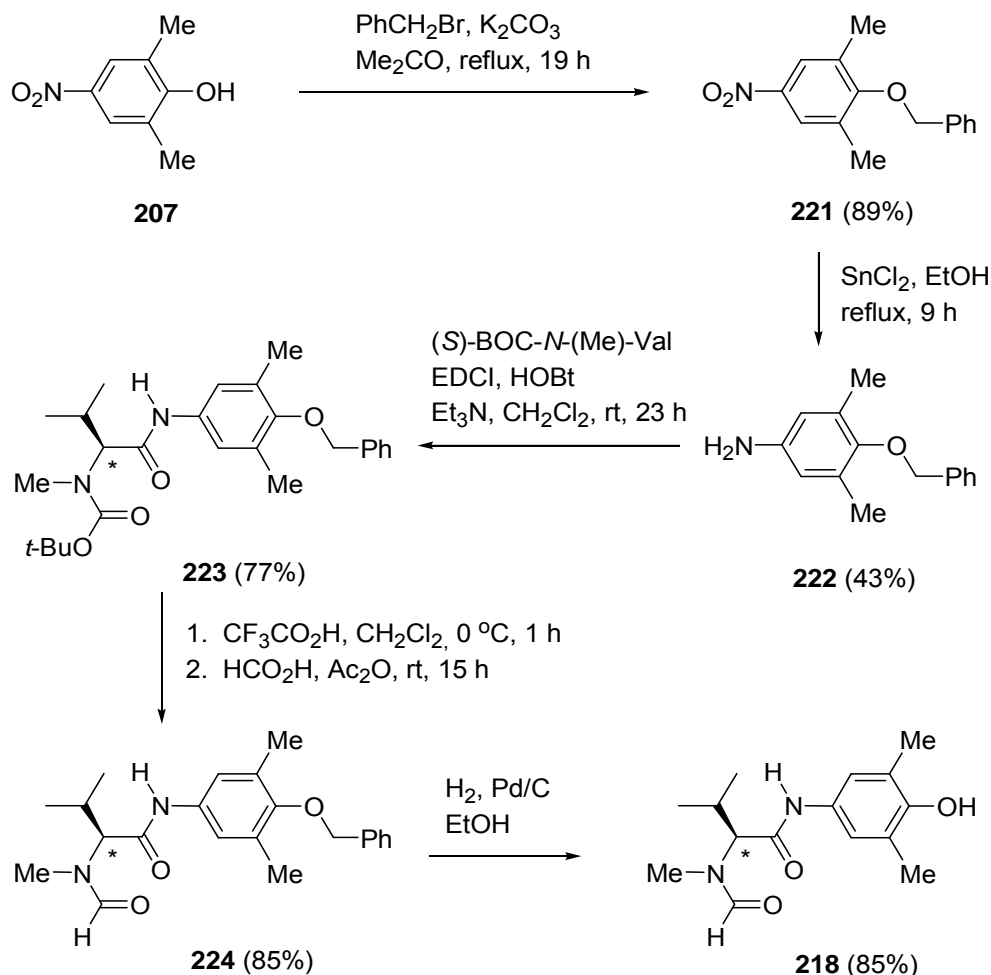


Figure 32. Amino-acid moieties for immobilization on the polymer

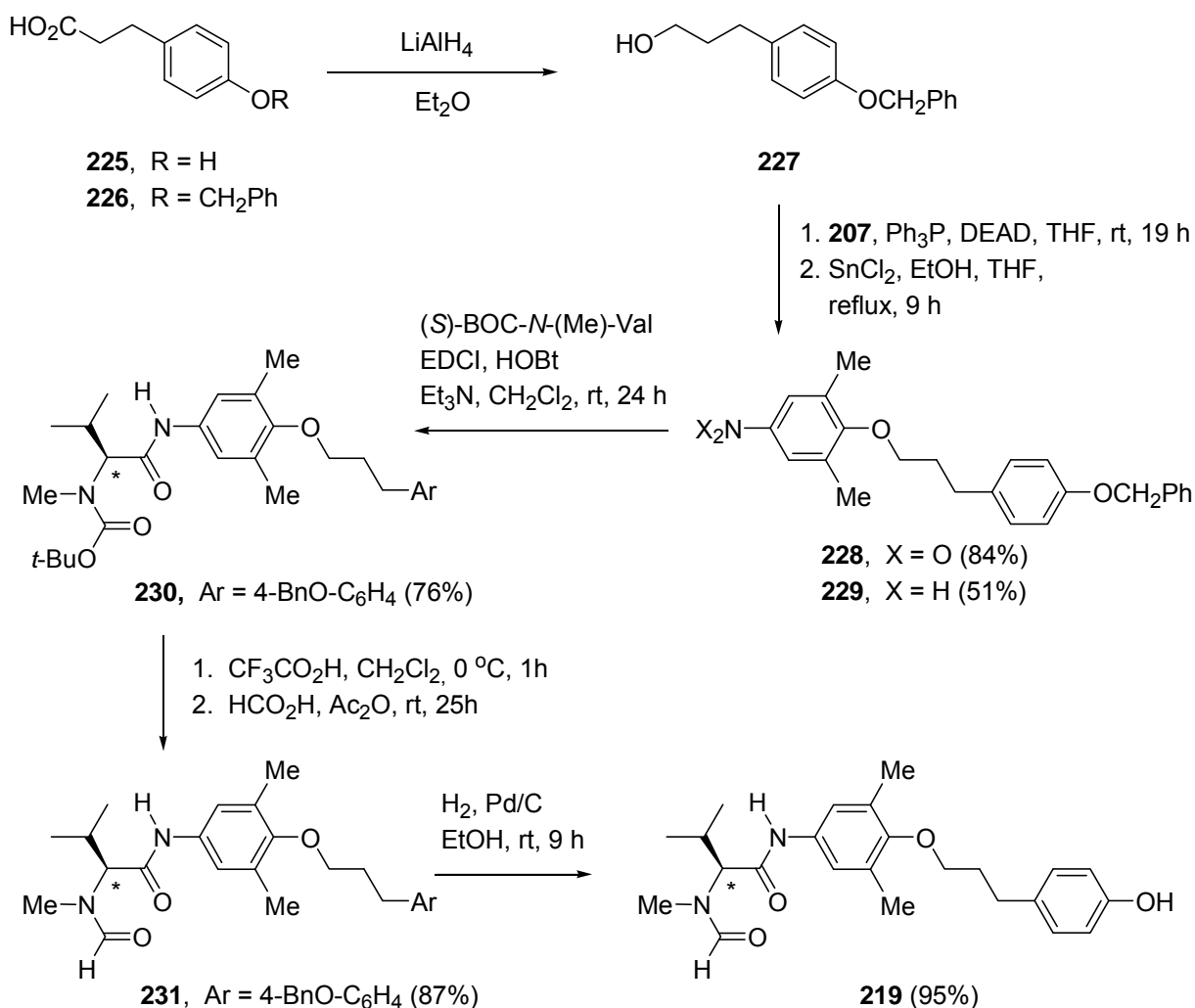
5.2.1 Synthesis of the amino-acid moieties suitable for immobilization

The synthesis of phenolic derivative **218** (Scheme 70) commenced with the protection of nitrophenol **207** by benzylation, and the resulting nitro ether **221** (89%)¹⁵² was reduced with SnCl₂ under our previously described conditions¹⁵⁰ to afford the aniline derivative **222** (43%).



Scheme 70. Synthesis of the phenol **218**

Extension of the reaction time at the same temperature resulted in the formation of a significant amount of the debenzylated product, whereas at lower temperature the reaction did not proceed to completion. Acylation of the latter product with the BOC-protected *N*-methyl valine by using the carbodiimide method furnished amide **223** (77%), whose deprotection with trifluoroacetic acid, followed by formylation in one pot¹⁵¹, gave rise to formamide **224** (85%). Finally, the protecting benzyl group was removed by catalytic hydrogenation to produce the desired phenol **218** (85%).

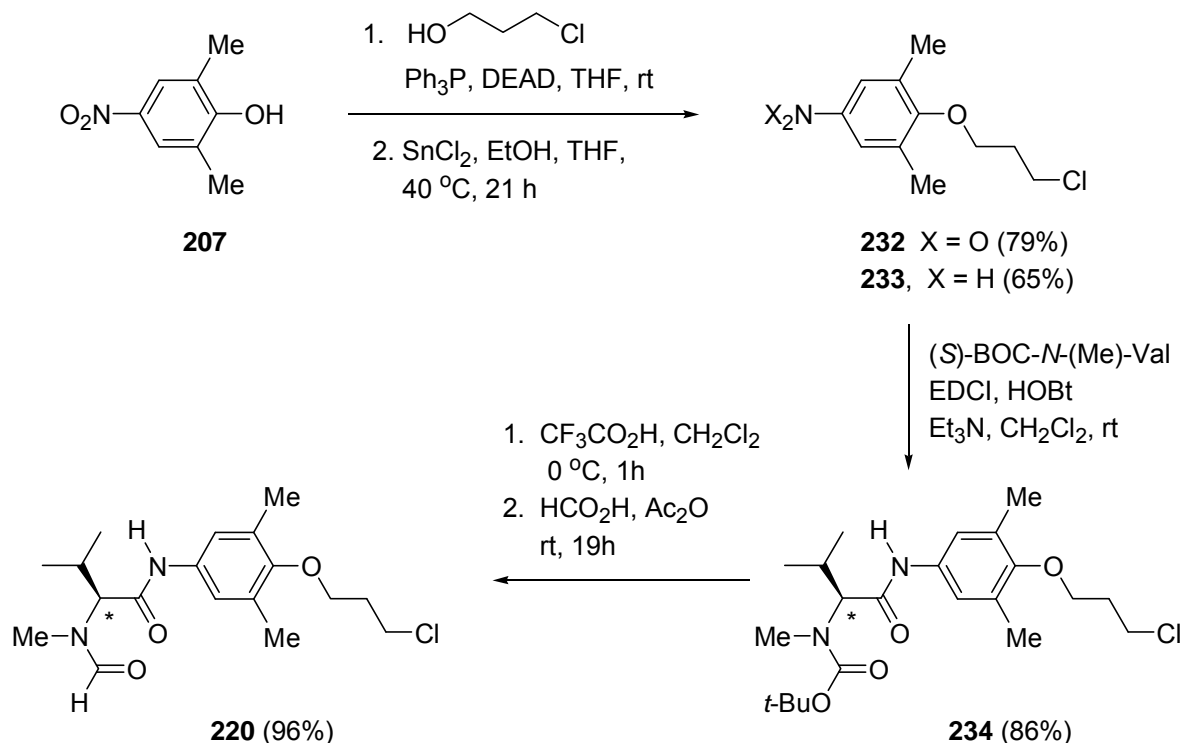


Scheme 71. Synthesis of elongated phenol **219**

For the synthesis of the elongated phenol **219**, alcohol **227** was selected as the electrophilic reagent to alkylate phenol **207**. Alcohol **227** itself was prepared in two steps from acid **225**, by protection of the hydroxyl by benzylation (BnBr, NaOH, EtOH; 56%),¹⁵³ followed by reduction of the resulting acid **226** with LiAlH₄ (95%).¹⁵⁴ A Mitsunobu reaction was then employed to effect the alkylation of nitro phenol **207** with alcohol **227**,¹⁴⁸ and the resulting nitro derivative **228** (84%) was then reduced with SnCl₂ to produce amine **229** (51%).¹⁵⁰ Acylation of the latter amine with the BOC-protected *N*-methylvaline provided amide **230** (76%),¹⁵¹ whose deprotection (TFA), followed by formylation (HCO₂H, Ac₂O), gave formamide **231** (87%).¹⁵¹ The final hydrogenation released phenol **219** (95%).

In the synthesis of the intermediate **220** (Scheme 72), the phenolic hydroxyl in **207** was first derivatized by alkylation with 3-chloropropan-1-ol under Mitsunobu conditions¹⁴⁸ to afford ether **232** (79%), in which the chloropropyl group served both as a protecting group and as the final moiety to be used for the attachment. The rest of the synthesis followed the original scheme: the nitro derivative **232** was reduced and the resulting amine **233** (65%)¹⁵⁰

was converted into amide **234** (86%) by the carbodiimide method.¹⁵¹ A one-pot deprotection with TFA and formylation with HCO₂H and Ac₂O afforded **220** (96%).¹⁵¹

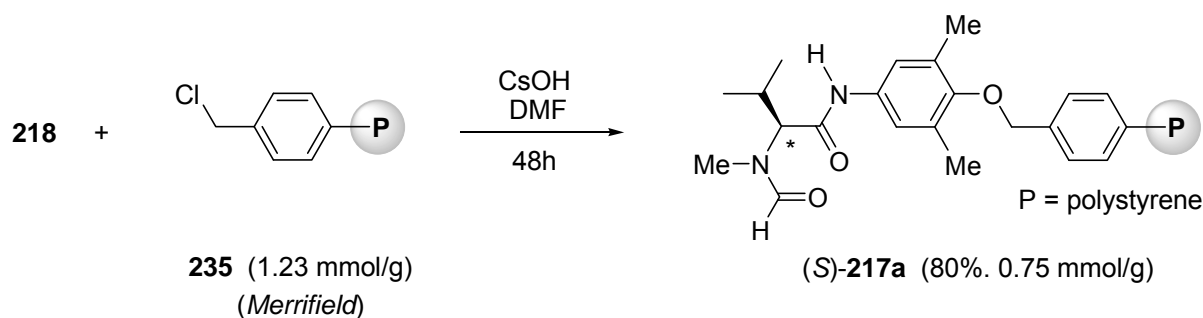


Scheme 72. Synthesis of intermediate **220**

5.2.2 Immobilization of amino-acid moieties

While the reduction with fluorous catalysts was carried out in a solution, the solid-supported catalysts operate in a heterogeneous system, which creates problems related to heterogeneous reactions. Here, many factors have to be carefully considered when choosing the appropriate support, including the swelling properties of the polymer, the accessibility of the catalyst to the reaction partners, the compatibility of the polymer with the reaction conditions, etc. From a variety of commercially available resins we selected the most common (Merrifield and Wang resin, TentaGel, etc.), which were believed to be compatible with our chemistry.

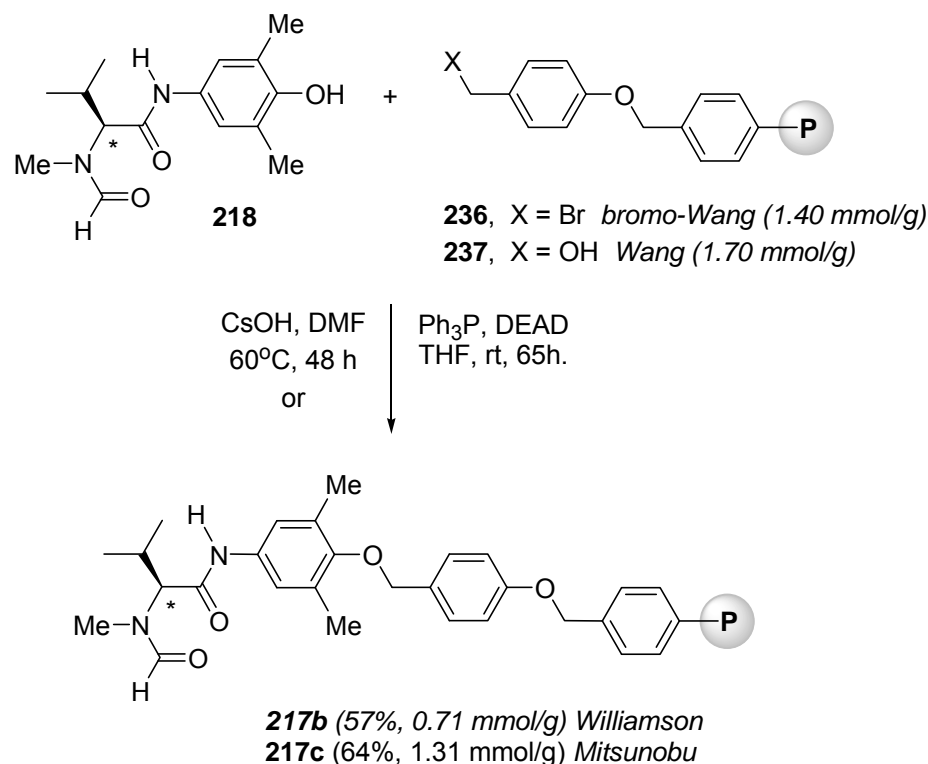
In the first part of this investigation, we chose to attach the amino-acid moiety **218** to the Merrifield resin **235**. The phenolic hydroxyl in **218** was alkylated with polymeric benzyl chlorides under modified Williamson condition (CsOH, DMF, 60 °C).



Scheme 73. Immobilization of phenol **218** on the Merrifield resin

After completion of the reaction, the polymer was repeatedly washed with MeOH and DCM to furnish catalyst **217a** as a brown solid. Mass comparison of the resin before and after the reaction indicated 80% yield, and the content of amino-acid moiety was established by the elemental analysis (0.75 mmol/g). An alternative work-up involved additional washing of the immobilized catalyst with a 1:1 mixture of H₂O and MeOH, and a 1:1 mixture of H₂O and THF but no significant difference was observed compared to the latter experiment. Analogous reaction at 45 °C allowed to immobilize phenol **218** in 62% yield whereas at 80 °C the yield decreased to 31%. Attempts to increase the yield of immobilization by using THF or various mixtures of THF and DMF as solvents, failed.

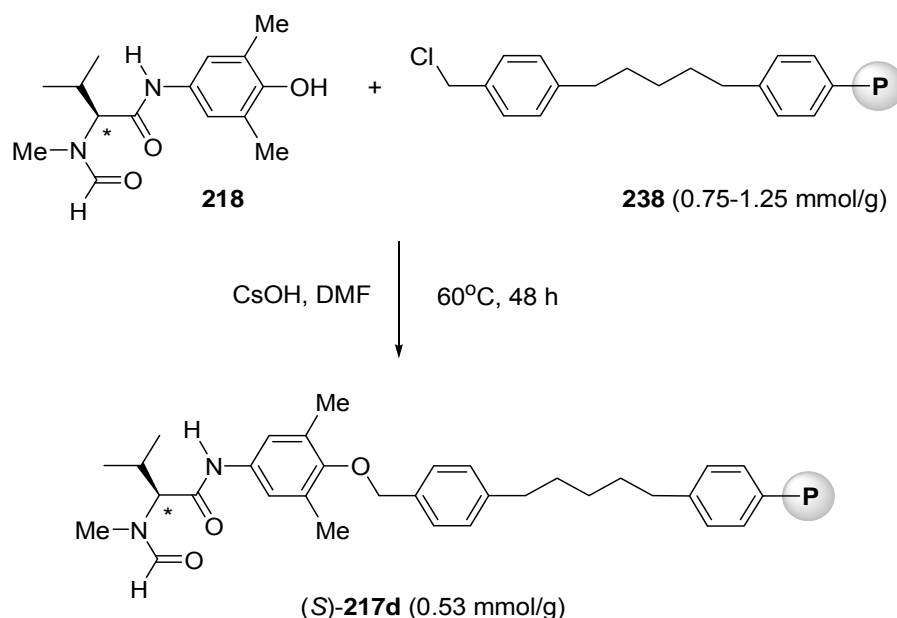
With this data in hands, two approaches for the immobilization of phenol **218** on a Wang resin were explored next. First, the Bromo-Wang resin **236**, which could be regarded as a more reactive analogue of the Merrifield resin with an additional benzyl moiety, was used in the reaction with phenol **218**, applying the optimal reaction conditions (CsOH, DMF, 60 °C).



Scheme 74. Immobilization of phenol **218** on Wang resin

After 48 h reaction and work up involving intensive washing with DMF, MeOH, DCM, Et₂O, an H₂O-MeOH (1:1) and H₂O-THF mixture (1:1), the catalyst immobilized on a Wang resin (**217b**) was obtained in 57% (0.71 mmol/g). An alternative way of anchoring involved the use of phenol **218** and the Wang resin **237** under Mitsunobu reaction conditions. Thus, in the presence of triphenylphosphine, diethylazodicarboxylate, and double excess of phenol **218**, the Wang resin was functionalized with the amino-acid moiety in 64% yield (cat **217c**, 1.31 mmol/g).

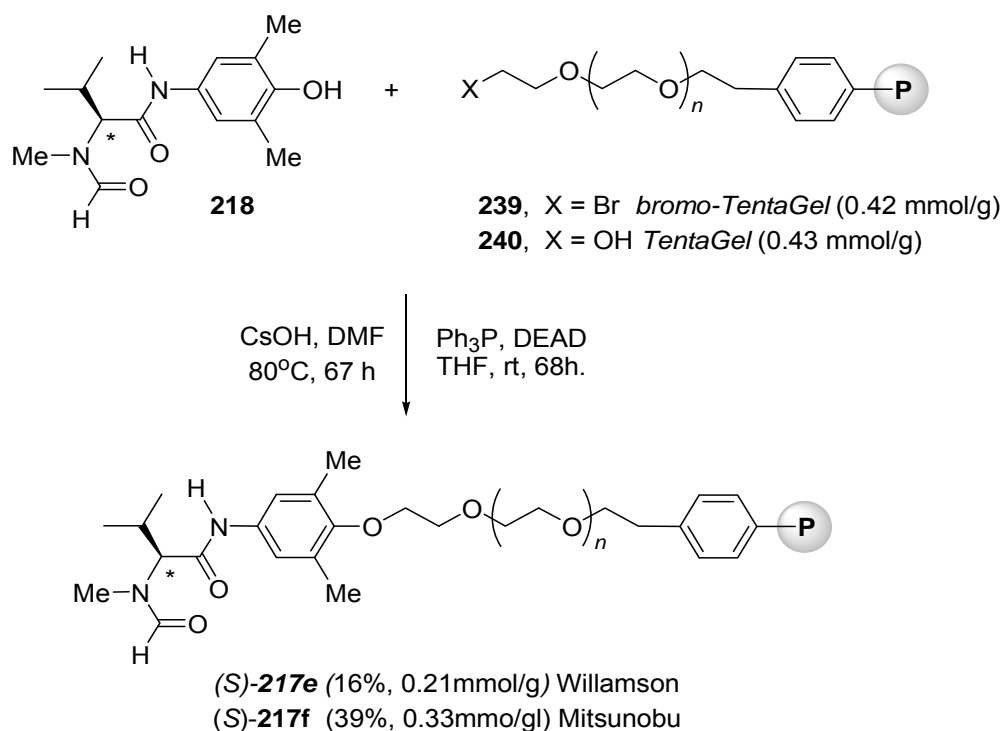
Following the general rule³ stating that the catalyst should be placed as far away from the resin as possible, the next step in our research was a preparation of catalysts with a long spacer between amino acid moiety and a polymer.



Scheme 75. Immobilization of phenol **218** on modified Merrifield resin **238**

With optimal reaction conditions in hands, we decided to prepare an analogue of catalyst **217a** with additional 5 carbons in the chain (**217d**, Scheme 75). Using the optimal reaction conditions (CsOH, DMF, 60 °C, 48h), phenol **218** was anchored to the resin **238** in 51% yield (0.53 mmol/g).

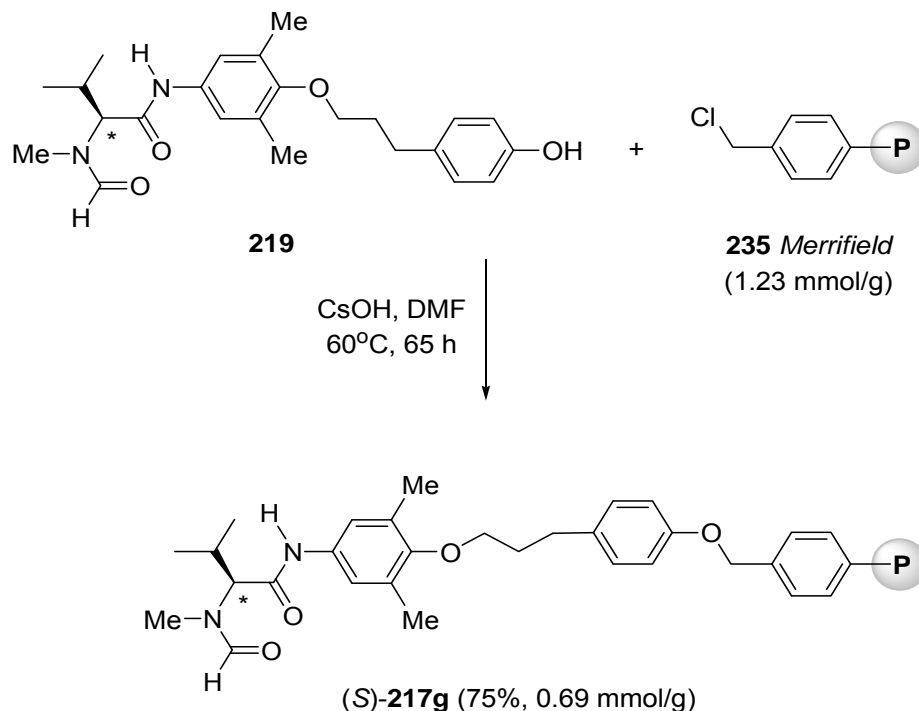
Immobilization of organocatalyst on the polystyrene-based TentaGel resins, with long polyglycol chains, was carried out in a similar way (Scheme 76). First, phenol **218** was treated with bromo-TentaGel resin **239** in the presence of cesium hydroxide. The reaction was carried out in DMF at 80 °C for 67 h. After completion, the crude polymer was intensively washed with DMF, MeOH, DCM, Et₂O, a 1:1 mixture of H₂O and MeOH and a 1:1 mixture of H₂O and THF, furnishing polymer **217e** in 16% yield (0.21 mmol/g).



Scheme 76. Immobilization of phenol **218** on modified TentaGel resins

For comparison, when TentaGel resin **240** and phenol **218** were used under Mitsunobu reaction conditions, the catalyst **217f** was obtained in 39% yield (0.33 mmol/g).

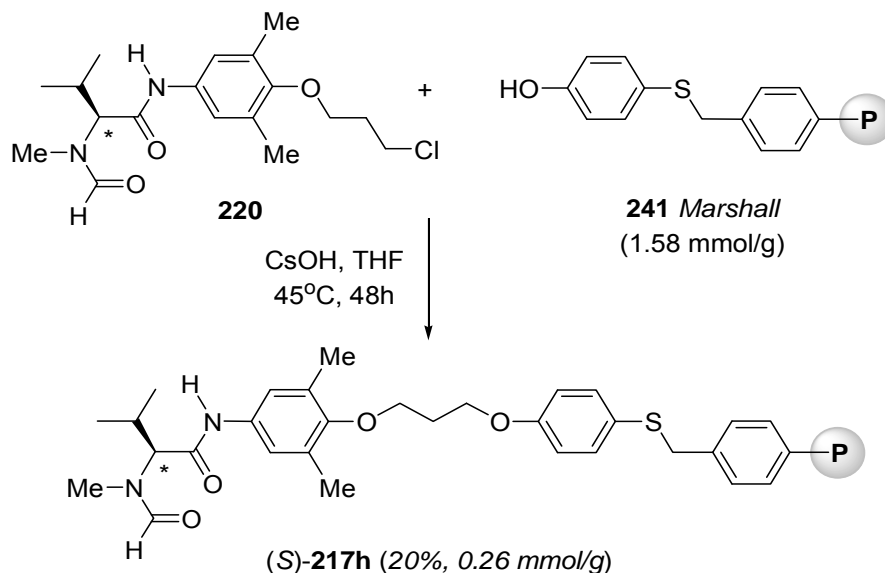
An interesting approach to the preparation of a solid supported catalyst with a long carbon spacer, involved the use of a substrate with the linker being part of the amino acid moiety.



Scheme 77. Immobilization of phenol **219** on Merrifield resin

Thus, phenol **219** (Scheme 77) was treated with Merrifield resin in the presence of CsOH in DMF at 60 °C for 65 h. After completion the polymer was washed with MeOH, DCM, a (1:1) mixture of H₂O and MeOH and a (1:1) mixture of H₂O and THF, furnishing polymer **217g** in 75% yield (0.69 mmol/g).

In all the previously described examples, the amino acid moiety served as a nucleophile when reacting with electrophilic functional groups of various resins. A complementary other approach could be the use of an amino acid moiety with an electrophilic functionality, and investigate its activity toward “nucleophilic” resin. Thus, the intermediate **220** was treated with Marshall resin **241** in the presence of cesium hydroxide and cesium iodide in THF (45 °C for 48 h). After aqueous and acidic work ups followed by intensive washing with organic solvents (MeOH, DCM, Et₂O), the catalyst **217h** was obtained in 20% yield (0.26 mmol/g).



Scheme 78. Immobilization of fomamide **220** on Marshall resin

5.2.3 Asymmetric reduction of imines catalysed by solid-supported formamides

The activity of immobilized catalysts in the reduction of imines was investigated by using a modified version of the standard protocol.¹³⁶ Thus, a porous reaction vessel with catalyst **217a** and imine **185a** were left in toluene for 30 min to ensure a proper swelling of the polymer, after which Cl₃SiH was added at 0 °C. The reaction was continued at room temperature overnight. After separation from the mother liquor, the reaction vessel with the immobilized catalyst was washed with toluene to elute the rest of the product, followed by further washing with CH₂Cl₂, MeOH, and Et₂O to regenerate the immobilized catalyst. Aqueous workup of the toluene solution¹³⁶ afforded pure amine **216a** (84% yield, 63% ee; Table 24, entry 2). For comparison, the reduction of imine **215a**, catalysed by **224** under homogenous reaction conditions in toluene, gave amine **216a** in 87% yield with 91% ee

(entry 36) with a marginal decrease of the reactivity and selectivity in chloroform (88%, 88% ee, entry 37). These results confirmed that the partial loss of catalytic activity observed for the heterogeneous system was related to unidentified physical factors rather than to the presence of the benzyl ether moiety in the catalyst.

When the reduction of imine **185a** catalysed by **217a** was carried out in chloroform, an improvement of enantioselectivity was observed, indicating a strong influence of the solvent (80%, 76% ee, entry 3). Repeated use of the regenerated catalyst **217a** has demonstrated retention of the activity (entries 4-8). Interestingly, the enantioselectivity turned out to be slightly higher in runs 2-5 than in the first cycle (82 vs 76%, entries 4 and 3), suggesting that “conditioning” of the catalyst was required to attain its optimal performance.

Catalyst **217d** (15 mol%), exhibited similar reactivity and selectivity (entries 9-14) as its lower “homologue” **217a** that has a shorter spacer. An attempt to improve the catalytic performance by increasing the loading to 30 mol% was fruitless (entries 15 and 16).

When the catalyst immobilized on the Wang resin (**217b**) was tested in the model reduction, a dramatic influence of the solvent was observed. While the reduction of **185a** in toluene exhibited 20% ee (entry 17), the reaction in chloroform gave **186a** in 73% ee (entry 18). The 2nd run, as in the previous case, gave an improved result (78% ee; entry 19) and this remained almost constant in the next runs (entries 19-23). Interestingly, **217c** prepared by Mitsunobu reaction exhibited inferior results (entries 24-25). However, a considerable improvement was attained in the 2nd and 3rd run (entries 25 and 26), suggesting that the polymer was contaminated by impurities, which were partly removed during the first run.

The catalyst immobilized on TentaGel **217e** exhibited a similar level of activity as **217a** (entries 27-29), whereas the catalyst **217f** appeared to be slightly less active (entry 32) with significantly worse results attained in toluene (entries 30 and 31).

The catalyst anchored on the Marshall resin (**217h**) exhibited very low reactivity and selectivity, and can be regarded as a failure (entry 33). Acetylation of any possible unfunctionalized phenolic groups on the polymer with acetyl chloride and using this product as a modified catalyst had only a marginal effect on the activity (entry 34).

The catalyst **217g** also turned out to be inefficient as it induced only 51% ee even in chloroform (entry 35).

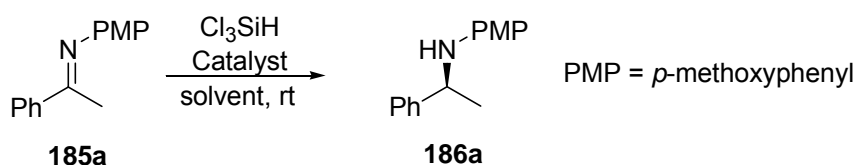


Table 24. Reduction of Ketimine **185a with Trichlorosilane, Catalysed by the Valine-Derived *N*-Methyl Formamides (*S*)-**187b**, **224**, and (*S*)-**217a-h**.**

entry	catalyst (mol%)	solvent	run	yield (%)	186a % ee ^a
1	187b (10)	toluene	1	85	91
2	217a (25)	toluene	1	84	63
3	217a (25)	CHCl ₃	1	80	76
4	217a (25)	CHCl ₃	2	81	82
5	217a (25)	CHCl ₃	3	82	81
6	217a (25)	CHCl ₃	4	80	82
7	217a (25)	CHCl ₃	5	81	82
8	217a (25)	CHCl ₃	6	78	81
9	217d (15)	CHCl ₃	1	87	77
10	217d (15)	CHCl ₃	2	84	82
11	217d (15)	CHCl ₃	3	85	81
12	217d (15)	CHCl ₃	4	83	81
13	217d (15)	CHCl ₃	5	84	82
14	217d (15)	CHCl ₃	6	83	81
15	217d (35)	CHCl ₃	1	90	78
16	217d (35)	CHCl ₃	2	92	81
17	217b (20)	toluene	1	86	20
18	217b (20)	CHCl ₃	1	83	73
19	217b (20)	CHCl ₃	2	76	78
20	217b (20)	CHCl ₃	3	77	79
21	217b (20)	CHCl ₃	4	76	77
22	217b (20)	CHCl ₃	5	76	77
23	217b (20)	CHCl ₃	6	74	77
24	217c (40)	CHCl ₃	1	34	22
25	217c (40)	CHCl ₃	2	53	61
26	217c (40)	CHCl ₃	3	52	68
27	217e (15)	toluene	1	74	73
28	217e (15)	CHCl ₃	2	68	77
29	217e (15)	CHCl ₃	3	69	76
30	217f (25)	toluene	1	72	47
31	217f (25)	toluene	2	69	47
32	217f (25)	CHCl ₃	3	72	63
33	217h (5)	toluene	1	72	30
34	217h (5)	toluene	1	82	45
35	217g (30)	CHCl ₃	1	71	51
36	224 (10)	toluene	1	87	91
37	224 (10)	CHCl ₃	1	88	88

^a Determined by chiral HPLC

The scope of the imine reduction was extended to other representative examples, including electron-rich and electron-poor aromatic and heteroaromatic imines. Keeping in mind the suitability of the new catalysts to a multiple use and the necessity of conditioning,

catalyst **217d** (30 mol%) was first conditioned (reduction of imine **185a**) and its activity confirmed in a model reaction (82%, 81% ee, [second run](#)). The regenerated catalyst **217d** was then applied to the reduction of a number of substrates under optimal reaction conditions (CHCl₃, rt) and the results are summarized in Table 25 ([runs 3-6](#)).

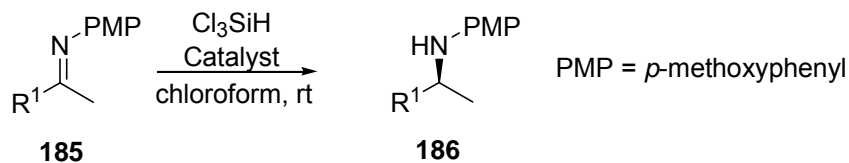


Table 25. Asymmetric reduction of imines **186a-e with trichlorosilane catalysed by the reused **217d** (30 mol%) in CHCl₃.**

run	imine	R ¹	yield in %	186 %ee ^a
2	185a	Ph	82	81
3	185b	2-Naphthyl	72	79
4	185c	4-CF ₃ -C ₆ H ₄	67	81
5	185d	4-MeO-C ₆ H ₄	62	77
6	185e	2,5-Me ₂ -3-furyl	67	78

^a Determined by chiral HPLC

Good enantioselectivities and chemical yields were obtained, regardless of the substitution pattern and as expected, little variation of yields and enantioselectivities was observed for **185b-e**. These results are consistent with those obtained with homogeneous catalyst, which confirms the value of the new methodology.

The last problem, which required explanation, was the difference in the results of the reductions performed under homogenous and heterogeneous reaction conditions, including the significant difference in application of toluene and chloroform. Toluene, the optimum solvent in the reduction of imines under homogenous reactions conditions, appeared to be significantly less useful in the heterogeneous catalysis.

Table 26. Reduction of imine **185a with trichlorosilane catalysed by resins **235-241**.**

entry	resin (mol %) ^a	run	solvent	conversion in % ^b
1	235 (40)	1	CHCl ₃	15
2	235 (40)	2	CHCl ₃	10
3	235 (40)	3	toluene	40
4	238 (30)	1	CHCl ₃	6
5	236 (40)	1	toluene	70
6	237 (40)	1	CHCl ₃	7
7	239 (30)	1	CHCl ₃	9
8	240 (30)	1	CHCl ₃	9
9	241 (35)	1	toluene	85

^a The mol % loading of the resin relates to the mmol/g content of the active group in the resin. ^b Established by ¹H NMR spectroscopy of the isolated crude mixture of the starting material and product.

To shed more light on these issues, we decided to investigate the possible catalytic activities of our resins in both solvents. The reaction was carried out as usual¹³⁶ but using the unfunctionalized resins as the potential catalyst. The results are presented in Table 26. Some catalytic activity of all resins was observed when the reactions were carried out in chloroform with significantly higher yields in toluene, especially for the Br-Wang resin **236** and Marshall resin **241** (entries 5, 9). The reaction catalysed by achiral source leads obviously to a racemic product, which could be the explanation of lower enantiomeric excess induced under heterogeneous reactions conditions. A comparison of catalytic activity of Merrifield resin in chloroform after the first and second run (Table 26, entries 1 and 2) could explain the changes observed between the first and second run as well as a meaning of conditioning when immobilized catalysts were tested. In the case of the reaction performed in toluene, the Merrifield resin exhibited a high catalytic activity even after conditioning (entry 3), which definitely eliminates this solvent from the application in our heterogeneous catalysis.

The mechanism of the conditioning is not fully understood but the following facts can be presented and discussed. With polymers containing hydroxyl or mercapto groups, it can be assumed that some of the remaining functional groups would interfere. Then, once exposed to the excess of trichlorosilane in the first run, the groups became less active, as observed in the second run. This explanation, however, cannot be applied for Merrifield or bromo-Wang resin, so the real reason must be different. It was observed in this study that the amount of the solid catalyst **217a** increased after the first run by about 25%, which was not repeated after the following runs. The increased mass can be related to the formation of small amount of a gel as a result of decomposition of trichlorosilane by water or methanol during the work up. The gel could not be removed from the polymer, and its presence is probably associated with the improved enantioselectivity after the first run. In the IR spectra of the regenerated catalyst **217a**, two new peaks were observed, namely at 841 cm^{-1} (Si-O) and 2253 cm^{-1} (Si-H), which is consistent with the mass increase.

Table 27. A solvent effect in the reduction of imine **185a with trichlorosilane catalysed by **217a****

run	solvent	yield [%]	ee [%] ^a
1	chloroform	83	78
2	chloroform	80	82
3	toluene	72	62
4	dichloromethane	80	79

^a Determined by chiral HPLC

Although all previously presented results clearly indicated the influence of solvent on the level of enantioselectivities obtained, in the last experiment we decided to show a

measurable relationship between the solvent and optical purity of product. Keeping in mind that regenerated catalysts can be reused a minimum of 5 times while preserving the same level of activity, the catalyst **217a** was used in a reduction of imine **185a** in different solvents and the results are presented in Table 27. The results indicated that the reaction carried out in toluene affords the product with 20% lower enantiomeric excess compared to chloroform. This eliminates toluene from application in asymmetric reduction of imines with trichlorosilane under heterogeneous reaction conditions.

5.2.4 Conclusions

In conclusions, an effective methodology for asymmetric reductions of imines with trichlorosilane, catalysed by organocatalysts immobilized on a solid support, was developed. This methodology simplifies the separation of the product from the catalyst and enables the preparation of chiral amines with good yields and enantioselectivities regardless of the substitution pattern of substrates. The champion catalysts **217a,d** can be reused over 5 times without any loss of activity, which confirms their suitability for multiple use. High level of catalytic activity was observed both when the catalysts were attached to a polymer directly or via suitable spacer. This creates an opportunity for the use of a simple intermediate, and its immobilization on inexpensive polymer (Merrifield). A strong influence of solvents on the catalytic performance was observed with the best results obtained for chloroform. High catalytic activity of unfunctionalized resins in toluene as well as its poor ability to swell resins, eliminated this solvent from our reduction attempts under heterogeneous reaction conditions.

5.3 Asymmetric reduction of imines with trichlorosilane catalysed by ionic modification of *N*-methylvaline-derived formamides

One of the main fields of interests for further studies in chemistry is the avoidance of toxic and environmentally unfriendly organic solvents. Ionic liquids, which combine good solubility properties with a negligible vapor pressure and excellent thermal stability, have rapidly gained popularity as valuable substitutes for many volatile solvents. Numerous organic, organometallic, and biocatalytic reactions have been performed with success in these new media. Furthermore, ionic liquids allow an easy product recovery as well as possible recycling of homogeneous catalysts. After the success with fluorous phase and catalysts immobilization on solid support, we decided to explore the application of this new methodology in the reduction of imines with trichlorosilane. We chose to synthesize the

imidazolium salt **242** (Figure 33) as an ionic modification of our champion catalyst **187b**, for we believed that the polarity induced by the positively charged ring should fit into the polar nature of ionic liquids, thus enabling an easy recovery of the new catalyst. A three-carbon spacer was chosen to minimize the influence of the positively charged ring on the active part of the catalyst.

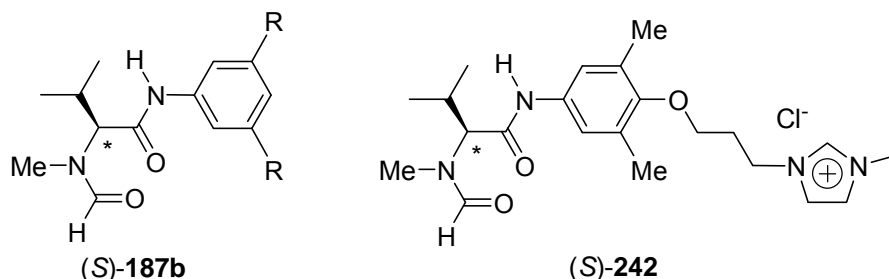
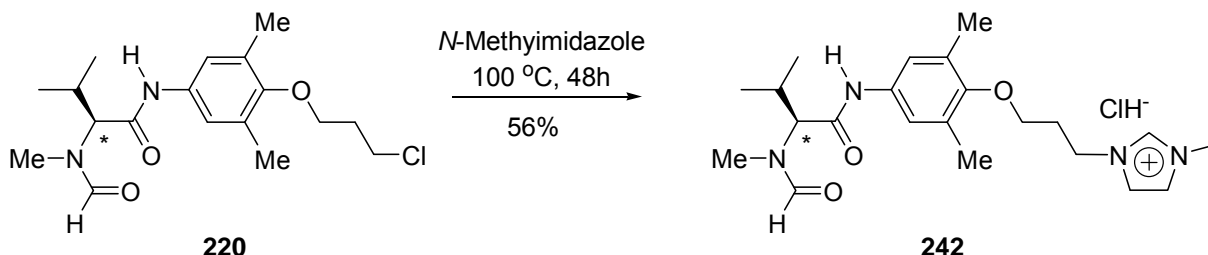


Figure 33. Champion catalyst for asymmetric reduction of imines with trichlorosilane **187b** and its proposed polymer modification **242**

The preparation of the imidazolium salt was based on the synthetic route developed previously with a synthesis of formamide **220** as a key intermediate (for its synthesis see Scheme 71). In the final step, chloride **220** was treated with an excess of *N*-methylimidazole at 100 °C to furnish the desired imidazolium salt **242** in 56% yield.



Scheme 79. A key transformation from the synthetic way of preparation of imidazolium salt **242**

The activity of the ionic catalyst **242** and its precursor **220** was evaluated under various reaction conditions using our standard protocol.¹³⁶ Following the requirements associated with the workup of the reaction mixture, 1-*n*-butyl-3-methylimidazolium hexafluoro phosphate was chosen as an ionic co-solvent due to its immiscibility with water. The results are summarized in Table 28. According to our prediction, the imidazolium salt precursor **220** exhibited an excellent catalytic activity in toluene (entry 1) with marginal loss of asymmetric induction in dichloromethane (entry 2). When the reaction catalysed by **220** was performed in toluene/[bmim]Cl biphasic system, amine **186a** was formed in 57% enantiomeric excess (entry 3). An analogous transformation in a mixture of DCM and [bmim]PF₆ (monophasic system) afforded the racemic product (entry 5). These results indicated a possible catalytic activity of [bmim]PF₆. The higher asymmetric induction in the biphasic system could be related to the better solubility of formamide **220** in toluene than in

IL and limited penetration of IL into the toluene phase. As a result, the enantioselective reaction catalysed by **220** in a toluene phase was faster than the reaction catalysed by achiral [bmim]PF₆. When DCM was used as a solvent and the system was monophasic, the accessibility of IL and formamide **220** towards the molecules of reagent was similar and the reaction, which leads to a racemic product, was significantly faster than enantioselective one.

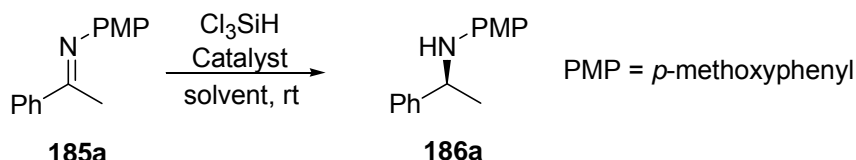


Table 28. Reduction of Ketimine **185a with Trichlorosilane, Catalysed by the Valine-Derived *N*-Methyl Formamides (*S*)-**220** and **242**.^a**

entry	catalyst (mol%)	solvent	additive	yield [%]	ee [%] ^c
1	220 (10)	toluene	-	88	90
2	220 (10)	DCM	-	90	86
3	220 (10)	toluene	[bmim] PF ₆	52 ^b	57
4	220 (10)	DCM	[bmim] PF ₆	70 ^b	racemic
5	242 (10)	toluene	[bmim] PF ₆	60 ^b	racemic
6	242 (10)	DCM	[bmim] PF ₆	70 ^b	racemic
7	242 (10)	DCM	-	92	37

^aThe reaction was carried out at 0.2 mmol scale with 2.0 equiv of Cl₃SiH at 18 °C for 16 h in solvent (1.5 mL) with or without an additive (0.2 mL). ^bPurified two times by the chromatography. ^cDetermined by chiral HPLC

When the reduction of imine **185a** was catalysed by imidazolium salt **242** in DCM, the amine **186a** was obtained in 37% enantiomeric excess (entry 7), whereas the application of biphasic toluene/[bmim]PF₆ (entry 5) or monophasic DCM/[bmim]PF₆ (entry 6) systems afforded racemic products. Low asymmetric excess induced by ionic modification of the champion catalyst could be related to the presence of imidazolium salt in the structure and its ability to catalyse the reaction that leads to a racemic product. The worst results were observed when [bmim]PF₆ was used as an additive. To confirm that the imidazolium salt can activate trichlorosilane in the reduction of imine, catalytic performance of 1-*n*-butyl-3-methylimidazolium hexafluorophosphate was investigated using standard conditions. The results are summarized in Table 29.

Table 29. Reduction of Ketimine **185a with Trichlorosilane, Catalysed by 1-*n*-Butyl-3-methylimidazolium hexafluorophosphate.^a**

entry	solvent	additive	Yield [%]
1	toluene	[bmim] PF ₆	96
2	DCM	[bmim] PF ₆	50

^aThe reaction was carried out at 0.2 mmol scale with 2.0 equiv of Cl₃SiH at 18 °C for 16 h in solvent (1.5 mL) with additive (0.2 mL).

High catalytic activity of IL was observed both in DCM and toluene. These results disqualified ionic liquids as a medium suitable for asymmetric reduction of imines with trichlorosilane. Because of an aqueous workup of the crude reaction mixture, the only ionic liquids that could potentially suit to our protocol, were those immiscible with water. Therefore, imidazolium salts with counter ions other than hexafluorophosphates were excluded from this study

5.4 Immobilization of the catalyst on gold nanoparticles

As mentioned before, the attempt at immobilization of homogeneous catalyst on an insoluble support can result in the loss of catalytic activity due to a limited catalyst mobility. For example, the catalyst immobilized on Merrifield resin is surrounded by the mass of the polymer and the catalytic site remains deep inside the polymer backbone. This effect can limit the access to the reaction partners and can result in a substantial decrease in activity. The reinstatement of homogeneous reaction conditions combined with the benefits of heterogeneous catalysis can be achieved by the use of metal nanoparticles as support for homogeneous catalysts. In this case, functionalized metal nanoparticles with appropriate surface coating can act nearly as homogeneous catalysts at the stage of reaction in one solvent and at the work-up stage, they are aggregated in another solvent, so that the catalyst can be separated from the product by filtration. If the catalyst is sufficiently stable under the reaction conditions, it can be isolated and reused. Nanoparticles can thus be viewed as novel supports to prepare heterogenized asymmetric catalyst.

Our success in the field of recoverable catalysts based on fluorous technology and insoluble polymers prompted us to employ gold nanoparticles as a new support for our catalyst and to explore the potential benefits of this new system in the reduction of imines with trichlorosilane.

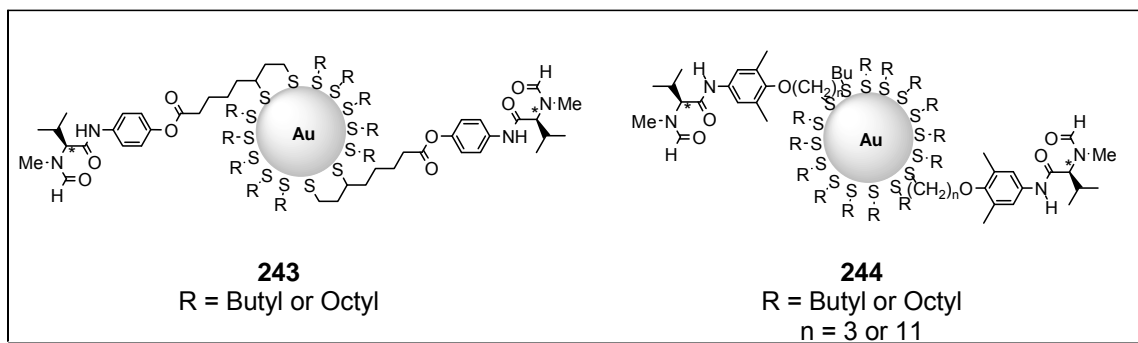


Figure 34. Proposed structures of the catalysts immobilized on gold-nanoparticles

Among the factors determining the physical properties and a performance of gold nanoparticles supported catalysts, the particles size, the nature of the coating layer, and the spacer length between the catalyst and the surface of gold have to be carefully considered.⁴⁷⁻⁴⁹ We decided therefore to synthesize amino-acid moieties (**245**, **246**, and **247**) with different attachment points and linkers length and investigate their catalytic properties when anchored to gold colloids with different coating layers.

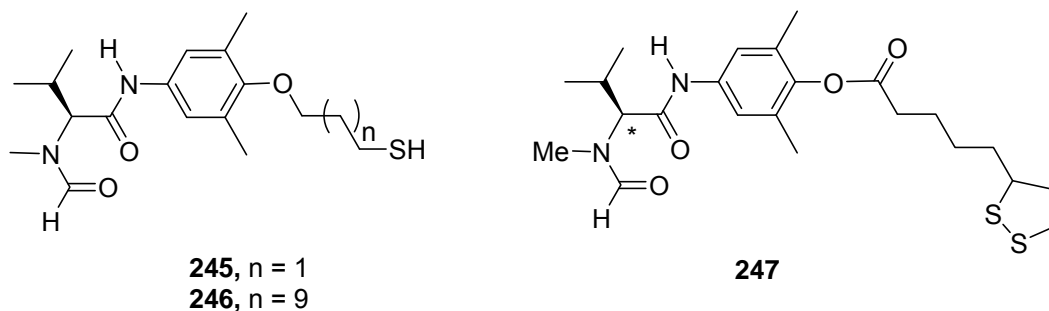
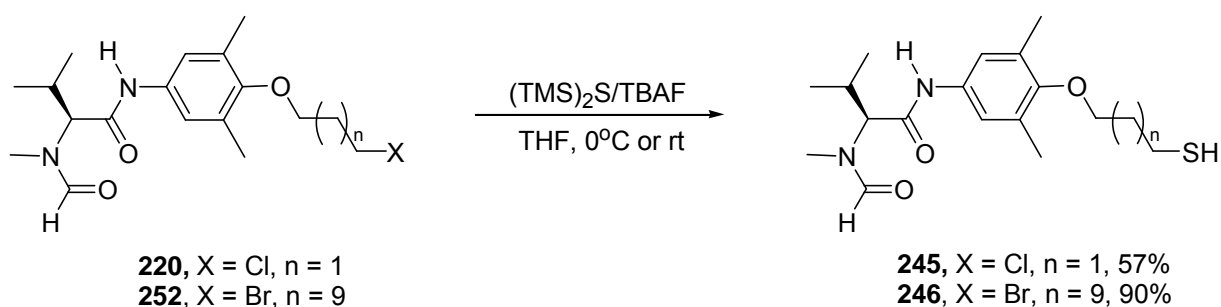


Figure 35. Intermediates for immobilization on the surface of gold nanoparticles

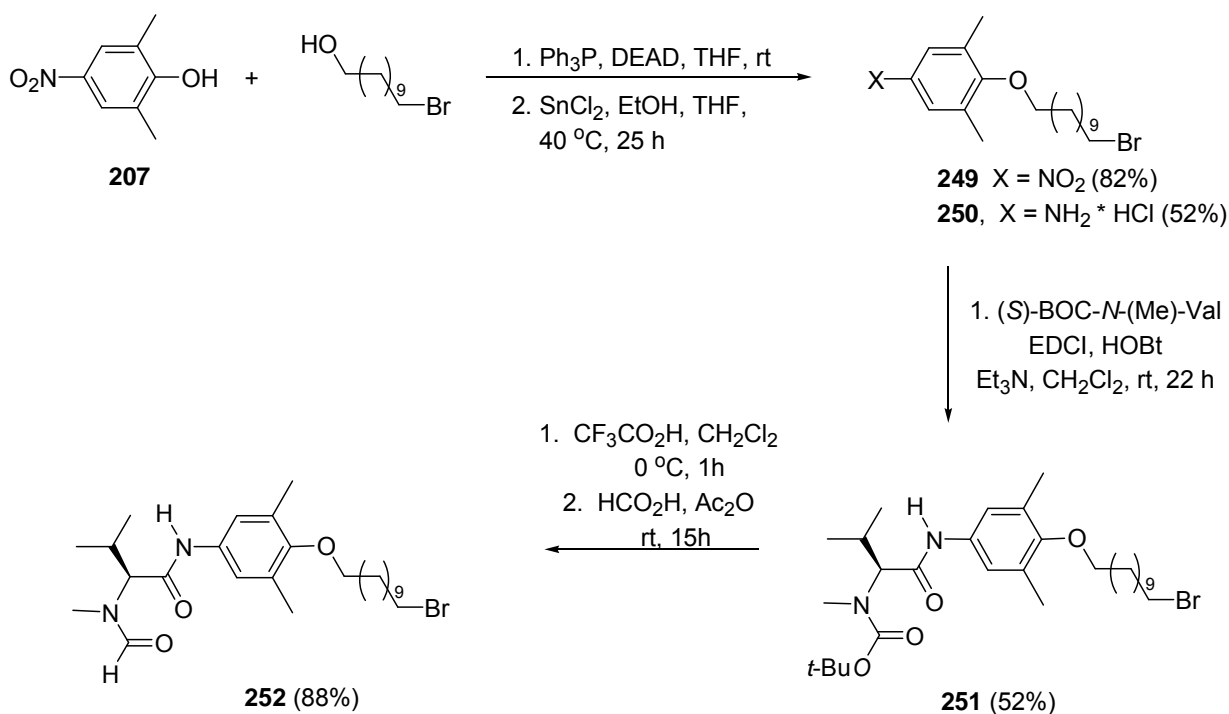
5.4.1 Synthesis of organic intermediates for immobilization on the surface of gold

A key step from the synthesis of thiols **245** and **246** was derivatization of the terminal carbon of the spacer in formamides **220** and **252** with a mercapto group. Thus, chloride **220** (for its synthesis see Scheme 72) was treated with hexamethyldisilathiane¹⁵⁵ in THF at room temperature to obtain the desired product **245** in 57% yield. Derivatization of the more reactive bromide **252** was carried out at 0 °C and the corresponding product was formed in 90% yield.



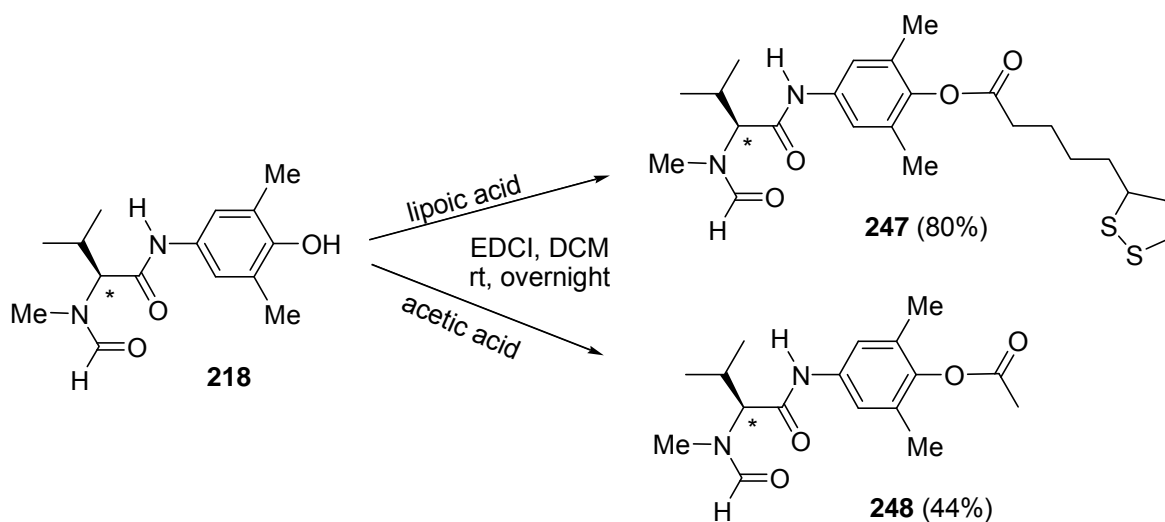
Scheme 80. A key step from the synthesis of thiols **245** and **246**

Synthesis of formamide **252** was an adaptation of the method developed previously for chloride **220** and commenced with alkylation of nitro phenol **207** with 1-bromo-11-undecanol under Mitsunobu reaction condition (82%).¹⁴⁸ The nitro ether **249** was reduced with tin(II) chloride and the resulting amine **250** (52%)¹⁵⁰ was converted into amide **251** (51%) by the carbodiimide method. The one-pot deprotection with TFA and formylation with HCO₂H and Ac₂O afforded **251** in 88%.¹⁵¹



Scheme 81. Synthesis of formamide **252**

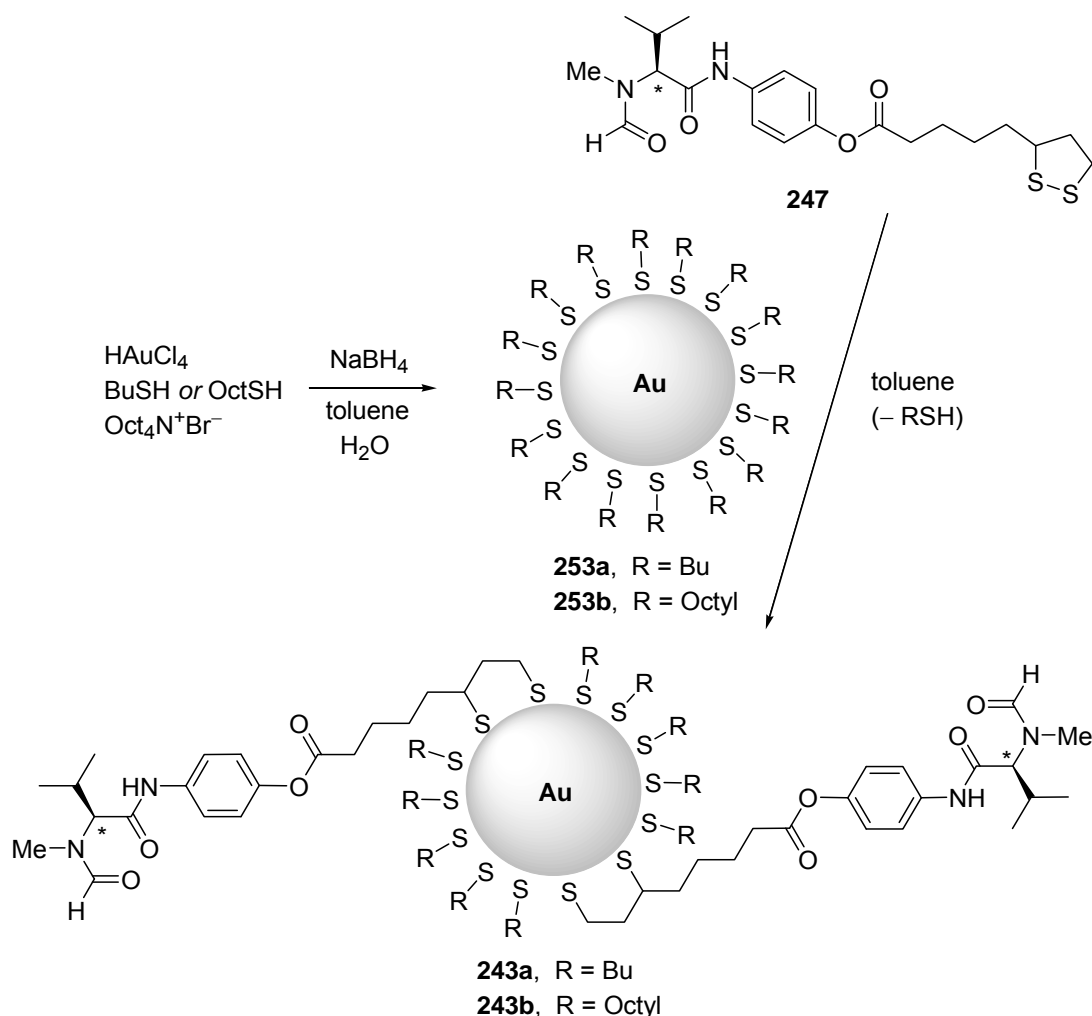
A key step in the synthesis of disulfide **247** was the derivatization of phenol **218** (for its synthesis see Scheme 70) with (±)-lipoic acid in the presence of EDCI. After optimization of reaction conditions, the desired product was obtained in 80% yield. Ester **248** was prepared in an analogous way using glacial acetic acid (44%).



Scheme 82. Synthesis of disulfide **247** and ester **248**

5.4.2 Immobilization of the catalyst on the surface of gold nanoparticles

To immobilize amino-acid moieties on the surface of gold nanoparticle a suitable support had to be prepared first.



Scheme 83. Preparation of the supports **253a,b** and immobilization of **247**

In the initial attempt, the support was synthesized by treatment of tetrachloroaurate with 10 equivalents of solid sodium borohydride (slow addition over 2-3 min) while stirring with 1.3 equivalents of 1-butanethiol and 2 equivalents of tetraoctylammonium bromide in a 1:1 mixture of toluene and water.¹⁵⁶ After 3 h, the butyl thiol-functionalized gold nanoparticles were isolated by precipitation from absolute ethanol. Changing 1-butanethiols to 1-octylthiols afforded octylthiol-functionalized gold nanoparticles. However, this procedure was not reproducible; therefore another protocol was explored next.¹⁵⁷ In the second attempt, 10 equivalents of sodium borohydride were added over 10 seconds as an aqueous solution and, the reaction was performed in the presence of 0.25 equivalent of 1-butyl thiol or 1-octyl thiol. This procedure was reproduced multiple times with the improvement of yields for both **253a,b**. Note that the exact calculation of yields is not possible; hence, the term yield refers to the higher amount of product that was

obtained from the analogous amount of substrate). The presence of the coating layers was confirmed by ^1H NMR spectroscopy and elemental analysis (**253a**, S = 3.74, **253b**, S = 3.23). The average size of the gold nanoparticles **253a** was 2.3 nm as shown by TEM images.

Having prepared support **253a**, immobilization of the amino acid moiety was performed by stirring **247** and **253a** (1:1 mass ratio, 2:1 mol ratio) in toluene for 4 days.¹⁵⁶ After completion of the reaction, functionalized gold nanoparticles were isolated by precipitation from absolute ethanol to afford **243a** as a black powder. The presence of the amino acid moiety was confirmed by ^1H NMR spectroscopy; however, the amount of **247** on the surface of the nanoparticles was very small as the attempt to determine the content of nitrogen in a sample by elemental analysis failed. The average size of **243a** was found to be 2.5 nm.

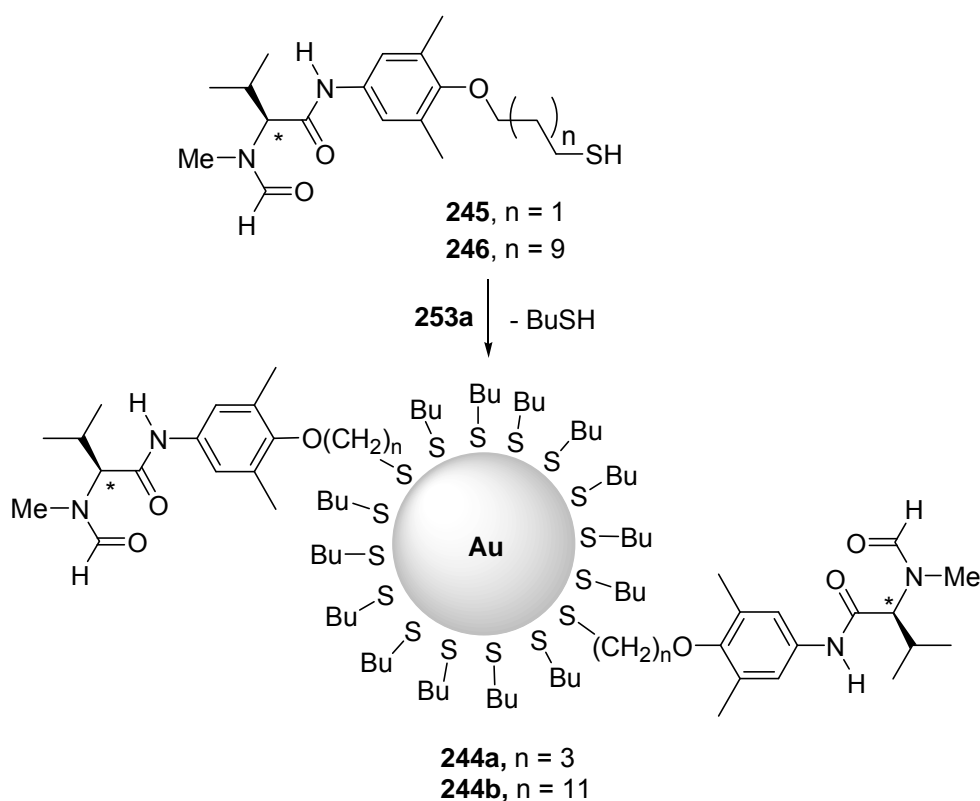
Treatment of **253b** with **247** following the protocol developed for **243a** afforded catalyst **243b** (Scheme 83). Similarly to the previous catalyst, the presence of the amino acid moiety was confirmed by ^1H NMR spectroscopy, but the attempt to analyze the content of the catalyst by elemental analysis was fruitless.

The place exchange reaction between disulfide **247** and the thiol functionalized gold nanoparticles **253a** and **253b** (Scheme 83) did not represent the most efficient way of immobilization of the amino acid moiety on the surface of gold nanoparticles. On the other hand, a functionalization of gold nanoparticles with 1-butanethiols worked well due to high affinity of the SH group to gold. It was decided to reduce the disulfide bond in **247** and use it both as a coating layer and the source of the catalyst. We envisaged that the reduction of the disulfide bond could be carried out in one pot with the reduction of the gold salt using sodium borohydride; however, the stability of the ester bond in **247** remained unknown. Therefore, in a controlled experiment, derivative **247** was treated with sodium borohydride and after 3 hours the reaction mixture showed no traces of product decomposition. This result opened the way for the initial idea. Following the protocol for the preparation of support **243a** and using **247** instead of 1-butanethiol, the functionalized nanoparticles were formed as indicated by the appearance of black color and by ^1H NMR spectroscopy. However, due to excellent solubility properties, the attempts to separate the supported catalyst by precipitation from any available solvents failed.

The physical properties of the functionalized gold nanoparticles strongly depend on the character of the coating layer.¹⁵⁸ It was therefore of great interest to synthesize derivatives of the champion catalyst with a different length of the carbon spacer and to investigate the influence of the chain length on the physical properties and catalytic performance of the

system. Thus, a 1:1 mixture of tetrachloroaurate and thiol **246** in toluene was treated with an aqueous solution of sodium borohydride added over 2-3 min. The reaction mixture became dark and was left to be stirred for an additional 3 h. The solvent was evaporated and the solubility of the dark residue, which contained functionalized gold nanoparticles, was examined in various solvents (MeOH, EtOH, AcOEt, THF, Et₂O, and hexane). Unfortunately, the black residue was soluble in all solvents except hexane, from which the nanoparticles precipitated as a mixture with the PTC catalyst. A similar result was obtained when the attempted precipitation was performed in MeOH at -80 °C. Following the same protocol and changing the gold salt/thiol **246** ratio from the original 1:1 to 4:1 and 6:1 did not improve the results, as similar solubility problems were observed. Changing the rate of addition of the sodium borohydride solution from the original slow (15 min) to fast (10 s) also proved fruitless. In view of these results, it seemed clear that in our case the surface of gold nanoparticles cannot be coated with the amino acid moieties exclusively as their presence influenced the solubility of the system.

In the next attempt, immobilization of **246** was carried out using the place exchange reaction. Therefore, support **253a** was treated with 2 equivalents of thiol **246** in DCM overnight.



Scheme 84. Immobilization of **245** and **246** on gold nanoparticles **253a**

The gold nanoparticles thus obtained were soluble in all previously tested solvents, except petroleum ether, which allowed a separation of the supported catalyst from the unreacted thiol by precipitation; note that the use of non-polar solvent was possible for the isolation of the supported catalyst as the reaction mixture was free of any hardly soluble reagent like PTC in a previous example. The formation of the catalyst **244b** was confirmed by NMR spectroscopy and elemental analysis (N, 2.15%). Although precipitation from petroleum ether afforded the catalyst for testing in a model reaction, we were aware that the application of a non-polar solvent at the separation stage limits the catalyst as a candidate for multiple use in a cycle of reductions.

Treatment of **253a** with 0.5 equiv of **246** under analogous reaction conditions afforded a gold nanoparticles-supported catalyst with physical properties similar to **244b** (soluble in all solvents except petroleum ether). Changing the support from **253a** to **253b** with octyl thiol as a coating layer was fruitless as the resulting catalyst could only be separated by precipitation from hexane.

Finally, catalyst **244a** with three carbon spacer between the aminoacid moiety and the surface of gold was prepared by reacting the buthyl thiol-functionalized nanoparticles **253a** with 0.5 equivalent of formamide **245** in DCM overnight (Scheme 84). Similar to previous examples, the new catalytic system **244a** was soluble in all solvents except petroleum, with which it was precipitated after the reaction completion (N, 0.89%).

5.4.3 Asymmetric reduction of imines with trichlorosilane catalysed by gold nanoparticles supported formamides

As shown earlier, due to the poor solubility in polar solvents only catalysts **247a,b** could be regarded as suitable candidates for an easy separation and multiple use in a cycle of transformation. As the amount of nitrogen in the samples of **247a** and **247b** was lower than 0.35% (which is within the experimental error of the elemental analysis), we assumed that in a test reaction performed on a 0.22 mmol scale, the catalyst loading was below 5 mol%. The model reduction was performed using a modification of our standard protocol: thus, the black powder of **247a** and imine **185a** were dissolved in dry toluene; trichlorosilane was then added at 0 °C and the mixture was stirred overnight at room temperature. The most significant change compared to the original protocol was the catalyst recovery. Thus, when the reaction was complete, toluene was evaporated and the residue was treated with methanol. The solution was then centrifuged, allowing separation of the solid catalyst from the amine, which stayed in the solution. The solvent from the methanolic solution was evaporated and the

residue was worked up as in the original procedure.¹³⁶ The recovered catalyst was used in the next transformation without further purification; the results are summarized in Table 30.

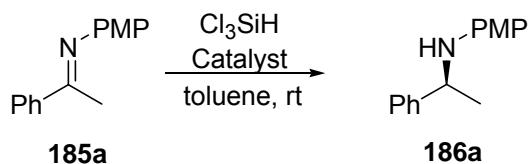


Table 30. Reduction of imine **185a with trichlorosilane, catalysed by **243a,b**, **244a,b**, **247**, **248**, and **253a**.**

entry	run	catalyst (mol%)	yield (%)	ee (%) ^b
1	–	187b (10)	85	91
2	–	247 (10)	80	89
3	–	248 (10)	80	91
4	–	253a	51	–
5	1	243a (<5) ^a	90	84
6	2	243a	92	82
7	3	243a	92	80
8	4	243a	89	68
9	–	243b (<5) ^a	88	70
10	–	244a (15)	91	39
11	–	244b (20)	86	79

^aThe reaction was carried using 100 mg of **243a** or 79 mg of **243b**. ^b Determined by chiral HPLC

Although the catalyst **243a** was used at less than 5% loading, high enantioselectivity and excellent chemical yield were obtained in the first run (entry 5). Note that the modification of the structure of the original catalyst **187b** with an ester functionality (catalysts **247** and **248**, entries 2 and 3) did not influence the reaction outcome significantly. Subsequent reuse of the regenerated catalyst in the next two cycles afforded the product with almost unchanged enantiopurity, and in very good yields (entries 6 and 7). However, after the third cycle the enantioselectivity decreased by about 15%. Similarly to the experiments with soluble and insoluble polymers, the support exhibited some catalytic activity, which obviously resulted in the formation of a racemic product (entry 4). We assumed therefore that the catalytic activity of the support was the main reason for lower enantiopurities obtained in comparison to the original transformation catalysed by **187b**. A decrease of the enantiomeric excess after the third run could be explained as follows: the original powder of **243a** forms a clear dispersion in toluene, and as a result the catalyst acts as nearly as the homogeneous one. However, after each run the functionalized gold nanoparticles aggregated (a well known phenomenon described in the literature and one of the most important difficulty related to the use of functionalized gold nanoparticles as reusable catalysts¹⁵⁸); as a result, their solubility in

toluene decrease. In other words, after each run the reaction character shifted from clearly homogeneous (first run) to almost heterogeneous (fourth run). (The TEM images of regenerated catalysts after the fourth run could not be prepared as the sample was insoluble in chloroform). Another problem observed was the appearance of the second component in the regenerated catalyst after the first run. Similarly to the catalyst immobilized on insoluble supports, after the first run, a peak at 2484 cm^{-1} appeared in the IR spectrum, which corresponds to the Si-H bond. This can derive from a partial hydrolysis or methanolysis of the excess trichlorosilane, yielding an insoluble solid, whose amount increased after each run. The solid component does not probably possess catalytic activity; however, due to its insolubility in toluene, the character of the reduction becomes more heterogeneous. Although the decomposition of the catalytic system by cleavage of the S-Au bond cannot be confirmed by analytical methods (note that the presence of the amino acid moiety is hardly detectable by ^1H MNR and undetectable by elemental analysis), this probably occurs as the reaction mixture is characterized by the characteristic smell of thiols after each run. As a result, the amount of the amino acid moiety on the surface of gold nanoparticles decreased slightly after each run and the damage to the coating surface made of butyl thiol units can increase the tendency of nanoparticles to aggregate.

Catalyst **243b** with the coating layer formed by octyl thiol exhibited similar activity and decreased stereoselectivity (88%, 70% ee, entry 9) compared to its lower homologue **243a** (entry 5).

The catalysts prepared by place exchange reaction form thiols **245** and **246** were not suitable for recycling due to their unlimited solubility in polar solvent. However, their activity was evaluated using a standard protocol. Good yields and enantiselectivities were observed for the catalyst **244b** (86%, 79% ee, entry 11), whereas its lower homologue with a three carbon spacer **244a** afforded product of significantly lower enantiopurity (39% ee, entry 10).

5.4.4 Conclusions

We have demonstrated a possibility of the use of the gold nanoparticles as a support for the *N*-methyvaline-derived formamide **187b** in the reduction of imines with trichlorosilane. Among the catalysts prepared the best results were obtained with **243a** (up to 84% ee), which represent some improvement compared to the solid supported catalysts as the new catalyst operates in a nearly homogeneous solution. The new catalyst can easily be separated from the reaction mixture by changing the polarity of the solvent, which simplified the isolation procedure and allowed its undemanding recovery. In addition the regenerated

catalyst could be reused twice without a significant loss of activity or selectivity. This work may be viewed as a proof of concept, which could be further extended to other, less expensive nanoparticle systems, such as those based on iron.

5.5 Immobilization of the catalyst on a soluble polymer

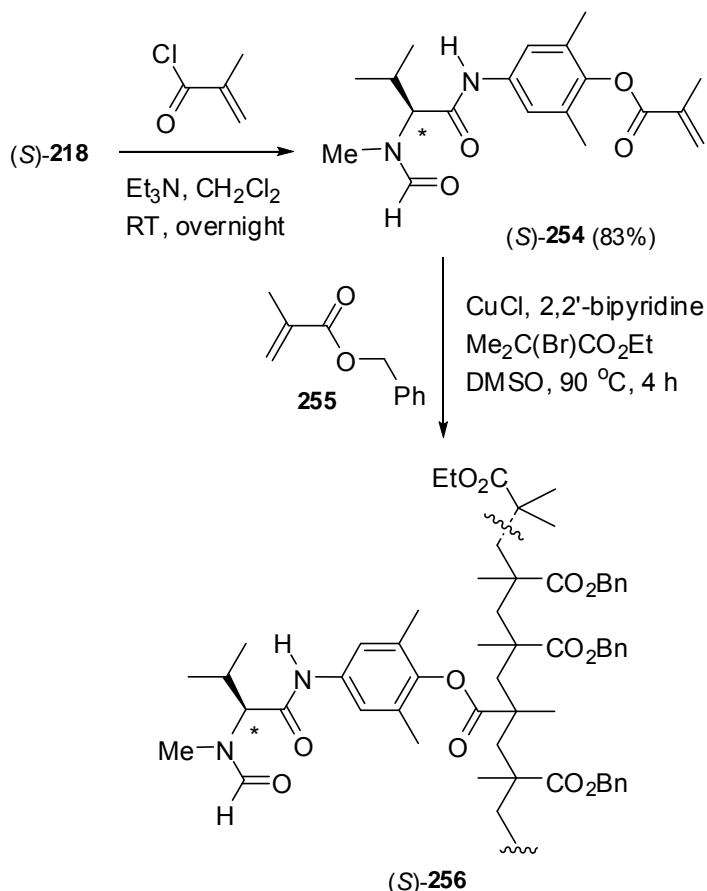
As shown above, the catalyst with a fluorine tag works in a solution and the difference between its performance and that of the untagged predecessor is negligible. On the other hand, the catalyst attached to an insoluble polymer exhibited lower stereoselectivity (by ~10-15%) due to the heterogeneous nature of the transformation. The catalyst immobilized on gold nanoparticles proved the concept of a heterogeneous catalyst operating in solution; a small increase of enantioselectivities was observed. However, the stability of the latter catalyst, its overall performance, preparation, ease of the use and recycling could still be improved. We decided to design a catalyst supported on polymer, whose solubility would depend on the solvent polarity. Our idea was to create the polymeric catalyst soluble in toluene (the optimized solvent for our reduction) and insoluble in a polar solvent, such as methanol, to simplify the isolation of the catalyst. If successful, this methodology would serve as a remedy to the problems associated with the heterogeneous system observed in our previous work.

5.5.1 Catalyst synthesis

The synthesis of the required linear polymer commenced with the preparation of an amino-acid moiety suitable for co-polymerization with selected monomers under atomic transfer radical polymerization (ATRP).¹⁵⁹ Thus, phenol **218** (for its synthesis see Scheme 70) was first transformed into ester **254** (Scheme 85) by using methacryloyl chloride (83%). The resulting methacrylic ester **254** was then reacted with an excess of benzyl methacrylate **255** (1:99) in the presence of CuCl (1 mol% with respect to **255**), α,α' -bipyridine (3 mol%), and ethyl α -bromo-isobutyrate (1 mol%) in DMSO at 90 °C for 4 h (Scheme 85). After the reaction completion, the resulting copolymer **256** was precipitated by pouring the cooled mixture into an excess of methanol.

In the initial experiments, the amount of monomer **254** was varied in the range of 1, 5, and 10% with respect to benzyl methacrylate **255**, whereas the molar ratio of CuCl was kept constant (1 mol%). Copolymerization of **254** (1 mol%) with **255** produced **256a** in 46% isolated yield, which contained 0.13 mmol•g⁻¹ of the active moiety, as revealed by elemental analysis. However, when the amount of monomer **254** in the initial mixture was increased to 5 mol%, the copolymerization, carried out under identical reaction conditions, afforded the

copolymer **256** in only 9% yield. Further decrease of the yield (to 4%) was observed with 10 mol% of **254**. Clearly, **254** had a negative effect on the activity of the catalysts, which can be caused by the chelation of CuCl by the amide moieties of **254**. Therefore, in the subsequent experiments, the amount of CuCl was increased to equal that of **254**, which proved to have a beneficial effect. In a scaled-up, optimized experiment, carried out with a 5:95 mixture of **254** and **255** in the presence of CuCl (5 mol%), α,α' -bipyridine (15 mol%) and ethyl α -bromo-isobutyrate (1 mol%), copolymer **256b** ($0.19 \text{ mmol}\cdot\text{g}^{-1}$) was obtained in 48% yield.



Scheme 85. Synthesis of the supported catalyst; Bn = benzyl.

Further increase in the content of monomer **254** in the mixture did not lead to any increase in its incorporation into the copolymer **256**, showing that the copolymerization reached its saturation point.

The average molecular weight (M_n) of the copolymers **256a** and **256b** thus obtained was ~ 7800 and $6000 \text{ g}\cdot\text{mol}^{-1}$, respectively, as shown by gel permeation chromatography (GPC). The polydispersity index (PDI) of the copolymers **256a** and **256b** varied from 1.35 (**256a**) to 1.18 (**256b**), indicating the formation of a fairly homogeneous polymer.

The attempt to use methyl methacrylate instead of benzyl methacrylate yielded the polymers soluble in polar solvents thus making them unpractical for application in our reductions.

5.5.2 Asymmetric Reduction of Imines with Trichlorosilane catalysed by **256a,b**.

The catalysts immobilized on a soluble polymer were tested in our model reaction, using a modification of the standard protocol. The imine and catalyst **256** were dissolved in toluene, followed by the addition of trichlorosilane and an overnight reaction. The most significant difference compare to our original protocol was the catalyst separation. Thus, when the reaction was completed, the crude mixture (a solution in toluene), was added to a vigorously stirred methanol, which induced a precipitation of the catalyst, while the crude amine remained in a solution. However, due to the presence of toluene, which acted as a co-solvent, the catalyst precipitation was not quantitative. Therefore, the solvent from the methanolic solution was evaporated and the crude amine, contaminated with traces of the catalyst (~5% of the initial amount) was washed with methanol again. This procedure allowed a quantitative removal of the catalyst from the product. When the catalyst **256a** was used in a model reaction at 20 mol% loading, amine **186b** was formed in 90% chemical and 85% ee (entry 1). Similar performance was observed for catalyst **256b** at 7, 3, even at 1 mol% loading; the catalyst could then be recovered almost quantitatively (entries 2-4).

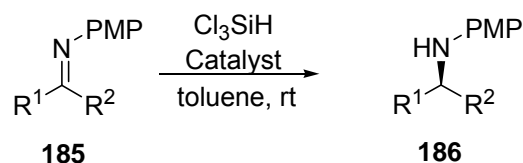


Table 31. Reduction of Ketimines **185a-k with Trichlorosilane, Catalysed by the Valine-Derived *N*-Methyl Formamides (*S*)-**256a/b**.**

entry	catalyst (mol%)	imine	R ¹	R ²	% catalyst recovery	yield %	186 % ee ^a
1	256a (20)	185a	Ph	Me	99	90	85
2	256b (7)	185a	Ph	Me	99	90	86
3	256b (3)	185a	Ph	Me	98	90	86
4	256b (1)	185a	Ph	Me	99	90	88
5	256b (7)	185b	4-CF ₃ -C ₆ H ₄	Me	92	75	86
6	256b (7)	185c	4-MeO-C ₆ H ₄	Me	85	87	82
7	256b (7)	185d	2-Naphth	Me	90	88	86
8	256b (7)	185f	3-thienyl	Me	96	78	65
9	256b (7)	185g	Ph	CH ₂ Cl	94	70	91
10	256b (7)	185h	Ph	CH ₂ CO ₂ Et	99	77	81
11	256b (7)	185i	Ph	<i>c</i> -Pr	99	71	73
12	256b (7)	185j	Ph	<i>c</i> -Bu	99	81	75
13	256b (7)	185k	Ph	<i>c</i> -Hex	98	85	55

^a Determined by chiral HPLC

The scope of application was then briefly elucidated with the substrates characterized by a different substitution pattern; the results are summarized in Table 31. In consonance with the previous observations, high enantioselectivities were attained for imines derived from aromatic ketones **185b-d** with both electron-withdrawing and electron-donating groups (entries 4-7). Imine **185f** with the β -thiophene nucleus (entry 8) exhibited lower enantioselectivity as observed previously for aromatic heterocycles.¹⁶⁰ By contrast, the presence of a heteroatoms in the alkyl part (**185g,h**) had a positive effect (entries 9 and 10), reaching the maximum of 91% ee. The cyclopropyl and cyclobutyl derivatives **185i,j** also exhibited acceptable enantioselectivities (entries 11 and 12), whereas a larger decrease was observed for the bulkier cyclohexyl derivative **185k** (entry 13).

The suitability of the catalyst for a multiple use was confirmed in the experiment with subsequent reuse of the recovered catalyst in a cycle of transformation. At least 5 runs were possible without the loss of activity or selectivity. In sharp contrast to the catalyst immobilized on insoluble polymer, the new catalytic system did not required conditioning.

Table 32. Asymmetric reduction of imines **185a with trichlorosilane catalysed by the reused **256b** (20 mol%) in toluene.**

run	catalyst recovery in %	yield %	(<i>S</i>)- 186a % ee ^a
1	99	86	86
2	95	87	86
3	94	90	84
4	93	90	86
5	95	90	86

^a Determined by chiral HPLC

5.5.3 Conclusions

In conclusion, an effective soluble polymer supported catalyst for asymmetric reduction of imines with trichlorosilane has been developed. The methodology simplifies the recovery of the catalyst and produces chiral amines **186a-k** in high chemical yields and with good enantioselectivity ($\leq 91\%$ ee) at low catalyst loading. The catalyst can be reused at least 5 times without any loss of activity, which demonstrates its suitability for multiple and parallel use. The main advantage of the present system over our previous solid-supported catalysts can be seen in the homogeneous conditions. Most of the existing soluble immobilized catalysts were prepared by anchoring the homogeneous catalyst to a polyethylene glycol (PEG) support.¹⁶¹ Separation of the product from this type of catalysts requires precipitation by adding a nonpolar solvent (hexane or ether) and, as a result, polar products and inorganic impurities also tend to precipitate (at least partly), which complicates the workup and the purification of the catalyst for re-use and lowers the yields. By contrast, **256b** can be

precipitated from a toluene solution (i.e., non-polar) by methanol, so that the coprecipitation of the inorganics and polar products is either avoided or minimized. The narrow range of the molecular weight of the copolymer **256b** can be regarded as a contributor to the overall behavior of the anchored catalyst.

5.6 Immobilization of the Catalyst on Inorganic Support

The application of inorganic materials as support for heterogeneous catalysts offers a number of benefits: their rigid structure does not allow the aggregation of active catalysts, they do not swell, and are insoluble in organic solvent. The lack of swelling properties and the insolubility in organic solvents make them an interesting material for the use in a continuous flow process. Our successful attempts to immobilize the *N*-methyl-L-valine derived formamide **187b** on soluble and insoluble polymers inspired us to attach the amino-acid moiety to the surface of silica gel (Figure 36) and to explore the area of inorganic supports.

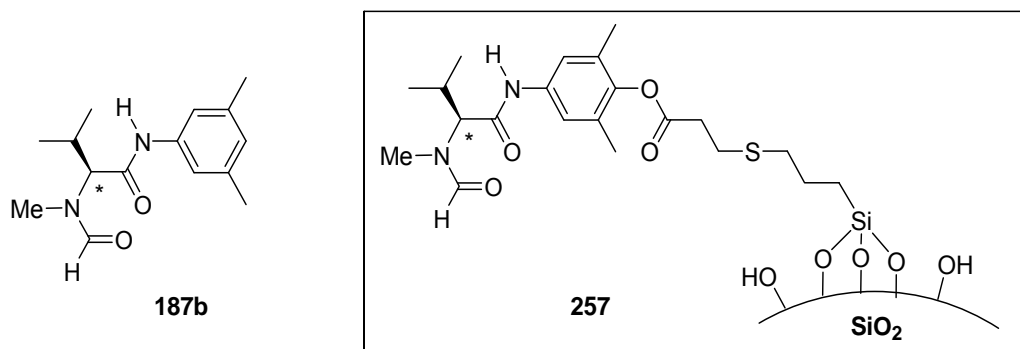
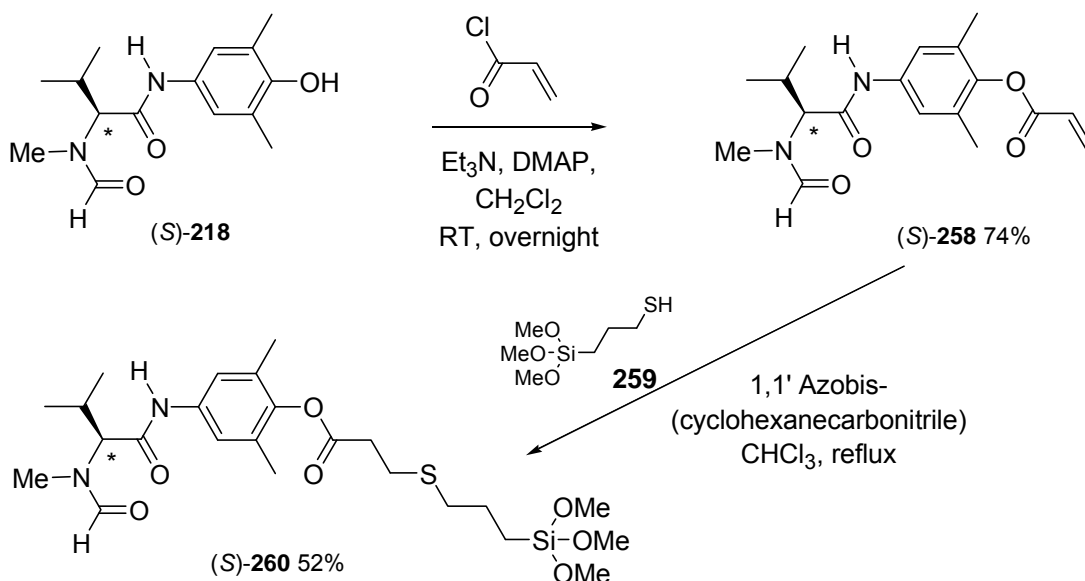


Figure 36.Champion organocatalyst for asymmetric reduction of imines with trichlorosilane **187b** and its silica gel supported derivative **257**

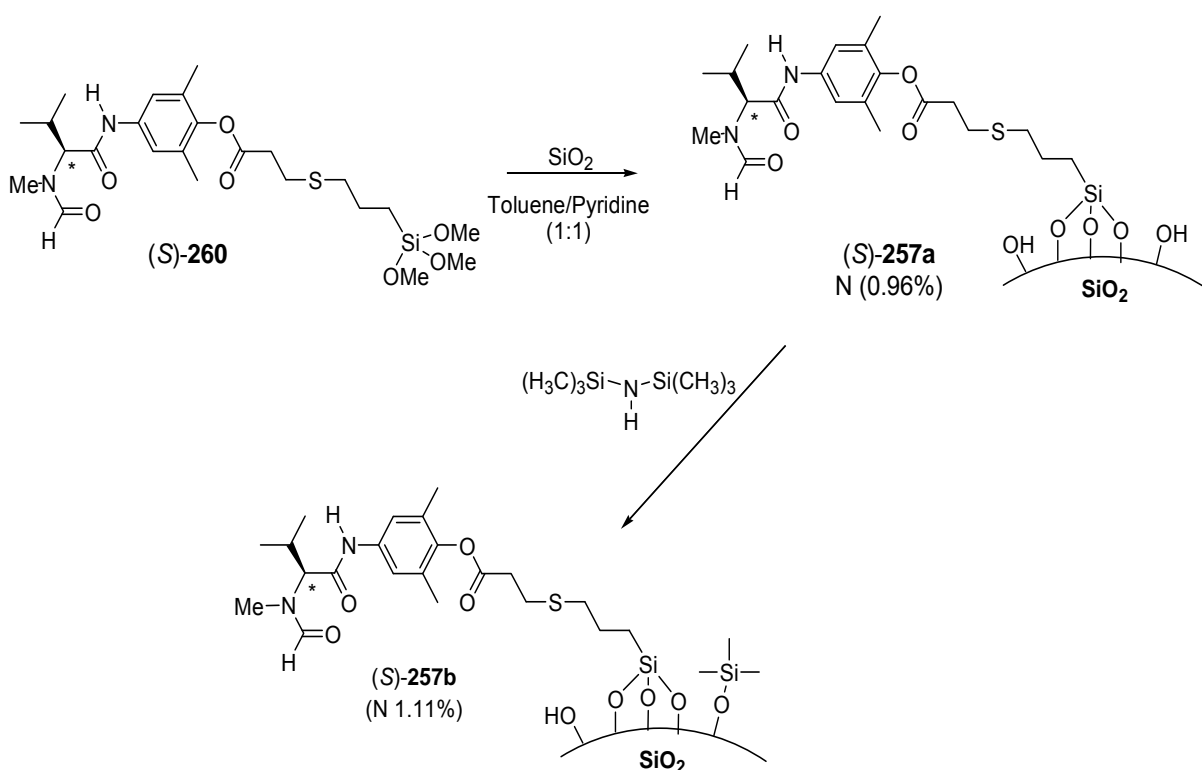
The key organic intermediated suitable for the attachment of amino acid moiety to the surface of silica gel was formamide **260**, whose synthesis commenced with esterification of phenol **218** (for its synthesis see Scheme 70) with acryloyl chloride (74%).



Scheme 86. Synthesis of the key intermediate **260**

The resulting ester **258** was then treated with an excess of (3-mercaptopropyl) trimethoxysilane **259** in the presence of radical initiator¹⁶² to afford the desired product **260** in 52% yield.

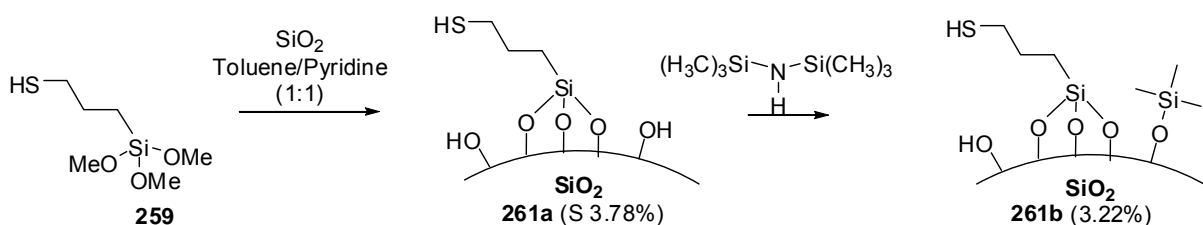
Immobilization of **260** on the inorganic support was performed using an adaptation of the method described by Song.¹⁶³ Silica gel was stirred with the silane derivative **260** at 90 °C in a 1:1 mixture of toluene and pyridine for 40 h. To ensure a removal of any potential impurities, the crude product was washed exhaustingly with methanol and dichloromethane and after an overnight drying the catalyst **257a** was obtained as a yellow powder. The attachment of the amino acid moiety was confirmed by elemental analysis (0.96% of N). An attempt to improve the immobilization by doubling the **260** : silica gel ratio failed. In the next step, protection of the remaining hydroxyl groups at the surface of silica gel had to be performed as we were aware that those functionalities can negatively influence the outcome of the imine reduction. To this end, a sample of **257a** was subjected to an exhausting silylation with hexamethyldisilazane¹⁶⁴ at 60 °C for 48 h. Indeed, the population of hydroxyl functionalities observed in IR spectrum decreased in comparison to the substrate, though only by about 25 % (cat. **257b**).



Scheme 87. Preparation of catalysts **257a,b**

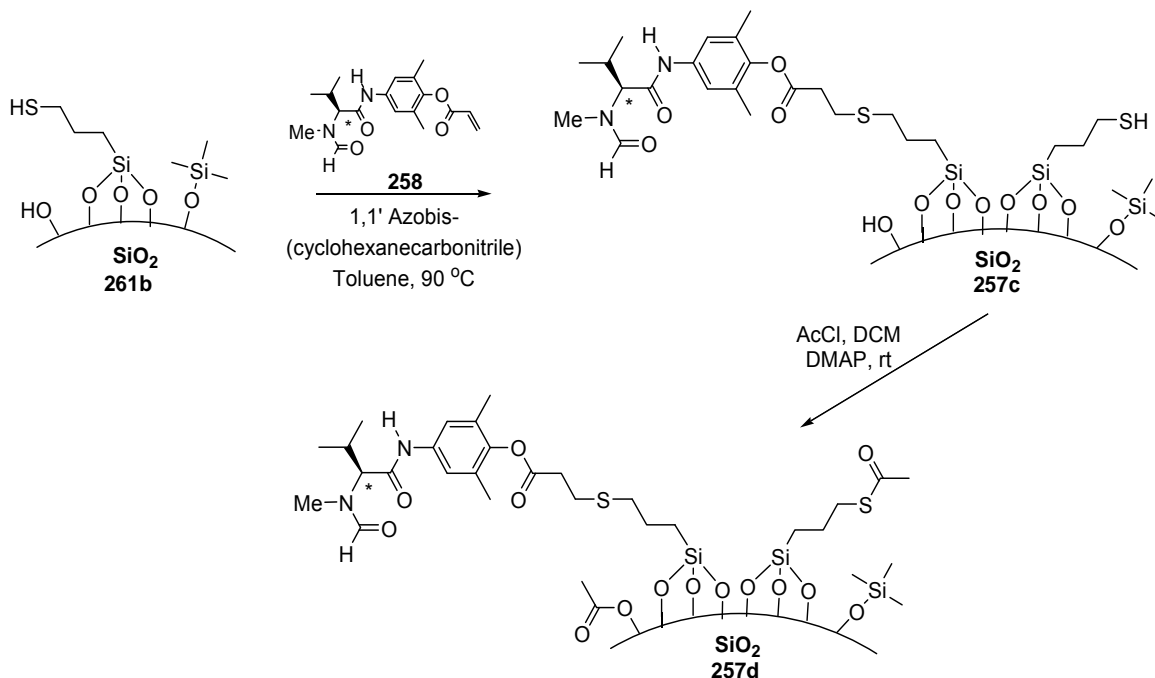
An alternative way of immobilization of the catalyst could also be possible by derivatization of the silica gel with the thiol-functionalized linker first, followed by protection

of the free hydroxyl functionalities. The amino acid moiety could then be introduced via a radical transformation using formamide **258**. The advantage of the new approach would be a simplification of the synthesis of key organic intermediate (**258** instead of **260**) first and the possibility of using much more vigorous conditions during the protection of hydroxyl functionalities from the support without a potential danger of affecting the amino acid moiety.



Scheme 88. Preparation of the support for an immobilization of amino acid moiety **258**

Derivatization of silica gel with silane **259** was carried out as described for the attachment of **260**, and after a 24 h reaction the functionalized support **261a** was obtained as a yellowish solid (3.78% of S.). Protection of hydroxyl groups with hexamethyldisilazane at 100 °C for 72 h afforded silica gel **261b** (3.22% of S) suitable for the attachment of formamide **258**.



Scheme 89. Derivatization of silica gel via intermediate **258**

In the next step the support **261b** was derivatized with the amino acid moiety using an in excess of acryloyl ester **258** and a radical initiator and the reaction was carried out in toluene at 90 °C¹⁶⁴. After 48 h the immobilized catalyst **257c** was obtained as a yellow solid

(Anal. 0.70% of N). Treatment of **257c** with acetyl chloride at room temperature for 24 h afforded the catalyst **257d** (0.65% of N).

5.7 Asymmetric reduction of imine **185a** in the presence of silica gel supported catalyst

The activity of the silica gel-supported catalysts was examined by using a modification of the standard protocol. Thus, to a suspension of imine **185a** and the catalyst in toluene, trichlorosilane was added and the reaction was carried out overnight. After reaction completion the mixture was diluted with methanol, and the solid catalyst was separated by filtration. The solvent from the methanolic solution was evaporated and the crude product was worked up as usual by washing with NaHCO₃. To regenerate the catalyst, the solid from the filter was washed intensively with methanol, dichloromethane, and ether and dried. The regenerated catalyst was used in the next transformation without further purification and the results are summarized in Table 33. When catalyst **257a** was used for the reduction of imine **185a** at 20 mol%, the product was obtained with high yield, though with moderate enantioselectivity (entry 1). In contrast to the insoluble polymer-supported catalysts, where an improvement of enantioselectivities was observed after the first run, repeated use of **257a** afforded the product of slightly lower enantiopurity (entry 2). In both cases the catalyst could be recovered with high 90% yield. Some improvement of enantioselectivities was observed when catalyst **257b** with partially protected hydroxyl groups on the surface of silica gel was used in the reduction (entries 3-4). However, the enantiopurities of the product were still moderate (~50% ee). Finally, catalyst **257c** afforded an almost racemic product (entry 5) and only some improvement was observed after conditioning with acetyl chloride (cat **257d**, entry 6). All these results clearly point toward the negative influence of silica gel on the outcome of the reaction. Therefore, the potential ability of the support to catalyse the reduction was investigated next. Application of silica gel and the support **261b** afforded product with good chemical yields (entries 8-9), which was obviously racemic. Therefore, it can be assumed that the ability of the achiral support to activate trichlorosilane is the main factor responsible for the low asymmetric inductions observed in previous experiments.

The ability of silica gel to activate trichlorosilane eliminated this material as a potential support for our chiral catalysts.

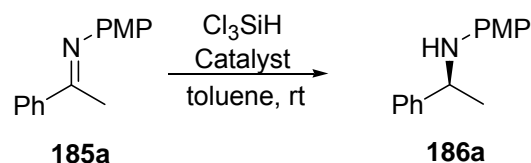


Table 33. Reduction of imine **185a with trichlorosilane, catalysed by **257a-d**, **SiO₂**, and **261b**.**

entry	catalyst (mol%)	run	yield (%)	ee (%) ^b	catalyst recovery (%)
1	257a (20)	1	88	41	89
2		2	90	31	90
3	257b (20)	1	90	48	95
4		2	86	50	94
5	257c (15)	1	88	14	88
6	257d (15)	1	92	41	88
7	257d (15)	2	92	29	90
8	SiO₂ ^a	-	72	-	-
9	261b ^a	-	83	-	-

^a The reaction was carried out on 0.22 mmol scale using 100 mg of the support. ^b Determined by chiral HPLC

5.8 General Conclusions

The practicality of the asymmetric reduction of ketimines with trichlorosilane catalysed by Lewis-basic formamides derived from *N*-methylvaline has now been considerably enhanced by fluorine tagging of the catalyst, which allows a very easy isolation of the product and an undemanding recovery of the catalyst that can be used in the next cycle. The fluorine catalysts operate in a solution and the difference between their efficiency and that of their untagged predecessors is negligible. Immobilization of the catalysts on a solid support simplifies the isolation procedure even further (simple filtration), though some loss of catalytic efficiency was observed due to the heterogeneous nature of the reaction. The reinstatement of homogeneous reaction conditions combined with the simplicity of separation of the heterogeneous catalyst was achieved by attaching the amino acid moiety to gold nanoparticles and soluble polymer. In both cases an improvement of the catalytic efficiency was observed in comparison to the solid support and separation from the product was simplified to a simple mechanical filtration after precipitation of the catalyst by addition of a polar solvent. These technologies appear to be particularly suitable to the small-scale parallel chemistry.

Attempts to immobilize our catalyst on the surface of silica gel and in ionic liquids have been made. However, silica gel and ionic liquids have been found to activate trichlorosilane, which results in the formation of racemic amines, and disqualifies these two classes from further consideration.

EXPERIMENTAL

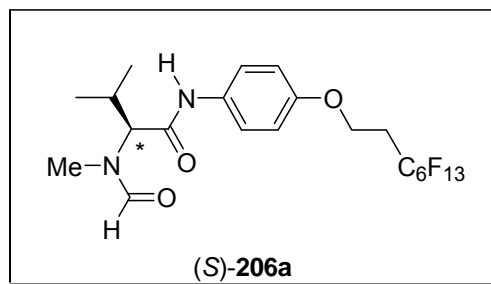
6 Experimental

General Methods. Melting points were determined on a Kofler block and are uncorrected. Optical rotations were recorded in CHCl_3 at 25 °C unless otherwise indicated, with an error of $\leq \pm 0.1$. The $[\alpha]_D$ values are given in $10^{-1} \text{ deg cm}^3 \text{ g}^{-1}$. The NMR spectra were recorded in CDCl_3 , ^1H at 400 MHz and ^{13}C at 100.6 MHz, with chloroform- d_1 (δ 7.26, ^1H ; δ 77.0, ^{13}C) as internal standard unless otherwise indicated. ^{19}F spectra were recorded at 376.5 MHz in CDCl_3 using CFCl_3 (δ 0) as a standard. Various 2D-techniques and DEPT experiments were used to establish the structures and to assign the signals. The IR spectra were recorded for KBr discs or for a thin film between NaCl plates. The mass spectra (EI and/or CI) were measured on a dual sector mass spectrometer using direct inlet and the lowest temperature enabling evaporation. All reactions were performed under an atmosphere of dry, oxygen-free nitrogen in oven-dried glassware, twice evacuated and filled with inert gas. Solvents and solutions were transferred by syringe-septum and cannula techniques. All solvents for the reactions were of reagent grade and were dried and distilled under nitrogen immediately before use as follows: toluene from sodium/benzophenone, dichloromethane from calcium hydride, triethylamine from calcium hydride. Petroleum ether refers to the fraction boiling in the range of 60–80 °C. Yields are given for isolated products showing one spot on a TLC plate and no impurities detectable in the NMR spectrum. The identity of the products prepared by different methods was checked by comparison of their NMR, IR, and MS data and by the TLC behavior. The chiral HPLC methods were calibrated with the corresponding racemates. Imines **185a-k** and amines **186a-k** are known compounds, previously prepared in this Laboratory;^{136,138a,b,165a,b} The molecular weight of the polymers (M_n and M_w) and the polydispersity index (PDI) were determined by gel permeation chromatography (GPC) using THF as eluent and polymethyl methacrylate as calibration standard. The content of the catalyst anchored to the polymer and gold nanoparticles was determined by elemental analysis (C, H, N, S).

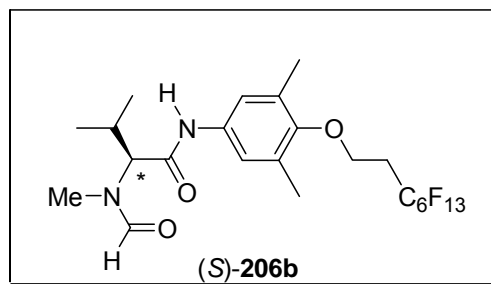
The following resins were employed in this study: (a) Chloromethylpolystyrene (**235**) 1.23 mmol/g 75–150 μm (StratoSphere), obtained from Polymer Laboratories; (b) 5-[4 (Chloromethyl)phenyl]pentyl]styrene (**238**), polymer-bound 0.75–1.25 mmol/g 100–200 μm , obtained from Aldrich; (c) Bromomethylphenoxyethyl polystyrene (**236**) 1.40 mmol/g (StratoSphere) 150–300 μm , obtained from Polymer Laboratories; (d) 4-Hydroxymethylphenoxyethyl polystyrene (**237**) 1.70 mmol/g (StratoSphere) 150–300 μm , obtained from Polymer Laboratories; (e) TentaGel HL Br resin (**239**), 0.43 mmol/g, 110 μm ,

obtained from Rapp Polymere GmbH; (f) TentaGel HL OH resin (**240**) 0.43 mmol/g 110 μm , obtained from Rapp Polymere GmbH; (g) 4-Hydroxytiophenol resin (**241**), 1.58 mmol/g, 150–300 μm (StratoSphere), obtained from Polymer Laboratories.

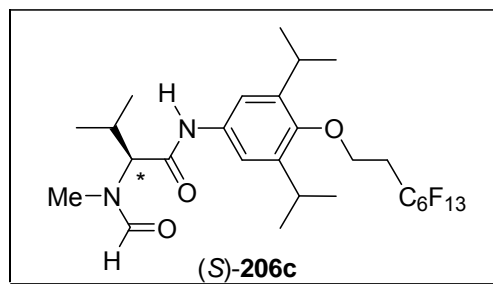
Silicagel used for immobilization of the catalyst was Kieselgel Typ 60, 70-230 mesh, 60Å, Porendurchmesser obtained from Aldrich.



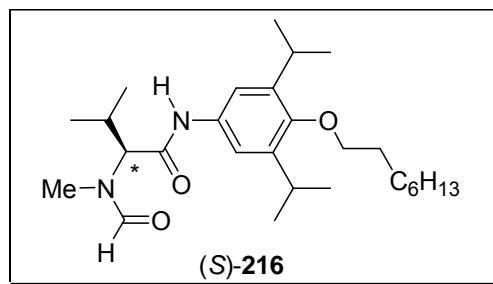
Formamide (S)-(-)-206a. The BOC derivative **214a** (340 mg, 0.51 mmol) was dissolved in trifluoroacetic acid (2 mL) at room temperature. After 1 h the acid was evaporated under reduced pressure and the residue was coevaporated with toluene (2 x 5 mL) to afford a TFA salt of the deprotected amine as brownish oil, which was used in the following step without further purification. The crude salt was dissolved in formic acid (1.5 mL) and the resulting solution was cooled to 0 °C. Acetic anhydride (0.7 mL, 7.42 mmol) was added dropwise and the mixture was allowed to stir at room temperature for 18 h. The volatiles were then removed under reduced pressure and the residue (347 mg) was dissolved in CH₂Cl₂ (25 mL) and washed with a saturated solution of NaHCO₃ (3 x 10 mL) and brine (10 mL). The organic solution was dried over MgSO₄ and evaporated. The residue (272 mg) was purified by chromatography on a column with silica gel (70 g) with a mixture of CH₂Cl₂ and MeOH (209:1) to afford formamide (S)-(-)-**206a** (228 mg, 73%) as a yellowish wax: *R_f* 0.45/0.22 (CH₂Cl₂-MeOH, 49:1); [α]_D -42.4 (*c* 0.5, EtOH); ¹H NMR (400 MHz, CDCl₃, a mixture of rotamers in ca. 4:1 ratio; the signals for the minor rotamer are marked with an *) δ 0.91 (d, *J* = 6.6 Hz, 3H), 1.05 (d, *J* = 6.3 Hz, 3H), 2.40-2.52 (m, 1H), 2.60 (tt, *J*_{H-H} = 6.8 Hz, *J*_{H-F} = 18.4 Hz, 2H), 2.93 (s, 0.44H*), 3.01 (s, 2.44H), 3.63 (d, *J* = 10.4 Hz, 0.17H*), 4.24 (t, *J* = 6.6 Hz, 2H), 4.43 (d, *J* = 11.3 Hz, 0.83H), 6.83-6.86 (m, 2H), 7.44-7.48 (m, 2H), 8.15 (s, 0.83H), 8.31 (s, 0.84H), 8.38 (s, 0.23H*), 8.50 (s, 0.2H*); ¹³C NMR δ 18.58 (CH₃), 19.52 (CH₃), 25.39 (CH), 31.23 (t, *J* = 21.4 Hz, CH₂), 31.63 (CH₃), 60.31 (CH₂), 63.01 (CH), 114.88 (CH), 121.62 (CH), 131.62 (C), 154.80 (C), 163.93 (CHO), 167.07 (CO); IR (KBr) ν 3467, 1658, 1606, 1546, 1512, 1472, 1239, 1145, 835, 809, 698 cm⁻¹; ¹⁹F NMR (CCl₃F) δ -81.23 (t, *J*_{F-F} = 10.3 Hz, 3F), -113.82 (m, 2F), -122.37 (m, 2F), -123.36 (m, 2F), -124.07 (m, 2F), -126.65 (m, 2F); MS (FAB) *m/z* (%) 597 ([MH]⁺, 38), 596 (58), 595 (16), 567 (14), 524 (13), 494 (12), 455 (48), 454 (11), 115 (100), 88 (82); HRMS (FAB) 597.1425 (C₂₁H₂₂O₃N₂F₁₃ requires 597.1423).



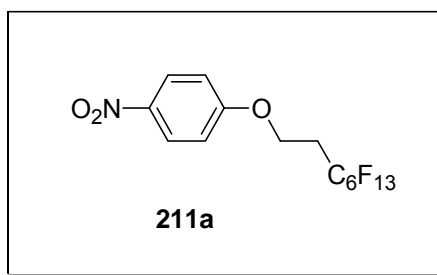
Formamide (S)-(-)-206b. Trifluoroacetic acid (3 mL) was added dropwise to a solution of BOC derivative **214b** (382 mg, 0.55 mmol) in CH₂Cl₂ (3 mL) at 0 °C and the stirring and cooling were continued for 1 h. The acid was removed under reduced pressure and the residue was coevaporated with toluene (2 x 5 mL) to afford a TFA salt of the deprotected amide as a brownish oil, which was used in the following step without further purification. The crude amine salt was dissolved in formic acid (1.7 mL) and the resulting solution was cooled to 0 °C. Acetic anhydride (1.3 mL) was then added dropwise and the mixture was allowed to stir at room temperature for 18h. The volatiles were then evaporated and the residue was coevaporated with toluene (3 x 5 mL). The residue (341 mg) was purified by chromatography on a column of silica gel (70 g) with a mixture of CH₂Cl₂ and MeOH (209:1) to afford formamide (S)-(-)-**206b** (278 mg; 82%) as a white solid: mp 25-26 °C; *R_f* 0.50/0.29 (CH₂Cl₂-MeOH, 49:1); [α]_D -37.1 (*c* 0.5, EtOH); ¹H NMR (400 MHz, CDCl₃, a mixture of rotamers in ca. 4:1 ratio; the signals for the minor rotamer are marked with an *) δ 0.91 (d, *J*) 6.6 Hz, 3H), 1.04 (d, *J* = 6.6 Hz, 3H), 2.24 (s, 6H), 2.40-2.51 (m, 1H), 2.61 (tt, *J*_{H-H} = 6.7 Hz, *J*_{H-F} = 18.7 Hz, 2H), 2.95 (s, 0.46H*), 3.00 (s, 2.46H), 3.65 (d, *J* = 10.6 Hz, 0.15H*), 3.99 (t, *J* = 6.6 Hz, 2H), 4.39 (d, *J* = 11.4 Hz, 0.83H), 7.20 (s, 1.34 H), 7.22 (s, 0.66H*), 8.14 (s, 0.80H), 8.17 (s, 0.81H), 8.38 (s, 0.15H*), 8.42 (s, 0.15H*); ¹³C NMR δ 16.24 (CH₃), 18.55 (CH₃), 19.53 (CH₃), 25.21 (CH), 31.56 (CH₃), 31.78 (t, *J* = 22.0 Hz, CH₂), 63.16 (CH), 63.75 (CH₂), 120.42 (CH), 131.39 (C), 133.58 (C), 151.89 (C), 163.99 (CHO), 167.07 (CO); ¹⁹F NMR (CCl₃F) δ -81.29 (t, *J*_{F-F} = 10.3 Hz, 3F), -113.77 (m, 2F), -122.35 (m, 2F), -123.34 (m, 2F), -124.06 (m, 2F), -126.61 (m, 2F); IR (KBr) ν 3444, 1658, 1615, 1556, 1487, 1241, 1145, 874, 808, 697 cm⁻¹; MS (FAB) *m/z* (%) 647 ([MNa]⁺, 100), 624 (55), 597 (11), 483 (36), 115 (87), 88 (76); HRMS (FAB) 647.1546 (C₂₃H₂₅O₃N₂NaF₁₃ ([MNa]⁺ requires 647.1555).



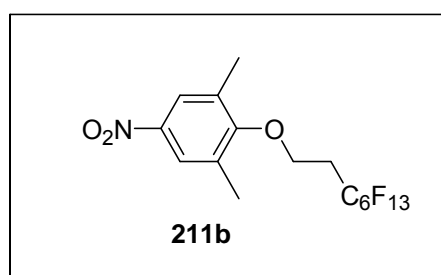
Formamide (S)-(-)-206c. Trifluoroacetic acid (2.3 mL) was added dropwise to a solution of BOC derivative **214c** (350 mg, 0.46 mmol) in CH_2Cl_2 (3.5 mL) at 0 °C and the stirring and cooling were continued for 1 h. The acid was removed under reduced pressure and the residue was coevaporated with toluene (2 x 10 mL) to afford a TFA salt of the deprotected amide as a brownish oil, which was used in the following step without further purification. The crude amine salt was dissolved in formic acid (2.6 mL) and the resulting solution was cooled to 0 °C. Acetic anhydride (1.9 mL) was then added dropwise and the mixture was allowed to stir at room temperature for 26 h. The volatiles were then evaporated and the residue was coevaporated with toluene (3 x 5 mL). The residue (352 mg) was purified by chromatography on a column of silica gel (50 g) with a mixture of CH_2Cl_2 and MeOH (260:1) to afford formamide (S)-(-)-**206c** (250 mg; 78%) as a white solid: mp 46-48 °C; R_f 0.70/0.50 (CH_2Cl_2 -MeOH, 49:1); $[\alpha]_D$ -33.6 (c 0.5, EtOH); ^1H NMR (400 MHz, CDCl_3 , a mixture of rotamers in ca. 4:1 ratio; the signals for the minor rotamer are marked with an *) δ 0.92 (d, J) 6.6 Hz, 3H), 1.06 (d, J = 6.6 Hz, 3H), 1.21 (d, J = 6.8 Hz, 6H), 1.23 (d, J = 6.8 Hz, 6H), 2.42-2.52 (m, 1H), 2.65 (tt, $J_{\text{H-H}}$ = 6.7 Hz, $J_{\text{H-F}}$ = 18.7 Hz, 2H), 2.97 (s, 0.32H*), 3.00 (s, 2.68H), 3.22 (hept, J = 6.8 Hz, 2H), 3.61 (d, J = 10.7 Hz, 0.18H*), 3.98 (t, J = 6.8 Hz, 2H), 4.40 (d, J = 11.3 Hz, 0.82H), 7.27 (s, 1.70 H), 7.32 (s, 0.25 H*), 7.97 (s, 0.82H), 8.15 (s, 0.84H), 8.43 (s, 0.13H*); ^{13}C NMR δ 18.58 (CH_3), 19.70 (CH_3), 23.90 (CH_3), 25.20 (CH), 26.81 (CH), 31.55 (CH_3), 31.99 (t, J = 21.6 Hz, CH_2), 63.12 (CH), 66.17 (CH_2), 115.99 (CH), 134.70 (C), 142.47 (C), 149.31 (C), 164.03 (CHO), 166.92 (CO); ^{19}F NMR (CCl_3F) δ -81.25 (t, $J_{\text{F-F}}$ = 10.1 Hz, 3F), -113.84 (m, 2F), -122.37 (m, 2F), -123.40 (m, 2F), -124.08 (m, 2F), -126.64 (m, 2F); IR (KBr) ν 3455, 2967, 1660, 1607, 1554, 1468, 1242, 1206 cm^{-1} ; MS (EI) m/z (%) 680 (M^+ , 62), 539 (72), 192 (56), 114 (100), 86 (35), 55 (11); HRMS (EI) 680.2281 ($\text{C}_{27}\text{H}_{33}\text{O}_3\text{N}_2\text{F}_{13}$ requires 680.2284).



Formamide (S)-(-)-216. Trifluoroacetic acid (5.6 mL) was added dropwise to a solution of BOC derivative **215** (580 mg, 1.12 mmol) in CH_2Cl_2 (9 mL) at 0 °C and the stirring and cooling were continued for 1 h. The acid was removed under reduced pressure and the residue was coevaporated with toluene (2 x 10 mL) to afford a TFA salt of the deprotected amide as a brownish oil, which was used in the following step without further purification. The crude amine salt was dissolved in formic acid (6.3 mL) and the resulting solution was cooled to 0 °C. Acetic anhydride (4.8 mL) was then added dropwise and the mixture was allowed to stir at room temperature for 19 h. The volatiles were then evaporated and the residue was coevaporated with toluene (3 x 5 mL). The residue (540 mg) was purified by chromatography on a column of silica gel (50 g) with a mixture of CH_2Cl_2 and MeOH (260:1) to afford formamide (S)-(-)-**216** (302 mg; 60%) as a colorless oil: R_f 0.72/0.42 (CH_2Cl_2 -MeOH, 49:1); $[\alpha]_D -48.2$ (c 0.5, EtOH); ^1H NMR (400 MHz, CDCl_3) δ 0.87-0.92 (m, 3H), 0.91 (t, J = 6.4 Hz, 3H partly overlapped with the latter multiplet), 1.06 (d, J = 6.5 Hz, 3H), 1.20 (d, J = 6.9 Hz, 6H), 1.21 (d, J = 6.9 Hz, 3H), 1.29-1.37 (m, 8H), 1.44-1.52 (m, 2H), 1.76-1.83 (m, 2H), 2.40-2.55 (m, 1H), 2.96 (s, 0.49H*), 3.00 (s, 2.51H), 3.28 (hept, 2H, J = 6.9 Hz), 3.61 (d, J = 10.5 Hz, 0.17H), 3.67 (t, J = 6.6 Hz, 2H), 4.42 (d, J = 11.2 Hz, 0.84H), 7.26 (s, 1.75H), 7.29 (s, 0.25H*), 8.03 (s, 0.74H), 8.14 (s, 0.86H), 8.42 (s, 0.14H*); ^{13}C NMR δ 14.09 (CH_3), 18.53 (CH_3), 19.64 (CH_3), 22.64 (CH_2), 23.95 (CH_3), 25.18 (CH), 26.03 (CH_2), 26.53 (CH), 29.24 (CH_2), 29.44 (CH_2), 30.34 (CH_2), 31.49 (CH_3), 31.83 (CH_2), 62.91 (CH), 75.03 (CH_2), 115.77 (CH), 133.96 (C), 142.55 (C), 150.09 (C), 163.92 (CO), 166.74 (CO); IR (KBr) ν 3425, 2962, 1659, 1606, 1551, 1466, 1244, 1207 cm^{-1} ; MS (EI) m/z (%) 446 (M^+ , 100), 339 (10), 305 (100), 219 (12), 193 (93), 142 (100), 114 (100), 86 (85), 43 (49); HRMS (EI) 446.3510 ($\text{C}_{27}\text{H}_{46}\text{O}_3\text{N}_2$ requires 446.3508).

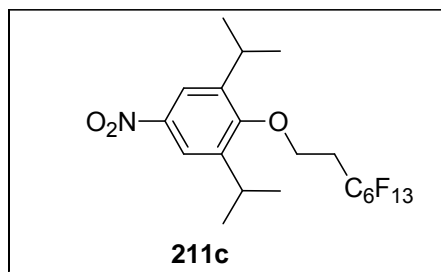


Ether 211a. A 28% aqueous solution of NaOH (6 mL) was slowly added dropwise to a mixture of *p*-fluoronitrobenzene **209** (5.30 g, 37.6 mmol), 1,1,2,2-tetrahydroperfluorooctanol **210** (2.00 g, 5.5 mmol), and tetrabutylammonium iodide (520 mg, 1.4 mmol) and the mixture was stirred at 45 °C for 48 h. After this time water (30 mL) was added and the mixture was extracted with CH₂Cl₂ (3 x 40 mL). The organic phase was dried over MgSO₄ then the solvent was evaporated to give a mixture of white solid and brown oil (7.39 g). The crude product was purified by chromatography on a column of silica gel (180 g) with a mixture of petroleum ether and CH₂Cl₂ (6:1) to afford ether **211a** (2.14 g, 80%) as a yellowish oil, which became a solid after cooling in a fridge: mp 26-27 °C; *R_f* 0.30 (petroleum ether-dichloromethane, 4:1); ¹H NMR (400 MHz, CDCl₃) δ 2.69 (tt, *J*_{H-H} = 6.6 Hz, *J*_{H-F} = 18.1 Hz, 2H), 4.37(t, *J* = 6.6 Hz, 2H), 6.98 (br d, *J* = 9.3 Hz, 2H), 8.22 (br d, *J* = 9.3 Hz, 2H); ¹³C NMR δ 31.13 (t, *J* = 21.9 Hz, CH₂), 60.74 (CH₂), 114.45 (CH), 125.97 (CH), 142.09 (C), 162.88 (C); ¹⁹F NMR (CCl₃F) δ -81.24 (t, *J*_{F-F} = 9.2 Hz, 3F), -113.77 (m, 2F), -122.32 (m, 2F), -123.34 (m, 2F), -123.99 (m, 2F), -126.61 (m, 2F); MS (FAB) *m/z* (%) 486 ([MH]⁺, 100), 469 (94), 124 (19), 71 (42); HRMS (FAB) 486.0377 (C₁₄H₉O₃NF₁₃ [MH]⁺ requires 486.0375).

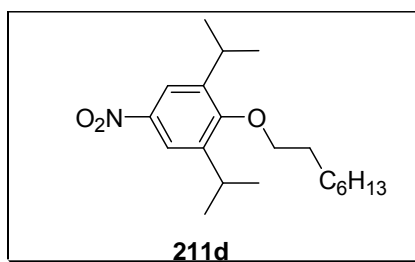


Ether 211b. Triphenylphosphine (690 mg, 2.63 mmol), 1,1,2,2-tetrahydroperfluorooctanol **210** (0.6 mL, 2.75 mmol), and diethylazodicarboxylate (0.42 mL, 2.6 mmol) were added successively to a stirred solution of 2,6-dimethyl-4-nitrophenol **207** (370 mg, 2.2 mmol) in THF (5 mL) at 0 °C and the resulting mixture was stirred at 25 °C for 18 h. The mixture was partitioned between brine (20 mL) and ethyl acetate (40 mL), the organic phase was dried

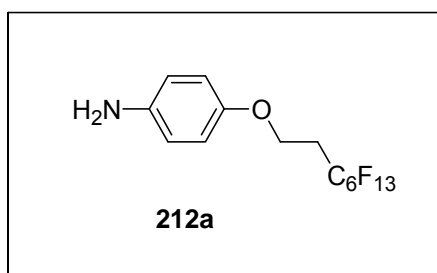
over MgSO_4 and concentrated, and then ether (40 mL) was added to induce the precipitation of triphenylphosphine oxide, which was separated by filtration. The filtrate was evaporated and the residue (1.9 g) was purified by chromatography on a column of silica gel (60 g) with a mixture of petroleum ether and dichloromethane (6:1, R_f 0.25) to afford ether **211b** (470 mg, 41%) as a white solid: mp 53-54 °C; ^1H NMR (400 MHz, CDCl_3) δ 2.36 (s, 6H), 2.68 (tt, $J_{\text{H-H}} = 6.6$ Hz, $J_{\text{H-F}} = 18.5$ Hz, 2H), 4.11 (t, $J = 6.6$ Hz, 2H), 7.94 (s, 2H); ^{13}C NMR δ 16.46 (CH_3) 31.81 (t, $J = 22.0$ Hz, CH_2), 63.95 (CH_2), 124.36 (CH), 132.35 (C), 143.89 (C), 160.41 (C); ^{19}F NMR (CCl_3F) δ -81.26 (t, $J_{\text{F-F}} = 10.3$ Hz, 3F), -113.70 (m, 2F), -122.30 (m, 2F), -123.31 (m, 2F), -123.99 (m, 2F), -126.59 (m, 2F); MS (FAB) m/z (%) 514 ($[\text{MH}]^+$, 100), 497 (41), 152 (10), 71 (18); HRMS (FAB) 514.0696 ($\text{C}_{16}\text{H}_{13}\text{O}_3\text{NF}_{13}$ $[\text{MH}]^+$ requires 514.0688).



Ether 211c. Triphenylphosphine (1.38 g, 5.26 mmol), 1,1,2,2-tetrahydroperfluorooctanol **210** (1.2 mL, 5.5 mmol), and diethylazodicarboxylate (0.84 mL, 5.3 mmol) were added successively to a stirred solution of 2,6-diisopropyl-4-nitrophenol **208** (1.00 g, 4.5 mmol) in THF (10 mL) at 0 °C and the resulting mixture was stirred at 25 °C for 20 h. The mixture was partitioned between brine (40 mL) and ethyl acetate (80 mL), the organic phase was dried over MgSO_4 , and a solvent was evaporated affording 4.21 g of a residue. The residue was purified by chromatography on a column of silica gel (100 g) with a mixture of petroleum ether and ethyl acetate (6:1) to afford ether **211c** (840 mg, 33%) as a white solid: mp 58-59 °C; R_f 0.60 (petroleum ether-dichloromethane, 5:1); ^1H NMR (400 MHz, CDCl_3) δ 1.28 (d, $J = 6.9$ Hz, 12H), 2.71 (tt, $J_{\text{H-H}} = 6.7$ Hz, $J_{\text{H-F}} = 18.4$ Hz, 2H), 3.28 (hept, $J = 6.9$ Hz, 2H), 4.07 (t, $J = 6.6$ Hz, 2H), 8.01 (s, 2H); ^{13}C NMR δ 23.66 (CH_3) 27.08 (CH), 31.91 (t, $J = 22.5$ Hz, CH_2), 66.43 (CH_2), 120.16 (CH), 143.65 (C), 145.27 (C), 157.93 (C); ^{19}F NMR (CCl_3F) δ -81.26 (t, $J_{\text{F-F}} = 10.1$ Hz, 3F), -113.73 (m, 2F), -122.28 (m, 2F), -123.31 (m, 2F), -123.97 (m, 2F), -126.58 (m, 2F); MS (EI) m/z (%) 569 (M^+ , 100), 554 (90), 511 (17), 221 (77), 208 (40), 164 (36), 82 (27), 43 (14); HRMS (EI) 569.1230 ($\text{C}_{20}\text{H}_{20}\text{O}_3\text{NF}_{13}$ requires 569.1236).

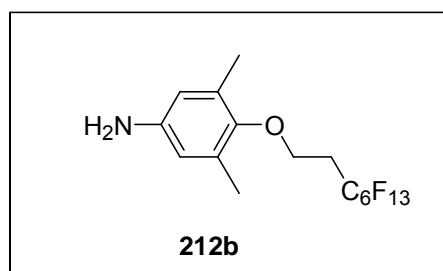


Ether 211d. Potassium carbonate (1.00 g, 7.23 mmol) and iodoctane (1.00 mL, 5.50 mmol) were consequently added to a stirred solution of 2,6-diisopropyl-4-nitrophenol **208** (0.53 g, 2.37 mmol) in dry acetone (11 mL). A mixture was heated at 45 °C for 19 h followed by evaporation of the solvent. Ether (50 mL) and water (20 mL) were added to a residue and after separation an organic phase was additionally washed with water (20 mL). The organic solution was dried over MgSO₄ and evaporation of the solvent afforded a crude product (1.52 g). The crude product was purified on a column of silica gel (50 g) with a mixture of petroleum ether and dichloromethane (8:1) to give ether **211d** (750 mg, 94%) as a colorless oil; *R_f* 0.52 (petroleum ether-dichloromethane, 5:1); ¹H NMR (400 MHz, CDCl₃) δ 0.88-0.92 (m, 3H), 1.26 (d, *J* = 6.9 Hz, 12H), 1.29-1.41 (m, 8H), 1.47-1.53 (m, 2H), 1.81-1.88 (m, 2H), 3.33 (hept, *J* = 6.9 Hz, 2H), 3.77 (t, 2H, *J* = 6.6 Hz), 7.98 (s, 2H); ¹³C NMR δ 14.09 (CH₃), 22.65 (CH₂), 23.74 (CH₃), 25.95 (CH₂), 26.90 (CH), 29.23 (CH₂), 29.39 (CH₂), 30.30 (CH₂), 31.82 (CH₂), 75.38 (CH₂), 120.00 (CH), 143.71 (C), 144.69 (C), 159.22 (C); MS (EI) *m/z* (%) 335 (M⁺, 18), 223 (99), 208 (82), 71 (38), 57 (53), 43 (56); HRMS (EI) 335.2461 (C₂₀H₃₃O₃N requires 335.2460).

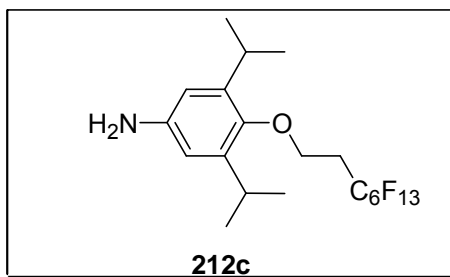


Aniline 212a. Tin(II) chloride dihydrate (2.59 g, 11.47 mmol) was added to a solution of nitroether **211a** (1.40 g, 2.89 mmol) in ethanol (22 mL) and the mixture was refluxed for 12 h; no trace of starting material was detected by the TLC after this period. The mixture was cooled and a satd solution of NaHCO₃ (40 mL) was added to reach pH 10. The solution was extracted with ether (3 x 120 mL) and the organic phase was dried over MgSO₄ and evaporated to furnish a brownish solid (1.25 g). The latter solid was purified by

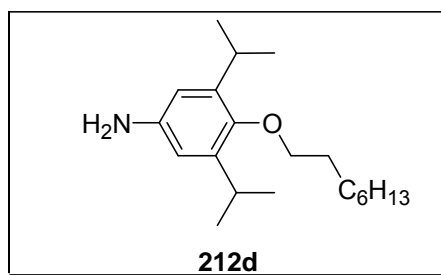
chromatography on a column of silica gel (75 g) with a mixture of petroleum ether and CH_2Cl_2 (1:1) to afford aniline **212a** (1.09 g, 83%) as a white solid: mp 47-48 °C; ^1H NMR (400 MHz, CDCl_3) δ 2.58 (tt, $J_{\text{H-H}} = 6.8$ Hz, $J_{\text{H-F}} = 18.5$ Hz, 2H), 3.45 (br s, 1.71H), 4.20 (t, $J = 6.9$ Hz, 2H), 6.65 (d, $J = 8.8$ Hz, 2H), 6.75 (d, $J = 8.8$ Hz, 2H); ^{13}C NMR δ 31.27 (t, $J = 21.9$ Hz, CH_2), 60.80 (CH_2), 115.94 (CH), 116.34 (CH), 140.74 (C), 151.11 (C); ^{19}F NMR (CCl_3F) δ -81.26 (t, $J_{\text{F-F}} = 10.3$ Hz, 3F), -113.82 (m, 2F), -122.39 (m, 2F), -123.39 (m, 2F), -124.09 (m, 2F), -126.64 (m, 2F); MS (FAB) m/z (%) 456 ($[\text{MH}]^+$, 96), 455 (100), 454 (22), 109 (79), 94 (17); HRMS (FAB) 456.0628 ($\text{C}_{14}\text{H}_{11}\text{ONF}_{13}$ requires 456.0633).



Aniline 212b. Tin(II) chloride dihydrate (2.18 g, 9.66 mmol) was added to a solution of nitroether **211b** (1.00 g, 1.95 mmol) in ethanol (14 mL) and the mixture was refluxed for 10 h. The mixture was then cooled and a saturated aqueous solution of NaHCO_3 (45 mL) was added to reach pH 10 and the product was extracted with ether (3 x 90 mL). The organic phase was dried over MgSO_4 and evaporated and the yellow oily residue (1.05 g) was purified by chromatography on a column of silica gel (90 g) with a petroleum ether- CH_2Cl_2 mixture (1:1, R_f 0.2) to afford aniline **212b** (0.72 g, 76%) as a white solid: mp 69-70 °C; ^1H NMR (400 MHz, CDCl_3) δ 2.20 (s, 6H), 2.61 (tt, $J_{\text{H-H}} = 6.8$ Hz, $J_{\text{H-F}} = 18.8$ Hz, 2H), 3.98 (t, $J = 6.8$ Hz, 2H), 6.36 (s, 2H); ^{13}C NMR δ 16.17 (CH_3), 31.81 (t, $J = 21.9$ Hz, CH_2), 63.86 (CH_2), 115.32 (CH), 131.42 (C), 142.52 (C), 147.89 (C); ^{19}F NMR (CCl_3F) δ -81.26 (t, $J_{\text{F-F}} = 10.3$ Hz, 3F), -113.70 (m, 2F), -122.30 (m, 2F), -123.31 (m, 2F), -123.99 (m, 2F), -126.58 (m, 2F); MS (FAB) m/z (%) 484 ($[\text{MH}]^+$, 98), 483 (100), 482 (19), 137 (85), 121 (31); HRMS (FAB) 484.0961 ($\text{C}_{16}\text{H}_{15}\text{ONF}_{13}$ $[\text{MH}]^+$, requires 484.0946).

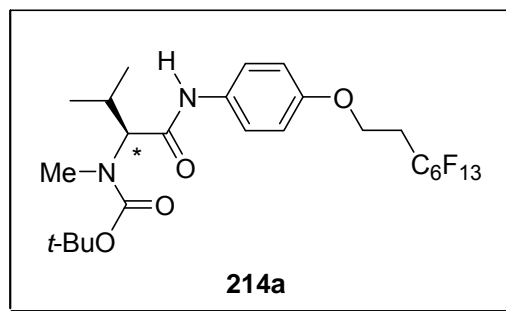


Aniline 212c. Tin(II) chloride dihydrate (1.30 g, 5.76 mmol) was added to a solution of nitroether **211c** (0.82 g, 1.44 mmol) in ethanol (10 mL) and the mixture was refluxed for 19 h. The mixture was then cooled and a saturated aqueous solution of NaHCO₃ (21 mL) was added to reach pH 10 and the product was extracted with ether (3 x 60 mL). The organic phase was dried over MgSO₄ and evaporated and the residue (0.74 g) was purified by chromatography on a column of silica gel (50 g) with a petroleum ether-CH₂Cl₂ mixture (3:2, *R_f* 0.30) to afford aniline **212c** (0.61 g, 79%) as a white solid: mp 41-43 °C; ¹H NMR (400 MHz, CDCl₃) δ 1.20 (d, *J* = 6.9 Hz, 12H), 2.64 (tt, *J*_{H-H} = 6.9 Hz, *J*_{H-F} = 18.7 Hz, 2H), 3.19 (hept, *J* = 6.9 Hz, 2H), 3.96 (t, *J* = 6.9 Hz, 2H), 4.17 (br s, 1.62H), 6.49 (s, 2H); ¹³C NMR δ 23.93 (CH₃), 26.61 (CH), 31.97 (t, *J* = 21.5 Hz, CH₂), 66.13 (CH₂), 111.55 (CH), 141.95 (C), 142.50 (C), 145.92 (C); ¹⁹F NMR (CCl₃F) δ -81.29 (t, *J*_{F-F} = 9.6 Hz, 3F), -113.73 (m, 2F), -122.35 (m, 2F), -123.35 (m, 2F), -124.04 (m, 2F), -126.60 (m, 2F); MS (EI) *m/z* (%) 539 (M⁺, 22), 192 (62), 150 (9), 44 (22); HRMS (EI) 539.1495 (C₂₀H₂₂ONF₁₃ requires 539.1494).



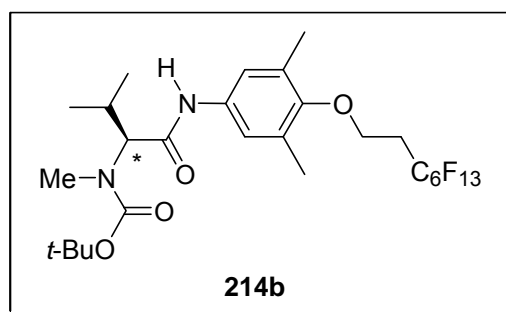
Aniline 212d. Tin(II) chloride dihydrate (2.50 g, 11.08 mmol) was added to a solution of nitroether **211d** (0.93 g, 2.77 mmol) in ethanol (19 mL) and the mixture was refluxed for 20 h. The mixture was then cooled and a saturated aqueous solution of NaHCO₃ (40 mL) was added to reach pH 10 and the product was extracted with ether (3 x 120 mL). The organic phase was dried over MgSO₄ and evaporated and the residue (0.81 g) was purified by chromatography on a column of silica gel (70 g) with a mixture of petroleum ether and CH₂Cl₂ (3:2) to afford aniline **212d** (0.62 g, 74%) as a slightly orange oil: *R_f* 0.37 (petroleum ether-CH₂Cl₂, 1:1); ¹H NMR (400 MHz, CDCl₃) δ 0.88-0.91 (m, 3H), 1.19 (d, *J* = 6.9 Hz,

12H), 1.30-1.34 (m, 8H), 1.44-1.51 (m, 2H), 1.75-1.82 (m, 2H), 3.26 (hept, $J = 6.9$ Hz, 2H), 3.65 (t, $J = 6.6$ Hz, 2H), 6.54 (s, 2H); ^{13}C NMR δ 14.10 (CH_3), 22.66 (CH_2), 24.05 (CH_3), 26.09 (CH_2), 26.37 (CH), 29.27 (CH_2), 29.48 (CH_2), 30.39 (CH_2), 31.85 (CH_2), 75.04 (CH_2), 111.22 (CH), 141.79 (C), 142.56 (C), 146.41 (C); MS (EI) m/z (%) 305 (M^+ , 35), 192 (100), 150 (17), 122 (4), 106 (3), 57 (4), 43 (11); HRMS (EI) 305.2718 ($\text{C}_{20}\text{H}_{35}\text{ON}$ requires 305.2719).

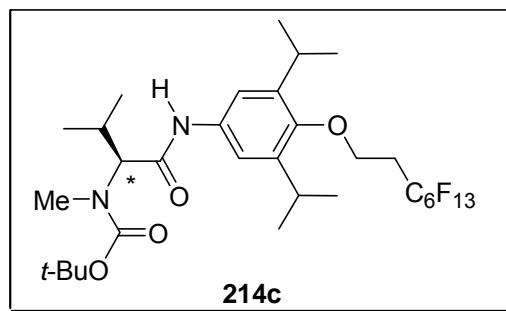


Amide (S)-(-)-214a. Triethylamine (0.45 mL, 3.27 mmol) was added to a solution of (S)-**213** (0.5 g, 2.16 mmol) in dry CH_2Cl_2 (15 mL) at 0 °C. To the resulting clear solution were consequently added aniline **212a** (890 mg, 1.95 mmol), 1-hydroxybenzotriazole hydrate (HOBt; 430 mg, 2.75 mmol), and 1-(3-dimethylaminopropyl)-3-ethylcarbodiimide hydrochloride (EDCI; 530 mg, 2.76 mmol). The reaction mixture was stirred at 0 °C for 1 h and then at room temperature for 24 h. The mixture was then diluted with ethyl acetate (110 mL) and washed successively with water (45 mL), cold 0.5 M HCl (2 x 45 mL), saturated NaHCO_3 (2 x 45 mL), and brine (45 mL), dried over MgSO_4 , filtered, and evaporated. The residue (1.18 g) was purified by chromatography on a column of silica gel (50 g) with a hexane-ethyl acetate mixture (19:1, 600 mL), which eluted impurities. Continued elution with the same mixture in 14:1 ratio afforded pure (S)-(-)-**214a** (880 mg, 68%) as a slightly yellowish oil: R_f 0.3 (petroleum ether-ethyl acetate, 9:1); $[\alpha]_D$ -59.6 (c 0.5, EtOH); ^1H NMR (400 MHz, CDCl_3) δ 0.91 (d, $J = 6.6$ Hz, 3H), 1.02 (d, $J = 6.3$ Hz, 3H), 1.48 (s, 9H), 2.33-2.42 (m, 1H), 2.61 (tt, $J_{\text{H-H}} = 6.8$ Hz, $J_{\text{H-F}} = 18.5$ Hz, 2H), 2.83 (s, 3H), 4.09 (d, $J = 11.4$ Hz, 1H), 4.25 (t, $J = 6.8$ Hz, 2H), 6.85 (d, $J = 9.0$ Hz, 2H), 7.43 (d, $J = 9.0$ Hz, 2H), 8.20 (br s, 1H); ^{13}C NMR δ 18.57 (CH_3), 19.83 (CH_3), 25.96 (CH_3), 28.33 (CH_3), 30.89 (CH), 31.20 (t, $J = 21.5$ Hz, CH_2), 60.31 (CH_2), 65.95 (CH), 80.65 (C), 114.90 (CH), 121.37 (CH), 131.99 (C), 154.55 (C), 157.43 (CO), 168.61 (CO); ^{19}F NMR (CCl_3F) δ -81.27 (t, $J_{\text{F-F}}$ 9.7 Hz, 3F), -113.82 (m, 2F), -122.37 (m, 2F), -123.37 (m, 2F), -124.07 (m, 2F), -126.64 (m, 2F); MS

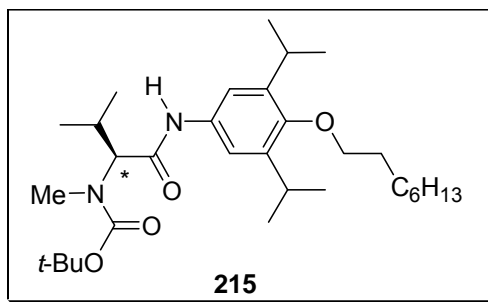
(FAB) m/z (%) 669 ($[MH]^+$, 27), 668 (42), 613 (47), 569 (45), 456 (100), 455 (100), 131 (49), 88 (49), 59 (48); HRMS (FAB) 669.1997 ($C_{25}H_{30}O_4N_2F_{13}$ $[MH]^+$ requires 669.1998).



Amide (S)-(-)-214b. Triethylamine (0.19 mL, 1.39 mmol) was added to a solution of (S)-**213** (217 mg, 0.94 mmol) in dry dichloromethane (9 mL) at 0 °C. To the resulting clear solution were consequently added aniline **212b** (540 mg, 1.12 mmol), 1-hydroxybenzotriazole hydrate (HOBt; 190 mg, 1.22 mmol), and 1-(3-dimethylaminopropyl)-3-ethylcarbodiimide hydrochloride (EDCI; 234 mg, 1.22 mmol). The reaction mixture was stirred at 0 °C for 1 h and then at room temperature for 18 h. The mixture was then diluted with ethyl acetate (50 mL) and washed successively with water (20 mL), cold 0.5 M HCl (2 x 20 mL), saturated NaHCO₃ (2 x 20 mL), and brine (20 mL) then dried over MgSO₄ and evaporated. The residue (540 mg) was purified by chromatography on a column of silica gel (90 g) with a petroleum ether-ethyl acetate mixture (12:1) to afford pure amide (S)-(-)-**214b** (380 mg, 58%) as a yellowish oil: R_f 0.32 (petroleum ether-dichloromethane, 12: 1); $[\alpha]_D$ -45.2 (c 0.5, EtOH); 1H NMR (400 MHz, CDCl₃) δ 0.91 (d, J = 6.6 Hz, 3H), 1.01 (d, J = 6.3 Hz, 3H), 1.47 (s, 9H), 2.24 (s, 6H), 2.31-2.40 (m, 1H), 2.61 (tt, J_{H-H} = 6.5 Hz, J_{H-F} = 18.6 Hz, 2H), 2.84 (s, 3H), 3.99 (t, J = 6.8 Hz, 2H), 4.10 (d, J = 10.8 Hz, 1H), 7.18 (s, 2H), 8.21 (br s, 0.75H); ^{13}C NMR δ 16.22 (CH₃), 18.57 (CH₃), 19.80 (CH₃), 25.99 (CH₃), 28.33 (CH₃), 30.44 (CH), 31.78 (t, J = 22 Hz, CH₂), 63.73 (CH₂), 65.91 (CH), 80.61 (C), 120.20 (CH), 131.28 (C), 134.03 (C), 151.61 (C), 157.40 (CO), 168.75 (CO); ^{19}F NMR (CCl₃F) δ -81.28 (t, J_{F-F} 10.3 Hz, 3F), -113.75 (m, 2F), -122.34 (m, 2F), -123.30 (m, 2F), -124.05 (m, 2F), -126.60 (m, 2F); MS (FAB) m/z (%) 719 ($[MNa]^+$, 56), 597 (38), 595 (16), 484 (100), 483 (100), 131 (100), 88 (100), 59 (94); HRMS (FAB) 719.2124 ($C_{27}H_{33}O_4N_2F_{13}Na$ $[MNa]^+$ requires 719.2130).



Amide (S)-(-)-214c. Triethylamine (0.30 mL, 2.18 mmol) was added to a solution of (S)-**213** (350 mg, 1.51 mmol) in dry dichloromethane (10 mL) at 0 °C. To the resulting clear solution were consequently added aniline **212c** (730 mg, 1.35 mmol), 1-hydroxybenzotriazole hydrate (HOBt; 270 mg, 1.75 mmol), and 1-(3-dimethylaminopropyl)-3-ethylcarbodiimide hydrochloride (EDCI; 330 mg, 1.72 mmol). The reaction mixture was stirred at 0 °C for 1 h and then at room temperature for 20 h. The mixture was then diluted with ethyl acetate (60 mL) and washed successively with water (30 mL), cold 0.5 M HCl (2 x 30 mL), saturated NaHCO₃ (2 x 40 mL), and brine (30 mL) then dried over MgSO₄ and evaporated. The residue (1.05 g) was purified by chromatography on a column of silica gel (50 g) with a petroleum ether-ethyl acetate mixture (25:1 for the first 250 mL and then 19:1) to afford pure amide (S)-(-)-**214c** (810 mg, 80%) as a white solid: *R_f* 0.60 (petroleum ether- ethyl acetate, 9:1); mp 94-96 °C; [α]_D -52.2 (*c* 0.5, EtOH); ¹H NMR (400 MHz, CDCl₃) δ 0.92 (d, *J* = 6.6 Hz, 3H), 1.03 (d, *J* = 6.4 Hz, 3H), 1.20-1.24 (m, 12 H), 1.49 (s, 9H), 2.32-2.42 (m, 1H), 2.65 (tt, *J*_{H-H} = 6.8 Hz, *J*_{H-F} = 18.6 Hz, 2H), 2.83 (s, 3H), 3.22 (hept, *J* = 6.8 Hz, 2H), 3.98 (t, *J* = 6.8 Hz, 2H), 4.12 (d, *J* = 10.2 Hz, 1H), 7.25 (s, 2H), 8.19 (br s, 0.92H); ¹³C NMR δ 18.61 (CH₃), 19.97 (CH₃), 23.86 (CH₃), 25.84 (CH), 26.72 (CH), 28.35 (CH₃), 30.38 (CH₃), 31.92 (t, *J* = 21.8 Hz, CH₂), 66.11 (CH and CH₂), 80.67 (C), 115.80 (CH), 135.06 (C), 142.31 (C), 148.98 (C), 157.52 (CO), 168.53 (CO); ¹⁹F NMR (CCl₃F) δ -81.27 (t, *J*_{F-F} = 10.4 Hz, 3F), -113.79 (m, 2F), -122.37 (m, 2F), -123.38 (m, 2F), -124.06 (m, 2F), -126.62 (m, 2F); MS (EI) *m/z* (%) 752 (M⁺, 35), 539 (92), 192 (66), 158 (65), 130 (100), 86 (62), 69 (60), 57 (55); HRMS (EI) 752.2853 (C₃₁H₄₁O₄N₂F₁₃ requires 752.2859).



Amide (S)-(-)-215. Triethylamine (0.30 mL, 2.18 mmol) was added to a solution of (S)-**213** (370 mg, 1.60 mmol) in dry dichloromethane (7 mL) at 0 °C. To the resulting clear solution were consequently added aniline **212d** (440 mg, 1.44 mmol) in DCM (3 mL), 1-hydroxybenzotriazole hydrate (HOBt; 280 mg, 1.83 mmol), and 1-(3-dimethylaminopropyl)-3-ethylcarbodiimide hydrochloride (EDCI; 350 mg, 1.83 mmol). The reaction mixture was stirred at 0 °C for 1 h and then at room temperature for 16 h. The mixture was then diluted with ethyl acetate (70 mL) and washed successively with water (35 mL), cold 0.5 M HCl (2 x 35 mL), saturated NaHCO₃ (2 x 45 mL), and brine (35 mL) then dried over MgSO₄ and evaporated. The residue (0.81 g) was purified by chromatography on a column of silica gel (70 g) with a petroleum ether-ethyl acetate mixture (24:1) to afford pure amide (S)-(-)-**215** (620 mg, 83%) as a yellowish oil: *R_f* 0.62 (petroleum ether ethyl acetate, 9:1); [α]_D -58.6 (*c* 0.5, EtOH); ¹H NMR (400 MHz, CDCl₃) δ 0.87-0.92 (m, 3H), 0.91 (t, *J* = 6.5 Hz, 3H, partly overlapped with the multiplet), 1.03 (d, *J* = 6.4 Hz, 3H), 1.19-1.22 (m, 12H), 1.30-1.35 (m, 8H), 1.45-1.54 (m, 11H), 1.76-1.83 (m, 2H), 2.32-2.41 (m, 1H), 2.82 (s, 3H), 3.28 (hept, *J* = 6.9 Hz, 2H), 3.67 (t, *J* = 6.6 Hz, 2H), 4.12 (d, *J* = 10.7 Hz, 1H), 7.23 (s, 2H), 8.12 (br s, 1.32H); ¹³C NMR δ 14.09 (CH₃), 18.59 (CH₃), 19.96 (CH₃), 22.64 (CH₂), 23.95 (CH₃), 25.83 (CH), 26.04 (CH₂), 26.51 (CH), 28.35 (CH₃), 29.25 (CH₂), 29.44 (CH₂), 30.35 (CH₂ and CH₃), 31.83 (CH₂), 65.87 (CH), 75.02 (CH₂), 80.58 (C), 115.64 (CH), 134.35 (C), 142.44 (C), 149.83 (C), 157.45 (CO), 168.39 (CO); MS (EI) *m/z* (%) 518 (M⁺, 19), 305 (75), 192 (54), 130 (64), 86 (99), 57 (51), 44 (21); HRMS (EI) 518.4081 (C₃₁H₅₄O₄N₂ requires 518.4084).

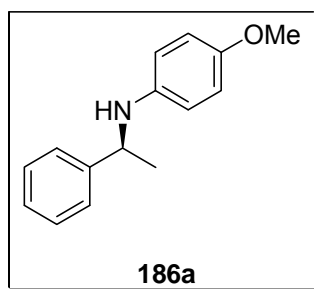
General Procedure for the Catalytic Hydrosilylation of Imines **185a-d** with Fluorous Catalysts **206a-c**.

Trichlorosilane (50 μ L, 0.5 mmol) was added dropwise to a stirred solution of the imine **185a-c** (0.2 mmol) and the catalyst (0.02 mmol) in anhydrous toluene (1.5 mL) at 0 °C; and the mixture was allowed to stir overnight at room temperature (or at 10 °C; see Table 22)

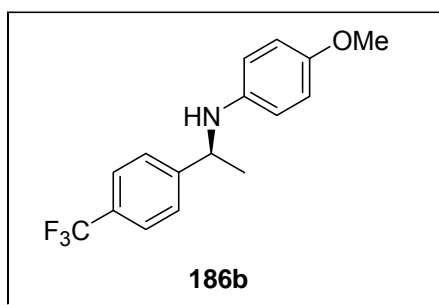
under an argon atmosphere. The reaction was quenched with a saturated solution of NaHCO_3 (10 mL) and the product was extracted with ethyl acetate (3 x 30 mL). The extract was washed with brine and dried over anhydrous MgSO_4 and the solvent was evaporated. The residue was dissolved in a mixture of methanol and water (80:20) and the resulting solution was filtered through a column of fluorous silica gel (2.8 g) to afford pure amine **186a-d**. The yields and enantioselectivities are given in Table 22. The results of the reduction of **185a** with recycled catalyst are shown in Table 23.

General Procedure for Recovery of the Fluorous Catalyst.

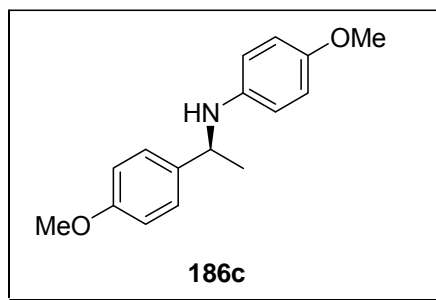
After elution of the product from the column of fluorous silica, methanol was employed to elute the fluorous catalyst. The methanolic eluate was evaporated, the residue was dissolved in CH_2Cl_2 (25 mL), and the resulting solution was dried over MgSO_4 . The latter solution was then evaporated to afford the regenerated fluorous catalyst **206a-c**, which was used for the next catalytic reduction without further purification.



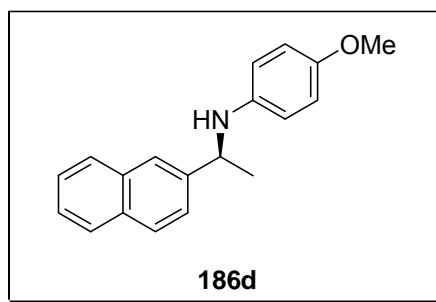
Amine (S)-(-)-186a Purified by column chromatography on silica gel with a petroleum ether-ethyl acetate mixture (15:1, R_f = 0.3): $[\alpha]_D$ -4.0 (c 1.0, CHCl_3); ^1H NMR (400 MHz, CDCl_3) δ 1.50 (d, J = 6.7 Hz, 3H), 3.70 (s, 3H), 3.79 (br s, 1H), 4.42 (q, J = 6.7 Hz, 1H), 6.46-6.50 (m, 2H), 6.68-6.72 (m, 2H), 7.20-7.25 (m, 1H), 7.30-7.38 (m, 4H) in agreement with the data for an authentic sample^{136,138a}; chiral HPLC (Chiracel OD-H, hexane/2-propanol 99:1, 0.75 $\text{mL} \cdot \text{min}^{-1}$) showed 86% ee (t_R = 21.6 min, t_S = 24.4 min).



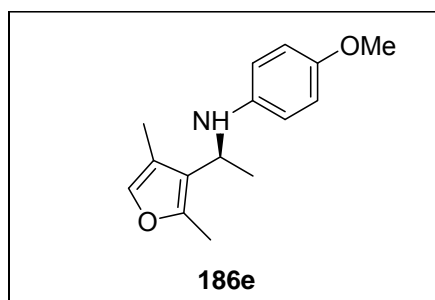
Amine (S)-(+)-186b. Purified by column chromatography on silica gel with a petroleum ether-ethyl acetate mixture (10:1, $R_f = 0.2$): $[\alpha]_D +6.5$ (c 1.0, CHCl_3); ^1H NMR (400 MHz, CDCl_3) δ 1.51 (d, $J = 6.7$ Hz, 3H), 3.70 (s, 3H), 3.83 (br s, 1H), 4.46 (q, $J = 6.7$ Hz, 1H), 6.41-6.45 (m, 2H), 6.67-6.71 (m, 2H), 7.48 (d, $J = 8.2$ Hz, 2H), 7.57 (d, $J = 8.2$ Hz, 2H) in agreement with the data for an authentic sample^{136,138a}; chiral HPLC (Chiracel OD-H, hexane/2-propanol 95:5, $0.9\text{ mL}\cdot\text{min}^{-1}$) showed 86% ee ($t_R = 15.7$ min, $t_S = 21.8$ min).



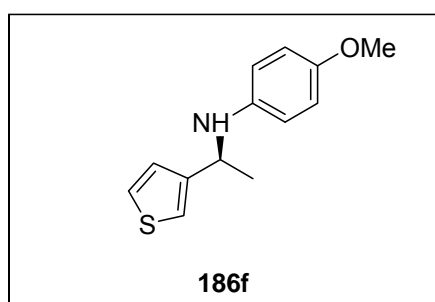
Amine (S)-(-)-186c. Purified by column chromatography on silica gel with a petroleum ether-ethyl acetate mixture (9:1, $R_f = 0.24$): $[\alpha]_D -16.1$ (c 1.0, CHCl_3); ^1H -NMR (400 MHz, CDCl_3) δ 1.47 (d, $J = 6.7$ Hz, 3H), 3.70 (s, 3H), 3.78 (s, 3H), 4.37 (q, $J = 6.7$ Hz, 1H), 6.46-6.70 (m, 2H), 6.67-6.71 (m, 2H), 6.84-6.87 (m, 2H), 7.25-7.29 (m, 2H) in agreement with the data for an authentic sample^{136,138a}; chiral HPLC (Chiracel OD-H, hexane/2-propanol 98:2, $0.6\text{ mL}\cdot\text{min}^{-1}$) showed 82% ee ($t_R = 28.8$ min, $t_S = 33.9$ min).



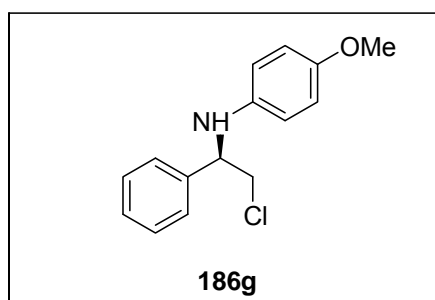
Amine (S)-(-)-186d. Purified by column chromatography on silica gel with a hexane-ethyl acetate mixture (10:1, $R_f = 0.24$): $[\alpha]_D -23.2$ (c 1.0, CHCl_3); ^1H NMR (400 MHz, CDCl_3) δ 1.58 (d, $J = 6.7$ Hz, 3H), 3.68 (s, 3H), 3.90 (br s, 1H), 4.57 (q, $J = 6.7$ Hz, 1H), 6.50-6.54 (m, 2H), 6.66-6.70 (m, 2H), 7.41-7.52 (m, 3H), 7.79-7.83 (m, 4H) in agreement with the data for an authentic sample^{136,138a}; chiral HPLC (Chiracel OD-H, hexane/2-propanol 99:1, $0.9\text{ mL}\cdot\text{min}^{-1}$) showed 86% ee ($t_R = 27.4$ min, $t_S = 33.4$ min).



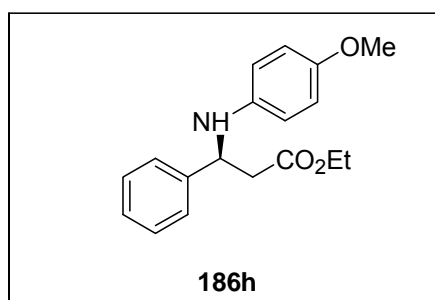
Amine (S)-(-)-186e. Purified by column chromatography on silica gel with a petroleum ether-ethyl acetate mixture (10:1): $[\alpha]_D -4.5$ (*c*, 2, CHCl₃); ¹H NMR (400 MHz, CDCl₃) δ 1.42 (d, *J* = 6.7, 3H), 2.21 (br s, 3H), 2.25 (br s, 3H), 3.36 (br s, 1H), 3.74 (s, 3H), 4.29 (q, *J* = 6.6 Hz, 1H), 5.88 (br s, 1H), 6.53–6.57 (m, 2H), 6.73–6.77 (m, 2H) in agreement with the data for an authentic sample^{165b}; chiral HPLC (Chiralpak IB, hexane/propan-2-ol 99:1, 0.75 mL•min⁻¹) showed 79% ee (*t*_R = 12.8 min, *t*_M = 14.6 min).



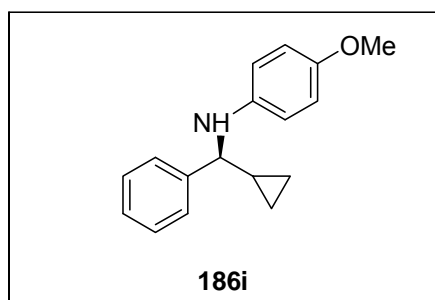
Amine (S)-(-)-186f. Purified by column chromatography on silica gel with a petroleum ether-ethyl acetate mixture (19:1, *R*_f = 0.24): $[\alpha]_D -9.0$ (*c*, 1.0, CHCl₃); ¹H NMR (400 MHz, CDCl₃) δ 1.61 (d, *J* = 6.6 Hz, 3H), 3.73 (s, 3H), 4.74 (q, *J* = 6.6 Hz, 1H), 6.58–6.62 (m, 2H), 6.74–6.78 (m, 2H), 6.94 (dd, *J* = 4.9, 3.5 Hz, 1H), 6.97 (ddd, *J* = 3.5, 1.2, 0.9 Hz, 1H), 7.14 (dd, *J* = 4.9, 1.4 Hz, 1H); in agreement with the data for an authentic sample^{165b} chiral HPLC (Chiracel OD-H, hexane/propan-2-ol 99:1, 0.70 mL•min⁻¹) showed 65% ee (*t*_{minor} = 27.4 min, *t*_{major} = 30.9 min).



Amine(S)-(-)-186g. Purified by column chromatography on silica gel with a petroleum ether-ethyl acetate mixture (24:1, $R_f = 0.25$): $[\alpha]_D -21.6$ (c 1.0, CHCl_3); ^1H NMR (400 MHz, CDCl_3) δ 3.70 (s, 3H), 3.72 (dd, $J = 11.3$ and 7.9 Hz, 1H), 3.87 (dd, $J = 11.3$ and 4.3 Hz, 1H), 4.24 (br s, 1H), 4.54 (dd, $J = 7.9$ and 4.3 Hz, 1H), 6.50-6.54 (m, 2H), 6.69-6.73 (m, 2H), 7.28-7.43 (m, 5H) in agreement with the data for an authentic sample^{138b}; chiral HPLC (Chiralpak IB, hexane/2-propanol 99:1, $0.75 \text{ mL}\cdot\text{min}^{-1}$) showed 91% ee ($t_{\text{major}} = 17.7 \text{ min}$, $t_{\text{minor}} = 19.9 \text{ min}$).

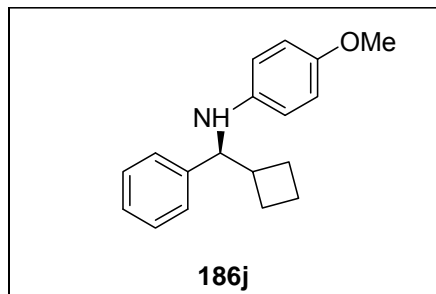


Amine (S)-(-)-186h. Purified by column chromatography on silica gel with a petroleum ether-ethyl acetate mixture (9:1, $R_f = 0.32$): $[\alpha]_D +6.0$ (c 1.0, CHCl_3); ^1H NMR (400 MHz, CDCl_3) δ 1.19 (t, $J = 7.2$ Hz, 3H), 2.77 (d, $J = 6.0$ Hz, 2H), 3.69 (s, 3H), 4.10 (q, $J = 6.8$ Hz, 2H), 4.30 (br s, 1H), 4.74 (t, $J = 6.8$ Hz, 1H), 6.51-6.53 (m, 2H), 6.68-6.70 (m, 2H), 7.24-7.38 (m, 5H) in agreement with the data for an authentic sample^{165a}; chiral HPLC (Chiralpak IB, hexane/2-propanol 9:1, $0.75 \text{ mL}\cdot\text{min}^{-1}$) showed 81% ee ($t_{\text{minor}} = 13.67 \text{ min}$, $t_{\text{major}} = 15.22 \text{ min}$).

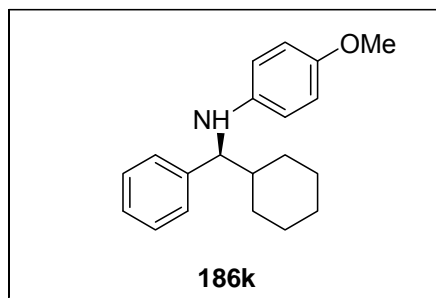


Amine (S)-(-)-186i. Purified by column chromatography on silica gel with a petroleum ether-ethyl acetate mixture (30:1, $R_f = 0.29$): $[\alpha]_D +66.1$ (c 1.0, CHCl_3); ^1H NMR (400 MHz, CDCl_3) δ 0.29 (ddd, $J = 14.3$, 5.2 , 4.1 Hz, 1H), 0.36 (ddd, $J = 9.5$, 5.0 , 4.5 Hz, 1H), 0.39-0.49 (m, 1H), 0.51 (dddd, $J = 14.2$, 8.0 , 5.4 , 4.0 Hz, 1H), 1.08 (dtd, $J = 8.2$, 5.0 , 5.0 Hz, 1H), 3.48 (d, $J = 8.4$ Hz, 1H), 3.58 (s, 3H), 4.02 (br s, 1H), 6.32-6.36 (m, 2H), 6.55-6.59 (m, 2H), 7.14

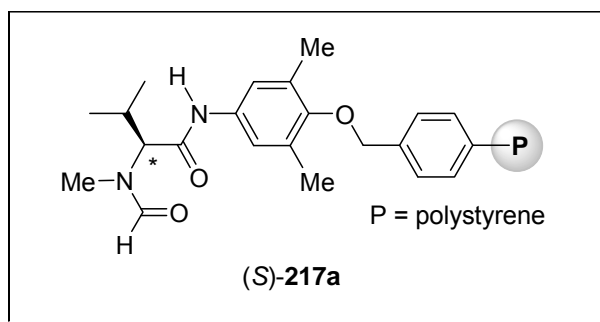
(dddd, $J = 8.1, 6.4, 2.2, 1.4$ Hz, 1H), 7.20-7.25 (m, 2H), 7.29-7.32 (m, 2H) in agreement with the data for an authentic sample^{165b}; chiral HPLC (Chiralpak IB, hexane/2-propan-2-ol 99:1, 0.75 mL•min⁻¹) showed 73% ee ($t_{\text{minor}} = 12.9$ min, $t_{\text{major}} = 15.2$ min).



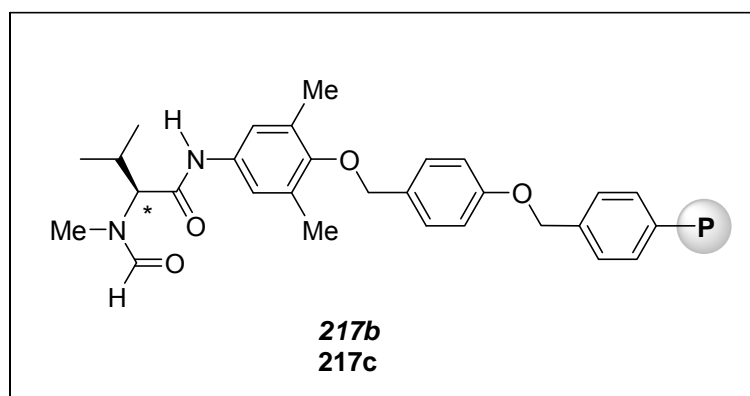
Amine (S)-(-)-186j. Purified by column chromatography on silica gel with a petroleum ether-ethyl acetate mixture (30:1, $R_f = 0.27$): $[\alpha]_D -0.8$ ($c, 1.0, \text{CHCl}_3$); ^1H NMR (400 MHz, CDCl_3) δ 1.63-1.85 (m, 5H), 1.98-2.08 (m, 1H), 2.38-2.48 (m, 1H), 3.57 (s, 3H), 3.67 (br s, 1H), 4.01 (d, $J = 9.1$ Hz, 1H), 6.34-6.38 (m, 2H), 6.55-6.59 (m, 2H), 7.12 (dddd, $J = 7.7, 6.2, 2.4, 1.6$ Hz, 1H), 7.17-7.25 (m, 3H) in agreement with the data for an authentic sample^{165b}; chiral HPLC (Chiralpak IB, hexane/2-propan 99:1, 0.75 mL•min⁻¹) showed 75 % ee ($t_{\text{minor}} = 10.4$ min, $t_{\text{major}} = 10.9$ min).



Amine (S)-(-)-186k. Purified by column chromatography on silica gel with a petroleum ether-ethyl acetate mixture (30:1, $R_f = 0.27$): $[\alpha]_D -11.6$ ($c, 1.0, \text{CHCl}_3$); ^1H NMR (400 MHz, CDCl_3) δ 1.02-1.30 (m, 5H), 1.57 (br d, $J = 12.9$ Hz, 1H), 1.63-1.81 (m, 4H), 1.93 (br d, $J = 12.6$, 1H), 3.70 (s, 3H), 4.07 (d, $J = 6.2$ Hz, 1H), 6.46-6.50 (m, 2H), 6.67-6.71 (m, 2H), 7.20-7.26 (m, 1H), 7.29-7.34 (m, 4H) in agreement with the data for an authentic sample^{165b}; chiral HPLC (Chiracel OJ-H, hexane/2-propan-2-ol 85:15, 0.75 mL•min⁻¹) showed 55 % ee ($t_{\text{minor}} = 12.8$ min, $t_{\text{major}} = 15.8$ min).



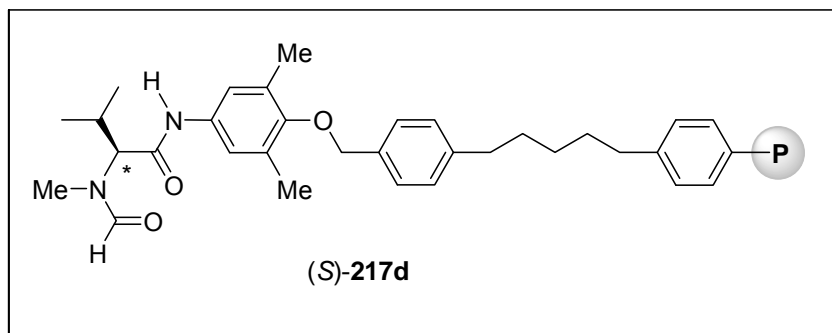
Merrifield Resin-Supported Catalyst **217a.** Cesium hydroxide monohydrate (57 mg, 0.34 mmol) was added to a reaction tube with a solution of phenol **218** (90 mg, 0.32 mmol) in DMF (3 mL), followed by shaking at 60 °C for 30 min. A small porous polypropylene reactor vessel (2.4 mL internal volume and 74 μm pore size) with chloromethylpolystyrene **235** [1.23 mmol/g (130 mg, 0.16 mmol)] was placed into the reaction tube, and the shaking was continued at 60 °C for 48 h. The porous reactor vessel was then removed from the organic solution and successively washed with DMF (2×25 mL) and then alternately with MeOH and CH_2Cl_2 (4×25 mL of each solvent) and ether (25 mL). Vacuum drying afforded a brownish solid (160 mg, 80%): IR (KBr) ν 3444, 2919, 1942, 1869, 1802, 1661, 1602, 1541, 1491, 1450 cm^{-1} . Anal. Found: C, 84.77; H, 7.15; N, 2.11. This corresponds to 0.75 mmol/g loading.



Wang Resin-Supported Catalyst **217b.** Cesium hydroxide monohydrate (57 mg, 0.34 mmol) was added to a reaction tube with a solution of phenol **218** (90 mg, 0.32 mmol) in DMF (3 mL), followed by shaking at 60 °C for 30 min. A small porous polypropylene reactor vessel (2.4 mL internal volume and 74 μm pore size) with bromomethylphenoxymethyl polystyrene **236** [1.40 mmol/g (114 mg, 0.16 mmol)] was placed into the reaction tube, and shaking was continued at 60 °C for 48 h. The porous reactor vessel was then removed from

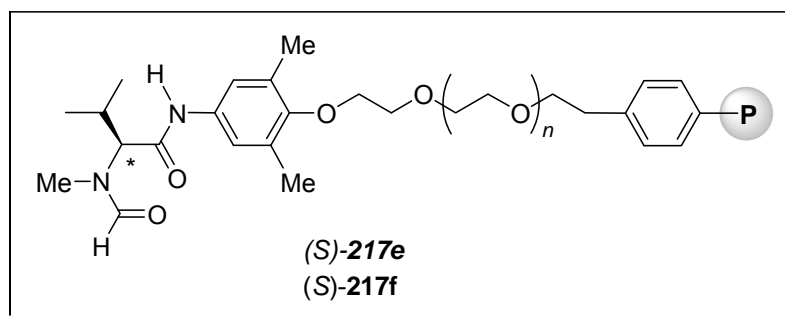
the organic solution and successively washed with MeOH (2×25 mL), a 1:1 mixture of MeOH and H₂O (25 mL), a 1:1 mixture of THF and H₂O (25 mL), and then alternately with MeOH and CH₂Cl₂ (4×25 mL of each solvent) and ether (25 mL). Vacuum drying afforded a brownish solid (130 mg, 57%): IR (KBr) ν 3431, 3024, 2920, 1943, 1877, 1805, 1725, 1674, 1602, 1550, 1512, 1451 cm⁻¹. Anal. Found: C, 82.30; H, 7.55; N, 1.98; this corresponds to 0.71 mmol/g loading.

Wang Resin-Supported Catalyst 217c. Diethyl azodicarboxylate (80 μ L, 0.51 mmol) was added to a reaction tube containing a small porous polypropylene reactor vessel (2.4 mL internal volume and 74 μ m pore size) with hydroxymethylphenoxymethyl polystyrene 237 [1.70 mmol/g (100 mg, 0.17 mmol)], phenol 218 (142 mg, 0.51 mmol), and triphenylphosphine (134 mg, 0.51 mmol) in THF (3 mL) at 0 °C. The mixture was shaken at 25 °C for 65 h, and the porous reactor vessel was then removed from the organic solution and washed alternately with MeOH and THF (4×25 mL of each solvent), then CH₂Cl₂ (3×25 mL), and ether (25 mL). Vacuum drying afforded a white solid (128 mg, 64%): IR (KBr) ν 3315, 3061, 2337, 1944, 1876, 1799, 1600, 1512, 1493, 1454 cm⁻¹. Anal. Found: C, 79.10; H, 7.25; N, 3.68; this corresponds to 1.31 mmol/g loading.



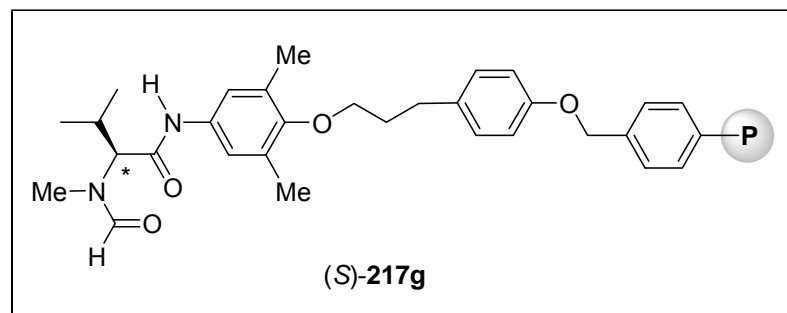
Modified Merrifield Resin-Supported Catalyst 217d. Cesium hydroxide monohydrate (57 mg, 0.34 mmol) was added to a reaction tube with a solution of phenol 218 (90 mg, 0.32 mmol) in DMF (3 mL), followed by shaking at 60 °C for 30 min. A small porous polypropylene reactor vessel (2.4 mL internal volume and 74 μ m pore size) with [5-[4-(chloromethyl)phenyl]pentyl]styrene, polymerbound 238 [0.75–1.25 mmol/g (130 mg, 0.097–0.16 mmol)] was placed into the reaction tube, and the shaking was continued at 60 °C for 48 h. The porous reactor vessel was then removed from the organic solution and successively washed with MeOH (2×25 mL), a 1:1 mixture of MeOH and H₂O (2×25 mL), a 1:1 mixture

of THF and H₂O (2 × 25 mL), and then alternately with MeOH and CH₂Cl₂ (4 × 25 mL of each solvent), and ether (25 mL). Vacuum drying afforded a brownish solid (142 mg, 51%): IR (KBr) ν 3317, 2916, 1942, 1871, 1803, 1694, 1600, 1547, 1490, 1449, 1372 cm⁻¹. Anal. Found: C, 85.08; H, 7.76; N, 1.49; this corresponds to 0.53 mmol/g loading.

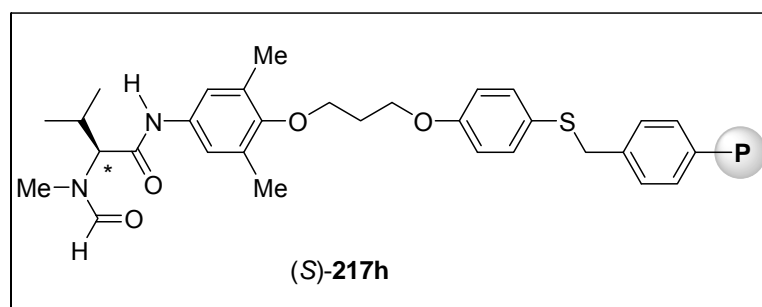


TentaGel Resin-Supported Catalyst 217e. Cesium hydroxide monohydrate (57 mg, 0.34 mmol) was added to a reaction tube with a solution of phenol **218** (90 mg, 0.32 mmol) in DMF (3 mL), followed by shaking at 80 °C for 30 min. A small porous polypropylene reactor vessel (2.4 mL internal volume and 74 μ m pore size) with TentaGel HL Br resin **239** [0.43 mmol/g (300 mg, 0.13 mmol)] was placed into the reaction tube, and the shaking was continued at 80 °C for 67 h. The porous reactor vessel was then removed from the organic solution and successively washed with MeOH (2 × 25 mL), a 1:1 mixture of MeOH and H₂O (2 × 25 mL), a 1:1 mixture of THF and H₂O (2 × 25 mL), and then alternately with MeOH and CH₂Cl₂ (4 × 25 mL of each solvent) and ether (25 mL). Vacuum drying afforded a brownish solid (304 mg, 16%): IR (KBr) ν 3448, 2917, 2870, 1664, 1602, 1492, 1453, 1106 cm⁻¹. Anal. Found: C, 67.67; H, 8.56; N, 0.59; this corresponds to 0.21 mmol/g loading.

TentaGel Resin-Supported Catalyst 217f. Diethyl azodicarboxylate (55 μ L, 0.35 mmol) was added to a reaction tube containing a small porous polypropylene reactor vessel (2.4 mL internal volume and 74 μ m pore size) with TentaGel HL OH resin **240** [0.43 mmol/g (300 mg, 0.129 mmol)], phenol **218** (90 mg, 0.32 mmol), and triphenylphosphine (92 mg, 0.35 mmol) in THF (3.5 mL) at 0 °C. The mixture was shaken at 25 °C for 68 h, and the porous reactor vessel was then removed from the organic solution and washed with THF (2 × 25 mL), then alternately with MeOH and CH₂Cl₂ (4 × 25 mL of each solvent) and ether (25 mL). Vacuum drying afforded a white solid (314 mg, 39%): IR (KBr) ν 3509, 2869, 1948, 1733, 1695, 1601, 1492, 1453, 1349 cm⁻¹. Anal. Found: C, 67.69; H, 8.56; N, 0.93; this corresponds to 0.33 mmol/g loading.

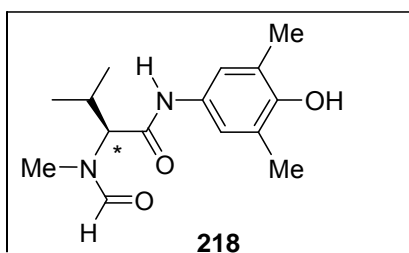


Merrifield Resin-Supported Catalysts with a Long Spacer 217g. Cesium hydroxide monohydrate (57 mg, 0.34 mmol) was added to a reaction tube with a solution phenol **219** (132 mg, 0.32 mmol) in DMF (3 mL), followed by shaking at 60 °C for 30 min. A small porous polypropylene reactor vessel (2.4 mL internal volume and 74 μm pore size) with chloromethylpolystyrene **235** [1.23 mmol/g (130 mg, 0.16 mmol)] was placed into the reaction tube and shaking was continued at 60 °C for 65 h. The porous reactor vessel was then removed from the organic solution and successively washed with MeOH (2×25 mL), a 1:1 mixture of MeOH and H₂O (25 mL), a 1:1 mixture of THF and H₂O (25 mL), and then alternately with MeOH and CH₂Cl₂ (4×25 mL of each solvent) and ether (25 mL). Vacuum drying afforded a brownish solid (177 mg, 75%): IR (KBr) ν 3318, 2915, 1942, 1872, 1803, 1694, 1599, 1546, 1489, 1448, 1374 cm^{-1} . Anal. Found: C, 84.20; H, 7.46; N, 1.93; this corresponds to 0.69 mmol/g loading.

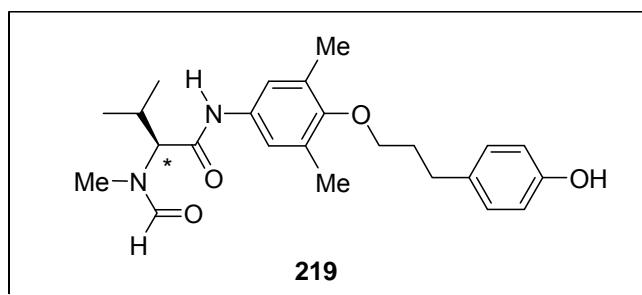


Marshall Resin-Supported Catalyst 217h. A solution of formamide **220** (90 mg, 0.25 mmol) in THF (3 mL) was added dropwise to a reaction tube containing a small porous polypropylene reactor vessel (2.4 mL internal volume and 74 μm pore size) with 4-hydroxytiophenol resin **241** [1.58 mmol/g (80 mg, 0.13 mmol)], cesium hydroxide monohydrate (27 mg, 0.16 mmol), and cesium iodide (44 mg, 0.17 mmol), and the mixture

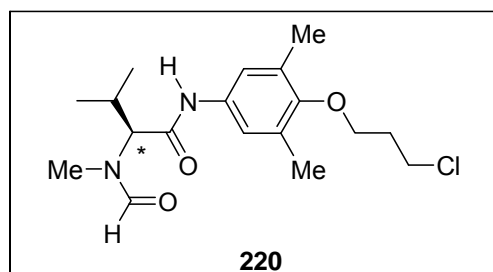
was shaken at 45 °C for 48 h. The porous reactor vessel was then removed from the organic solution and successively washed with THF (20 mL), a 1:1 mixture of THF and water (2 × 20 mL), a 1:1 mixture of THF and 1 M HCl (2 × 20 mL), and alternately with MeOH and CH₂Cl₂ (4 × 25 mL of each solvent) and ether (25 mL). Vacuum drying afforded a brownish solid (88 mg, 20%): IR (KBr) ν 3429, 2920, 1944, 1873, 1804, 1655, 1599, 1580, 1491, 1451 cm⁻¹. Anal. Found: C, 77.67; H, 6.67; N, 0.72; this corresponds to 0.26 mmol/g loading.



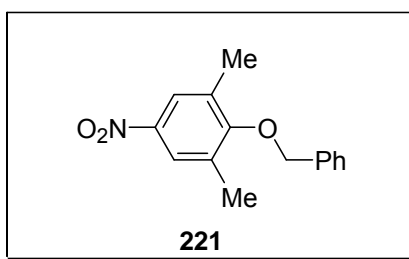
Formamide (S)-(-)-218. A mixture of the benzyl derivative **224** (280 mg, 0.76 mmol) and 10% palladium on activated charcoal (80 mg, 10 mol%) in absolute ethanol (14 mL) was stirred under a hydrogen atmosphere for 9 h. The mixture was then filtered through Celite, and the solvent was evaporated. The residue (220 mg) was purified by chromatography on a column of silica gel (30 g) with a mixture of CH₂Cl₂ and MeOH (49:1) to afford (S)-(-)-**218** (180 mg, 85%) as an enamel: R_f = 0.37 and 0.25 (two spots; CH₂Cl₂-MeOH, 49:1); $[\alpha]_D$ -141.30 (c 1.0, CHCl₃); ¹H NMR (400 Hz, CDCl₃, a mixture of rotamers in ca. 4:1 ratio; the signals for the minor rotamer are marked with an *) δ 0.91 (d, J = 6.5 Hz, 3H), 1.04 (d, J = 6.5 Hz, 3H), 2.18 (s, 6H), 2.39–2.50 (m, 1H), 2.92 (s, 0.60H*), 3.00 (s, 2.35H), 3.51 (d, J = 10.5 Hz, 0.19H*), 4.40 (d, J = 11.2, 0.78H), 5.18 (s, 0.77H), 5.25 (s, 0.20H), 7.07 (s, 0.36 H*), 7.10 (s, 1.59H), 8.10 (s, br. 0.81H), 8.13 (s, 0.89H), 8.21 (s, 0.23H); ¹³C NMR δ 16.1 (CH₃), 18.5 (CH₃), 19.5 (CH₃), 25.3 (CH), 31.6 (CH₃), 62.9 (CH), 120.7 (CH), 123.8 (C), 129.8 (C), 149.3 (C), 163.9 (CHO), 167.0 (CO); IR (KBr) ν 3433, 3086, 3069, 2965, 1655, 1557, 1490, 1469, 1410, 1210 cm⁻¹; MS (EI) m/z 278 (M⁺, 39), 137 (66), 114 (100), 86 (38) 55 (19), 42 (19); HRMS (EI) 278.1632 (C₁₅H₂₂N₂O₃ requires 278.1630).



Formamide (S)-(-)-219. A mixture of the benzyl derivative **231** (870 mg, 1.73 mmol) and a 10% palladium on activated charcoal (180 mg, 10 mol%) in absolute ethanol (40 mL) was stirred under a hydrogen atmosphere for 8 h. Ethanol (300 mL) was then added, and the mixture was filtered through Celite and evaporated. The residue (720 mg) was purified by chromatography on a column of silica gel (70 g) with a mixture of CH₂Cl₂ and MeOH (49:1) to afford (S)-(-)-**219** (670 mg, 95%) as an enamel: $R_f = 0.37$ and 0.25 (two spots, CH₂Cl₂-MeOH, 49:1); $[\alpha]_D -140.60$ (c 0.5, CHCl₃); ¹H NMR (400 Hz, CDCl₃, a mixture of rotamers in ca. 4:1 ratio; the signals for the minor rotamer are marked with an *) δ 0.90 (d, $J = 6.6$ Hz, 3H), 1.02 (d, $J = 6.5$ Hz, 3H), 2.02–2.09 (m, 2H), 2.21 (s, 6H), 2.40–2.50 (m, 1H), 2.75 (t, $J = 7.7$ Hz, 2H), 2.94 (s, 0.43H*), 3.02 (s, 2.60H), 3.51 (d, $J = 10.4$ Hz, 0.14H*), 3.71 (t, $J = 6.4$ Hz, 2H), 4.37 (d, $J = 11.2$ Hz, 0.86H), 6.37 (br s, 0.96H), 6.79 (d, $J = 8.5$ Hz, 2H), 7.07 (d, $J = 8.5$ Hz, 2H), 7.14 (s, 0.14H*), 7.16 (s, 1.69H), 8.03 (br s, 0.12H*), 8.14 (s, 0.93H), 8.19 (s, 0.78H), 8.25 (s, 0.13H*); ¹³C NMR δ 16.4 (CH₃), 18.5 (CH₃), 19.4 (CH₃), 25.4 (CH), 31.4 (CH₂), 31.7 (CH₃), 32.2 (CH₂), 63.1 (CH), 71.7 (CH₂), 115.3 (CH), 120.5 (CH), 129.4 (CH), 131.5 (C), 132.8 (C), 133.5 (C), 152.8 (C), 154.0 (C), 164.1 (CHO), 167.0 (CO); IR (KBr) ν 3396, 2960, 2871, 1654, 1549, 1517, 1480, 1218 cm⁻¹; MS (CI) m/z 413 ([MH]⁺, 40), 412 (68), 271 (27), 143 (90), 115 (100), 88 (28); HRMS (CI) 413.2436 (C₂₄H₃₃N₂O₄ [MH]⁺ requires 413.2440).

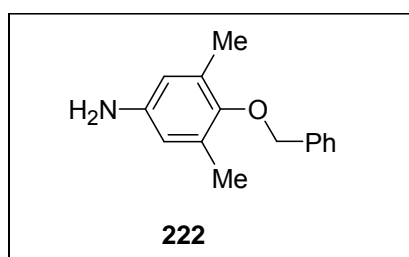


Formamide (S)-(-)-220. Trifluoroacetic acid (3.5 mL) was added dropwise to a solution of the BOC derivative **234** (300 mg, 0.70 mmol) in CH₂Cl₂ (6 mL) at 0 °C, and stirring was continued at the same temperature for 1 h. The acid was removed under reduced pressure, and the residue was coevaporated with toluene (2 × 10 mL) to afford a TFA salt of the deprotected amine as a brownish oil, which was used in the following step without further purification. The crude amine salt was dissolved in formic acid (4 mL), and the resulting solution was cooled to 0 °C. Acetic anhydride (3 mL) was then added dropwise and the mixture was allowed to stir at room temperature for 19 h. The volatiles were then evaporated, and the residue (290 mg) was purified by chromatography on a column of silica gel (40 g) with a mixture of CH₂Cl₂ and MeOH (70:1) to afford formamide (S)-(-)-**220** (230 mg; 96%) as a white solid: mp 117–119 °C; *R_f* = 0.50 and 0.42 (two spots; CH₂Cl₂-MeOH, 49:1); [α]_D –154.20 (*c* 0.5, CHCl₃); ¹H NMR (400 Hz, CDCl₃ a mixture of rotamers in ca. 4:1 ratio; the signals for the minor rotamer are marked with an *) δ 0.91 (d, *J* = 6.5 Hz, 3H), 1.04 (d, *J* = 6.5 Hz, 3H), 2.21 (pent, *J* = 6.0 Hz, 2H) partly overlapped with 2.24 (s, 6H), 2.40–2.52 (m, 1H), 2.98 (s, 0.6 H*), 2.99 (s, 2.42 H), 3.74 (d, *J* = 10.6 Hz, 0.18H*), 3.82 (t, *J* = 6.3 Hz, 2H), 3.85 (t, *J* = 5.7 Hz, 2H), 4.37 (d, *J* = 11.3 Hz, 0.83H) 7.18 (s, 1.69H), 8.05 (s, br, 0.74 H), 8.14 (s, 0.86 H), 8.57 (s, 0.29 H); ¹³C NMR δ 16.3 (CH₃), 18.5 (CH₃), 19.5 (CH₃), 25.2 (CH), 31.6 (CH₃), 33.2 (CH₂), 41.6 (CH₂), 63.1 (CH), 68.2 (CH₂), 120.4 (CH), 131.5 (C), 133.2 (C), 162.2 (C), 164.0 (CO), 167.0 (CO); IR (KBr) ν 3285, 3215, 3148, 3081, 2965, 2875, 1658, 1613, 1555, 1485, 1411, 1215 cm⁻¹; MS (EI) *m/z* 354 (M⁺, 54), 213 (96), 166 (15), 142 (82), 114 (100), 86 (52), 55 (28), 41 (28); HRMS (EI) 354.1715 (C₁₈H₂₇ClN₂O₃ requires 354.1710).

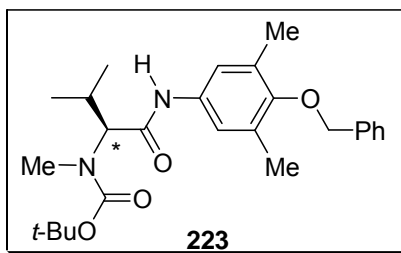


4-Benzyloxy-3,5-dimethylnitrobenzene 221. Benzyl bromide (3.56 mL, 29.99 mmol) and K₂CO₃ (5.00 g, 36.20 mmol) were consecutively added to a stirred solution of 2,6-dimethylnitrophenol **207** (2.00 g, 11.96 mmol) in dry acetone (50 mL), and the mixture was refluxed for 19 h. The mixture was then evaporated, the residue was partitioned between ether (80 mL) and water (40 mL), and the organic phase was additionally washed with a 1M aqueous

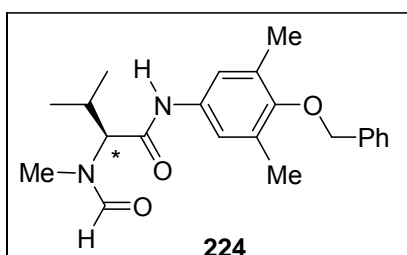
solution of NaOH (40 mL). The organic solution was dried over MgSO₄ and evaporated to afford the crude product (6.05 g), which was purified by chromatography on a column of silica gel (50 g) with a mixture of petroleum ether and CH₂Cl₂ (5:1) to remove benzyl bromide. Continued elution with a mixture of CH₂Cl₂ and petroleum ether (2:1) afforded **221** (2.74 g, 89%) as a white solid: mp 68–69 °C; *R_f* = 0.25 (petroleum ether-CH₂Cl₂, 5:1); ¹H NMR (400 Hz, CDCl₃) δ 2.24 (s, 6H), 4.88 (s, 2H), 7.36–7.47 (m, 5H), 7.94 (s, 2H); ¹³C NMR δ 16.7 (CH₃), 74.4 (CH₂), 124.3 (CH), 127.9 (CH), 128.5 (CH), 128.7 (CH), 132.7 (C), 136.5 (C), 143.6 (C), 161.1 (C); MS (EI) *m/z* 257 (M⁺, 4), 91 (100), 89 (5), 65 (27), 39 (9); HRMS (EI) 257.1053 (C₁₅H₁₅NO₃ requires 257.1052).



4-Benzyloxy-3,5-dimethylaniline 222. Tin(II) chloride dehydrate (3.16 g, 14 mmol) was added to a solution of nitro ether **221** (900 mg, 3.5 mmol) in ethanol (20 mL), and the mixture was refluxed for 9 h. The mixture was then cooled, a saturated aqueous solution of NaHCO₃ (50 mL) was added to reach pH 10, and the product was extracted with ether (3 × 150 mL). The organic phase was dried over MgSO₄ and evaporated, and the residue (820 mg) was purified by chromatography on a column of silica gel (30 g) with CH₂Cl₂ to afford contaminated **222** (530 mg) as a red oil. The oil was dissolved in Et₂O (20 mL), followed by the addition of 1 M hydrochloric acid (10 mL). The white solid amine salt thus formed was isolated by filtration and washed with Et₂O to remove impurities and then dissolved in a mixture of Et₂O (20 mL), water (10 mL), and saturated NaHCO₃ (10 mL) and stirred for 10 min. The organic phase was separated, dried over MgSO₄, and evaporated to afford pure **222** (340 mg, 43%) as a yellowish oil: *R_f* = 0.25 (CH₂Cl₂-petroleum ether 2:1); ¹H NMR (400 Hz, CDCl₃) δ 2.24 (s, 6H), 4.75 (s, 2H), 6.44 (s, 2H), 7.32–7.49 (m, 5H); ¹³C NMR δ 16.4 (CH₃), 74.3 (CH₂), 115.9 (CH), 127.8 (CH), 127.8 (CH), 128. Five (CH), 131.8 (C), 137.9 (C), 141.1 (C), 148.9 (C); MS (EI) *m/z* (%) 227 (M⁺, 19), 136 (100), 108 (18), 91 (28); HRMS (EI) 227.1311 (C₁₅H₁₇NO requires 227.1310).

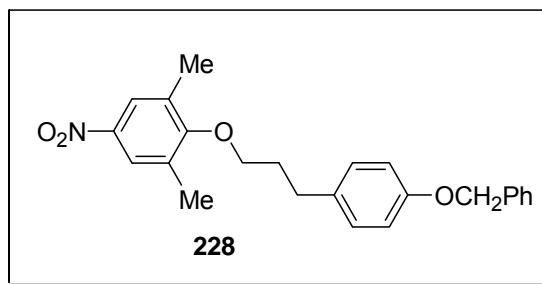


Amide (S)-(-)-223. Triethylamine (0.32 mL, 2.30 mmol) was added to a solution of (S)-BOC-N-methylvaline (390 mg, 1.69 mmol) in dry CH₂Cl₂ (8 mL) at 0 °C. To the resulting clear solution were successively added a solution of aniline **222** (340 mg, 1.50 mmol) in CH₂Cl₂ (3 mL), 1-hydroxybenzotriazole (HOBt; 230 mg, 1.70 mmol), and 1-(3-dimethylaminopropyl)-3-ethylcarbodiimide hydrochloride (EDCI; 330 mg, 1.72 mmol). The reaction mixture was stirred at 0 °C for 1 h and then at room temperature for 23 h. The mixture was then diluted with ethyl acetate (70 mL) and washed successively with water (30 mL), cold 0.5 M HCl (2 × 30 mL), saturated NaHCO₃ (2 × 30 mL), and brine (30 mL) and dried over MgSO₄ and evaporated. The residue (680 mg) was purified by chromatography on a column of silica gel (50 g) with a mixture of petroleum ether and ethyl acetate (8:1) to afford pure amide (S)-(-)-**223** (510 mg, 77%) as a white solid: mp 132–134 °C; *R_f* = 0.50 (petroleum ether-AcOEt, 6:1); [α]_D –81.6 (*c* 0.5, EtOH); ¹H NMR (400 Hz, CDCl₃) δ 0.91 (d, *J* = 6.5 Hz, 3H), 1.02 (d, *J* = 6.5 Hz, 3H), 1.49 (s, 9H), 2.28 (s, 6H), 2.32–2.41 (m, 1H), 2.83 (s, 3H), 4.10 (d, *J* = 10.7 Hz, 1H), 4.76 (s, 2H), 7.20 (s, 2H), 7.33–7.49 (m, 5H), 8.07 (br s, 0.78H); ¹³C NMR δ 16.5 (CH₃), 18.6 (CH₃), 19.9 (CH₃), 25.9 (CH), 28.4 (CH₃), 30.4 (CH₃), 66.0 (CH), 74.2 (CH₂), 80.6 (C), 120.2 (CH), 127.8 (CH), 128.0 (CH), 128.5 (CH), 131.6 (C), 133.7 (C), 137.5 (C), 152.2 (C), 157.4 (CO), 168.6 (CO); MS (EI) *m/z* 440 (M⁺, 22), 214 (36), 158 (95), 136 (100), 91 (54), 57 (49); HRMS (EI) 440.2674 (C₂₆H₃₆N₂O₄ requires 440.2675).



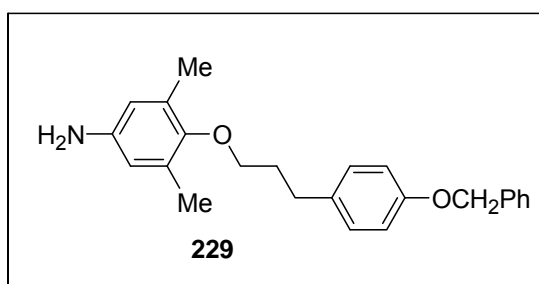
Formamide (S)-(-)-224. Trifluoroacetic acid (18.5 mL) was added dropwise to a solution of the BOC derivative **223** (1.62 g, 4.40 mmol) in CH₂Cl₂ (30 mL) at 0 °C and stirring continued at the same temperature for 1 h. The acid was removed under reduced pressure, and the

residue was coevaporated with toluene (2×20 mL) to afford a TFA salt of the deprotected amine as a brownish oil, which was used in the following step without further purification. The crude amine salt was dissolved in formic acid (20.7 mL), and the resulting solution was cooled to 0 °C. Acetic anhydride (15.4 mL) was then added dropwise and the mixture was allowed to stir at room temperature for 15 h. The volatiles were then evaporated and the residue (1.58 g) was purified by chromatography on a column of silica gel (75 g) with a mixture of CH_2Cl_2 and MeOH (99:1) to afford formamide (*S*)-(-)-**224** (1.15 g; 85%) as a light orange solid: mp 123–124 °C; R_f = 0.62 and 0.37 (two spots; CH_2Cl_2 -MeOH, 49:1); $[\alpha]_D -153.40$ (c 0.5, CHCl_3); ^1H NMR (400 Hz, CDCl_3 , a mixture of rotamers in ca. 4:1 ratio; the signals for the minor rotamer are marked with an *) δ 0.92 (d, J = 6.5 Hz, 3H), 1.05 (d, J = 6.5 Hz, 3H), 2.27 (s, 6H), 2.41–2.54 (m, 1H), 2.98 (s, 0.59H*), 3.00 (s, 2.36H), 3.68 (d, J = 10.95, 0.16H*), 4.37 (d, J = 11.0, 0.86H), 4.76 (s, 2H) 7.21 (s, 1.86 H), 7.24 (s, 0.13 H*), 7.32–7.47 (m, 5H), 8.01 (s, br. 0.85H), 8.15 (s, 0.91H), 8.50 (s, 0.16H); ^{13}C NMR δ 16.5 (CH_3), 18.6 (CH_3), 19.6 (CH_3), 25.2 (CH), 31.6 (CH_3), 63.2 (CH), 74.2 (CH_2), 120.4 (CH), 127.8 (CH), 128.0 (CH), 128.5 (CH) 131.7 (C), 133.2 (C), 137.5 (C), 152.5 (C), 164.0 (CO), 167.0 (CO); IR (KBr) ν 3459, 3317, 3069, 2965, 1658, 1613, 1551, 1482, 1411, 1211 cm^{-1} ; MS (EI) m/z 368 (M^+ , 9), 277 (17), 164 (12), 142 (91), 114 (100), 91 (75) 86 (23), 55 (13), 42 (11); HRMS (EI) 368.2103 ($\text{C}_{22}\text{H}_{28}\text{N}_2\text{O}_3$ requires 368.2100).

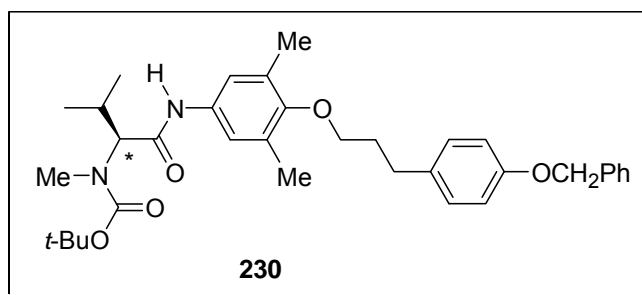


4-[3-(4-Benzyloxyphenyl)-1-propyloxy]-3,5-dimethylnitro-benzene **228**. Triphenylphosphine (4.31 g, 16.42 mmol), alcohol **227** (3.98 g, 16.42 mmol), and diethyl azodicarboxylate (2.58 mL, 16.42 mmol) were added successively to a stirred solution of 2,6-dimethyl-4-nitrophenol **207** (2.22 g, 13.28 mmol) in THF (30 mL) at 0 °C, and the resulting mixture was stirred at 25 °C for 19 h. The solvent was evaporated, and the residue was purified by chromatography on a column of silica gel (100 g) with a mixture of petroleum ether and dichloromethane (3:2) to afford a slightly contaminated product as a brownish solid. The solid was washed with ether (2×15 mL) to give pure ether **228** (4.36 g, 84%) as a yellowish solid: mp 97–99 °C; R_f = 0.3 (petroleum ether- CH_2Cl_2 , 3:2); ^1H NMR (400 MHz,

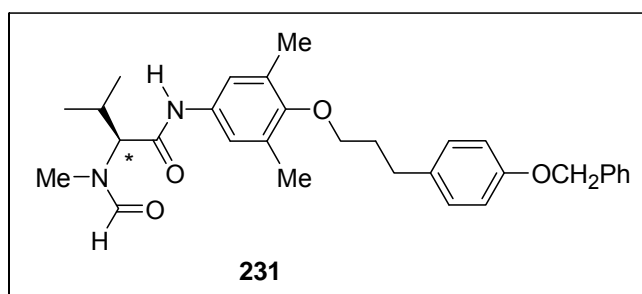
CDCl₃) δ 2.09–2.17 (m, 2H), 2.33 (s, 6H), 2.81 (t, J = 7.7 Hz, 2H), 3.84 (t, J = 6.4 Hz, 2H), 5.06 (s, 2H), 6.93 (d, J = 8.6 Hz, 2H), 7.15 (d, J = 8.6 Hz, 2H), 7.33–7.45 (m, 5H), 7.91 (s, 2H); ¹³C NMR δ 16.7 (CH₃), 31.3 (CH₂), 32.1 (CH₂), 70.1 (CH₂), 71.9 (CH₂), 114.9 (CH), 124.2 (CH), 127.4 (CH), 127.9 (CH), 128.6 (CH), 129.3 (CH), 132.3 (C), 133.5 (C), 137.1 (C), 143.4 (C), 157.2 (C), 161.6 (C); MS (EI) m/z 391 (M⁺, 82), 285 (8), 256 (9), 225 (5), 197 (7), 167 (6), 133 (8), 91 (100), 86 (100), 47 (93); HRMS (EI) 391.1781 (C₂₄H₂₅NO₄ requires 391.1784).



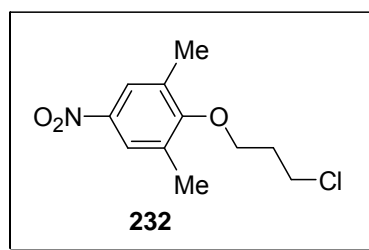
4-[3-(4-Benzyloxyphenyl)-1-propyl]oxy-3,5-dimethylaniline 229. Tin(II) chloride dihydrate (4.82 g, 21.36 mmol) was added to a solution of nitro ether **228** (2.00 g, 5.11 mmol) in a 1:1 mixture of ethanol and THF (30 mL), and the mixture was refluxed for 9 h. The mixture was then cooled, and a saturated aqueous solution of NaHCO₃ (75 mL) was added to reach pH 10. The product was extracted with ethyl acetate (3 × 125 mL), and the organic phase was dried over MgSO₄. The solvent was evaporated, and the residue (2.60 g) was purified by chromatography on a column of silica gel (70 g) with CH₂Cl₂ to afford aniline **229** (950 mg, 51%) as a reddish solid: mp 53–55 °C; R_f = 0.20 (CH₂Cl₂); ¹H NMR (400 MHz, CDCl₃) δ 2.03–2.10 (m, 2H), 2.20 (s, 6H), 2.78 (t, J = 7.8 Hz, 2H), 3.72 (t, J = 6.4 Hz, 2H), 5.05 (s, 2H), 6.47 (s, 2H), 6.92 (d, J = 8.6 Hz, 2H), 7.16 (d, J = 8.6 Hz, 2H), 7.31–7.45 (m, 5H); ¹³C NMR δ 16.3 (CH₃), 31.6 (CH₂), 32.2 (CH₂), 70.0 (CH₂), 71.8 (CH₂), 114.7 (CH), 116.5 (CH), 127.5 (CH), 127.9 (CH), 128.5 (CH), 129.3 (CH), 131.8 (C), 134.2 (C), 137.1 (C), 139.2 (C), 149.8 (C), 157.0 (C); MS (EI) m/z 361 (M⁺, 55), 136 (69), 91 (100), 84 (19), 65 (13); HRMS (EI) 361.2044 (C₂₄H₂₇NO₂ requires 361.2042).



Amide (S)-(-)-230. Triethylamine (0.85 mL, 6.12 mmol) was added to a solution of (S)-BOC-N-methylvaline (850 mg, 3.68 mmol) in dry CH₂Cl₂ (25 mL) at 0 °C. To the resulting clear solution were consecutively added aniline **229** (950 mg, 2.63 mmol), 1-hydroxybenzotriazole (HOBt; 630 mg, 4.66 mmol), and 1-(3-dimethylaminopropyl)-3-ethylcarbodiimide hydrochloride (EDCI; 780 mg, 4.07 mmol), and the reaction mixture was stirred at 0 °C for 1h and then at room temperature for 24 h. The mixture was then diluted with ethyl acetate (150 mL) and washed successively with water (75 mL), cold 0.5 M HCl (2 × 75 mL), saturated NaHCO₃ (2 × 75 mL), and brine (75 mL), dried over MgSO₄, and evaporated. The residue (1.92 g) was purified by chromatography on a column of silica gel (100 g) with a mixture of petroleum ether and ethyl acetate (8:1) to afford pure amide (S)-(-)-**230** (1.15 g, 76%) as an orange oil: R_f = 0.42 (petroleum ether-AcOEt, 6:1); $[\alpha]_D -70.4$ (c 0.5, CHCl₃); ¹H NMR (400 MHz, CDCl₃) δ 0.91 (d, J = 6.6 Hz, 3H), 1.01 (d, J = 6.5 Hz, 3H), 1.49 (s, 9H), 2.04–2.11 (m, 2H), 2.24 (s, 6H), 2.32–2.41 (m, 1H), 2.79 (t, J = 7.7 Hz, 2H), 2.83 (s, 3H), 3.73 (t, J = 6.4 Hz, 2H), 4.09 (d, J = 11.0 Hz, 1H), 5.05 (s, 2H), 6.92 (d, J = 8.6 Hz, 2H), 7.15 (d, J = 8.6 Hz, 2H) partly overlapped with 7.16 (s, 2H), 7.30–7.45 (m, 5H), 8.05 (br s, 0.84H); ¹³C NMR δ 16.4 (CH₃), 18.6 (CH₃), 19.9 (CH₃), 25.9 (CH), 28.4 (CH₃), 30.5 (CH₃), 31.5 (CH₂), 32.2 (CH₂), 66.0 (CH), 70.1 (CH₂), 71.7 (CH₂), 80.6 (C), 114.8 (CH), 120.1 (CH), 127.5 (CH), 127.9 (CH), 128.5 (CH), 129.3 (CH), 131.5 (C), 133.4 (C), 134.1 (C), 137.2 (C), 152.5 (C), 157.1 (C), 157.4 (CO), 168.6 (CO); MS (EI) m/z 574 (M⁺, 26), 361 (53), 130 (54), 91 (100), 86 (69), 57 (44); HRMS (EI) 574.3404 (C₃₅H₄₆N₂O₅ requires 574.3407).

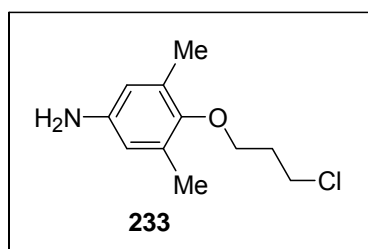


Formamide (S)-(-)-231. Trifluoroacetic acid (10.1 mL) was added dropwise to a solution of the BOC derivative **230** (1.15 g, 2.00 mmol) in CH₂Cl₂ (17 mL) at 0 °C and stirring continued at the same temperature for 1 h. The acid was removed under reduced pressure, and the residue was coevaporated with toluene (2 × 20 mL) to afford a TFA salt of the deprotected amine as a brownish oil, which was used in the following step without further purification. The crude amine salt was dissolved in formic acid (12.1 mL), and the resulting solution was cooled to 0 °C. Acetic anhydride (9 mL) was then added dropwise, and the mixture was allowed to stir at room temperature for 25 h. The volatiles were then evaporated, and the residue was coevaporated with toluene (2 × 10 mL). The latter residue (940 mg) was purified by chromatography on a column of silica gel (100 g) with a mixture of CH₂Cl₂ and MeOH (90:1) to afford formamide (S)-(-)-**231** (870 mg; 87%) as a colorless oil: *R_f* = (2 spots 0.70 and 0.50) (CH₂Cl₂-MeOH, 49:1); [α]_D -95.20 (*c* 0.5, CHCl₃); ¹H NMR (400 MHz, CDCl₃, a mixture of rotamers in ca. 4:1 ratio; the signals for the minor rotamer are marked by an *) δ 0.91 (d, *J* = 6.6 Hz, 3H), 1.05 (d, *J* = 6.5 Hz, 3H), 2.04–2.11 (m, 2H), 2.23 (s, 6H), 2.39–2.52 (m, 1H), 2.78 (t, *J* = 7.7 Hz, 2H), 2.93 (s, 0.41H*), 2.99 (s, 2.55H), 3.49 (d, *J* = 10.3 Hz, 0.11H*), 3.73 (t, *J* = 6.4 Hz, 2H), 4.38 (d, *J* = 11.2 Hz, 0.83H), 5.05 (s, 2H), 6.92 (d, *J* = 8.6 Hz, 2H), 7.15 (d, *J* = 8.6 Hz, 2H), 7.17 (s, 2H), 7.30–7.45 (m, 5H), 7.76 (s, 0.12H*), 8.02 (br s, 0.83H), 8.14 (s, 0.86H), 8.24 (s, 0.13H*); ¹³C NMR δ 16.4 (CH₃), 18.5 (CH₃), 19.5 (CH₃), 25.2 (CH), 31.5 (CH₂), 31.6 (CH₃), 32.2 (CH₂), 63.1 (CH), 70.1 (CH₂), 71.7 (CH₂), 114.8 (CH), 120.3 (CH), 127.4 (CH), 127.9 (CH), 128.5 (CH), 129.3 (CH), 131.5 (C), 133.0 (C), 134.1 (C) 137.2 (C), 152.8 (C) 157.1 (C), 163.9 (CHO), 167.0 (CO); IR (KBr) ν 3448, 2925, 1655, 1552, 1509, 1484, 1215 cm⁻¹; MS (EI) *m/z* 502 (M⁺⁺, 18), 361 (25), 276 (10), 233 (100), 231 (40), 121 (47), 78 (92), 44 (55); HRMS (EI) 502.2831 (C₃₁H₃₈N₂O₄ requires 502.2832).

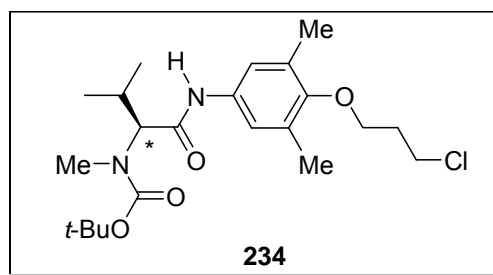


4-(3-Chloro-1-propyloxy)-3,5-dimethylnitrobenzene 232. Triphenylphosphine (980 mg, 3.74 mmol), 3-chloropropanol (0.31 mL, 3.70 mmol), and 97% diethyl azodicarboxylate (0.59 mL, 3.73 mmol) were added consecutively to a stirred solution of 2,6-dimethyl-4-nitrophenol **207** (500 mg, 2.99 mmol) in THF (7 mL) at 0 °C. The resulting mixture was stirred at 25 °C

for 21 h, and the solvent was then evaporated to afford the crude product (2.04 g), which was purified by chromatography on a column of silica gel (40 g) with a mixture of petroleum ether and CH₂Cl₂ (4:1) to give **232** (580 mg, 79%) as a white solid: mp 53–55 °C; *R_f* = 0.42 (petroleum ether-CH₂Cl₂, 5:1); ¹H NMR (400 Hz, CDCl₃) δ 2.27 (pent, 2H, *J* = 5.9 Hz), 2.36 (s, 6H), 3.84 (t, 2H, *J* = 6.2 Hz), 3.97 (t, *J* = 5.8 Hz, 2H), 7.92 (s, 2H); ¹³C NMR δ 16.5 (CH₃) 33.0 (CH₂), 41.2 (CH₂), 68.3 (CH₂), 124.3 (CH), 132.4 (CH), 143.6 (C), 160.9 (C); MS (EI) *m/z* (%) 243 (M⁺, 37), 167 (86), 137 (77), 121 (15), 91 (54), 82 (100), 47 (59); HRMS (EI) 243.0658 (C₁₁H₁₄ClNO₃ requires 243.0662).



4-(3-Chloro-1-propyloxy)-3,5-dimethylaniline 233. Tin(II) chloride dihydrate (4.30 g, 19.04 mmol) was added to a solution of the nitro ether **232** (1.16 g, 4.76 mmol) in a 1:1 mixture of THF and EtOH (24 mL), and the resulting solution was stirred at 40 °C for 23 h. The mixture was then cooled, and a saturated aqueous solution of NaHCO₃ (70 mL) was added to reach pH 10. The product was extracted with ether (3 × 200 mL) and the organic phase was dried over MgSO₄ and evaporated. The residue (1.15 g) was purified by chromatography on a column of silica gel (50 g) with CH₂Cl₂ to afford aniline **233** (660 mg, 65%) as a brownish solid: mp 62–63 °C; *R_f* = 0.40 (CH₂Cl₂); ¹H NMR (400 Hz, CDCl₃) δ 2.20–2.23 (m, 8H), 3.54 (s, br, 1.94 H), 3.83 (t, *J* = 6.4 Hz, 2H), 3.84 (t, *J* = 5.8 Hz, 2H), 6.38 (s, 2H); ¹³C NMR δ 16.2 (CH₃) 33.3 (CH₂), 41.8 (CH₂) 68.3 (CH₂), 115.5 (CH), 131.7 (C), 141.5 (C), 148.4 (C); MS (CI) *m/z* 213 (M⁺, 45), 136 (100), 120 (9), 108 (52), 93 (38), 91 (19), 41 (52); HRMS (EI) 213.0916 (C₁₁H₁₆ClON requires 213.0920).

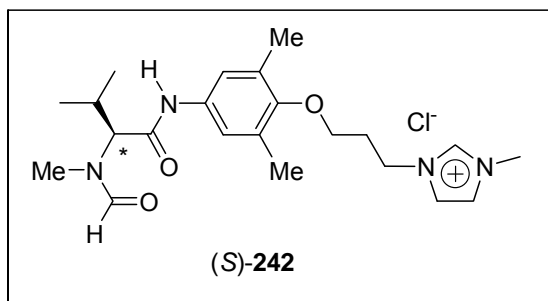


Amide (S)-(-)-234. Triethylamine (0.16 mL, 1.15 mmol) was added to a solution of (S)-BOC-N-methylvaline (210 mg, 0.91 mmol) and aniline **233** (180 mg 0.84 mmol) in dry CH₂Cl₂ (6 mL) at 0 °C. To the resulting clear solution were consecutively added 1-hydroxybenzotriazole (HOBt; 160 mg, 1.18 mmol) and 1-(3-dimethylaminopropyl)-3-ethylcarbodiimide hydrochloride (EDCI; 210 mg, 1.09 mmol). The reaction mixture was stirred at 0 °C for 1 h and then at room temperature for 22 h. The mixture was then diluted with ethyl acetate (35 mL), washed successively with water (20 mL), cold 0.5 M HCl (2 × 20 mL), saturated NaHCO₃ (2 × 20 mL), and brine (20 mL), dried over MgSO₄, and evaporated. The residue (430 mg) was purified by chromatography on a column of silica gel (40 g) with a mixture of petroleum ether and ethyl acetate (8:1) to afford pure amide (S)-(-)-**234** (310 mg, 86%) as a yellowish oil: *R_f* = 0.27 (petroleum ether-ethyl acetate, 8:1); [*α*]_D −81.6 (*c* 0.5, CHCl₃); ¹H NMR (400 Hz, CDCl₃) δ 0.90 (d, *J* = 6.5 Hz, 3H), 1.00 (d, *J* = 6.5 Hz, 3H), 1.48 (s, 9H), 2.22 (pent, *J* = 6.0 Hz, 2H) partly overlapped with 2.25 (s, 6H), 2.31–2.41 (m, 1H), 2.82 (s, 3H), 3.83 (t, *J* = 6.3 Hz, 3H), 3.85 (t, *J* = 5.7 Hz, 2H), 4.09 (d, *J* = 11.1 Hz, 1H), 7.18 (s, 2H), 8.08 (s, 0.87 H); ¹³C NMR δ 16.3 (CH₃), 18.6 (CH₃), 19.8 (CH₃), 25.9 (CH), 28.4 (CH₃), 30.4 (CH₃), 33.2 (CH₂), 41.6 (CH₂), 65.9 (CH), 68.1 (CH₂), 80.6 (C), 120.2 (CH), 131.4 (C), 133.6 (C), 151.9 (C), 157.4 (CO), 168.6 (CO); MS (CI) *m/z* 426 (M⁺, 25), 213 (75), 136 (79), 130 (100), 82 (92), 57 (95); HRMS (EI) 426.2291 (C₂₂H₃₅ClN₂O₄ requires 426.2285).

General Procedure for the Asymmetric Reduction of 185a-e, Catalysed by 217a-h or 235–241. The imine **185a** (100 mg, 0.44 mmol) was added to a reaction tube containing a small porous polypropylene reactor vessel (2.4 mL internal volume and 74 μm pore size) with an immobilized catalyst or resin (for the number of mmol, see Tables 1 and 3) in a solvent (4 mL), and the tube was shaken at room temperature for 30 min. Trichlorosilane (100 μL) was added at 0 °C, followed by overnight shaking at room temperature. The porous reactor vessel was separated from the mother liquor and washed with chloroform (2 × 30 mL). Combined organic solutions were quenched with a saturated aqueous solution of NaHCO₃ (25 mL), the

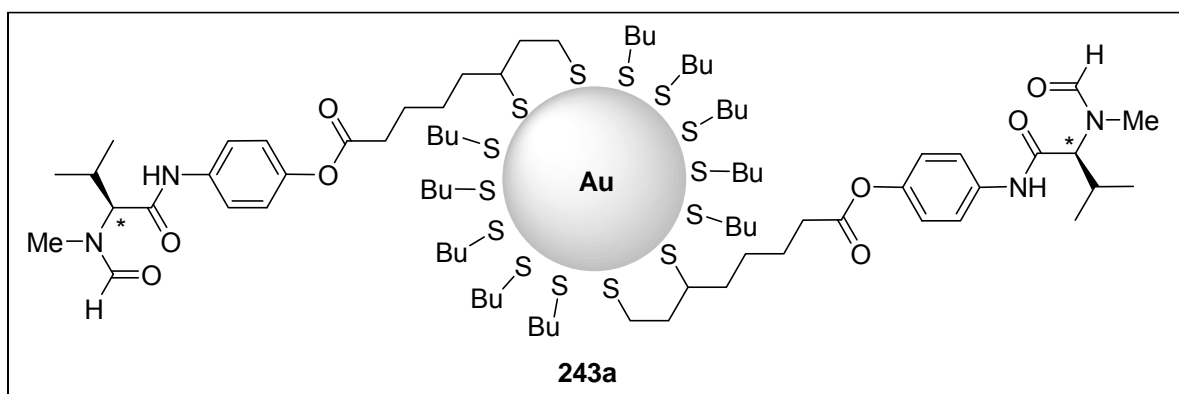
layers were separated, and the aqueous layer was additionally extracted with chloroform (60 mL). Combined chloroform solutions were dried over MgSO_4 , and the solvent was evaporated to give a crude product, which was purified by chromatography on a column of silica gel (15 g) to afford pure amines **185a**. The results are summarized in the Tables 24, 25 and 26.

Regeneration of Immobilized Catalysts. After separation from the mother liquor and washing with chloroform, the porous reactor vessel with immobilized catalyst was alternately washed with methanol and CH_2Cl_2 (4×25 mL of each solvent) and ether (25 mL). An overnight drying under vacuum afforded the regenerated catalyst, which was used for the next transformation without further purification.

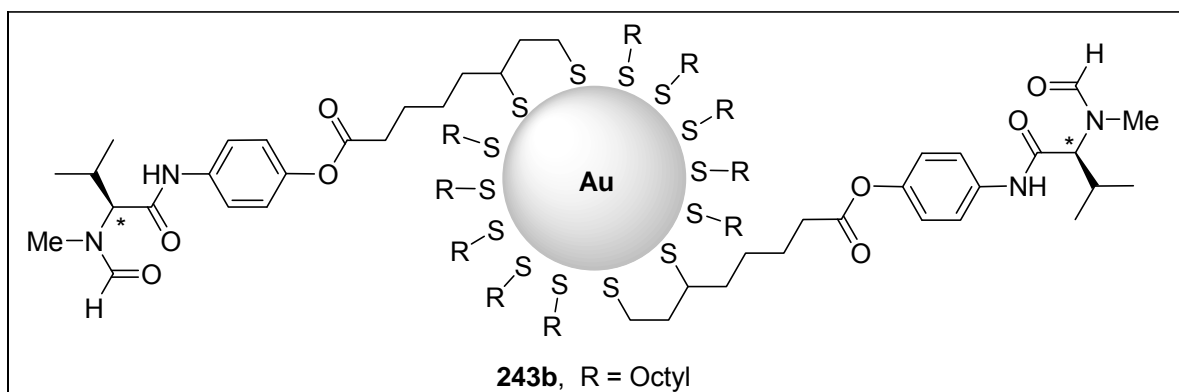


Imidazolium salt 242. Formamide **220** (100 mg, 0.28 mmol) and *N*-methyl-imidazole were stirred at 100 °C for 48 h. After cooling, chloroform (1.5 mL) was added, followed by the addition of ether (40 mL). The organic solution was separated from an insoluble residue and the process was repeated two more times. Evaporation of the solvent afforded the desired salt (56 mg, 51%) as a white solid (extremely moisture sensitive; when exposed to the air, the solid was quickly transformed to an oil): $[\alpha]_D -25.6$ (c 0.5, MeOH); ^1H NMR (400 Hz, D_2O , a mixture of rotamers in ca. 2:1 ratio) δ 0.77 (d, $J = 6.5$ Hz, 3H), 0.86 (d, $J = 6.5$ Hz, 3H), 2.06 (s, 6H), 2.26 (t, $J = 6.8$ Hz, 2H) partly overlapped with 2.14-2.30 (m, 3H), 2.79 (s, 2H), 2.93 (s, 1H), 3.66 (d, $J = 10.9$ Hz, 0.55H), 3.76 (s, 3H) partly overlapped with 3.73-3.76 (m, 5H), 4.31 (t, $J = 7.3$ Hz, 2H), 4.36 (d, $J = 11.1$ Hz, 0.38H), 6.97 (s, 0.68H), partly overlapped with 6.98 (s, 1.20H), 7.32 (s, 1H), 7.41 (s, 1H), 8.01 (s, 0.33H), 8.07 (s, 0.68H), 8.66 (s, 1H); ^{13}C NMR δ 15.44 (CH_3), 17.74 (CH_3), 18.22 (CH_3), 25.72 (CH), 26.77 (CH), 27.80 (CH_3), 29.88 (CH_2), 31.55 (CH_3), 35.60 (CH_3), 46.68 (CH_2), 61.80 (CH), 68.90 (CH_2), 68.99 (CH), 122.17 (CH), 122.47 (CH), 122.57 (CH), 123.63 (CH), 131.88 (C), 131.93 (C), 131.93 (C), 132.10 (C), 132.16 (C), 152.16 (C), 152.21 (C), 165.80 (CHO), 166.14 (CHO), 169.88 (CO), 169.94 (CO); IR (KBr) ν 3445, 3070, 2962, 1681, 1557, 1486, 1213 cm^{-1} ; MS (CI) m/z (%)

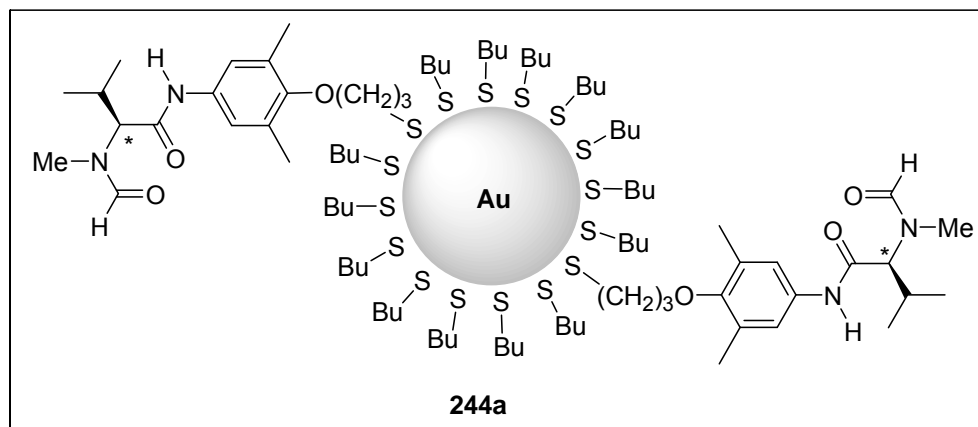
402 ($[MH]^+$, 76), 401 (100), 286 (14), 97 (60); HRMS (CI) 402.2631 ($C_{22}H_{34}N_4O_3$ requires 402.2577).



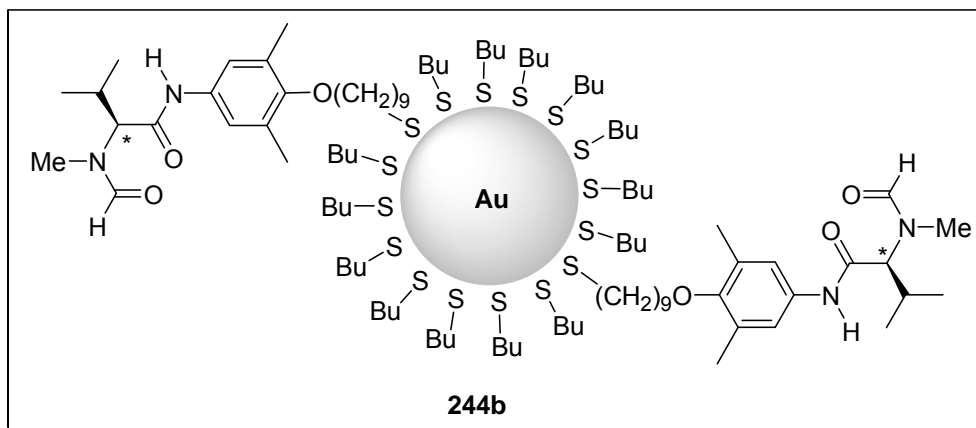
Gold nanoparticles 243a. Disulfide (-)-**247** (538 mg, 1.15 mmol) was added to a solution of butylthiolate-stabilised gold nanoparticles **253a** (538 mg, 3.74% S, 0.63 mmol) in toluene (70 mL) and the resulting solution was stirred at room temperature for 3 days. The solution was then concentrated under vacuum and EtOH (50 mL) added. The resulting precipitate was filtered by gravity filtration and washed with EtOH (150 mL) and acetone (150 mL) to furnish nanoparticles **243a** (493 mg) as a black powder: 1H NMR (400 Hz, $CDCl_3$) δ 0.89 (broad signal), 1.55 (broad signal), 2.97 (broad signal), 3.54 (broad signal), 4.33 (broad signal), 8.14 (broad signal); IR (KBr) ν 3446, 2954, 2923, 2869, 1757, 1655, 1560, 1456, 1416, 1375, 1261, 1210, 1094 cm^{-1} . Anal. Found: C, 7.14; H, 1.15; N, nil. TEM – 2.5 nm, an average core size. The filtrate was concentrated under vacuum then passed quickly through a plug of silica gel, eluting with a CH_2Cl_2 - Me_2CO mixture (3:1) to give unreacted lipoic ester **247** (371 mg).



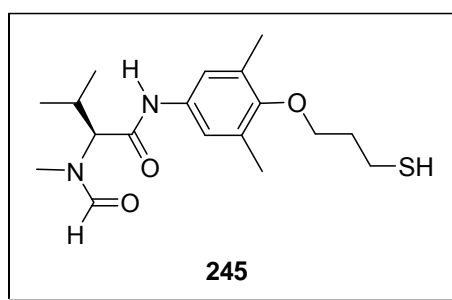
Gold nanoparticles 243b. Disulfide (-)-**247** (59 mg, 0.13 mmol) was added to a solution of octylthiolate-stabilised gold nanoparticles **253b** (100 mg, 3.23% S, 0.10 mmol) in DCM (20 mL) and the resulting solution was stirred at room temperature for 2 days. The solution was then concentrated under vacuum and EtOH (50 mL) added. The resulting precipitate was filtered by gravity filtration and washed with EtOH (100 mL) and acetone (100 mL) to furnish nanoparticles **243b** (88 mg) as a black powder: ^1H NMR (400 Hz, CDCl_3) δ 0.93 (broad signal), 1.12 (s), 1.61 (broad signal), 1.79 (broad signal), 2.10 (s), 2.42-2.51 (m), 2.60 (t, $J = 7.6$ Hz), 2.97 (s), 4.33 (d, $J = 10.3$ Hz), 8.00 (broad signal), 8.13 (broad signal); IR (KBr) ν 3440, 2951, 2927, 2869, 1760, 1649, 1560, 1460, 1418, 1375, 1266, 1211, 1094 cm^{-1}



Gold nanoparticles 244a. Thiol (S)-(-)-**245** (60 mg, 0.17 mmol) was added to a solution of the butylthiolate-stabilized gold nanoparticles **253a** (400 mg, 0.35 mmol of thiols on the surface) in CH_2Cl_2 (25 mL) (~0.5:1 **245**/butanethiol mol ratio) and the resulting solution was stirred at room temperature overnight. The solution was concentrated under vacuum to near dryness then petroleum ether (50 mL) was added to precipitate the product. The solid thus formed was isolated by filtration and washed with petroleum ether (200 mL) to give the functionalised nanoparticles **244a** (282 mg) as a black powder, soluble in most solvents except for petroleum ether: ^1H NMR (400 Hz, CDCl_3) δ 0.85 (broad signal), 1.26 (broad signal), 1.62 (broad signal), 2.17 (broad signal), 2.96 (broad signal), 6.99 (broad signal), 8.16 (broad signal); IR (KBr) ν 3462, 3277, 2954, 2922, 2868, 1656, 1611, 1549, 1482, 1409, 1374, 1213, 1214, 1060, 1007 cm^{-1} . Anal. Found: C, 9.87; H, 1.33; N, 0.89.

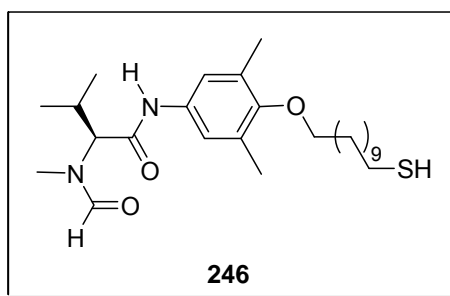


Gold nanoparticles 244b. Thiol (-)-**246** (6.7 mL of a ~60mg/mL solution in CH₂Cl₂, ~0.87 mmol) was added to a solution of butylthiolate-stabilized gold nanoparticles **253a** (400 mg, 0.47 mmol of thiols on the surface) in CH₂Cl₂ (60 mL) (~2:1 **246**/butanethiol mol ratio) and the resulting solution was stirred at room temperature overnight. The solution was concentrated under vacuum to near dryness and petroleum ether (70 mL) was added. The resulting solid was isolated by filtration and washed with petroleum ether (300 mL) to give the functionalised nanoparticles **244b** (521 mg) as a black powder, soluble in most solvents except petroleum ether: ¹H NMR (400 Hz, CDCl₃) δ 0.92 (broad signal), 1.03 (broad signal), 1.28 (broad signal), 1.60 (broad signal), 2.00 (broad signal), 2.24 (broad signal), 2.44 (broad signal), 2.97 (broad signal), 3.06 (broad signal), 3.51 (broad signal), 4.51 (broad signal), 7.00 (broad signal), 8.14 (broad signal), 8.29 (broad signal); IR (KBr) ν 3465, 3286, 2921, 2851, 1655, 1611, 1551, 1484, 1409, 1214, 1062. Anal. Found: C, 24.97; H, 3.40; N, 2.15.



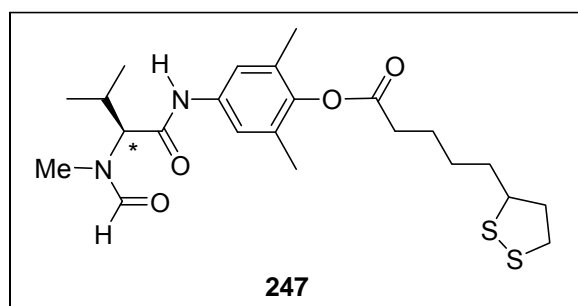
Formamide (S)-(-)-245. Tetra-*n*-butyl-ammonium fluoride (TBAF, 1M soln. in THF; 1.51 mL, 1.51 mmol) was slowly added to a solution of formamide **220** (490 mg, 1.38 mmol) and hexamethyldisilathiane (0.29 mL, 1.62 mmol) in THF (7 mL) at 0 °C and the mixture was stirred at this temperature for 30 min. The temperature was then increased to 25 °C and the reaction continued for 5h. Sat. NH₄Cl (50 mL) was added and the stirring was continued for an additional 5 min. The mixture was then washed with CH₂Cl₂ (2 × 100 mL), dried, and

evaporated. The residue (623 mg) was purified by chromatography on a column of silica gel (70 g) with a mixture of CH₂Cl₂ and MeOH (70:1) to afford pure formamide **245** (280 mg, 57%) as a yellowish oil: R_f = (2 spots 0.50 and 0.42) (CH₂Cl₂ – MeOH, 49:1); $[\alpha]_D$ -106.00 (c 1.0, CHCl₃); ¹H NMR (400 Hz, CDCl₃; a mixture of rotamers in ca. 4:1 ratio; the signals for the minor rotamer are marked with an *) δ 0.91 (d, J = 6.6 Hz, 3H), 1.03 (d, J = 8.8 Hz, 3H), 1.41 (t, , J = 8.0 Hz, 0.82H), 2.06 (pent., J = 6.4 Hz, 2H), 2.23 (s, 6H), 2.39-2.52 (m, 1H), 2.79 (q, J = 7.5 Hz, 2H), 2.91 (s, 0.41H*), 3.00 (s, 2.51H), 3.53 (d, J = 10.4 Hz, 0.13H*), 3.80 (t, J = 6.0 Hz, 2H), 4.40 (d, J = 11.3 Hz, 0.82H), 7.15 (s, 0.27H*), 7.18 (s, 1.55H), 8.10 (s, 0.14H*), 8.12 (s, 0.63H), 8.14 (s, 0.95H), 8.25 (s, 0.14H*); ¹³C NMR δ 16.33 (CH₃), 18.55 (CH₃), 19.51 (CH₃), 21.53 (CH₂), 25.27 (CH), 31.56 (CH₃), 34.47 (CH₂), 63.01 (CH), 69.87 (CH₂), 120.36 (CH), 131.40 (C), 133.11 (C), 152.35 (C), 163.90 (CHO), 167.05 (CO); IR (KBr) ν 3433, 3316, 2963, 2928, 2873, 1656, 1611, 1550, 1484, 1437, 1409, 1385, 1214, 1061, 1027, 874, 798; MS (EI) m/z (%) 352 (M⁺, 30), 211 (28), 142 (36), 114 (100), 86 (23); HRMS (EI) 352.1824 (C₁₈H₂₈N₂O₃S requires 352.1821).



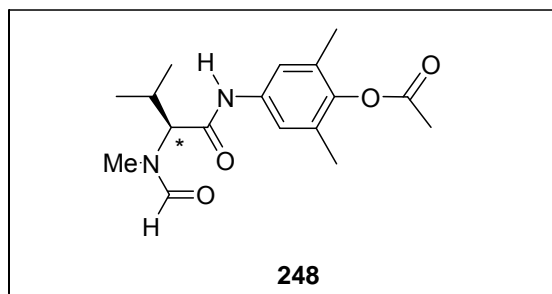
Formamide (S)-(-)-246. Tetra-*n*-butyl-ammonium fluoride (TBAF, 1M soln. in THF; 1.22 mL, 1.22 mmol) was slowly added to a solution of formamide **252** (571 mg, 1.12 mmol) and hexamethyldisilathiane (0.28 mL, 1.35 mmol) in THF (6 mL) at 0 °C and the mixture was stirred at this temperature for 100 min. Sat. NH₄Cl (35 mL) was added and the stirring was continued for an additional 5 min. The mixture was then washed with CH₂Cl₂ (2 × 100 mL), dried, and evaporated. The residue (623 mg) was purified by chromatography on a column of silica gel (70 g) with a mixture of CH₂Cl₂ and MeOH (70:1) to afford pure formamide **246** (461 mg, 90%) as a yellowish oil: R_f = 0.42 and 0.30 (two spots; CH₂Cl₂–MeOH, 70:1); $[\alpha]_D$ -77.00 (c 1.0, CHCl₃); ¹H NMR (400 Hz, CDCl₃; a mixture of rotamers in ca. 4:1 ratio; the signals for the minor rotamer are marked with an *) δ 0.91 (d, J = 6.6 Hz, 3H), 1.04 (d, J = 6.5 Hz, 3H), 1.29-1.41 (m, 13H), 1.44-1.51 (m, 2H), 1.61 (pent, J = 7.2 Hz, 2H), 1.77 (pent, J = 7.3 Hz, 2H), 2.24 (s, 4.94H), 2.25 (s, 0.75H*) 2.39-2.48 (m, 1H), 2.52 (q, J = 7.5 Hz, 2H), 2.93 (s, 0.53H*), 2.98 (s, 2.48H), 3.46 (d, J = 10.3 Hz, 0.12H*), 3.53 (t, J = 6.6 Hz, 0.10H),

3.69 (t, $J = 6.6$ Hz, 2H), 4.35 (d, $J = 11.3$ Hz, 0.83H), 7.14 (s, 0.24H*), 7.16 (s, 1.64H), 7.88 (s, 0.79H), 8.14 (s, 0.81H), 8.22 (s, 0.11H*); ^{13}C NMR δ 16.35 (CH₃), 18.53 (CH₃), 19.56 (CH₃), 24.66 (CH₂), 25.14 (CH), 26.13 (CH₂), 28.36 (CH₂), 29.05 (CH₂), 29.47 (CH₂), 29.50 (CH₂), 29.52 (CH₂), 29.55 (CH₂), 30.35 (CH₂), 31.55 (CH₃), 34.04 (CH₂), 63.10 (CH), 72.48 (CH₂), 120.25 (CH), 131.54 (C), 132.84 (C), 152.77 (C), 163.94 (CO), 166.91 (CO); IR (KBr) ν 3433, 2962, 2925, 2853, 1656, 1612, 1552, 1485, 1409, 1261, 1215, 1069, 1024, 802; MS (EI) m/z (%) 464 (M^+ , 48), 523 (83), 142 (58), 114 (100), 86 (25), 55 (12); HRMS (EI) 464.3076 (C₂₆H₄₄N₂O₃S requires 464.3073).

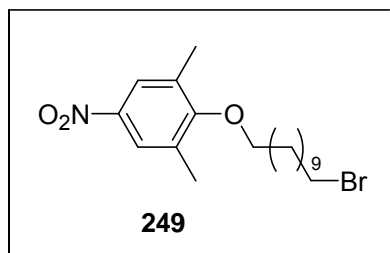


Formamide (S)-(-)-247. Phenol **218** (200 mg, 0.72 mmol) and 4-(dimethylamino)-pyridine (DMAP, 28 mg, 0.23 mmol) were consecutively added to a solution of (3-dimethylaminopropyl)-3-ethylcarbodiimide hydrochloride (EDCI; 344 mg, 1.79 mmol) and (±)-lipoic acid (296 mg, 1.43 mmol) in CH₂Cl₂ (10 mL) and the reaction mixture was stirred at 25 °C for 20 h. The mixture was then diluted with ethyl acetate (30 mL) and washed consecutively with water (2 × 40 mL), 0.5M HCl (40 mL), saturated NaHCO₃ (2 × 40 mL), water (40 mL), and brine (40 mL) and dried over MgSO₄ and evaporated. The residue (357 mg) was purified by chromatography on a column of silica gel (25 g) with a mixture of CH₂Cl₂ and MeOH (100:1) to afford pure formamide (S)-(-)-**247** (280 mg, 80%) as a yellow oil: $R_f = 0.44$ and 0.26 (two spots; CH₂Cl₂–MeOH, 49:1); $[\alpha]_D -89.20$ (c 0.65, CHCl₃); ^1H NMR (400 Hz, CDCl₃, a mixture of rotamers in ca. 4:1 ratio; the signals for the minor rotamer are marked with an *) δ 0.91 (d, $J = 6.6$ Hz, 3H), 1.03 (d, $J = 6.5$ Hz, 3H), 1.48–1.64 (m, 2H), 1.66–1.77 (m, 2H), 1.78–1.85 (m, 2H), 1.88–1.96 (m, 1H), 2.10 (s, 6H), 2.36–2.51 (m, 2H), 2.60 (t, $J = 7.5$ Hz, 2H), 2.91 (s, 0.37H*), 2.99 (s, 2.63H*) 3.09–3.22 (m, 2H), 3.50 (d, $J = 10.4$ Hz, 0.14H*), 3.54–3.62 (m, 1H), 4.39 (d, $J = 11.3$, 0.89H), 7.23 (s, 0.31 H*), 7.27 (s, 1.63H), 7.99 (s, br. 0.11H*), 8.13 (s, 0.89H), 8.19 (s, 0.77H), 8.22 (s, 0.18H*); ^{13}C NMR δ 16.49 (CH₃), 18.53 (CH₃), 19.52 (CH₃), 24.81 (CH₂), 25.20 (CH), 28.85 (CH₂), 31.60 (CH₃), 33.74 (CH₂), 34.59 (CH₂), 38.42 (CH₂), 40.21 (CH₂), 56.26 (CH), 63.26 (CH), 119.83 (CH),

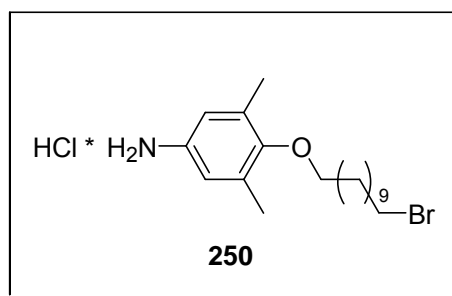
130.74 (C), 135.10 (C), 144.52 (C), 163.98 (CHO), 167.06 (CO), 171.26 (CO); IR (KBr) ν 3434, 2926, 1753, 1656, 1556, 1485, 1411, 1372, 1187 1124 cm^{-1} ; MS (CI) m/z (%) 467 ($[\text{MH}]^+$, 14), 278 (22), 189 (16), 1432 (94), 115 (100), 88 (30), 79 (23); HRMS (CI) 467.2043 ($\text{C}_{23}\text{H}_{35}\text{N}_2\text{O}_4\text{S}_2$ requires 467.2038).



Formamide (S)-(-)-248. Phenol **218** (50 mg, 0.18 mmol) and 4-(dimethylamino)-pyridine (DIMP, 5 mg, 0.04 mmol) were consecutively added to a solution of (3-dimethylaminopropyl)-3-ethylcarbodiimide hydrochloride (EDCI; 69 mg, 0.36 mmol) and glacial acetic acid (21 μL , 0.37 mmol) in DCM (1.5 mL). The reaction mixture was stirred at 25 $^{\circ}\text{C}$ for 15 h. The mixture was diluted with ethyl acetate (20 mL) and washed consecutively with water (2×10 mL), 0.5M HCl (2×10 mL), saturated NaHCO_3 (2×10 mL), brine (10 mL) and dried over MgSO_4 and evaporated. The residue (50 mg) was purified by chromatography on a column of silica gel (10 g) with a mixture of CH_2Cl_2 and MeOH (75:1) to afford pure formamide (S)-(-)-**248** (25 mg, 44%) as a colourless oil: R_f = 0.43 and 0.29 (two spots; CH_2Cl_2 –MeOH, 49:1); $[\alpha]_D$ -175.40 (c 0.5, CHCl_3); ^1H NMR (400 Hz, CDCl_3 , a mixture of rotamers in ca. 4:1 ratio; the signals for the minor rotamer are marked with an *) δ 0.91 (d, J = 6.5 Hz, 3H), 1.03 (d, J = 6.5 Hz, 3H), 2.11 (s, 6H), 2.31 (s, 2.29H), 2.32 (s, 0.69H*) 2.40–2.50 (m, 1H), 2.90 (s, 0.39H*), 2.99 (s, 2.55H), 3.50 (d, J = 10.4 Hz, 0.13H*), 4.40 (d, J = 11.2, 0.86H), 7.23 (s, 0.23 H*), 7.27 (s, 1.76H), 8.12 (br s, 0.11H*), 8.13 (s, 0.85H), 8.23 (s, 1H); ^{13}C NMR δ 16.38 (CH_3), 18.54 (CH_3), 19.50 (CH_3), 20.39 (CH_3), 25.24 (CH), 31.57 (CH_3), 63.15 (CH), 119.82 (CH), 130.76 (C), 135.19 (C), 144.55 (C), 163.95 (CHO), 167.10 (CO), 168.91; IR (KBr) ν 3450, 2965, 1759, 1658, 1562, 1485, 1410, 1372, 1187 cm^{-1} ; MS (EI) m/z (%) 320 (M^+ , 13), 278 (16), 225 (9), 142 (52), 114 (100), 83 (78), 47 (23); HRMS (EI) 320.1738 ($\text{C}_{17}\text{H}_{24}\text{N}_2\text{O}_4$ requires 320.1736).

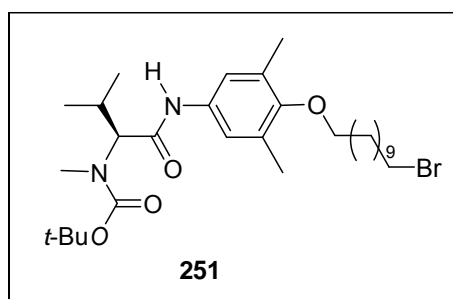


4-(11'-Bromo-1'-undecyloxy)-3,5-dimethylnitrobenzene 249. Triphenylphosphine (1.96 g, 7.47 mmol), 11-bromo-1-undecanol (1.86 g, 7.40 mmol) and 97% diethyl azodicarboxylate (1.17 mL, 7.46 mmol) were added consecutively to a stirred solution of 2,6-dimethyl-4-nitrophenol **207** (1.0 g, 5.98 mmol) in THF (14 mL) at 0 °C. The resulting mixture was stirred at 25 °C for 18 h and the solvent was then evaporated to afford the crude product (6.12 g), which was purified by chromatography on a column of silica gel (80 g) with a mixture of petroleum ether and CH₂Cl₂ (4:1) to give **249** (1.96 g, 82%) as a yellowish oil; *R_f* = 0.42 (petroleum ether–CH₂Cl₂, 4:1); ¹H NMR (400 Hz, CDCl₃) δ 1.30-1.56 (m, 14H), 1.82 (pent, *J* = 6.6 Hz, 2H), overlapped with 1.85 (pent, *J* = 6.9 Hz, 2H), 2.34 (s, 6H), 3.41 (t, 2H, *J* = 6.8 Hz), 3.81 (t, *J* = 6.6 Hz, 2H), 7.91 (s, 2H); ¹³C NMR δ 16.60 (CH₃), 26.00 (CH₂), 28.13 (CH₂), 28.73 (CH₂), 29.38 (CH₂), 29.43 (CH₂), 29.50 (CH₂), 30.32 (CH₂), 32.79 (CH₂), 34.06 (CH₂), 72.75 (CH₂), 124.19 (CH), 132.32 (C), 143.28 (C), 161.66 (C); MS (CI) *m/z* (%) 401 and 399 (M⁺, 14), 167 (100), 137 (33), 97 (30), 55 (62); HRMS (EI) 399.1415 (C₁₉H₃₀⁷⁹BrNO₃ requires 399.1409).



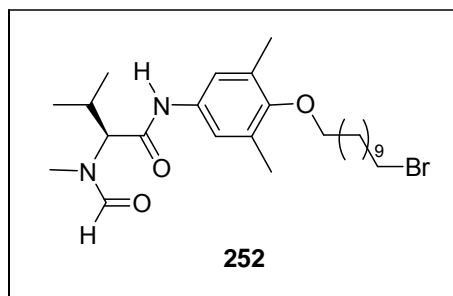
4-(11'-Bromo-1'-undecyloxy)-3,5-dimethylaniline hydrochloride 250. Tin(II) chloride dihydrate (4.50 g, 19.94 mmol) was added to a solution of the nitro ether **249** (2.00 g, 5.00 mmol) in EtOH (25 mL) and the resulting solution was stirred at 40 °C for 25 h. The mixture was then cooled and a saturated aqueous solution of NaHCO₃ (80 mL) was added to reach pH 10. The product was extracted with ether (3 × 150 mL) and the organic phase was dried over MgSO₄. The filtrate was condensed to ~250 mL followed by addition of 1M HCl (20 mL). The mixture was stirred for 10 min., the white solid was collected by filtration and

the product was washed with ether (3 x 100 mL). Drying in the air afforded the aniline salt **250** (1.05 g, 52%) as a white powder: ^1H NMR (400 Hz, CDCl_3) δ 1.30-1.52(m, 14H), 1.78 (pent, $J = 6.7$, Hz 2H), 1.85 (pent, $J = 7.3$ Hz, 2H), 2.27 (s, 6H), 3.41 (t, $J = 6.9$ Hz, 2H), 3.71 (t, $J = 6.5$ Hz, 2H), 7.16 (s, 2H), 10.33 (br s, 2.65H); ^{13}C NMR δ 16.26 (CH_3), 26.08 (CH_2), 28.16 (CH_2), 28.74 (CH_2), 29.40 (CH_2), 29.45 (CH_2), 29.48 (CH_2), 29.51 (CH_2), 30.31 (CH_2), 32.83 (CH_2), 34.02 (CH_2), 72.56 (CH_2), 123.12 (CH), 124.50 (C), 133.23 (C), 156.55 (C); MS (CI) m/z 370 (M^+ , 100), 369 (22), 290 (13), 138 (78), 137 (21), 69 (48); HRMS (EI) 370.1752 ($\text{C}_{19}\text{H}_{33}^{79}\text{BrNO}_3$ requires 370.1746).

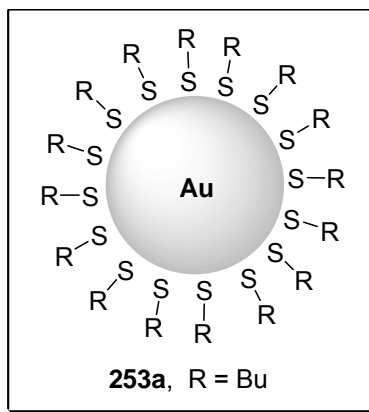


Amide (S)-(-)-251. The aniline salt **250** (1.00 g, 2.46 mmol) was added to a stirred solution of CH_2Cl_2 (50 mL), H_2O (10 mL), and sat. NaHCO_3 (10 mL) and stirring was continued for 10 min. The organic phase was separated, dried over MgSO_4 , and concentrated to ~10 mL by evaporation, furnishing solution A. To a stirred solution of (S)-BOC-N-methyl-valine (0.69 g, 2.98 mmol) in CH_2Cl_2 (7 mL) were successively added at 0°C : solution A, triethylamine (0.46 mL, 3.30 mmol), 1-hydroxy-benzotriazole (HOBt; 0.46 g, 3.41 mmol), and 1-(3-dimethylaminopropyl)-3-ethylcarbodiimide hydrochloride (EDCI; 0.61 g, 3.19 mmol). The reaction mixture was stirred at 0°C for 1 h and then at room temperature for 22 h. The mixture was then diluted with ethyl acetate (100 mL) and washed successively with water (60 mL), cold 0.5M HCl (2×55 mL), saturated NaHCO_3 (2×55 mL), and brine (55 mL) and dried over MgSO_4 and evaporated. The residue (0.95 g) was purified by chromatography on a column of silica gel (100 g) with a mixture of petroleum ether and ethyl acetate (12:1) to afford pure amide (S)-(-)-**251** (0.74 mg, 51%) as a lightly orange oil: $R_f = 0.52$ (petroleum ether - ethyl acetate, 8:1); $[\alpha]_D -55.00$ (c 1, CHCl_3); ^1H NMR (400 Hz, CDCl_3) δ 0.90 (d, $J = 6.6$ Hz, 3H), 1.00 (d, $J = 6.4$ Hz, 3H), 1.48 (s, 9H), as a part of 1.29-1.52 (m, 23H), 1.77 (pent, $J = 7.3$ Hz, 2H), 1.85 (pent, $J = 7.3$ Hz, 2H), 2.24 (s, 6H), 2.30-2.40 (m, 1H), 2.82 (s, 3H), 3.40 (t, $J = 6.9$ Hz, 2H), 3.69 (t, $J = 6.6$ Hz, 2H), 4.09 (d, $J = 11.0$ Hz, 1H), 7.16 (s, 2H), 8.03 (br s, 0.74 H); ^{13}C NMR δ 16.36 (CH_3), 18.55 (CH_3), 19.84 (CH_3), 25.88 (CH), 26.12 (CH_2), 28.14 (CH_2), 28.34 (CH_3), 28.73 (CH_2), 29.38 (CH_2), 29.45 (CH_2), 29.52 (CH_2), 30.34 (CH_2),

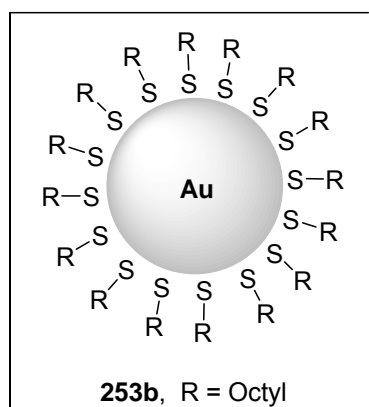
32.80 (CH₂), 34.08 (CH₂), 65.85 (CH), 72.45 (CH₂), 80.54 (C), 120.04 (CH), 131.46 (C), 133.28 (C), 152.49 (C), 157.33 (CO), 168.56 (CO); MS (EI) *m/z* (%) 584 and 582 (M⁺, 8), 368 (37), 157 (52), 129 (95), 86 (100), 57 (48); HRMS (EI) 582.3038 (C₃₀H₅₁⁷⁹BrN₂O₄ requires 582.3032).



Formamide (S)-(-)-252. Trifluoroacetic acid (13.5 mL) was added dropwise to a solution of the BOC derivative **251** (1.54 g, 2.64 mmol) in CH₂Cl₂ (20 mL) at 0 °C and the stirring was continued at the same temperature for 1 h. The acid was removed under reduced pressure and the residue was co-evaporated with toluene (2 × 20 mL) to afford a TFA salt of the deprotected amine as a brownish oil, which was used in the following step without further purification. The crude ammonium salt was dissolved in formic acid (15.2 mL) and the resulting solution was cooled to 0 °C. Acetic anhydride (11.5 mL) was then added dropwise and the mixture was allowed to stir at room temperature for 15 h. The volatiles were then evaporated and the residue (1.42 g) was purified by chromatography on a column of silica gel (140 g) with a mixture of CH₂Cl₂ and MeOH (70:1) to afford formamide (S)-(-)-**252** (1.19 g; 88%) as a yellow oil: *R_f* = 0.42 and 0.30 (two spots; CH₂Cl₂–MeOH, 70:1); [α]_D -78.00 (*c* 1, CHCl₃); ¹H NMR (400 Hz, CDCl₃ a mixture of rotamers in ca. 4:1 ratio; the signals for the minor rotamer are marked with an *) δ 0.90 (d, *J* = 6.6 Hz, 3H), 1.03 (d, *J* = 6.3 Hz, 3H), 1.29-1.47 (m, 14H), 1.76 (pent, *J* = 7.2 Hz, 2H), 1.84 (pent, *J* = 7.1 Hz, 2H), 2.22 (s, 6H), 2.38-2.51 (m, 1H), 2.91 (s, 0.47H*), 3.00 (s, 2.49H), 3.40 (t, *J* = 6.9 Hz, 2H), 3.55 (d, *J* = 10.6 Hz, 0.18H*), 3.68 (t, *J* = 6.5 Hz, 2H), 4.42 (d, *J* = 11.2 Hz, 0.82H), 7.14 (s, 0.32H*), 7.18 (s, 1.64H), 8.13 (s, 0.82H), 8.22 (s, 0.77H), 8.25 (s, 0.22H*), 8.34 (s, 0.17H*); ¹³C NMR δ 16.32 (CH₃), 18.56 (CH₃), 19.48 (CH₃), 25.32 (CH), 26.09 (CH₂), 28.11 (CH₂), 28.70 (CH₂), 29.35 (CH₂), 29.42 (CH₂), 29.49 (CH₂), 30.31 (CH₂), 31.53 (CH₃), 32.77 (CH₂), 34.05 (CH₂), 62.86 (CH), 72.40 (CH₂), 120.27 (CH), 131.43 (C), 132.90 (C), 152.70 (C), 163.85 (CO), 169.97 (CO); MS (EI) *m/z* (%) 512 (23), 510 (M⁺, 22), 369 (36), 114 (100), 86 (25), 12 (55); HRMS (EI) 510.2455 (C₂₆H₄₃BrN₂O₃ requires 510.2457).



Gold nanoparticles 253a. A solution of hydrogen tetrachloroaurate hydrate $\text{HAuCl}_4 \cdot n\text{H}_2\text{O}$ (2.0 g, 49% Au metal basis, 4.98 mmol) in deionised water (150 mL) was added to a stirred solution of tetraoctylammonium bromide (6.80 g, 12.44 mmol, 2.5 equiv) in toluene (480 mL). The mixture was stirred for 10 min, the organic layer was separated and butanethiol (132 μL , 1.24 mmol, 0.25 equiv) was added. The solution was stirred for 10 min and then a solution of NaBH_4 (1.88g, 49.8 mmol, 10 eq.) in deionised water (150 ml) was added over ~ 10 s. The resulting black solution was stirred at room temperature for 3.5 h after which time the layers were separated and the toluene layer was concentrated to near dryness under vacuum. Ethanol (70 mL) was then added and the precipitate was isolated by gravity filtration, and then washed with ethanol (300 mL) and acetone (450 mL) to afford nanoparticles **253a** as a black powder (1.07 g): ^1H NMR (400 Hz, CDCl_3) δ 0.95 (broad signal), 1.27 (broad signal), 1.54 (broad signal), 1.68 (broad signal), 3.38 (broad signal). Anal. Found: S, 3.74. TEM – 2.3 nm, an average core size.



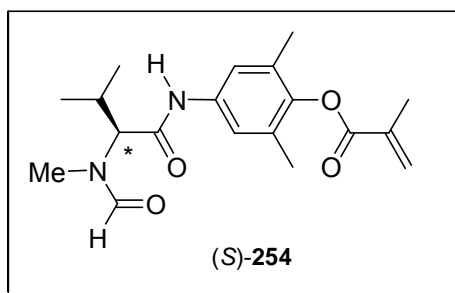
Gold nanoparticles 253b. Synthesised on a 1.0 g scale from $\text{HAuCl}_4 \cdot n\text{H}_2\text{O}$ (1.0 g, 2.49 mmol) in an identical manner to that shown above but using octanethiol (91 mg, 0.62

mmol) instead to butanethiol. ^1H NMR (400 Hz, CDCl_3) δ 0.88 (broad signal), 1.27 (broad signal), 1.55 (broad signal), 1.66 (broad signal), 3.37 (broad signal). Anal. Found: S, 3.23.

General Procedure for the Asymmetric Reduction of **185a** Catalyzed by **243a,b**.

The imine **185a** (50 mg, 0.22 mmol) was added to a suspension of catalyst **243a** (100 mg) or **243b** (79 mg) in toluene (1.5 mL), followed by the addition of trichlorosilane (50 μL) at 0 $^\circ\text{C}$ and the mixture was stirred at room temperature overnight. The solvent was evaporated and the residue was treated with methanol (25 mL) to form a dispersion which was centrifuged. The black solid was separated from the solution and dispersed again in MeOH (25 mL). Repeated centrifuge of the latter dispersion afforded a regenerated catalyst^A which was dried under high vacuum prior to the next use. Methanolic solution were combined, the solvent evaporated and the residue dissolved in chloroform (30 mL), followed by washing with NaHCO_3 (10 mL). After separation an aqueous phase was additionally washed with chloroform (30 mL). Combined organic solutions were dried over MgSO_4 and the solvent was evaporated. The crude product was purified by chromatography on a column of silica gel (10 g) using a mixture of petroleum ether – ethyl acetate (15:1) to give pure amine **186a**. The results are summarized in the Table 30.

^AThe catalyst **243b** was recovered only in 32% thus the repeated use in the next transformation was not performed.

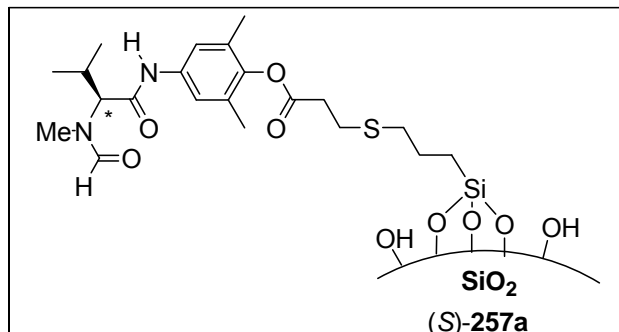


Formamide (S)-(-)-254. Methacryloyl chloride (0.12 mL, 1.2 mmol) was added to a solution of phenol **218** (300 mg, 1.08 mmol) and triethylamine (0.2 mL) in CH_2Cl_2 (9 mL) and the mixture was stirred at 25 $^\circ\text{C}$ for 18 h. The solvent was then evaporated (without external heating) and the residue (520 mg) was purified by chromatography on a column of silica gel (30 g) with a mixture of CH_2Cl_2 and MeOH (70:1) to afford pure formamide (S)-(-)-**254** (230 mg, 62%) as a yellowish oil; R_f = 0.50 and 0.36 (two spots; CH_2Cl_2 –MeOH, 49:1); $[\alpha]_D$ -162.6 (c 0.5, CHCl_3); ^1H NMR (400 Hz, CDCl_3 , a mixture of rotamers in ca. 4:1 ratio; the signals for the minor rotamer are marked with an *) δ 0.91 (d, J = 6.5 Hz, 3H), 1.04

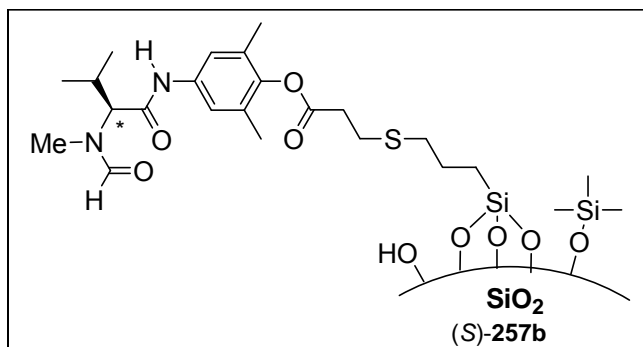
Catalyst 256b. Copper(I) chloride (80 mg, 0.82 mmol), 2,2'-bipyridine (384 mg, 2.46 mmol), benzyl methacrylate **255** (2.70 mL, 16 mmol), and ethyl 2-bromoisobutyrate (24 μ L, 0.16 mmol) were successively added to a solution of **254** (282 mg, 0.82 mmol) in DMSO (7 mL) and the mixture was stirred under nitrogen for 5 min. The heterogeneous mixture was then degassed by freeze pump thaw and stirred under nitrogen at 90 °C for 3 h. The mixture was then cooled to room temperature and poured into a rapidly stirring methanol (1 L). The precipitated polymer was isolated by filtration, washed with methanol (300 mL), dissolved in DMSO (7 mL) and the solution was poured into a rapidly stirring methanol (1000 mL) again. The precipitate was filtered, washed with methanol (300 mL), and dried under high vacuum to afford a contaminated product as a greenish powder (3.19 g). The latter powder was dissolved in CH₂Cl₂ (100 mL) and vigorously stirred with deionised water (100 mL) for 30 min. The organic layer was dried and evaporated and the residue was dissolved in chloroform (7 mL) and the solution was poured into a rapidly stirring methanol (1000 mL). The precipitated polymer was isolated by filtration, washed with methanol (300 mL), and dried under high vacuum to furnish the desired product **256b** (2.48 g, 48%) as a white powder: ¹H NMR (400 Hz, CDCl₃) δ : 0.72 (br s), 0.91 (br s), 1.07 (br s), 1.18 (br m), 1.31 (br m), 1.60 (br m), 1.78 (br s), 1.88-2.04 (br signal), 2.48 (br m), 2.98 (br s), 3.44 (br m), 4.00 (br m), 4.35 (br d), 4.88 (br d), 5.09 (br m), 5.15 (br m), 7.08 (br m), 7.28 (br s), 7.47 (br m), 8.00 (br s), 8.14 (br s); [α]_D -6.30 (c 1, CHCl₃); IR (KBr) ν 3437, 3064, 3032, 2959, 1728, 1487, 1482, 1455, 1388, 1367, 1262, 1142, 751, 697 cm⁻¹; GPC M_n = 6000 g•mol⁻¹, M_w = 7134 g•mol⁻¹, PDI = 1.19; Anal. Found: C, 73.78; H, 6.88; N, 0.53; this corresponds to 0.19 mmol•g⁻¹ loading.

General Procedure for the Asymmetric Reduction of 215a-k Catalysed by 256a/b. Trichlorosilane (50 μ L) was added to a solution of imine **215** (0.22 mmol) and catalyst **256a/b** (for the mol%, see Tables 31 and 32) in toluene (2 mL) at 0 °C and the mixture was stirred at room temperature overnight. The mixture was then poured into a rapidly stirring methanol (50 mL), and the precipitated polymer was filtered off and washed with methanol (50 mL). The combined filtrates were evaporated and the residue was treated with methanol (2 \times 30 mL), which dissolved the product and left the remaining traces of the catalyst undissolved. Combined polymer-supported catalyst was dried in a vacuum (for yields of the recovered catalyst, see Table 31 and 32). The methanolic solution, containing the amine and inorganic impurities, was evaporated and the residue was dissolved in chloroform (30 mL), and the solution was washed with aqueous saturated NaHCO₃ (10 mL). The aqueous phase was extracted with chloroform (30 mL) and the combined organic solutions were dried over

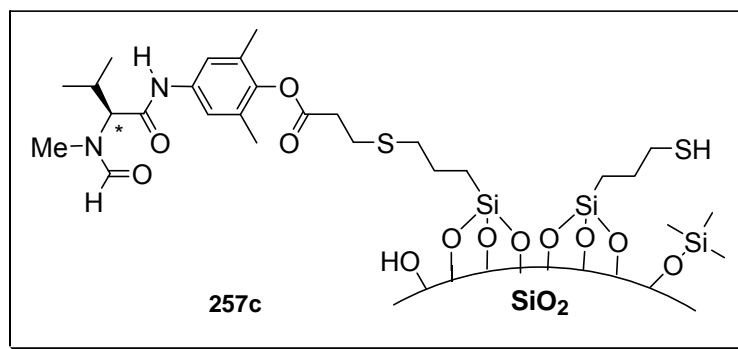
MgSO₄ and evaporated. The crude product was purified by chromatography on a column of silica gel (10 g) using a mixture of petroleum ether and ethyl acetate to give the pure amine. The results are summarized in the Tables 31 and 32.



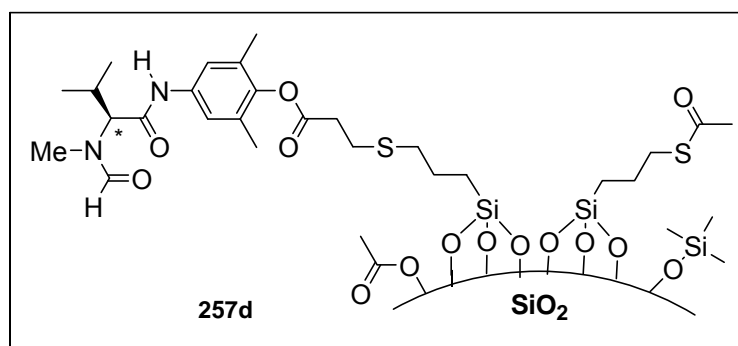
Silica Gel-Supported Formamide **257a.** Silica gel (dried at 250 °C for 4 h prior to the reaction) and formamide **260** (283 mg, 0.54 mmol) were stirred in a 1:1 mixture of dry pyridine and toluene (3 mL) at 90 °C for 40 h. The mixture was cooled to rt and the solid material was isolated by filtration under vacuum, followed by washing with MeOH (5 × 25 mL), DCM (2 × 25 mL) and Et₂O (25 mL). Overnight drying under vacuum afforded the supported catalyst **257a** (297 mg) as a yellow solid: IR (KBr) ν 3447, 2966, 1758, 1660, 1560, 1487, 1414, 1052, 950, 876, 801, 448 cm⁻¹. Anal. Found: C, 11.40; H, 1.68; N, 0.96.



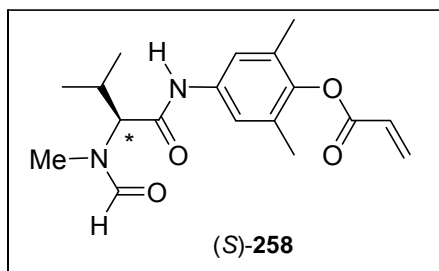
Silica Gel-Supported Formamide **257b.** Hexamethyldisilazane (3 mL) and the silica gel-supported formamide **257a** (170 mg) were stirred at 60 °C for 48 h. The mixture was cooled to room temperature and the solid material was isolated by filtration under vacuum, followed by washing with MeOH (5 × 25 mL), DCM (2 × 25 mL), and Et₂O (25 mL). Overnight drying under vacuum afforded catalyst **257b** (138 mg) as a yellow solid: IR (KBr) ν 3436, 2963, 1761, 1665, 1561, 1487, 1415, 1255, 1105, 1073, 1014, 844, 805, 462 cm⁻¹. Anal. Found: C, 14.27; H, 2.51; N, 1.11.



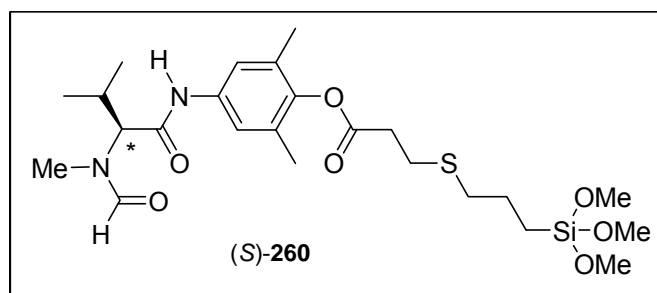
Silica Gel-Supported Formamide **257c.** A mixture of formamide **258** (115 mg, 0.35 mmol), derivatized silica **261b** (400 mg, 0.40 mmol SH), and 1,1'-azobis (cyclohexanecarbonitrile) (19 mg) in toluene was degassed by freeze pump thaw and stirred under nitrogen at 90 °C for 48 h. The mixture was cooled to room temperature and the solid material was isolated by filtration under vacuum, followed by washing with MeOH (5 × 25 mL), DCM (2 × 25 mL), and Et₂O (25 mL). Overnight drying under vacuum afforded catalyst **257c** (420 mg) as a yellow solid: IR (KBr) ν 3439, 2961, 2848, 1878, 1758, 1665, 1559, 1486, 1413, 1236, 1100, 1003, 811, 470 cm⁻¹. Anal. Found: C, 12.07; H, 2.00; N, 0.70.



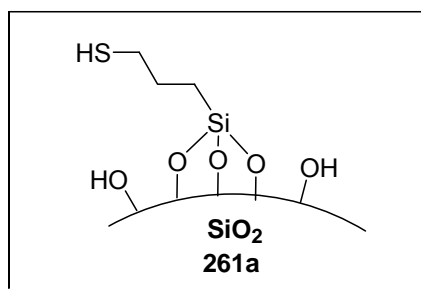
Silica Gel-Supported Formamide **257d.** To a stirred suspension of derivatized **257c** (253 mg), and 4-dimethylamino pyridine DMAP (120 mg) were successively added triethylamine (1.52 mL, 10.9 mmol) and acetyl chloride (0.7 mL, 10 mmol) and the mixture was stirred at room temperature for 24 h. The solid material was isolated by filtration under vacuum, followed by washing with MeOH (5 × 25 mL), DCM (2 × 25 mL), and Et₂O (25 mL). Overnight drying under vacuum afforded the catalyst **257d** (240 mg) as a yellow solid: IR (KBr) ν 3447, 2964, 2849, 1759, 1665, 1561, 1487, 1415, 1257, 1094, 1030, 808, 459 cm⁻¹. Anal. Found: C, 12.55; H, 1.94; N, 0.65.



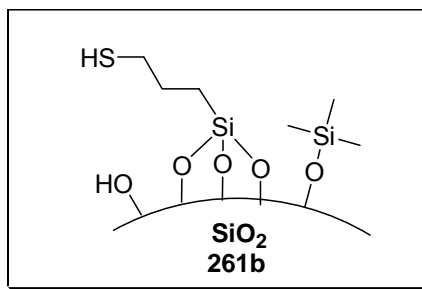
Formamide (S)-(-)-258. Acryloyl chloride (0.92 mL, 11.32 mmol) was added to a solution of phenol **218** (1.78 g, 6.39 mmol), triethylamine (1.95 mL, 14.02 mmol) and DMAP (80 mg) in CH₂Cl₂ (45 mL) and the mixture was stirred at 25 °C for 21 h. NaHCO₃ (80 mL, sat. solution) was added and the organic phase was separated. The aqueous layer was additionally extracted with CH₂Cl₂ (200 mL), the combined organic phase was dried over MgSO₄, and evaporated. The residue (2.25 g) was purified by chromatography on a column of silica gel (150 g) with a mixture of CH₂Cl₂ and MeOH (70:1) to afford pure formamide (S)-(-)-**258** (1.58 g, 74%) as a yellowish oil; R_f = 0.50 and 0.36 (two spots; CH₂Cl₂-MeOH, 49:1); $[\alpha]_D$ -113.00 (c 1, CHCl₃); ¹H NMR (400 Hz, CDCl₃, a mixture of rotamers in ca. 4:1 ratio; the signals for the minor rotamer are marked with an *) δ 0.91 (d, J = 6.6 Hz, 3H), 1.04 (d, J = 6.5 Hz, 3H), 2.11 (s, 6H), 2.40-2.53 (m, 1H), 2.91 (s, 0.37 H*), 2.99 (s, 2.55H), 3.50 (d, J = 10.3 Hz, 0.14H*), 4.39 (d, J = 11.3, 0.87H), 6.02 (dd, J = 10.4, J = 1.3 Hz, 1H), 6.35 (dd, J = 17.3, J = 10.40 Hz, 1H), 6.63 (dd, J = 17.3, J = 1.3 Hz, 1H), 7.24 (s, 0.22 H*), 7.28 (s, 1.69H), 8.14 (s, 1.51H), 8.22 (s, 0.13H*); ¹³C NMR δ 16.38 (CH₃), 18.54 (CH₃), 19.52 (CH₃), 25.22 (CH), 31.59 (CH₃), 63.14 (CH), 119.80 (CH), 127.37 (CH), 130.86 (C), 132.66 (CH₂), 135.21 (C), 144.30 (C), 163.97 (CHO), 167.09 (CO); IR (KBr) ν 3433, 2964, 2927, 1734, 1656, 1620, 1559, 1486, 1404, 1259, 1159, 1078, 1022, 804 cm⁻¹; MS (EI) m/z (%) 332 (M⁺, 28), 191 (8), 142 (57), 114 (100), 86 (18), 55 (12); HRMS (EI) 332.1738 (C₁₈H₂₄N₂O₄ requires 332.1736).



Formamide (S)-(-)-260. (3-Mercaptopropyl)trimethoxysilane (**259**) (1.48 mL, 8 mmol) and 1,1'-azobis(cyclohexanecarbonitrile) (68 mg) were added to a solution of **218** (340 mg, 1.02 mmol) in CHCl_3 (5 mL), the mixture was then degassed by freeze pump thaw and refluxed under nitrogen for 22 h. The solvent was evaporated and the residue (1.93 g) was purified by chromatography on a column of silica gel (80 g) with a mixture of CH_2Cl_2 and MeOH (70:1) to afford pure formamide (S)-(-)-**260** (283 mg, 52%) as a yellowish oil; R_f = 0.50 and 0.36 (two spots; CH_2Cl_2 -MeOH, 49:1); $[\alpha]_D$ -62.00 (c 1, CHCl_3); ^1H NMR (400 Hz, CDCl_3 , a mixture of rotamers in ca. 4:1 ratio; the signals for the minor rotamer are marked with an *) δ 0.74-0.78 (m, 2H) 0.90 (d, J = 6.6 Hz, 3H), 1.03 (d, J = 6.4 Hz, 3H), 1.72 (pent, J = 7.7 Hz, 2H), 2.11 (s, 6H), 2.40-2.49 (m, 1H), 2.60 (t, J = 7.7 Hz, 2H), 2.87-2.89 (s overlapped with m, 4.22H), 2.98 (s, 2.57 H), 3.56 (s, 9H), 4.39 (d, J = 11.3 Hz, 0.87H), 7.22 (s, 0.22 H*), 7.26 (s, 1.78H), 8.13 (s, 1H), 8.22 (s, 1H); ^{13}C NMR δ 8.48 (CH_2), 16.53 (CH_3), 18.53 (CH_3), 19.48 (CH_3), 22.90 (CH_2), 25.24 (CH), 26.83 (CH_2), 31.56 (CH_3), 34.57 (CH_2), 35.07 (CH_2), 50.53 (CH_3), 63.05 (CH), 119.80 (CH), 130.73 (C), 135.21 (C), 144.39 (C), 163.94 (CHO), 167.08 (CO), 169.85 (CO); IR (KBr) ν 3433, 2939, 2840, 2361, 1756, 1657, 1556, 1485, 1411, 1186, 1130, 1084, 814 cm^{-1} ; MS (CI) m/z (%) 529 ($[\text{M}+\text{H}]^+$, 100), 497 (13), 333 (13), 279 (17), 242 (11), 165 (31), 142 (65); HRMS (CI) 529.2402 ($\text{C}_{24}\text{H}_{41}\text{N}_2\text{O}_7\text{SSi}$ $[\text{M}+\text{H}]$ requires 529.2404).



Preparation of Support 261a. Silica gel (2 g) and (3-mercaptopropyl)-trimethoxysilane (**259**) (8.76 mL, 47.1 mmol) were stirred in a 1:1 mixture of dry pyridine and toluene (9 mL) at 90 °C for 24 h. The mixture was then cooled to room temperature and the solid material was isolated by filtration under vacuum, followed by washing with MeOH (5 × 25 mL), DCM (2 × 25 mL), and Et_2O (25 mL). Overnight drying under vacuum afforded derivatized silica **261a** (2.32 g) as a yellow solid: IR (KBr) ν 3440, 2948, 2848, 2571, 2001, 1865, 1633, 1455, 1271, 997, 806, 470 cm^{-1} . Anal. Found: S, 3.78.



Preparation of Support 261b. Hexamethyldisilazane (7.5 mL) and the support **261a** (500 mg) were stirred at 100 °C for 72 h. The mixture was cooled to rt and the solid material was isolated by filtration under vacuum, followed by washing with MeOH (5 × 25 mL), DCM (2 × 25 mL), and Et₂O (25 mL). Overnight drying under vacuum afforded the support **261b** (480 mg) as a yellow solid: IR (KBr) ν 3466, 2951, 2847, 1871, 1628, 1457, 1165, 960, 812, 455 cm⁻¹. Anal. Found: S, 3.22.

General Procedure for the Asymmetric Reduction of 185a, Catalysed by 257a-d or 261b or SiO₂^A. Trichlorosilane (100 μ L) was added to a stirred suspension of the imine **185a** (50 mg, 0.22 mmol) and the catalyst (for the mass or number of mmol, see Table 33) in toluene (1.5 mL) at 0 °C and the mixture was stirred at room temperature additional 16h. The catalyst was separated from the mother liquor by filtration and washed with MeOH (2 × 25 mL). Organic solutions were combined and the solvent was evaporated. The residue was dissolved in CHCl₃ (30 mL) and treated with a saturated aqueous solution of NaHCO₃ (10 mL). The layers were separated, and the aqueous layer was additionally extracted with chloroform (30 mL). Combined chloroform solutions were dried over MgSO₄, and the solvent was evaporated to give a crude product, which was purified by chromatography on a column of silica gel (15 g) with a mixture of petroleum ether and ethyl acetate (15:1) to afford pure amines **186a**. The results are summarized in the Table 33.

^A – Silicagel was dried at 200 °C for 4h prior to the use

Regeneration of Immobilized Catalysts. After separation from the mother liquor and washing with MeOH, the catalyst was additionally washed with MeOH (2 × 25 mL), CH₂Cl₂ (2 × 25 mL) and ether (25 mL). An overnight drying under vacuum afforded the regenerated catalyst, which was used for the next transformation without further purification.

References

- [1] – S. C. Stinson, *Chem. Eng. News* **2001**, 79(40), 79.
- [2] – *Principles and Practice of Heterogeneous Catalysis* (Eds.; J. M. Thomas, W. J. Thomas), Wiley-VCM, Weinheim, **1997**.
- [3] - M. Heitbaum, F. Glorius, I. Esher, *Angew. Chem. Int. Ed.* **2006**, 45, 4732.
- [4] - C. A. McNamar, M. J. Dixon, M. Bradley, *Chem. Rev.* **2002**, 102, 3275.
- [5] – Hodge, P. *Chem. Soc. Rev.* **1997**, 26, 417
- [6] – C. E. Song, J. W. Yang, E. J. Roh, S. G. Lee, J. H. Ahn, H. Han, *Angew. Chem.* **2002**, 114, 4008; *Angew. Chem. Int. Ed.* **2002**, 41, 3852.
- [7] Rapp Polymere www.rapp-polymere.com; Argonaut Technologies www.argotech.com
- [8] Sherrington, D. C. *J. Polym. Sci., Pol. Chem.* **2001**, 39, 2364.
- [9] D. J. Bayston, J. L. Fraser, M. R. Ashton, A. D. Baxter, M. E. C. Polywka, E. Moses, *J. Org. Chem.* **1998**, 63, 3137.
- [10] P. Guerriero, V. Ratovelomanana-Vidal, J. P. Genet, P. Dellis, *Tetrahedron Lett.* **1997**, 42, 3423.
- [11] T. Ohkuma, H. Takeno, Y. Honda, R. Noyori, *Adv. Synth. Catal.* **2001**, 343, 369.
- [12] A. Fuiji, M. Sodeoka, *Tetrahedron Lett.* **1999**, 40, 8011.
- [13] C. Chapuis, M. Barthe, J.-Y. de Saint Laumer, *Helv. Chim. Acta* **2001**, 84, 230.
- [14] a) C. Saluzzo, T. Lamouille, F. Le Guyader, M. Lemaire, *Tetrahedron: Asymmetry* **2002**, 13, 1141; b) R. ter Halle, B. Colasson, E. Schulz, M. Spagnol, M. Lemaire, *Tetrahedron Lett.* **2000**, 41, 643.
- [15] D. A. Annis, E. N. Jacobsen, *J. Am. Chem. Soc.* **1999**, 121, 4147.
- [16] S. Peukert, E. N. Jacobsen, *Org. Lett.* **1999**, 1, 1245.
- [17] T. S. Reger, K. D. Janda, *J. Am. Chem. Soc.* **2000**, 122, 6929.
- [18] a) H. Zhang, Y. Zhang, C. Li, *Tetrahedron: Asymmetry* **2005**, 16, 2417; b) H. Zhang, S. Xiang, C. Li, *Chem. Commun.* **2005**, 1209.
- [19] For a review see: Ghosh, A. K.; Mathivanan, P.; Cappiello, J. *Tetrahedron: Asymmetry* **1998**, 9, 1-45.
- [20] a) A. Mandoli, S. Orlandi, D. Pini, P. Salvadori, *Chem. Commun.* **2003**, 2466., b) Glos, M.; Reiser, O. *Org. Lett.* **2000**, 2, 2045.
- [21] Annunziata, R.; Benaglia, M.; Cinquini, M.; Cozzi, F.; Pitillo, M. *J. Org. Chem.* **2001**, 66, 3160.

- [22] a) Kamahori, K.; Tada, S.; Ito, K.; Itsuno, S. *Tetrahedron: Asymmetry* **1995**, *6*, 2547; b) Kamahori, K.; Ito, K.; Itsuno, S. *J. Org. Chem.* **1996**, *61*, 8321.
- [23] a) Irurre, J.; Fernandez-Serrata, A.; Rosanas, F. *Chirality* **1997**, *9*, 191. b) Altana, B.; Burguete, M. I.; Fraile, J. M.; Garcia, J. I.; Luis, S. V.; Mayoral, J. A.; Vicent, M. J. *Angew. Chem., Int. Ed. Engl.* **2000**, *39*, 1503.
- [24] Itsuno, S.; Frechet, J. M. J. *J. Org. Chem.* **1987**, *52*, 4140.
- [25] Soai, K.; Niwa, S.; Watanabe, M. *J. Org. Chem.* **1988**, *53*, 927.
- [26] Watanabe, M.; Soai, K. *J. Chem. Soc., Perkin. Trans. 1* **1994**, 837.
- [27] Lipshutz, B. H.; Shin, Y. *Tetrahedron Lett.* **2000**, *41*, 9515
- [28] a) Sellner, H.; Seebach, D. *Angew. Chem. Int. Ed. Engl.* **1999**, *38*, 1918; b) Sellner, H.; Rheiner, P. B.; Seebach, D. *Helv. Chim. Acta.* **2002**, *85*, 352.
- [29] Moon Kim, B.; Sharpless, K. B. *Tetrahedron Lett.* **1990**, *31*, 3003.
- [30] Han, H.; Janda, K. D. *J. Am. Chem. Soc.* **1996**, *118*, 7632.
- [31] Kuang, Y.-Q.; Zhang, S.-Y.; Wei, L.-L. *Tetrahedron Lett.* **2001**, *42*, 5925.
- [32] C. E. Song, S.-G. Lee, *Chem. Rev.* **2002**, *102*, 3495.
- [33] Tu, Q. Y.; Wang, F.; Gu, P. M.; Liu, P. N. *Org. Lett.* **2004**, *6*, 169
- [34] Shannon, I. J.; Clarke, R. J. *Chem. Commun.*, **2001**, 1936.
- [35] Burguete, M. I.; Fraile, J. M.; Garcia, J. I.; Garcia-Verdugo, E.; Herrerias, C. I.; Luis, S. V.; Mayoral, J. A. *J. Org. Chem.* **2001**, *66*, 8893.
- [36] Corma, A.; Garcia, H.; Moussaif, A.; Sabater, J. M.; Zniber, R.; Redouane, A. *Chem. Commun.*, **2002**, 1058.
- [37] Park, J. K.; Kim, S.-W.; Hyeon, T.; Kim, B. M. *Tetrahedron: Asymmetry*, **2001**, *12*, 2931
- [38] Rechavi, D.; Lemaire, M. *Org. Lett.* **2001**, *3*, 2493.
- [39] a) Thomas, J. M.; Maschmeyer, T.; Johnson, B. F. G.; Shephard, D. S. *J. Mol. Catal. A* **1999**, *141*, 139; b) Thomas, J. M. *Angew. Chem., Int. Ed.* **1999**, *38*, 3588; c) Borszeky, K.; Burgi, T.; Zhaohui, Z.; Mallet, T.; Baiker, A. *J. Catal.* **1999**, *187*, 160.
- [40] Jones, M. D.; Raja, R.; Thomas, J. M.; Johnson, B. F. G.; Lewis, D. W.; Rouzaud, J.; Harris, K. D. M. *Angew. Chem., Int. Ed.* **2003**, *42*, 4326.
- [41] Johnson, B. F. G.; Raynor, S. A.; Shephard, D. S.; Mashmeyer, T. Meurig-Thomas, J.; Sankar, G.; Bromley, S.; Oldroyd, R.; Gladden, L.; Mantle, M. D. *Chem. Commun.*, **1999**, 1167.
- [42] Shin, J.-H.; Kim, G.-J. *Tetrahedron Lett.* **1999**, *40*, 6827.
- [43] Song, C. E.; Yang, J. W.; Ha, H.-J. *Tetrahedron: Asymmetry*, **1997**, *8*, 841.
- [44] Kesali, B.; Lin, W.; *Chem. Commun.* **2004**, 2284.

- [45] Hu, A.; Ngo, H. L.; Lin, W. *Angew. Chem. Int. Ed.* **2004**, *43*, 2501.
- [46] Pugin, B.; Landert, H.; Spindler, F.; Blaser, H.-U. *Adv. Synth. Catal.* **2002**, *9*, 344.
- [47] Li, H.; Luk, Y.-Y.; Mrksich, M.; *Langmuir* **1999**, *15*, 4957.
- [48] Takizawa, S.; Patil, M. L.; Marubayashi, K.; Sasai, H.; *Tetrahedron* **2007**, *63*, 6512.
- [49] Ono, F.; Kanemasa, S.; Tanaka, J. *Tetrahedron Lett.* **2005**, *46*, 7623.
- [50] Fujihara, H.; Tamura, M. *J. Am. Chem. Soc.* **2003**, *125*, 15742.
- [51] Hu, A.; Yee, G. T.; Lin, W. *J. Am. Chem. Soc.* **2005**, *127*, 12486.
- [52] Belser, T.; Jacobsen, E. N. *Adv. Synth. Catal.* 000000
- [53] Belser, T.; Stohr, M.; Pfaltz, A. *J. Am. Chem. Soc.* **2005**, *127*, 8720.
- [54] a) Benaglia, M.; Puglisi, A.; Cozzi, F. *Chem. Rev.* **2003**, *103*, 3401. b) Cozzi, F. *Adv. Synth. Catal.* **2006**, *348*, 1367. c) Breslow, R. *Science* **1982**, *218*, 532.
- [55] a) Benaglia, M.; Celentato, G.; Cozzi, F. *Adv. Synth. Catal.* **2001**, *343*, 171. b) Benaglia, M.; Cinquini, M.; Cozzi, F.; Puglisi, A.; Celentato, G. *Adv. Synth. Catal.* **2002**, *344*, 533.
- [56] Kondo, K.; Yamano, T.; Takemoto, K. *Makromol. Chem.* **1985**, *186*, 1781.
- [57] Benaglia, M.; Cinquini, M.; Cozzi, F.; Puglisi, A.; Celentato, G. *J. Mol. Catal. A* **2003**, *204-205*, 157.
- [58] a) Enders, D.; Seki, A.; *Synlett* **2002**, 26. b) Hanessian, S.; Pham, V. *Org. Lett.* **2000**, *2*, 2975.
- [59] Clapham, B.; Cho, C.-W.; Janda, K. D. *J. Org. Chem.* **2001**, *66*, 868.
- [60] Szollosi, G.; London, G.; Balaspiri, L.; Somali, C. Bartok, M. *Chirality* **2003**, *15*, S90-S96
- [61] Calderon, F.; Fernandez, R.; Sanchez, F.; Fernandez-Mayoralas, A. *Adv. Synth. Catal.* **2005**, *347*, 1395.
- [62] Arendt, K. A.; Borths, C. J.; MacMillan, D. W. C. *J. Am. Chem. Soc.* **2000**, *122*, 4243
- [63] Selkala, S. A.; Tois, J.; Pihko, P. M.; Koskinen, A. M. P. *Adv. Synth. Catal.* **2002**, *344*, 941.
- [64] Jen, W. S.; Wiener, J. J. M.; MacMillan, D. W. C. *J. Am. Chem. Soc.* **2000**, *122*, 9874.
- [65] Puglisi, A.; Benaglia, M.; Cinquini, M.; Cozzi, F.; Celentato, G. *Eur. J. Org. Chem.* **2004**, 567.
- [66] Oyama, T. Yoshioka, H. Tomoi, M. *Chem. Commun.* **2005**, 1857.
- [67] a) Denmark, S. E.; Fu, J.; Lawler, M. J.; *J. Org. Chem.* **2006**, *71*, 1523; Denmark, S. E.; Fu, J.; Coe, D. M.; Su, X.; Pratt, N. E.; Griedel, B. D. *J. Org. Chem.* **2006**, *71*, 1513; and references cited therein, b) Priem, G. Pelotier, B.; Macdonald, S. J. F.; Anson, M.

- S.; Campbell, I. B. *J. Org. Chem.* **2003**, *68*, 3844.; Priem, G. Pelotier, B.; Macdonald, S. J. F.; Anson, M. S.; Campbell, I. B. *Synlett* **2003**, 679.
- [68] Sartori, G.; Armstrong, A.; Maggi, R.; Mazzacani, A.; Sartori, R.; Bigi, F.; Dominguez-Fernandez, B.; *J. Org. Chem.* **2003**, *68*, 3232.
- [69] Nelson, A. *Angew. Chem. Int. Ed.* **1999**, *38*, 1538; Kacprzak, K.; Gawronski, J. *Synthesis*, **2001**, *40*, 3131.
- [70] a) Chinchilla, R.; Mazon, P.; Najera, C.; *Tetrahedron: Asymmetry*, **2000**, *11*, 3277., b) Thierry, A.; Plaquevent, J.-C.; Cahard, D. *Tetrahedron: Asymmetry* **2001**, *12*, 983., c) Thierry, A.; Perrard, T.; Audouard, C.; Plaquevent, J.-C.; Cahard, D. *Synthesis* **2001**, 1742.
- [71] Danelli, T.; Annunziata, R.; Benaglia, M.; Cinquini, M.; Cozzi, F.; Tocco, G. *Tetrahedron: Asymmetry*, **2003**, *14*, 461.
- [72] Kobayashi, N.; Iwai, K. *J. Am. Chem. Soc.* **1978**, *100*, 7071.
- [73] Inagaki, M.; Hiratake, J.; Yamamoto, Y.; Oda, J. *Bull. Chem. Soc. Jpn.* **1987**, *60*, 4121.
- [74] Kobayashi, N.; Iwai, K. *Tetrahedron Lett.* **1980**, *21*, 2167.
- [75] Danda, H.; Chino, K.; Wake, S. *Chem. Lett.* **1991**, 731.
- [76] Yamashita, T.; Yasueda, H.; Miyauchi, Y.; Nakamura, N.; *Bull. Chem. Soc. Jpn.* **1977**, *50*, 1532.
- [77] Hermann, K.; Wynber, H.; *Helv. Chim. Acta.* **1977**, *60*, 2208;
- [78] Hafez, A. M.; Taggi, A. E.; Dudding, T.; Lectka, T. *J. Am. Chem. Soc.* **2001**, *123*, 10853.
- [79] a) Welton, T. *Chem. Rev.* **1999**, *99*, 2071. b) Dupont, J.; de Souza, R. F.; Suarez, P. A. Z. *Chem. Rev.* **2002**, *102*, 3667. c) Olivier-Bouribigou, H.; Magna, L.; *J. Mol. Cat. A* **2002**, *3484*, 1. d) Sheldon, R. *Chem. Commun.* **2001**, 2399. e) Wasserscheid, P.; Keim, W. *Angew. Chem., Int. Ed. Engl.* **2000**, *39*, 3772. f) Gordon, C. M. *Appl. Catal. A* **2001**, *222*, 101. g) Dyson, P. J. *Transition Met. Chem.* **2002**, *27*, 353.
- [80] Chauvin, Y.; Musmann, L.; Olivier, H. *Angew. Chem., Int. Ed. Engl.* **1995**, *34*, 2698.
- [81] Berger, A.; de Souza, R. F.; Delgado, M. R.; Dupont, J. *Tetrahedron: Asymmetry*, **2001**, *12*, 1825.
- [82] Guernik, S.; Wolfson, A.; Herskowitz, M.; Greenspoon, N.; Geresh, S. *Chem. Commun.* **2001**, 2314.
- [83] Monteiro, A. L. Zinn, F. K.; de Souza, R. F.; Dupont, J. *Tetrahedron: Asymmetry*, **1997**, *8*, 177.
- [84] Brown, R. A.; Pollet, P.; McKoon, E.; Eckert, C. A.; Liotta, C. L.; Jessop, P. G. *J. Am. Chem. Soc.* **2001**, *123*, 1254.

- [85] a) Wolfson, A.; Venkelecom, I. F. J.; Jacobs, P. A. *Tetrahedron Lett.* **2003**, *44*, 1195., b) selectivity to methyl hydroxybutyrate due to a formation of the corresponding acetal.
- [86] Baleizao, C. Gigante, B.; Garcia, H.; Corma, A. *Green Chemistry*, **2002**, *4*, 272.
- [87] Song, C. E.; Oh, C. R.; Roh, E. J.; Choo, D. J. *Chem. Commun.* **2000**, 1743.
- [88] Oh, C. R.; Choo, D. J.; Shim, W. H.; Lee, D. H.; Roh, E. J.; Lee, S.-gi.; Song, C. E. *Chem. Commun.* **2003**, 1100.
- [89] Song, C. E.; Roh, E. J. *Chem. Commun.* **2000**, 837.
- [90] Fraile, J. M.; Garcia, J. I.; Herrerias, C. I.; Mayoral, J. A.; Carrie, D.; Vaultier, M.; *Tetrahedron: Asymmetry*, **2001**, *12*, 1891.
- [91] Toma, S.; Gotov, B.; Kmentova, I.; Solcaniova, E. *Green Chemistry*, **2000**, *2*, 149.
- [92] Branco, L. C.; Alfonso, C. A. M. *Chem. Commun.* **2002**, 3036.
- [93] Song, C. E.; Jung, D.-un.; Roh, E. J.; Lee, S.-gi.; Chi, D, Y. *Chem. Commun.* **2002**, 3038.
- [94] Loh, T.- P.; Feng, L.- C.; Yang, H. -Y.; Yang, J.- Y. *Tetrahedron Lett.* **2002**, *43*, 8741.
- [95] Kotrusz, P.; Alemayehu, S.; Toma, S.; Schmalz, H.-G.; Adler, A. *Eur. J. Org. Chem.* **2005**, 4904.
- [96] Luo, S.; Mi, X.; Zhang, L.; Liu, S.; Xu, H.; Cheng, J.- P. *Tetrahedron* **2007**, *63*, 1923.
- [97] a) Xu, D.- Q.; Wang, B.- T.; Luo, S.- P.; Yue, H.- D.; Wang, L.- P.; Xu, Z.-Y. *Tetrahedron Asymmetry*, **2007**, *18*, 1788. b) Xu, D.; Luo, S.; Yue, H.; Wang, L.; Liu Y.; Xu, Z. *Synlett*, **2006**, *16*, 2569.
- [98] Ni, B.; Zhang, Q.; Headley, A.- D. *Green Chem.*, **2007**, *9*, 737.
- [99] a) Luo, S.; Mi, X.; Zhang, L.; Liu, S.; Xu, H.; Cheng, J.- P. *Angew. Chem., Int. Ed.* **2006**, *45*, 3093. b) For an overview and philosophy of fluorous tags, see: Gladysz, J. A.; Curran, D. P.; Horvath, I. T. *Handbook of Fluorous Chemistry*; Wiley: New York, **2004**.
- [100] Nakamura, Y.; Takeuchi. S.; Ohgo, Y.; Curran, D. P. *Tetrahedron* **2000**, *56*, 351.
- [101] (a) Nakamura, Y.; Takeuchi, S.; Okumura, K.; Ohgo, Y.; Curran, D. P. *Tetrahedron* **2002**, *58*, 3963. (b) Nakamura, Y.; Takeuchi. S.; Ohgo, Y.; Curran, D. P. *Tetrahedron* **2000**, *41*, 57.
- [102] Simonelli, B.; Orlandi, S.; Benaglia, M.; Pozzi, G. *Eur. J. Org. Chem.* **2004**, 2669.
- [103] Fache, F. *New J. Chem.*, 2004, **28**, 1277.
- [104] a) See: Hoffmann, S.; Seayad, A. M.; List, B. . *Angew. Chem., Int. Ed.* **2005**, *44*, 7424 and references cited therein, b) Langlois, N.; Dang, T.-P.; Kagan, H. B. *Tetrahedron Lett.* **1973**, 4865.
- [105] Itsuno, S.; Nakano, M.; Miyazaki, K.; Matsuda, H.; Ito, K.; Hirao, A.; Nakahama, S. *J. Chem. Soc., Perkin Trans. 1* **1985**, 2039.

- [106] a) Cho, B. T.; Chun, Y. S. *J. Chem. Soc., Perkin. Trans. I* **1990**, 3200. b) Cho, B. T.; Chun, Y. S. *Tetrahedron: Asymmetry* **1992**, 3, 1583.
- [107] Bolm, C.; Felder, M. *Synlett* **1994**, 655.
- [108] Brunel, J. M.; Buono, G. *Synlett* **1996**, 177.
- [109] Shimizu, M.; Kamei, M.; Fujisawa, T. *Tetrahedron Lett.* **1995**, 36, 8607.
- [110] a) Sugi, K. D.; Nagata, T.; Yamada, T.; Mukaiyama, T. *Chem. Lett.* **1997**, 493. b) Sugi, K. D.; Nagata, T.; Yamada, T.; Mukaiyama, T. *Chem. Lett.* **1996**, 737. c) Nagata, T.; Yoroazu, K.; Yamada, T.; Mukaiyama, T. *Angew. Chem., Int. Ed. Engl.* **1995**, 34, 2145. d) Nagata, T.; Sugi, K. D.; Yamada, T.; Mukaiyama, T. *Synlett* **1996**, 1076. e) Sugi, K. D.; Nagata, T.; Yamada, T.; Mukaiyama, T. *Chem. Lett.* **1996**, 1081.
- [111] Levi, A.; Modena, G.; Scorrano, G. *J. Chem. Soc., Chem. Commun.* **1975**, 6.
- [112] a) Vastag, S.; Bakos, J.; Toros, S.; Takach, N. S. E.; King, R. B.; Heil, B.; Marko, L. *J. Mol. Catal.* **1984**, 22, 283. b) Bakos, J.; Toth, I.; Heil, B.; Marko, L. *J. Organomet. Chem.* **1985**, 279, 23. c) Bakos, J.; Toth, I.; Heil, B.; Szalontai, G.; Parkanyi, L.; Fulop, V. *J. Organomet. Chem.* **1989**, 370, 263.
- [113] Kang, G.-J.; Cullen, W. R.; Fryzur, M. D.; James, B. R.; Kutney, J. P. *J. Chem. Soc., Chem. Commun.* **1998**, 1466.
- [114] a) Cullen, W. R.; Fryzur, M. D.; James, B. R.; Kutney, J. P. Kang, G.-J.; Herb, G.; Thorburn, I. S.; Spogliarich, R. *J. Mol. Catal.* **1990**, 62, 243. b) Becalski, A. G.; Cullen, W. R.; Fryzur, M. D.; James, B. R.; Kang, G.-J.; Retting, S. J. *Inorg. Chim.* **1991**, 30, 5002.
- [115] Longley, C. J.; Goodwin, T. J.; Wilkinson, G. *Polyhedron* **1986**, 5, 1625.
- [116] Becalski, A. G.; Cullen, W. R.; Fryzur, M. D.; James, B. R.; Kang, G.-J.; Retting, S. J. *Inorg. Chim.* **1991**, 30, 5002.
- [117] a) Amrani, Y.; Lecomte, L.; Sinou, D.; Bakos, J.; Toth, I.; Heil, B. *Organometallics* **1989**, 8, 542. b) Bakos, J.; Orosz, A.; Heil, B.; Laghmari, M.; Lhoste, P.; Sinou, D. *J. Chem. Soc., Chem. Commun.* **1991**, 1684.
- [118] a) Burk, M. J.; Feaster, J. E. *J. Am. Chem. Soc.* **1992**, 114, 6266. b) Burk, M. J.; Martinez, J. P.; Feaster, J. E.; Cosford, N. *Tetrahedron* **1994**, 50, 4399.
- [119] a) Chan, Y. N. C.; Osborn, J. A. *J. Am. Chem. Soc.* **1990**, 112, 9400. b) Chan, Y. N. C.; Meyer, D.; Osborn, J. A. *J. Chem. Soc., Chem. Commun.* **1990**, 869. c) Spindler, F.; Pugin, B.; Blaser, H.-U. *Angew. Chem., Int. Ed. Engl.* **1990**, 29, 558.
- [120] a) Togni, A. *Angew. Chem., Int. Ed. Engl.* **1996**, 35, 1475. See also: b) Spindler, F.; Pugin, B.; Jalett, H.-P.; Buser, H.-P.; Pittelkow, U.; Blaser, H.-U. *Proceedings of the*

Conference on Catalysis of Organic Reactions, Atlanta 1996; Catal. Org. React., Chem. Ind. (Dekker). **1996**, 68, 153.

- [121] Schnider, P.; Kock, G.; Pretot, R.; Wang, G.; Bohnen, F. M.; Kruger, C.; Pfaltz, A. *Chem. Eur. J.* **1997**, 3, 887.
- [122] Zhu, S.-F.; Xie, J.-B.; Hang, Y.-Z.; Li, S.; Zhou, Q.-L. *J. Am. Chem. Soc.* **2006**, 128, 12886.
- [123] Xiao, D.; Zhang, X. *Angew. Chem., Int. Ed.* **2001**, 40, 3425.
- [124] Ng, Y.; Chan, C.; Osborn, J. A.; *J. Am. Chem. Soc.* **1990**, 112, 9400.
- [125] a) Spindler, H.; Blaser, H.-U.; *Enantiomer* **1999**, 4, 557.; Togni, A. *Angew. Chem., Int. Ed.* **1996**, 108, 1581. *Angew. Chem., Int. Ed.* **1996**, 35, 1475.
- [126] Jiang, X.-b.; Minnaard, A. J.; Hessen, B.; Feringa, B. L.; Duchateau, A. L. L. Andrien, J. G. O.; Boogers, J. A. F.; de Vries, J. G. *Org. Lett.* **2003**, 5, 1503.
- [127] Guiu, E.; Munoz, B.; Castillon, S.; Claver, C. *Adv. Synth. Catal.* **2003**, 345, 169.
- [128] Willoughby, C. A.; Buchwald, S. L. *J. Am. Chem. Soc.* **1992**, 114, 7562.; *J. Am. Chem. Soc.* **1994**, 116, 8952.; *J. Am. Chem. Soc.* **1994**, 116, 11703.
- [129] Wang, Y.-Q.; Lu, S.-M.; Zhou, Y.-G. *J. Org. Chem.* **2007**, 72, 3729.
- [130] a) Cobley, C. J.; Foucher, E.; Lecouve, J.-P.; Lennon, I. C.; Ramsden, J. A.; Thomillot, G. *Tetrahedron: Asymmetry* **2003**, 14, 3431. b) Oppolzer, W.; Wills, M.; Starkemann, C.; Bernardinelli, G. *Tetrahedron Lett.* **1990**, 31, 4117.
- [131] a) Brunner, H.; Becker, R. *Angew. Chem., Int. Ed.* **1984**, 23, 222. b) Becker, R.; Brunner, H.; Mahboobi, S.; Wiegreb, W. *Angew. Chem., Int. Ed.* **1985**, 24, 995.
- [132] a) Verdaguer, X.; Lange, U. E. W.; Reding, M. T.; Buchwald, S. L. *J. Am. Chem. Soc.* **1996**, 118, 6784. Verdaguer, X.; Lange, U. E. W.; Reding, M. T.; Buchwald, S. L. *Angew. Chem., Int. Ed.* **1998**, 37, 1103. Hansen, M.; Buchwald, S. L. *Org. Lett.* **2000**, 2, 713. b) Reding, M. T.; Buchwald, S. L. *J. Org. Chem.* **1998**, 63, 6344.
- [133] Lipshutz, B. H.; Shimizu, H. *Angew. Chem., Int. Ed.* **2004**, 43, 2228.
- [134] Kobayashi, S.; Yasuda, M.; Hachiya, I.; *Chem. Lett.*, **1996**, 407.
- [135] a) Iwasaki, F.; Onomura, O.; Mishima, K.; Kanematsu, T.; Maki, T.; Matsamura, Y. *Tetrahedron Lett.* **2001**, 42, 2525. b) Onomura, O.; Kouchi, Y.; Iwasaki, F.; Matsamura, Y. *Tetrahedron Lett.* **2006**, 47, 3751.
- [136] Malkov, A. V.; Mariani, A.; MacDougall, K. N.; Kočovský, P. *Org. Lett.* **2004**, 6, 2253.
- [137] Malkov, A. V.; Figlus, M.; Stončius, S.; Kočovský, P. *J. Org. Chem.* **2007**, 72, 1315.

- [138] a) Malkov, A. V.; Stončius, S.; MacDougall, K. N.; Mariani, A.; McGeoch, G. D.; Kočovský, P. *Tetrahedron* **2006**, 62, 264. b) Malkov, A. V.; Stončius, S.; Kočovský, P. *Angew. Chem., Int. Ed.* **2007**, 46, 3722.
- [139] a) Wang, Z.; Ye, X.; Wei, S.; Wu, P.; Zhang, A.; Sun, J. *Org. Lett.* **2006**, 8, 999. b) Wang, Z.; Cheng, M.; Wu, P.; Wei, S.; Sun, J. *Org. Lett.* **2006**, 8, 3045. c) Pei, D.; Wang, Z.; Wei, S.; Zhang, Y.; Sun, J. *Org. Lett.* **2006**, 8, 5913.
- [140] Wang, Z.; Wei, S.; Wang, C.; Sun, J. *Tetrahedron: Asymmetry* **2007**, 18, 705.
- [141] a) Malkov, A. V.; Stewart Liddon, A. J. P.; Ramirez-Lopez, P.; Bendova, L.; Haigh, D.; Kočovský, P. *Angew. Chem., Int. Ed.* **2006**, 45, 1432. b) Zhou, L.; Wang, Z.; Wei, S.; Sun, J. *Chem. Commun.*, **2007**, 2977.
- [142] a) Uematsu, N.; Fujii, A.; Hashiguchi, S.; Ikariya, T.; Noyori, R.; *J. Am. Chem. Soc.* **1996**, 118, 4916. b) Noyori, R.; Hashiguchi, S. *Acc. Chem. Res.* **1997**, 30, 97.
- [143] a) Rueping, M.; Sugiono, E.; Azap, C.; Theissmann, T.; Botle, M. *Org. Lett.* **2005**, 7, 3781. b) Rueping, M.; Azap, C.; Sugiono, E.; Theissmann, T. *Synlett* **2005**, 2367
- [144] Hoffmann, S.; Seayad, A. M.; List, B. *Angew. Chem. Int. Ed.* **2005**, 44, 7424.
- [145] a) Rueping, M.; Antonchick, A. P. *Angew. Chem. Int. Ed.* **2007**, 46, 4562; b) Rueping, M.; Antonchick, A. P.; Theissmann, T. *Synlett* **2006**, 1071; *Angew. Chem.* **2006**, 118, 3765; *Angew. Chem. Int. Ed.* **2006**, 45, 3683; c) Rueping, M.; Antonchick, A. P.; Theissmann, T. *Angew. Chem. Int. Ed.* **2006**, 45, 6751; d) Rueping, M.; Sugiono, E.; Azap, C. *Angew. Chem.* **2006**, 118, 2679; *Angew. Chem. Int. Ed.* **2006**, 45, 2617; e) *J. Am. Chem. Soc.* **2006**, 128, 13074-13075.
- [146] Ether **211a** was prepared before in a similar way by another group but the conditions were not fully described and the product was only characterized by ¹H NMR: Beaune, O.; Bessière, J. M.; Boutevin, B.; Robin, J. J. *J. Fluorine Chem.* **1994**, 67, 159.
- [147] For the synthesis of **208**, see: Helfenbein, J.; Lartigue, C.; Noirault, E.; Azim, E.; Legailiard, J.; Galmier, M. J.; Madelmont, J. C. *J. Med. Chem.* **2002**, 45, 5806.
- [148] For the method, see: Ragnoli, M.; Pucci, E.; Bertolucci, M.; Gallot, B.; Galli, G. *J. Fluorine Chem.* **2004**, 125, 283.
- [149] Entwistle, I. D.; Gilkerson, T. *Tetrahedron* **1978**, 34, 215.
- [150] Thiele, T.; Prescher, D.; Ruhmann, R.; Wolff, D. *J. Fluorine Chem.*, 85, **1997**, 155.
- [151] For the method see 138a
- [152] When THF was used as solvent, the yield dropped to 30%.
- [153] Doherty, D. G. *J. Am. Chem. Soc.* **1955**, 77, 4887.

- [154] Henley-Smith, P.; Whiting, D. A.; Wood, A. F. *J. Chem. Soc., Perkin Trans. I* **1980**, 614.
- [155] Zhu, J.; Kell, A. J.; Workentin, M. S. *Org. Lett.* **2006**, 8, 4993.
- [156] Boal, A. K.; Otello, V. M. *J. Am. Chem. Soc.* **2002**, 124, 5019.
- [157] Hostetler, M. J.; Wingate, J. E.; Zhong, C.-J.; Harris, J. E.; Vachet, R. W.; Clark, M. R.; Londono, J. D.; Green, S. J.; Stokes, J. J.; Wignall, G. D.; Glish, G. L.; Porter, M. D.; Evans, N. D.; and Murray, R. W. *Langmuir* **1998**, 14, 17-30.
- [158] Lee, B. S.; Namgoong, S. K.; Lee, S.-g. *Tetrahedron Lett.* **2005**, 46, 4501.
- [159] For authoritative reviews on this method, see: (a) Matyjaszewsky, K.; Xia, J. *Chem. Rev.* **2001**, 101, 2921. (b) Matyjaszewski, K.; Braunecker, W. A. *Macromol. Eng.* **2007**, 1, 161. (c) Braunecker, W. A.; Matyjaszewski, K. *Prog. Polym. Sci.* **2007**, 32, 93.
- [160] Malkov, A. V.; Figlus, M.; Kočovský, P.; *J. Org. Chem.* 2008, 73, 3985
- [161] For reviews on other soluble polymers, see the following: (a) Dickerson, T. J.; Reed, N. N.; Janda, K. D. *Chem. Rev.* **2002**, 102, 3325. For the problems associated with nonpolar solvents, see: (b) Reger, T. S.; Janda, K. D. *J. Am. Chem. Soc.* **2000**, 122, 6929.
- [162] For the method see: Minutowo, F.; Pini, D.; Petri, A.; Salvadori, P. *Tetrahedron: Asymmetry*, **1996**, 7, 2293.
- [163] For the method see: 43.
- [164] For the method see: 37.
- [165] a) Malkov, A. V.; Stončius, S.; Vranková, K.; Arndt, M.; Kočovský, P. *Chem. Eur. J.* **2008**, 14, 8082., b) Malkov, A. V.; Vranková, K.; Stončius, S.; Kočovský, P. manuscript in preparation.

APPENDICES

